

**Investigating the Formation of Functional and Smart Materials by
Nanospinning and other Spinning Techniques**

KETANKUMAR VIJAYKUMAR VADODARIA

Submitted for the degree of Doctor of Philosophy

**Heriot-Watt University
The School of Textiles and Design**

December 2012

The copyright in this thesis is owned by the author. Any quotation from the thesis or use of any of the information contained in it must acknowledge this thesis as the source of the quotation or information.

ABSTRACT

Functional, smart fibres and fibres with different morphologies have been produced from different materials using different spinning methods. The effect of processing parameters on different nano fibre morphologies was studied by SEM. The spinning solution properties such as viscosity, surface tension, conductivity, UV-visible spectra were studied. The fibres were characterised by DSC, FTIR, XRD, strength test.

Antibacterial, hygroscopic, humectant Manuka honey (MH) functional nanofibres have been produced successfully by single needle electrospinning (SNE) using polyethylene oxide (PEO) as matrix. Electrospinning parameters such as higher feed rate, higher proportion of MH, lower applied voltage, lower needle to collector distance produced merged, thicker, flat 15% (wt/wt) MHPEO nanofibres and vice versa. 15%MHPEO fibres of diameters from 0.198 μ m to 0.924 μ m were produced using different parameters. The 50% and 65% (wt) MHPEO mats showed antibacterial property. DSC result showed reduction in melting temperature as the MH proportion increased. FTIR results showed respective peaks for MH and PEO. MHPEO nanofibres can be used for medical end use such as wound healing.

Ethyl cellulose (EC) nanofibres have been successfully electrospun using different combination of toluene and ethanol (0:100, 40:60, 50:50, 60:40, 100:0) as solvent by SNE. Round and elongated bead on string to smooth bead-less 15% (wt/wt)EC fibres produced as proportion of toluene increased in the solvent mixture. Thin, bead-less fibres were obtained by 60:40 (toluene: ethanol) with average fibre diameters ranging from 0.483 μ m to 0.631 μ m. EC nanofibres have been also produced by high output bubble electrospinning (BE) method. EC fibres of diameters from 0.188 μ m to 0.41 μ m were produced by BE. Comparison between effect of electorspinning parameters on fibre revealed that the fibre morphologies followed different trends in SNE and BE. The beaded structure can be used for loading drugs in advanced medical textiles and smooth bead-less fibrous mat can be used for application such as filtration.

In order to develop thermochromic (smart) nanofibres by meltelectrospinning, thermochromic polypropylene fibres have been developed by meltspinning. The pure polypropylene and thermochromic. DSC and FTIR results showed separate peaks for the thermochromic effect and for the polypropylene. SEM images verified the presence of thermochromic pigments. Thermochromic filaments can be used in garment fashion, or as sensors in yarn or fabric form.

DEDICATION

Thank you for all your unconditional support and effort from teaching me first few words up to the journey of Ph.D..

ACKNOWLEDGEMENT

First and foremost, I would like to express my utmost gratitude to my supervisor Prof. George K. Stylios for his guidance, support, invaluable advice and patience throughout the course of the research. I am grateful to my supervisor for giving me the chance to work under his supervision and giving me the freedom to explore and try my knowledge. I found him always motivating and encouraging.

I am also thankful to my second supervisor Mrs Fiona Waldron. I would also like to thank to Prof. Alison Harley (Head of School), Prof. Roger Wardman, Prof. Robert Christie, Dr. Alex Fotheringham, Dr. Britta Kalkeuter, Dr. Lisa Macintyre, Dr. Danmei Sun, Mr Jim Mcvee, Dr. Roger Spark, Mr. Peter Sandison and library staff, Mr Liang Luo, Mrs Ann, Mrs Jane Robertson, Eleanor Drummond, Dr. Abraham Daniel, Dr. Shah M ReduwanBillah, Dr. Michel Wan, Dr. Xiaoming Zhao, Mrs Margaret Robson, for their help, suggestions, advice and encouragement

I am deeply thankful to Dr. Susan Dewar from the School of life science at Heriot-watt University for her time and help in performing microbiology tests. I am also thankful to Dr. Vijay Vadodaria (My father), Dr. Alex Fotheringham and my wife for active discussions and advice in setting up microbiological experiments.

I would also like thanks to Mrs Christina Graham, Mrs. Marian Millar and Mr Thomas Doherty in the school of engineering and physics (EPS) of Heriot Watt University. I am thankful to all in the school of Textiles and Design, and its staff members providing me with constant help, facility and training to carry out this work. I would also like to extend my thanks to those, who contributed, advised, helped and supported directly or indirectly my PhD work research fellows for their participation in my research.

Finally, I take this opportunity to express the profound gratitude from my heart to my parents-Dr.Vijaykumar P.Vadodaria, Mrs. Saroj V.Vadodaria for their blessings and support, which I never forget. I am also thankful to my in laws Dr.Kanubhai K.Patel and Mrs. Vibhaben K. Patel for their encouragement and support. I want to thank my beloved wife Jalada Vadodaria for her patience, devotion and for being my inspiration. I am lucky to have a lovely daughter Sanavi, who brought lots of joy and happiness for me. I want to offer a very special thanks to my sisters and their family, who always took pride in my academic achievements.

Last but not least I give my warmest gratitude to the almighty God for giving me strength and wisdom without which I could do nothing

ACADEMIC REGISTRY

Research Thesis Submission



Name:			
School/PGI:			
Version: <i>(i.e. First, Resubmission, Final)</i>		Degree Sought (Award and Subject area)	

Declaration

In accordance with the appropriate regulations I hereby submit my thesis and I declare that:

- 1) the thesis embodies the results of my own work and has been composed by myself
- 2) where appropriate, I have made acknowledgement of the work of others and have made reference to work carried out in collaboration with other persons
- 3) the thesis is the correct version of the thesis for submission and is the same version as any electronic versions submitted*.
- 4) my thesis for the award referred to, deposited in the Heriot-Watt University Library, should be made available for loan or photocopying and be available via the Institutional Repository, subject to such conditions as the Librarian may require
- 5) I understand that as a student of the University I am required to abide by the Regulations of the University and to conform to its discipline.

* *Please note that it is the responsibility of the candidate to ensure that the correct version of the thesis is submitted.*

Signature of Candidate:		Date:	
-------------------------	--	-------	--

Submission

Submitted By <i>(name in capitals)</i> :	
Signature of Individual Submitting:	
Date Submitted:	

For Completion in the Student Service Centre (SSC)

Received in the SSC by <i>(name in capitals)</i> :			
Method of Submission <i>(Handed in to SSC; posted through internal/external mail):</i>			
E-thesis Submitted (mandatory for final theses)			
Signature:		Date:	

Please note this form should bound into the submitted thesis.

Updated February 2008, November 2008, February 2009, January 2011

TABLE OF CONTENTS

Chapter 1 : Materials and Its Processing at Macro to Nano Dimensions

1.1	Introduction	1
1.2	Material Science and Engineering	1
1.2.1	Smart Materials	2
1.2.2	Structural Materials and Functional Materials	2
1.2.3	Composites	2
1.2.4	Polymers	2
1.3	Textile Materials	3
1.3.1	Melt spinning:	4
1.3.2	Dry spinning:	5
1.3.3	Wet spinning:	6
1.4	Journey from Macro to Micro	7
1.5	Nanoscience, Nanotechnology and Nanomaterial	9
1.6	Nanomaterials	10
1.6.1	Engineered Nanomaterial	10
1.6.2	Composites and Nano Composites	11
1.7	How to Manufacture Nano Materials	12
1.7.1	The Electrospinning Process	13
1.8	Limitations in Nanotechnology	15
1.9	Characterization of Nano Materials	15
1.10	Thesis Aims and Objectives	16
1.11	Thesis Layout,	18
1.12	Bibliography	21

Chapter 2 : Nano Fibres and Principles of Electrospinning

2.1	Introduction	27
2.2	Methods of Producing Nanofibres	27
2.2.1	Drawing	31
2.2.2	Template Synthesis	31
2.2.3	Self-Assembly	32
2.2.4	Phase Separation	32

2.3	History of Electrospinning	33
2.4	Theories of The Electrospinning process	33
2.4.1	Jet Initiation / Base Region / Taylor Cone Region	34
2.4.2	Jet Thinning / Jet Region and Splaying Region	35
2.4.3	Jet Instabilities.....	37
2.4.4	Jet Solidification / Collection Region	39
2.5	Electrospinning Parameters and Properties of Electrospun Nanofibres.....	39
2.5.1	Solution Concentration & Viscosity	40
2.5.2	Electrical Property/Conductivity of Solution.....	41
2.5.3	Surface Tension.....	41
2.5.4	pH.....	42
2.5.5	Volatility of Solvent.....	42
2.5.6	Evaporation of Solvent.....	42
2.5.7	Solution Preparation Parameter /Method	42
2.5.8	Type of Solvent / Solvent Quality.....	42
2.5.9	Multi-component Solvent	42
2.5.10	Additives in Solvents	43
2.5.11	Molecular Weight of Polymer.....	43
2.5.12	Applied Voltage	43
2.5.13	Needle to Collector Distance (NTCD).....	44
2.5.14	Volume Feed Rate / Polymer Flow Rate.....	45
2.5.15	Needle / Extrusion / Capillary Tip Diameter	45
2.5.16	Spinneret Design	45
2.5.17	AC / DC Supply	45
2.5.18	Multi Needles / Nozzles	45
2.5.19	Net Charge Density	45
2.5.20	Effect of Polarity	46
2.5.21	Temperature	46
2.5.22	Humidity	46
2.5.23	Air Velocity /Gases / Surrounding Air /Vacuum Condition.....	46
2.5.24	Vapour Concentration of Solvent / Solvent Evaporation.....	47
2.5.25	Vibration	47
2.5.26	Electrical Field Distribution / Supplementary Electrode / Insulator.....	47
2.5.27	Gas-Assisted Effect.....	47
2.5.28	Time of Spinning	47

2.5.29	Method of Collection	47
2.5.30	Speed of Collector.....	48
2.5.31	Combination of Other Process with Electrospinning (Air Blowing System).....	48
2.6	Electrospinnability.....	48
2.6.1	Advances in Electrospinning	48
2.7	Bibliography	50

Chapter 3 : Experimental and Testing Techniques in Detail

3.1	Solution Preparation	62
3.1.1	Ultrasonic Bath	62
3.2	Solution Testing	63
3.2.1	Viscosity.....	63
3.2.2	Surface Tension.....	64
3.2.3	Conductivity of Solution	66
3.2.4	Ultra Violet-Visible Spectroscopy (UV-vis).....	68
3.3	Polymer and Nano Fibre and Mat Testing	69
3.3.1	Cold Field Emission Scanning Electron Microscope	69
3.3.2	X-Ray Diffraction (XRD)	72
3.3.3	Differential Scanning Calorimetry	76
3.3.4	Fourier Transform Infrared (FTIR) Spectrometry	79
3.3.5	Tensile Test	81
3.3.6	<i>Antibacterial Test</i>	82
3.4	Bibliography	83

Chapter 4 : Investigating, Formation and Characterisation of Manuka Honey Nanofibres and its Antibacterial Properties for Wound Healing

4.1	Introduction	85
4.1.1	Electrospinning Of Manuka Honey	86
4.2	Material and Methods.....	87
4.2.1	Materials.....	87
4.2.2	Solution Preparation.....	87

4.2.3	Solvent and Solution Properties (Viscosity, Surface Tension and Conductivity)	87
4.2.4	Ultra Violet - Visible Spectroscopy	87
4.2.5	Visual Observation.....	87
4.2.6	Electrospinning	87
4.2.7	Scanning Electron Microscopic (SEM) Studies.....	88
4.2.8	Differential Scanning Calorimetry (DSC) Studies.....	88
4.2.9	Fourier Transform Infrared Red Spectroscopy (FTIR).....	88
4.2.10	Antibacterial Test	88
4.3	Results and Discussion	88
4.3.1	Viscosity, Surface Tension and Conductivity	88
4.3.2	Photographs of Honey.....	90
4.3.3	Ultra Violet-Visible Spectroscopy (Uv-visible spectra)	92
4.3.4	Influence of MH:PEO Ratio on Fibre Properties.....	93
4.3.5	Influence of Applied Voltage on Fibre Properties	94
4.3.6	Influence of Needle to Collector Distance (NTCD) on Fibre Properties.....	96
4.3.7	Influence of Feed Rate on Fibre Property	97
4.3.8	Differential Scanning Calorimetry	98
4.3.9	FTIR	99
4.3.10	Antibacterial Activity.....	100
4.4	Conclusion.....	101
4.5	Bibliography	102

Chapter 5 : Investigating the Electrospinning of Ethylcellulose

5.1	Introduction	106
5.2	Materials and Experimental Methods.....	107
5.2.1	Materials.....	107
5.2.2	Solution Preparation.....	107
5.2.3	Electrospinning Setup	108
5.2.4	Solvent and Solution Properties (Viscosity, Surface Tension and Conductivity)	108
5.2.5	Visual Observation.....	108

5.2.6	Scanning Electron Microscopic (SEM) Studies.....	108
5.2.7	FTIR (Fourier Transform Infrared Spectroscopy)	109
5.2.8	Differential Scanning Calorimetry (DSC) Studies.....	109
5.3	Results and Discussions	109
5.3.1	Solvent and Viscosity.....	109
5.3.2	Conductivity and Surface Tension	110
5.3.3	Visual Observation.....	112
5.3.4	Effect of Solvent on Ethylcellulose Electrospinning	114
5.3.5	Effect of Applied Voltage on Fibre Morphology.....	117
5.3.6	Effect of Needle to Collector Distance on Fibre Morphology	119
5.3.7	FTIR (Fourier Transform Infrared Spectroscopy)	121
5.3.8	Differential Scanning Calorimetry	123
5.4	Conclusion.....	123
5.5	Bibliography.....	124

Chapter 6 : The Case of Bubble Electrospinning of Ethylcellulose Ultrafine Fibres

6.1	Introduction	130
6.2	Materials and Experimental Methods.....	131
6.2.1	Materials.....	131
6.2.2	Solution Preparation.....	132
6.2.3	Solvent and Solution Properties (Viscosity, Surface Tension and Conductivity)	132
6.2.4	Bubble Electrospinning Setup and Parameters	132
6.2.5	Scanning Electron Microscopic (SEM) Studies.....	132
6.2.6	FTIR (Fourier Transform Infrared Spectroscopy)	132
6.3	Results and Discussions	132
6.3.1	Viscosity.....	132
6.3.2	Effect of Solution Surface to Collector Distance on Fibre Property.....	134
6.3.3	Effect of Applied Voltage on Fibre Morphology.....	135
6.3.4	FTIR (Fourier Transform Infrared Spectroscopy)	138
6.4	Comparison between needle electrospinning and bubble electrospinning.....	140
6.4.1	Effect of Feed Rate.....	140

6.4.2	Effect of Needle / Solution Surface to Collector Distance on Fibre Morphology.	141
6.4.3	Effect of Applied Voltage on Fibre Morphology.....	142
6.5	Conclusion.....	142
6.6	Bibliography.....	143

Chapter 7 : Development and Characterisation of Thermochromic Polypropylene Filament Yarn

7.1	Introduction	148
7.2	The Principle of Leuco Dye Based Thermochromism	149
7.3	Materials and Methods	152
7.3.1	Materials.....	152
7.3.2	Melt Spinning Setup.....	153
7.3.3	Visual Observation.....	153
7.3.4	Scanning Electron Microscopic (SEM) Studies.....	153
7.3.5	Tensile Testing of the Yarns	154
7.3.6	Fourier Transform Infrared Spectroscopy.....	154
7.3.7	DSC Test:	154
7.3.8	X-ray Diffraction.....	154
7.4	Results and Discussion	155
7.4.1	Thermochromic Effect	155
7.4.2	Scanning Electron Microscopy Analysis	156
7.4.3	Tensile Properties.....	157
7.4.4	FTIR Characterisation.....	158
7.4.5	DSC Measurement	159
7.4.6	X-Ray Diffraction	161
7.5	Conclusion.....	161
7.6	Bibliography.....	162

Chapter 8 : End Uses and Further Work

8.1	Introduction	165
8.2	MHPEO (Needle) Electrospinning.....	167
8.2.1	End Use	168
8.2.2	Further Work.....	168

8.3	Ethylcellulose (needle) electrospinning	168
8.3.1	End Use	168
8.3.2	Further Work.....	169
8.4	Ethylcellulose (Bubble) Electrospinning.....	169
8.4.1	End Use	169
8.4.2	Further Work.....	169
8.5	Thermochromic Polypropylene	169
8.5.1	End Use	170
8.5.2	Further Work:.....	170
8.6	Bibliography	171

Chapter 9 : Conclusions

9.1	Antibacterial Manuka Honey Nano Fibres.....	172
9.2	Beaded and Smooth Ethylcellulose Nano Fibres by Needle Electrospinning.	174
9.3	Bubble Electrospinning of Ethylcellulose Eibres.....	176
9.4	Comparison between Ethylcellulose Needle Electeospinning and Bubble Electrospinning	177
9.5	Thermochromic Polypropylene	178

LISTS OF TABLES

Table 1:1 Unique features of the nanomaterial	8
Table 1:2 Property of different materials at macro and nano scale.....	9
Table 2:1 Effect of humidity on fibre morphology	46
Table 2:2 Comparison between needle electrospinning and needle-less electrospinning	49
Table 3:1 Specifications of ring (Kruss K6)	66
Table 4:1 Conductivity (micro Siemens), surface tension (mN/m) and UV-visible absorption peak (nm).....	92
Table 5:1 Conductivity of EC solvents	110
Table 5:2 Ethyl cellulose solution and film visual property	113
Table 5:3 Effect of solvent on ethyl cellulose electrospinning	116
Table 6:1 FTIR bands for Ethanol	139
Table 6:2 FTIR bands for Toluene.....	139
Table 6:3 FTIR bands of etylcellulose	140
Table 9:1 Effect of solvent on ethyl cellulose electrospinning	175
Table 9:2 Ethyl cellulose solution and film visual property	176

LISTS OF FIGURES

Figure 1:1 Principle of melt spinning	4
Figure 1:2 Schematic diagram of bench top meltspinning.....	5
Figure 1:3 Dry spinning	6
Figure 1:4 Principle of wet spinning.....	7
Figure 1:5 Principle of Top-down and Bottom-up approach	12
Figure 1:6 Schematic diagram of the electrospinning Process	13
Figure 1:7 Principle of bubble electrospinning.....	14
Figure 2:1 Principles of nanofibres by drawing.....	31
Figure 2:2 Principles of nanofibres by template synthesis	31
Figure 2:3 Principles of phase separation	32
Figure 2:4 Changes in the polymer droplet with applied potential.....	35
Figure 2:5 Instabilities	38
Figure 2:6 Onset development of bending instabilities.....	38
Figure 3:1 Ultrasonic bath (Decon Ultrasonic – F5 minor)	62
Figure 3:2 Brookfield DV II Pro Viscosimeter.....	63
Figure 3:3 Viscosimeter spindles (Brookfield DV II Pro viscosimeter).....	63
Figure 3:4 Schematic diagram of the ring methods	65
Figure 3:5 Surface tension meter accessories	65
Figure 3:6 Kruss surface tension meter.....	66
Figure 3:7 Oakton CON 110 conductivity meter.....	67
Figure 3:8 Perkin Elmer lambda 2 Ultra Violet-visible spectrometer	68
Figure 3:9 Cold Field Emission Scanning microscope Hitachi S-4300.....	70
Figure 3:10 Polaron (SC7620) Sputter coater.....	71
Figure 3:11 Bragg's Law	73
Figure 3:12 Typical X-Ray diffraction graph	74
Figure 3:13 Schematic diagram of XRD.....	75
Figure 3:14 Bruker-AXS D8Discover transmission X-ray diffractometer	76
Figure 3:15 Schematic DSC curve.....	77
Figure 3:16 METLER-TA instrument DSC12E	78
Figure 3:17 DSC Sampler	79
Figure 3:18 ATR-FTIR Perkin-Elmer Spectrum 100 FT-IR	80
Figure 3:19 Instron Tensile tester (Model 3345)	82
Figure 4:1 Viscosity of all solutions	89
Figure 4:2 Conductivity (μS) and surface tension (mN/M) of all the solutions	89

Figure 4:3 Electrospun mat 15MHPEO	90
Figure 4:4 SEM stubs of electrospun mats of (Left) 15PEO and 15MHPEO (Right)	91
Figure 4:5 Solutions of 15PEO, 10MHPEO, 15MHPEO (Left to right)	91
Figure 4:6 UV-Visible spectra	92
Figure 4:7 Effect of MH proportion on fibre morphology.....	93
Figure 4:8 Effect of MH proportion on fibre diameters.....	94
Figure 4:9 Effect of applied voltage on fibre morphology	95
Figure 4:10 Effect of applied voltage on fibre diameters	95
Figure 4:11 Effect of NTCD on fibre morphology	96
Figure 4:12 Effect of NTCD on fibre diameters	96
Figure 4:13 Effect of feed rate on fibre morphology	97
Figure 4:14 Effect of feed rate on fibre diameters	98
Figure 4:15 DSC curves of electrospun mats.....	98
Figure 4:16 FTIR of electrospun mats	99
Figure 4:17 Antibacterial activity	101
Figure 5:1 Chemical structure of Ethylcellulose.....	106
Figure 5:2 Viscosities of 15EC solutions in different solvent systems.....	109
Figure 5:3 Surface tension (mN/m)	111
Figure 5:4 Conductivity (μ S)	111
Figure 5:5 Comparison of Ethyl cellulose solutions	112
Figure 5:6 Comparison of Ethyl cellulose films from different solvent systems	113
Figure 5:7 Effect of solvent proportion on fibre morphology.....	115
Figure 5:8 Effect of applied voltage on 15EC60To fibre morphology.....	118
Figure 5:9 Effect of applied voltage on 15EC60To fibre diameter	119
Figure 5:10 Effect of NTCD on 15EC60To fibre morphology.....	120
Figure 5:11 Effect of NTCD on 15EC60To fibre diameter	120
Figure 5:12 FTIR of solvents	121
Figure 5:13 FTIR of solvents and EC solutions.....	121
Figure 5:14 FTIR of EC mats	122
Figure 5:15 Differential scanning calorimetry	123
Figure 6:1 Viscosity of 15%EC in toluene: ethanol (60:40).....	133
Figure 6:2 Effect of solution surface to collector distance on fibre morphology	134
Figure 6:3 Effect of solution surface to collector distance on average fibre diameter .	135
Figure 6:4 Effect of applied voltage on fibre morphology at 10cm SSCD.....	136
Figure 6:5 Effect of applied voltage on average fibre diameter (BE) at 10cm.....	136

Figure 6:6 Effect of applied voltage on fibre morphology at 20cm SSCD.....	137
Figure 6:7 Effect of applied voltage on average fibre diameter (BE) at 20cm.....	137
Figure 6:8 FTIR of electrospun mats	139
Figure 6:9 Effect of feed rate on SNE fibre morphology (a,b,c) and comparison with BE fibre morphology (d).....	140
Figure 6:10 Effect of feed rate on SNE average fibre diameter and comparison with BE average fibre diameter.....	141
Figure 7:1 The principle of thermochromism	149
Figure 7:2 Structure of Polypropylene.....	152
Figure 7:3 UMB Blue structure.....	152
Figure 7:4 Thermochromic effect by body temperature	155
Figure 7:5 Developed thermochromic filament under the temperature of (a) 17°C (b) 25°C (c) 32°C (d) 38°C.....	155
Figure 7:6 Scanning electron microscopy.....	156
Figure 7:7 Tensile test (Polypropylene and Thermochromic polypropylene)	157
Figure 7:8 FTIR curves	158
Figure 7:9 D.S.C. curves	160
Figure 7:10 X-ray diffraction.....	160
Figure 8:1 Classification of smart textiles	165
Figure 9:1 Effect of different parameters on Manuka honey electrospinning	173
Figure 9:2 Effects of different parameters on Ethylcellulose needle electrospinning ..	175
Figure 9:3 Effects of different parameters on Ethyl cellulose (fibre morphology) bubble electrospinning	177

LIST OF PUBLICATIONS

Conference proceedings

- [1] K. Vadodaria and G. K. Stylios, "Comparison of Bubble Electrospinning and Needle Electrospinning of Ethylcellulose Ultrafine fibres," in *3rd International Conference on Nano Science and Technology (ICNST 2012)*, Jimma Hotel, Beijing, China, 2012.
- [2] K. Vadodaria and G. K. Stylios, "Ultrafine Web Formation from Bee's Sweet Treasure," in *3rd International Conference on Nano Science and Technology (ICNST 2012)*, Jimma Hotel, Beijing, China, 2012.

Journal Publications

- [1] K. Vadodaria and G. K. Stylios, "Comparison of Bubble Electrospinning and Needle Electrospinning of Ethylcellulose Ultrafine fibres," *Advanced Materials Research* vol. 622-623, pp. 710-715, 2013 2013.
- [2] K. Vadodaria and G. K. Stylios, "Ultrafine Web Formation from Bee's Sweet Treasure," *Advanced Materials Research* vol. 622-623, pp. 1784-1788, 2013 2013.
- [3] D. Sun, K. V. Vadodaria, and G. K. Stylios, "Developing polymer composite filament for thermosensitive applications," *Polymers and Polymer Composites*, Accepted on July, 2012.

LIST OF ABBREVIATIONS

Abbreviations	Description
1. MMF	Man-made fibre
2. CNT	Carbon nanotubes
3. UV	Ultraviolet
4. ENM	Engineered nano materials
5. ATR-FTIR	Attenuated total reflectance-Fourier transform infrared spectroscopy
6. SEM	Scanning electron microscope
7. XRD	X-Ray diffraction
8. MH	Manuka honey
9. PEO	Polyethylene oxide
10. MHPEO	Manuka honey / Polyethylene oxide blend
11. NTCD	Needle to collector distance
12. DSC	Differential scanning calorimeter
13. EC	Ethylcellulose
14. SSCD	Solution surface to collector distance
15. BE	Bubble electrospinning
16. SNE	Single needle electrospinning
17. AC	Alternating current
18. DC	Direct current
19. PVA	Polyvinyl alcohol
20. PAN	Polyacrylonitrile
21. PLLA	Poly-L-lactide
22. BuOH	Butanol
23. DCM	Dichloromethane
24. DMF	Dimethylformamide
25. PAA	Polyacrylic acid (PAA)
26. PDLA	Poly-DL-lactic acid (PDLA)
27. PS	Polystyrene
28. PMMA	Poly(methyl methacrylate)
29. RH	Relative humidity
30. LCD	Liquid crystal display
31. UV-Vis	Ultraviolet visible spectrometer
32. EM	Electron microscope

33. CFE-SEM	Colf field emission – scanning electron microscope
34. FEG	Field emission gun
35. CRE	Constant rate of elongation
36. MRSA	<i>Methicillin-resistant Staphylococcus aureus</i>
37. UMF	Unique manuka factor
38. Et	Ethanol
39. To	Toluene
40. MNE	Multi needle electrospinning
41. ECM	Extracellular matrix
42. PP	Polypropylene
43. T _m	Melting peak
44. T _g	Glass transition temperature

LIST OF DEFINATIONS

1. Resilience an occurrence of rebounding or springing back
2. Malleable Able to be hammered or pressed permanently out of shape without breaking or cracking
3. Anitinflammatory refers to the property of a substance or treatment that reduces inflammation
4. Antimutagenic An agent that inhibits mutations. Mutagens are any agents (physical or environmental) that can induce a genetic mutation or can increase the rate of mutation.
5. Ductility It is a solid material's ability to deform under tensile stress; this is often characterized by the material's ability to be stretched into a wire.

Chapter 1 : Materials and Its Processing at Macro to Nano Dimensions

1.1 Introduction

Materials play a very important role in the progress of the human race. In different areas, progress is identified by the dominant materials used in that period, starting from the stone age, the bronze age, the iron age to the present silicon age [1, 2]. Even today the demand for new materials is growing [3]. Materials are converted into various products after the selection of low cost / cheap materials with required properties. The materials are converted into appropriate shape and dimensions to meet technical performance required [4, 5].

1.2 Material Science and Engineering

Material science and engineering encourages a wide spectrum of material types, their manufacturing and processing techniques [6, 7]. Materials can be classified according to their properties. Materials can be broadly categorised into several groups as: metals, polymers, elastomers, ceramics, glasses, hybrids, composites, natural organic materials etc. [8-12]. Product design, selection of material and technological process are interconnected to meet the end uses and cost [6]. Engineering product design is connected with the determination of the product shape and the selection of materials from which they are to be made, and the selection of the relevant technological processes. The designed product has to meet the parameters pertaining fully to its functionality and the requirements connected with its shape and dimensional tolerances [6]. Engineering product design involves 3 elements: structural design, material design and technical design [6]. Material selection is one of the most important tasks for product designers. Factors such as material properties (chemical, biological [13], electrical, magnetic, optical etc.), material processability and economical aspects are taken into account before selecting material [3].

- Structural design involves deciding shape, geometry and cost to meet function of the product.
- Material design involves material selection by considering the composition, constituent phases and microstructure to meet the end use application [6].
- The technical properties of materials (physical, chemical, biological) are considered with availability to meet the functionality and expected life considering cost.

- Technological design ensures assembling elements, their geometrical features and properties, automation and productivity at lowest cost possible [6].

Definitions of some of the materials are as given below.

1.2.1 Smart Materials

The word “Smart” describes a system which has capability of sensing, processing, actuating, self-changing and self-recovering. Smart materials change / improve their property in the presence of external stimuli such as temperature, pH, electric charge, magnetic field etc. The smart properties of smart materials can be used for energy saving/ harvesting, increase human comfort, increase product life span, waste reduction, self-repair, improve efficiency etc.

1.2.2 Structural Materials and Functional Materials

In past, more research was done on the development of the structural materials which were designed / engineered for improved load bearing capacity, mechanical and structural properties. Recently, research is diverted towards the development of the functional materials. Functional materials are different from structural materials. The physical, chemical, biological properties of functional materials are sensitive to the change in environment/external stimuli. The external stimuli can be temperature, pressure, electric field, magnetic field, optical wavelength, adsorbed gas molecules, pH, electromagnetic waves etc.. Functional materials cover a broad range of materials including smart materials and also materials with some special functionality, e.g. Ferroelectric, antibacterial, conductive polymers etc. [14, 15].

1.2.3 Composites

The electrical, mechanical, magnetic, strength and other properties of the polymers can be enhanced by engineering composites with adding appropriate constituents [16]. Polymers are ductile and light weight compared to metals which are stronger. Polymer properties can be improved by adding inclusions such as fibre, plastics, particles. Scientists have developed techniques for micro sized inclusions. Recent developments have allowed nano level inclusions. “Composites are engineered materials made from two or more constituents, each offering different properties which can be combined synergistically” [17]

1.2.4 Polymers

The word polymer comes from Greek word “poly” means many. Polymer has many numbers of identical repeating single basic chemical structural units called “monomer”.

The unit of repeating unit depends upon the number of repeating units or “mers” present in polymer chain. Polymers are used in various forms such as plastics, elastomers, coatings, adhesives, fibres etc. Polymers can be natural or synthetic [18]. The regularity of polymer structure and the relative intermolecular secondary valence bonds decides fibres, plastics or elastomers [19].

1.3 Textile Materials

Textile materials form a unique branch of natural and synthetic polymeric material [18, 20-23]. Textiles are made up of specially engineered selected materials, which can deliver essential properties such as flexibility, strength, feel, high length to strength ratio etc. [24, 25]. Depending on the end use either natural or synthetic textile materials are used [26]. Natural fibres were used for centuries. Disadvantage of natural fibres is that, their inherent physical properties such as diameter, length are dependent on natural factors such as atmosphere. These natural factors are beyond the control of humans. These limitations have been overcome, with the invention of manmade fibres. New textile materials are used for high end applications such as industrial textiles, geotextiles, construction, agricultural, biomedical, fashion, defence and many more. Textiles are used from as simple as wipes to high end defence applications such as bullet proof Kevlar jackets. Textiles are produced from different forms such as fibre, yarn, fabrics (woven, knitted, nonwoven). Fibres such as cotton, jute, silk, wool etc. are based on natural fibres. Polyester, nylon, acrylic, viscose rayon are manmade /synthetic fibres. Manmade fibres are formed from various polymers. Long-chain molecules with repeating units are formed by chemical reaction in textile polymers. The length of repeating unit depends on the type of raw material. Man-made fibres offer flexibility in terms of functionalization or engineering. Manmade fibres account about 65% of all fibres used in textile applications. Technical fibres are a very important area in today's textile sector. Manmade fibres are manufactured by processes such as wet spinning/dry spinning/melt spinning or combination of them [22]. Fibre spinning techniques such as melt, wet and dry spinning are described briefly by various authors and [22, 27, 28] are summarised further in the present chapter.

In all the above methods, textile polymers are melted or dissolved in solvents to make polymer solution with required viscoelastic properties for spinning. The polymer solution is forced by the extrusion process through spinneret. The strand of fibre solution coming out of spinneret is dried/coagulated/cross-linked to get solidified fibres depending on the type of process.

The spinneret decides shape, size and number of filaments. After spinning, some post spinning operations such as drawing, texturing, chopping are carried out to produce suitable for the next process or application.

1.3.1 Melt spinning:

Melt spinning (Figure 1:1) is used for thermoplastic polymers such as polyester, nylon, polypropylene, polyethylene etc. In melt spinning, the polymer chips are fed, heated and melted.

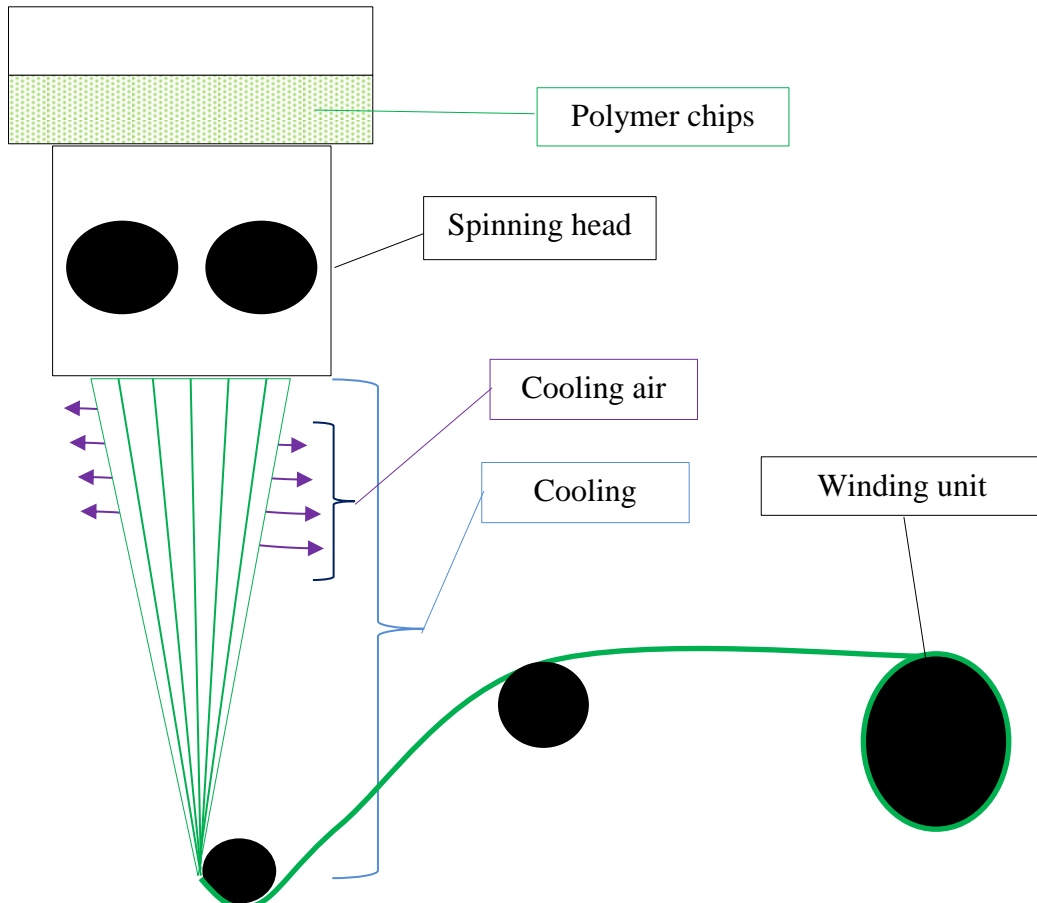


Figure 1:1 Principle of melt spinning

The molten viscous polymer solution is pumped through spinning head. The molten polymer passes through cooling zone. The cooling agent can be air or solvent. The polymer jet solidifies by the certain cooling medium and forms fibre. The filaments are collected on winding unit. The resultant fibres are drawn to improve its mechanical strength.

Melt Spinning setup in the experiment

In the present study, polypropylene and thermochromic polypropylene filaments were produced on a bench top screw extruder; ESL, U.K. as shown in the diagram (Figure 1:2), the bench top extruders has a single screw pump (F), a metering pump and die head system (B), water cooling bath (C), winding unit (D) and a control panel (A). The

temperature are controlled and regulated in the 3 extruder zones, pump and in the two die head zones. Polymer granules are fed through the hopper (E).

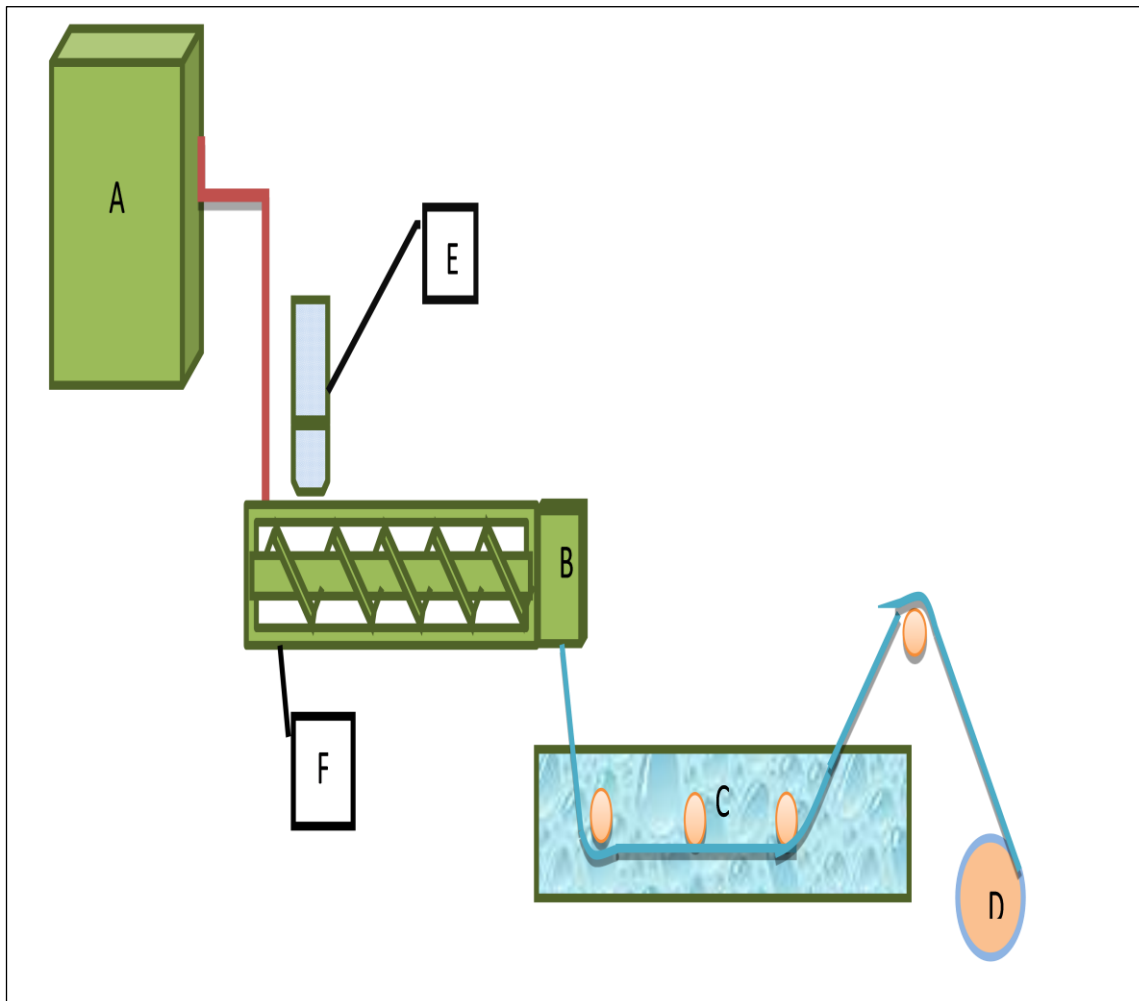


Figure 1:2 Schematic diagram of bench top meltspinning

The molten polymer is forced through a single hole spinneret as a jet. The speed is adjusted by the metering pump. All the speeds and temperatures can be controlled via the control panel (A). The extruded hot polymer jet can be cooled into a water bath and passed through guiding rollers to the lesona winding unit.

1.3.2 Dry spinning:

Dry spinning (Figure 1:3) is used for nylon, cellulose acetate, Acrylonitrile. In dry spinning the polymer is dissolved in a suitable solvent. The polymer solution is extruded through a spinneret. The hot air evaporates the solvent. Fibre becomes dry and solidifies due to inert gas or air. The solidified fibres are wound on the bobbins. The filaments are then stretched / drawn to improve mechanical strength.

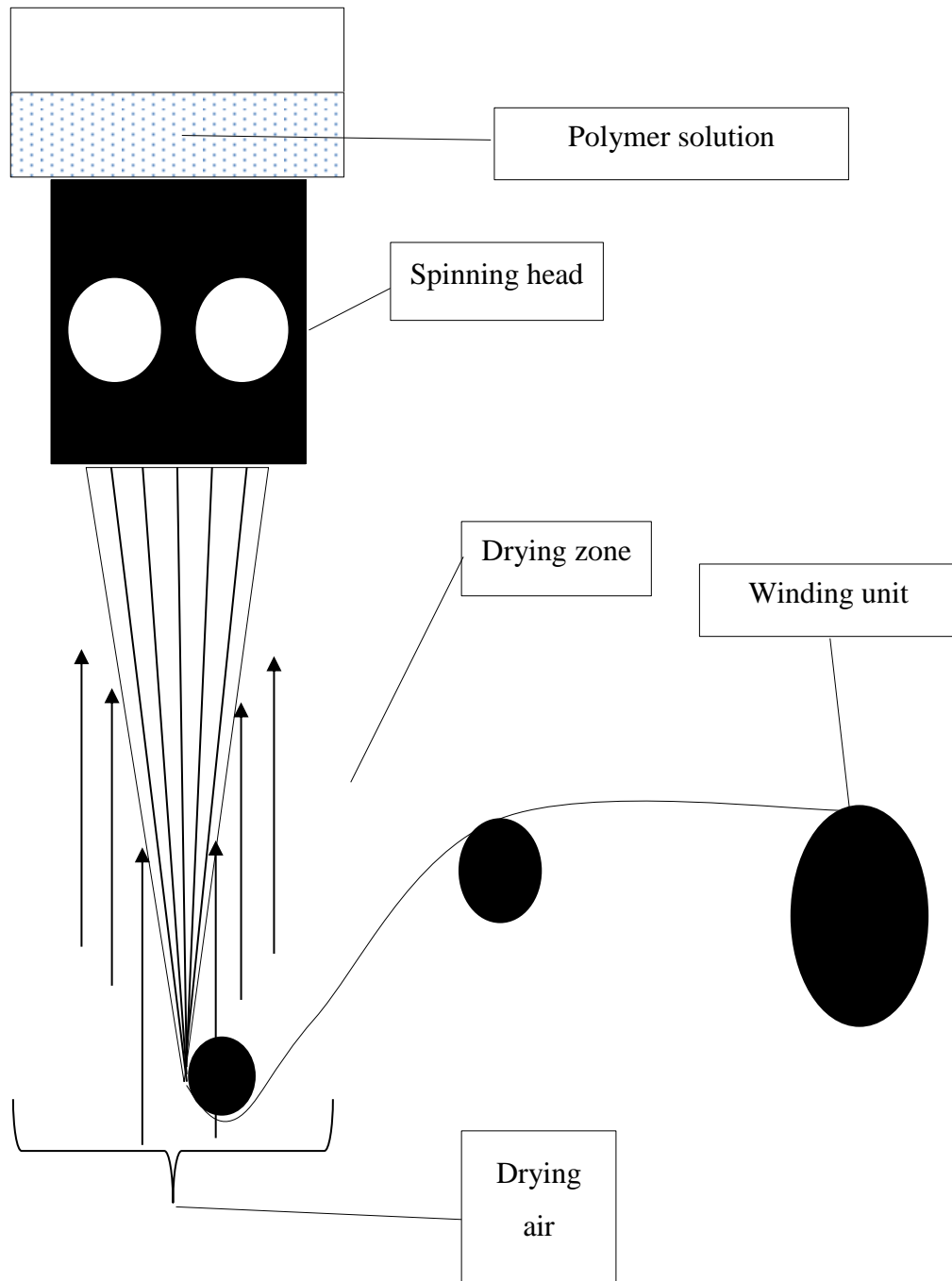


Figure 1:3 Dry spinning

1.3.3 Wet spinning:

Polymers which cannot be melted or dissolved in volatile solvent can be spun by wet spinning. Polymer solution is obtained by chemical reaction. The polymer solution is extruded into the coagulation bath. Polymer solution strand solidifies by coagulation.

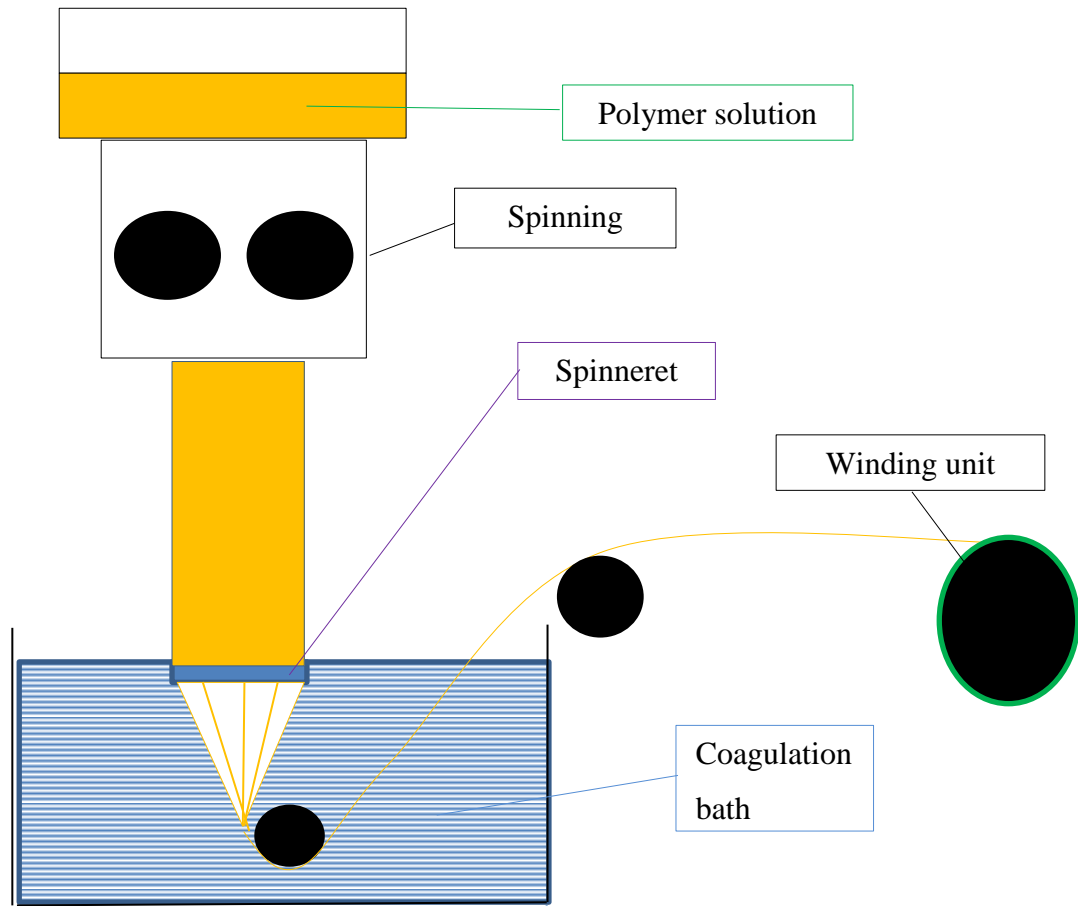


Figure 1:4 Principle of wet spinning

Fibres such as viscose rayon, casein, poly vinyl alcohol are spun by wet spinning (Figure 1:4).

All above methods can generate fibre diameters up to the micrometre range and used for normal textile applications. If fibre diameter can be reduced to nanometre, the fibres have unique properties added by the reduced dimension. Nano fibres have more surface area compared to micro or macro fibres of the same materials. Nano fibrous nonwoven mats have smaller pores. Nano fibrous filters are used for high efficiency filters, tissue scaffolds, and drug delivery or as an active surface. Nano is a Greek word meaning “dwarf” [35]. Nano is one billionth i.e. 10^{-9} of a meter [36, 37].

1.4 Journey from Macro to Micro

“In essence, the nanoscale of dimensions is the transition zone between the macro level and the molecular level” [47]. Changing materials from macro scale to nanoscale can change material’s physico-chemical properties (e.g. Electrical, chemical, biological, magnetic, optical etc.) as shown in Table 1:1 [33]. Properties of nano materials are controlled by their reduced transverse dimension and ultimately depend upon the

quantum effects of atoms/molecules of the material [33, 41]. The properties of the nano materials are unique to the nano dimension. The physico-chemical properties changes at nano scale compared to a macro scale of the same material. Nanotechnology gives opportunity to tailor the material at nano scale/atom level. With the use of nanotechnology, new family of materials and devices can be generated.

Table 1:1 Unique features of the nanomaterial	
High surface to mass ratio [33]	
High strength , conductivity, Increased resiliency , solubility, durability, reactivity [33]	
Higher catalytic effect for reactions [33]	
Ability to cross cellular and sub-cellular membranes [33]	

As particle dimensions are reduced to nano size, more atoms are exposed on surface i.e. increased surface area per volume. Surface molecules are the mostly active part in chemical or biological systems. For a given mass of material, nanoparticles prove to be more reactive than the same mass of large particles [42]. ‘The surface to volume ratio determines the potential number or reactive groups’ [33]. The effect of nano dimension on material property can be positive (i.e., increased strength, increased reactivity etc.) or negative (i.e. increased toxicity, increased instability etc.) [33]. Table 1:2 [30, 51] is the summary of unique features noted by various authors. Carbon nano tube (CNT) nanotubes are reported for their 100time more tensile strength and 5 time the Young’s modules of steel, in spite of its $1/6^{\text{th}}$ of the standard weight. CNTs are also stronger than diamond [52]. Increased surface area and quantum effects distinguish nano materials form others. A greater proportion of atoms can be found at the surface compared to the inside [42]. Optical UV reflective properties of titanium dioxide particles depend on size and particle aggregation [43]. Increased surface area can be beneficial (for eg drug delivery, conductance etc.)

Some of the examples quoted by various authors to describe these dimension in terms of scales are as below. In terms of dimensions a few examples are given below [29, 35, 38].

A nano meter is approx. $1/80000^{\text{th}}$ of human hair

Blood cell is approx. 7000nm

Ratio of human head to nanometre is nearly same as ratio of earth to human head.

DNA is about 2.5nm long while sodium atom is about 0.2nm.

Globular proteins are approximately 6 nm in diameter.

The oxide layers in metal oxide semiconductor devices are integrated electrons of 2 nm.

Quantum dots are approximately 1-2 nm diameters.

Table 1:2 Property of different materials at macro and nano scale

<u>Substance [30, 51]</u>	<u>Property at macro scale [30, 51]</u>	<u>Property at Nano scale [30, 51]</u>
Glass	Shatters	Flexible such as spaghetti
Steel	Hard	Malleable such as cheese
Diamond	Extremely hard	Rubbery, Spongy
Platinum and gold	Metal, Inert, Unreactive	Chemical catalyst
Silver	Metal	Bioactive
Aluminium		Combust, can be fuel
Carbon	Soft, malleable	Stronger then steel

1.5 Nanoscience, Nanotechnology and Nanomaterial

The capacity to control, synthesise and design materials in the nanometric scale (10^{-9} m) features one of the main progress directions to use those materials for the development of their new applications [31]. “These are all manufacturable dimensions today [29]”. Nanoscience and nanotechnology are defined as below [33, 39-42].

“Nano science is the study of phenomenon and manipulation of materials at atomic, molecular and supra-molecular scales, where the properties significantly differ from those at a larger scale” [39, 43]. “Nanotechnologies are the design, characterisation, production and application of structural devices and systems by controlling shape and size at the nanometre scale” [39, 43, 44]. Norio Taniguchi in 1974 used word ‘nanotechnology’ to refer the ability of engineering materials precisely at the nanometre level [42, 45]. In 1959, Richard Feynman in 1959 [46] discussed about possibility of rearranging the atoms, in his lecture ‘There’s plenty of room at the bottom’. Feynman in 1959 [46] said that we can hardly doubt that when we have some control of the arrangement of things on a small scale we will get an enormously greater range of possible properties that substances can have and of different things that can we do.

Nano science is interdisciplinary science between physics, chemistry, biology, engineering. The “nanotechnology tree” in reference number [47] demonstrates the interdisciplinary nature of nano science.

1.6 Nanomaterials

“There is a diversity of definitions. The US definition is that “at least one dimension of a nanoparticle or the relevant length scale of an exploited phenomenon must lie between 1 and 100 nanometres (nm)” [29, 30] British thinkers defines “the nanotechnological ranges between 0.2 and 100 nm”[29]. In the ISO standard “nano materials are split into “nano-objects” (having any external dimension on the nano scale) and “nanostructured materials” (having internal structure or surface structure on the nano scale)” [31]. Nanomaterial [32] is the ‘building blocks’ of nanotechnology [33]. Nano fibres, nanotubes/rods, nanoparticles etc. are examples of nano structuring. Considering dimensions, nano materials can be divided as below [13]:

Nanoparticles (3 dimensional particulates- spherical, granular, crystalline)

Nanotubes (2 nano dimensions and 3rd higher dimension – nanotubes etc.)

Nano layers (one dimensional – nano layers. sheets/flake etc.)

The reasons for the superior performance of nano sized fillers are high volume ratio, lower or fewer impurities (so more purity) [13]. Particles with smaller dimensions can disperse more homogeneously in to polymer matrix [34]. Nanoparticles can associate into extended structures which dominate the rheological, viscoelastic and mechanical properties of the nano composites.

1.6.1 Engineered Nanomaterial

Nanotechnology gives ability to engineer/tailor materials, structures, devices, systems of desired, altered functionalities at molecular/supra-molecular level compared to the same material at non-nano form [43]. Evolving definitions of ENMs are [48] as below:

“Materials meeting the following criteria are ENMs:

- Consist of particles, with one or more external dimensions in the size range 1nm-100nm, for more than 1% of their number size distribution.
- Have internal or surface structures of one or more dimensions in the size range 1 nm-100 nm [49, 50].
- Has a specific surface area by volume ratio greater than $60 \text{ m}^2/\text{cm}^3$, excluding particles with a size lower than 1 nm [48].

Som et al (2011)[49] discussed use of ENM for enhancing textile properties.

1.6.2 Composites and Nano Composites

In composite materials “one or more distinctive components dispersed in a continuous matrix”. The size of the reinforcement in composite material is reduced from macro, meso, micro to nano dimension over a period of time [56]. The use of nano reinforcement in polymer composites improves mechanical properties in some cases up to 1000% [16]. “Nano structured composites can produce and or enhance multifunctionality in ways that conventional composites could not” [16]. "Nano composite" is defined as a composite in which the distinctive component, or Gibbsian solid phase, is in the nanometre range. Nano composites are formed by blending nano fillers of different materials with different dimensions and shapes (nanotubes, flakes, clays, spherical etc.) with the material/polymer matrix. [53]. Nano composites are the composite with at least one nano dimensional fillers. Gibson et al (2010)[16] gave a few examples in his review article and stated that nano structured composites can enhance multifunctionality of material properties compared to conventional composites. Gibson [16] also commented that tensile strength increased with decrease in particle sizes in both micron and nano ranges as long as agglomeration is avoided ‘and even mechanical performance of nano sizes reinforcement is superior to its micronized counterpart’.[55]. The accepted length for the nano phase is less than 100 nm in at least one dimension. The continuous matrices can be ceramic, metallic or organic materials, either in bulk form or as thin films [54][57]. Addition of nanoparticles in nano composite enhanced / changed various properties such as glass transition temperature, crystallization time, stiffness, electrical conductivity, UV adsorption, strength, antimicrobial property, abrasion property [58]. The morphology of nanoparticles (i.e. specific geometrical dimensions, aspect ratios) influences final nanocomposite properties. The morphology of nanofiller can be layered, spherical, circular [53]. Hybrid composite materials are formed using nano sized fillers as well as conventional micro scale fibre or particle reinforcements [16].

The main filler characterization are given by

- Chemical composition
- Shape (often characterise by aspect ratios-spherical, rods, fillers etc.
- Mean particle diameter, size distribution, largest diameter, hardness, density
- Particle surface properties (surface area, surface energy)

1.7 How to Manufacture Nano Materials

Nano materials/ nano structures manufacturing process can be broadly categorized into two approaches “top up” and “bottom up” with different quality, productivity and cost involves (Figure 1:5).

In the bottom up approach, the material is built from molecule to macro form. The material is made atom by atom or molecule by molecule. Bottom up approach is broadly splitted into 3 categories: chemical synthesis, self-assembly and positional assembly [42].

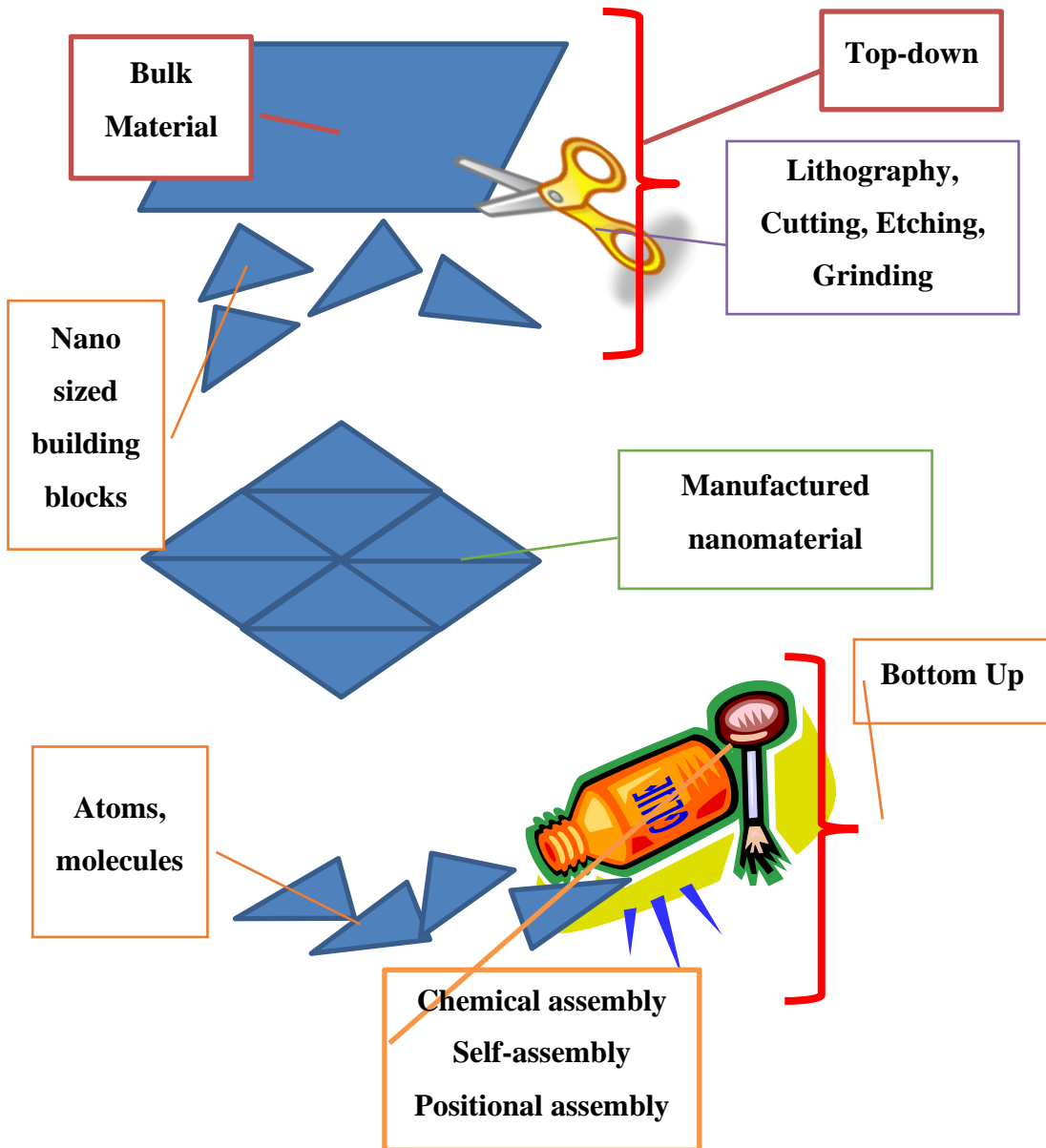


Figure 1:5 Principle of Top-down and Bottom-up approach

- In chemical synthesis, molecules, particulates are produced. These raw materials are used to make products in their bulk disordered form or ordered form.
- In self-assembly, atoms or molecules are arranged in order themselves by physical or chemical interaction between units. (e.g. Salt, crystals, snowflakes)[43]. Bottom

or collector) is connected to positive or negative supply. The other (collector or solution) is connected to opposing supply or neutral / earth to create an electric field. Direct current (DC) power supply is usually used for electrospinning although the use of Alternating current (AC) potential is also feasible [33, 35]. The solution in droplets becomes charged as the voltage is increased. The same charge generates Coulombic repulsions among the solution ions. The higher voltage causes the droplet to elongate, due to same charges. As the applied voltage increases, the droplet shape changes from round to elongated shape. This shape is called “Taylor cone”. As the applied voltage increased, the electrical forces oppose the surface tension. At a critical voltage V_c , the applied voltage overcomes the surface tension. At V_c , due to Coulombic repulsions the solution jet emerges from the droplet. The jet travels towards the collector in the influence of Coulombic force and electrical force between solution and collector. The jet splits and stretches due to Coulombic and electrical forces. The jet travels towards the collector in a chaotic and zigzag motion due to high voltage, the jet become thinner in its path towards the collector. The solution jet either dries out or remains semi wet before it reaches the Collector, the jet forms electropun nano fibres on the collector.

Bubble electrospinning

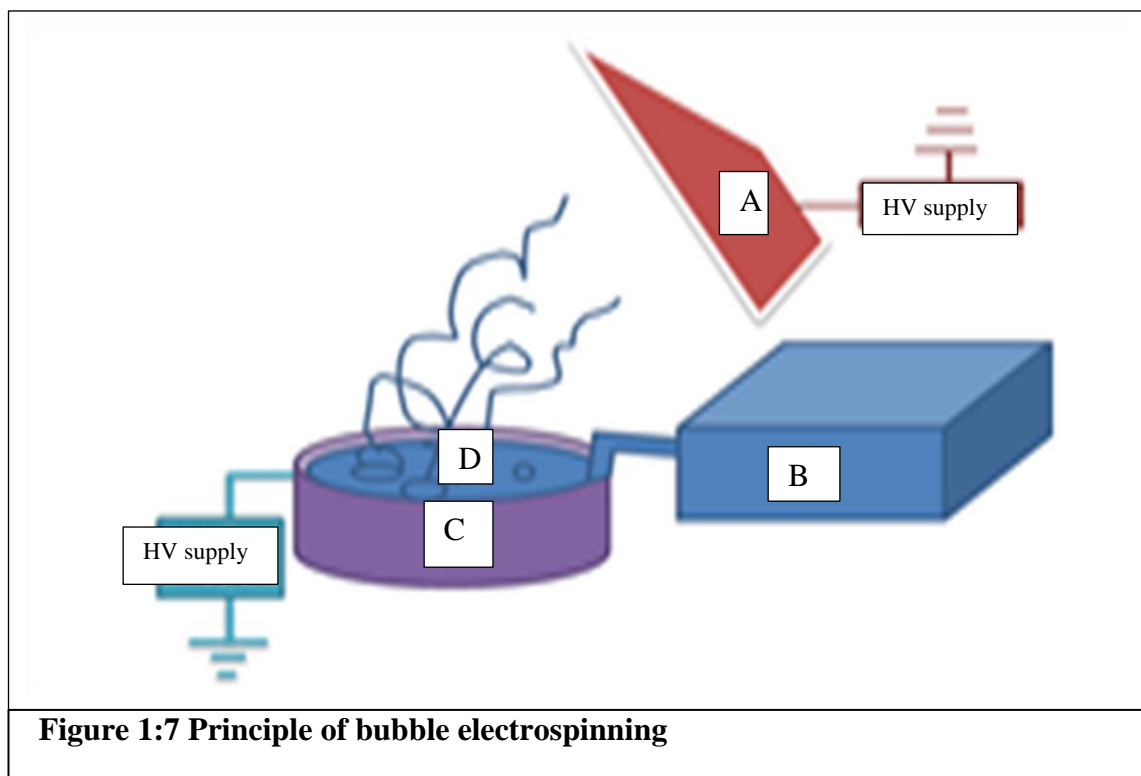


Figure 1:7 Principle of bubble electrospinning

In BE electrospinning,(Figure 1:7)a compressor (B)(B100SEC, Charles Austen Pumps Ltd.) was used to generate compressed air (0.7) bar pressure).

The compressed air was passed through a 15% EC solution reservoir (C) by a 0.8mm inner diameter tube. A high voltage supply (Glassman, MK35P2.0-22, U.S.A.) was

connected to 15% EC solution. The potential difference between bubble and collector generated multiple fibre forming jets, which are collected on the collector (A).

1.8 Limitations in Nanotechnology

Nanotechnology/science and nano materials are still at emerging stage and their positive effects and negative effects are still under investigation [60].

- Knowledge about the effect of ENMs on environment and human health is still unknown [61].
- Material rules at macro and micro level are not always the same and valid for nano domain as well in all circumstances [62].
- Probably there is a need to develop specific methods to study ENMs, which may be different at macro and micro materials [63].
- Theoretical hypotheses are needed to be developed for predicting material behaviour, property, and characteristics at nano scale.
- Data about material performance, hazards [64] are still not well established so effect of size, shape, surface functionality are relatively unknown at the nano scale [65].
- There are several ways of nanoparticle entry into human / animal bodies:-inhalation, ingestion, absorbance through skin, injection. Effect of nanoparticles by any of this method of entry in to human body needs further studies [66]. The mechanisms of nanoparticles on health outcome are still not well known [52, 67].
- Direct or indirect and short term as well as long term impact on environment, needs study in detail [68] Effect of nanoparticles on mass pollution [69], nanoparticle release rate and reaction rate with air, water.
- The boundaries/definitions of macro, micro, nano are not very clear.
- There are not enough data to make effective models/theoretical schemes to predict nano material behaviour.

1.9 Characterization of Nano Materials

Nanomaterial characterization is very important as nanomaterial properties can change with change in size, surface or structure of the material. These parameters not only affect functionality and property of the material but also the hazardous effects of them. It is very important to make nano materials with desired functional property with low/negligible hazard effect.

Nanoparticle size (i.e. diameter, length, width etc.) can affect various parameters such as change in melting temperature and glass transition temperature, toxicity for e.g. 2

(nanometer) nm gold particles melt at 650K and 6nm melts at 1150K. Toxicity of TiO₂ depends on particle size [64, 70].

Material properties depends on surface characteristics such as surface chemistry, surface charge, morphology, functionality, roughness, contamination for e.g. greater surface area with same surface chemistry will be more reactive [64, 70].

Material structural properties such as shape (fibre, tubes, spheres, cubes, cylinders, horns, rings etc), porosity, chemical composition, crystal structure, aggregation can affect nanoparticle properties for e.g. the cytotoxicity and bioactivity of carbon materials (carbon nanotubes, fluorescence, graphene, graphite etc.) depends on their geometry [64].

1.10 Thesis Aims and Objectives

The main aim of the thesis is to develop functional, structural and smart materials by different spinning methods and to characterise the material properties. The aims and objectives are divided in to 4 points as below.

- 1) To develop functional nanofibres by needle electrospinning
 - A) Specifically to investigate nano fibre formation from manuka honey by needle electrospinning. Manuka honey is a natural material and it is mainly consumed as food, medicine or beauty care product. Honey is consumed as liquid or powder. So, the fibrous form will widen the usage of manuka honey.
 - B) To study effect of different electrospinning parameters on the manuka honey fibre morphologies.
 - C) To study effect of different solution parameters on the manuka honey fibre morphologies.
 - D) To characterise the manuka honey electrospun mat.
 - E) To study the antibacterial property of manuka honey electrospun mat.

Manuka honey electrospun fibres can be used for different area such as medical, packaging, cosmetics.

- 2) To develop different electrospun fibrous morphologies by needle electrospinning.
 - A) Specifically to understand formation of ethylcellulose fibrous morphologies by needle electrospinning. Ethylcellulose is widely used in pharmaceutical industries.
 - B) To study effect of solvent combinations and proportions on the formation of ethylcellulose fibres. In the above study 1, effect of solution and electrospinning parameters on the fibre morphology is going to be studied. In study 2, the effect of solvent system on the electrospun fibre morphology will be studied. Fibre

functionality not only depends on chemical structure but it also depends on its shape. The enduse of the fibre is decided by its size and shape (morphology).

C) To characterise the ethylcellulose electrospun mat

Ethylcellulose nano fibres can be used for various applications in pharmaceuticals, for drug release, for food applications.

3) To develop different fibre morphologies by bubble electrospinning

A) To understand formation of different ethylcellulose fibrous morphologies by bubble electrospinning. In previous two studies, nano fibres will be produced by needle electrospinning. But needle electrospinning has drawbacks such as low productivity, needle clogging, limited width, uniform fibre density per cross section across the fabric width. Recently, needle-less electrospinning methods such as bubble electrospinning were developed to overcome above problems. It is important to develop different morphology of electrospun fibres by changing different bubble electrospinning parameters.

B) To study effect of different parameters on the morphology of bubble electrospun ethyl cellulose fibres

C) To characterise bubble electrospun ethylcellulose fibres

D) To compare morphologies of bubble electrospun and needle electrospun ethyl cellulose fibres.

4) To produce smart fibres by melt spinning process in order to understand processability by melt electrospinning.

A) To develop thermo sensitive polypropylene by melt extrusion. In order to develop smart thermochromic fibres by meltelectrospinning, thermochromic polypropylene filaments will be developed by meltspinning. It is very important to study processability of thermochromic material by melt spinning. Thermochromic material is very sensitive to heat and shear, so there are chances of damage to the thermochromic materials while melt processing. The same melt spinning process parameters can be used for melt electrospinning, if thermochromic fibres can be successfully melt spun.

B) To evaluate the thermochromic effect of the filament

C) To characterise thermochromic filament

Thermochromic filament can be used as sensor, fashion and design material.

The research objectives, findings, conclusions are presented in nine chapters as described below.

1.11 Thesis Layout,

Chapter 1. Materials and Its Processing at Macro to Nano Dimensions

The introduction and literature reviews were covered partly in chapter 1 and chapter 2. In chapter 1, fibre spinning methods are described with schematic diagrams.

Chapter 2. Nanofibres and Principles of Electrospinning

In chapter 2, the main emphasis was on electrospinning. The effect of various parameters on electrospun fibre morphology and advances in electrospinning are also discussed in chapter 2.

Chapter 3. Experimental and Testing Techniques in Details

Chapter 3 is focused on the description of the instruments used to manufacture, characterise spinning solutions and fibres. Principles of viscosity meter, conductivity meter, surface tension meter, ATR-Fourier transform infrared spectroscopy (ATR-FTIR) and ultra violet-visible spectroscopy is also described in details. Fibre characterisation methods such as scanning electron microscopy (SEM), X-ray diffraction (XRD), ATR-FTIR, tensile testing machine are also described in chapter 3.

Chapter 4. Investigation, Formation and Characterisation of Manuka Honey Nano Fibres and its Antibacterial Properties for Wound Healing

Manuka honey (MH) is well known due to its unique antibacterial property called unique Manuka factor (UMF). Higher the UMF better is the antibacterial property. Honey is utilised mainly in liquid or dry powder form. Honey is applied on wound in its liquid form. It would be more beneficial, if honey can be converted to nano fibrous form. Honey fibres can be applied directly on wound without need of gauge. Not only that fibrous material with honey can be used for packaging as well as cosmetics.

100% MH cannot be electrospun due to its viscoelastic properties. The objective of the present work was to electrospin Manuka honey in to nanofibres and maintains its antibacterial properties. MH has been successfully electrospun from aqueous solution by blending with poly ethylene oxide (PEO). PEO was used as matrix to form fibres from MH in the present study. PEO is non-toxic and biocompatible polymer. Different properties of Manuka honey (MH) – PEO (MHPEO) solution properties such as surface tension, viscosity, electrical conductivity and Ultra Violet-visible spectroscopy were measured. Effect of various parameters such as MH concentration, applied voltage, needle to collector distance (NTCD), feed rate on MHPEO fibre morphology was studied. The interaction between Manuka honey and PEO has been established by FTIR

and DSC. The morphological properties of the electrospun fibre mats have further shown that smooth, thicker and merged fibres were obtained with higher MH proportion and high feed rate. Thin, less merged fibres were obtained with long NTCD and high applied voltage. The antibacterial property of the Manuka honey-PEO has been studied. 50% and 65% MHPEO with 100% MH showed antibacterial property.

Chapter 5. Investigating the Electrospinning of Ethylcellulose

The fibre morphology is important for its enduse. The size and the shape of the fibres decide its enduse i.e. adds functionality to final fibres. The fibre morphologies are affected by various parameters in electrospinning. The objective of the work in this chapter was to investigate the formation of different fibre morphologies using different solvent system on the electrospun fibre morphology. The selection of desirable solvent or solvent system for a particular polymer is very important for the optimisation of electrospinning. Ethylcellulose is used as polymer in the present work. Ethyl cellulose (EC) is a cellulosic polymer and it is widely used in the drug industry. In the present work, 15% (wt./wt.) EC was electrospun with the solvent systems of toluene and ethanol in different ratios (100:0, 60:40, 50:50, 40:60, 0:100). The viscosity and surface tension showed major effects on the EC fibre morphology and formation of beads. Electrospinning was carried at different voltages and NTCD. The effects of different solvent ratios (ethanol: toluene) on morphology and/or size of the electrospun fibres were investigated by scanning electron microscopy (SEM). Electrospinning of 15% w/w EC solutions in 100% ethanol produced round shaped irregular beaded fibres. The shape of bead changed from elongated irregular shape to elongated shaped smooth bead as ethanol proportion reduced from 60% to 50% in solvent. 15% EC in toluene: ethanol (60:40) toluene: ethanol produced smoother and almost bead-less fibres. The 15% EC in toluene produced thick, smooth and bead-less fibres. Different properties of the EC mats were tested by DSC, FTIR etc.

Chapter 6. The Case of Bubble Electrospinning of Ultrafine Fibres

In chapter 4 and 5 production of Manuka honey and ethylcellulose nanofibres was done by single needle electrospinning method. Needle electrospinning systems (single or multiple) are not suitable for industrial scale production due to their limitations such as needle clogging. Bubble electrospinning (BE) is one of the new needle-less concepts developed for industrial scale production. Much more work is done on parameter optimisation in case of needle electrospun fibre, but needle-less electrospinning methods still lacks optimization of parameters [71]. In the present study EC fibres were

produced by bubble electrospinning. We studied the effect of applied voltage and solution surface to collector distance on the electrospun fibre morphology. In case of SNE, we can control feed rate, but in BE feed rate entirely depends on number and size of bubbles produced, which is unpredictable and entirely depends on various parameters such as compressed air force, hose pipe diameter, and hose pipe depth in reservoir etc. We found an increase in fibre diameter with an increase in distance. In BE, as applied voltage increased initially, the fibre diameter decreased but then started increasing with increasing applied voltage. The reasons for this behaviour are explained.

Chapter 7. Development and Characterisation of Thermochromic Polypropylene Filament Yarn

In chapter 4, 5 and 6 electrospinning methods used were based on solution by solvent system. Certain polymers and materials degrade or are not easily dissolved in common solvents, e.g. Thermochromic pigments can be damaged in most solvent systems. So it is very important to find out an alternative method to produce thermochromic nano fibres. In that case melt-electrospinning is another method, which could be used for the production of thermoplastic polymers. In order to develop melt-electrospinning, it is very important to study processing of thermochromic polypropylene by meltspinning.

In the present work, thermochromic polypropylene mono filaments were melt spun using a Lab spin Screw Extruder with water cooling. It is very important to use screw extruder to blend polypropylene and thermochromic pigment. Similar feeding mechanism can be used for melt-electrospinning. Hence, it is very important to understand effect of different parameters (temperature, shear stress, pressure etc) on fibre morphology.

In the present work, pure polypropylene filament and thermochromic polypropylene filament were produced with the same parameters. Both the filaments were studied and compared at various properties. Visual observation suggests uniform distribution of pigments in the polypropylene matrix. The colour change was gradual from blue to colourless above approximately 37°C. When cooled, the colour reversed back again to the original colour. SEM images suggest smoother surface for polypropylene compared to thermochromic polypropylene. The thermochromic pigments contributed in the formulation of rougher thermochromic filament surface. The maximum load value was found higher in polypropylene, and the elongation value was found higher in the thermochromic filament. The low strength of thermochromic filament is due to size, shape and distribution of the thermochromic pigment in the polypropylene. The DSC

results showed two endothermic peaks for the thermochromic bead. The lower endothermic peak suggests activation temperature. The thermochromic filament showed three endothermic peaks, the third endothermic peak is due to polypropylene. The XRD results have found all peaks of polypropylene and also the peak of the thermochromic pigment.

Chapter 8. End uses and Future Work

This chapter deals with the possible scope of the extension of the present work. The chapter also states the possible end use of the developed fibres in the present work.

Chapter 9. Conclusion

This chapter deals with the summary of the work and conclusion of the present work.

1.12 Bibliography

- [1.1] G. B. Olson, "Beyond Discovery: Design for a New Material World," *Calphad*, vol. 25, pp. 175-190, 2001.
- [1.2] M. Manoharan, "Research on the frontiers of materials science: The impact of nanotechnology on new material development," *Technology in Society*, vol. 30, pp. 401-404, 2008.
- [1.3] E. Karana, P. Hekkert, and P. Kandachar, "Material considerations in product design: A survey on crucial material aspects used by product designers," *Materials & Design*, vol. 29, pp. 1081-1089, 2008.
- [1.4] S. M. Sapuan, "A knowledge-based system for materials selection in mechanical engineering design," *Materials & Design*, vol. 22, pp. 687-695, 2001.
- [1.5] D. Pasini, "Shape transformers for material and shape selection of lightweight beams," *Materials & Design*, vol. 28, pp. 2071-2079, 2007.
- [1.6] L. A. Dobrzański, "Significance of materials science for the future development of societies," *Journal of Materials Processing Technology*, vol. 175, pp. 133-148, 2006.
- [1.7] W. Brostow, "Instruction in materials science and engineering: modern technology and the new role of the teacher," *Materials Science and Engineering: A*, vol. 302, pp. 181-185, 2001.
- [1.8] M. F. Ashby, Y. J. M. Bréchet, D. Cebon, and L. Salvo, "Selection strategies for materials and processes," *Materials & Design*, vol. 25, pp. 51-67, 2004.
- [1.9] L. Y. Ljungberg, "Materials selection and design for development of sustainable products," *Materials & Design*, vol. 28, pp. 466-479, 2007.

- [1.10] M. C. Flemings and R. W. Cahn, "Organization and trends in materials science and engineering education in the US and Europe," *Acta Materialia*, vol. 48, pp. 371-383, 2000.
- [1.11] Y. Li, "Predicting materials properties and behavior using classification and regression trees," *Materials Science and Engineering: A*, vol. 433, pp. 261-268, 2006.
- [1.12] F. Ashby, *Materials Selection In Mechanical Design*: Elsevier Butterworth-Heinemann, 2005.
- [1.13] K. Chrissafis and D. Bikiaris, "Can nanoparticles really enhance thermal stability of polymers? Part I: An overview on thermal decomposition of addition polymers," *Thermochimica Acta*, vol. 523, pp. 1-24, 2011.
- [1.14] Z. L. Wang and Z. C. Kang, *Functional and smart materials-Structural evolution and structure analysis* 1ed. Plenum Publishing Corp., Attn: Dept. M99-95, 233 Spring Street, New York, NY 10013-1578: Plenum Press, 1998.
- [1.15] R. W. Cahn, *The Coming of Materials Science* vol. 5. Department of Materials Science and Metallurgy, University of Cambridge, Cambridge, UK Elsevier Science, 2001.
- [1.16] R. F. Gibson, "A review of recent research on mechanics of multifunctional composite materials and structures," *Composite Structures*, vol. 92, pp. 2793-2810, 2010.
- [1.17] M. S. Scholz, J. P. Blanchfield, L. D. Bloom, B. H. Coburn, M. Elkington, J. D. Fuller, M. E. Gilbert, S. A. Muflahi, M. F. Pernice, S. I. Rae, J. A. Trevarthen, S. C. White, P. M. Weaver, and I. P. Bond, "The use of composite materials in modern orthopaedic medicine and prosthetic devices: A review," *Composites Science and Technology*, vol. 71, pp. 1791-1803, 2011.
- [1.18] S. B. Warner, *Fibre science*: Prentice Hall, 1995.
- [1.19] R. B. Seymour and C. E. Carraher, *Structure-property relationships in polymers*: Plenum Press, 1984.
- [1.20] S. Eichhorn, J. W. S. Hearle, and T. Kikutani, *Handbook of Textile Fibre Structure, Volume 2: Natural, Regenerated, Inorganic, and Specialist Fibres*: Taylor & Francis, 2009.
- [1.21] S. Eichhorn, *Handbook of Textile Fibre Structure, Volume 1: Fundamentals and Manufactured Polymer Fibres*: Taylor & Francis, 2009.
- [1.22] S. P. Mishra, *A Text Book of Fibre Science and Technology*: New Age International, 2000.

- [1.23] Z. Zhang and K. Friedrich, "Artificial neural networks applied to polymer composites: a review," *Composites Science and Technology*, vol. 63, pp. 2029-2044, 2003.
- [1.24] M. A. Ahmed, M. Iqbal, J. Mughal, and A. Moiz. (2009, 23/09/12). *Textile Fibres*. Available: <http://www.fibre2fashion.com/industry-article/23/2267/textile-fibres1.asp>
- [1.25] H. L. Needle, *Textile Fibres, Dyes, Finishes, and Processes: A Concise Guide*: Noyes Publications, 1986.
- [1.26] L. Y. Ljungberg, "Materials selection and design for structural polymers," *Materials & Design*, vol. 24, pp. 383-390, 2003.
- [1.27] J. G. Cook, *Handbook of Textile Fibres: Volume 2: Man-Made Fibres*, 5 ed.: Woodhead Publishing, 1984.
- [1.28] W. Klein, *Man-made fibres and their processing* vol. 6. Manchester, UK.: The textile institute, 1994.
- [1.29] D. Munshi, P. Kurian, R. V. Bartlett, and A. Lakhtakia, "A map of the nanoworld: Sizing up the science, politics, and business of the infinitesimal," *Futures*, vol. 39, pp. 432-452, 2007.
- [1.30] M. A. Van Hove, "From surface science to nanotechnology," *Catalysis Today*, vol. 113, pp. 133-140, 2006.
- [1.31] R. Hischer and T. Walser, "Life cycle assessment of engineered nanomaterials: state of the art and strategies to overcome existing gaps," *Sci Total Environ*, vol. 425, pp. 271-82, May 15 2012.
- [1.32] Z. L. Wang, *Characterization of nanophase materials*. the University of Michigan: Wiley-VCH, 2000.
- [1.33] W. Yang, J. I. Peters, and R. O. Williams, 3rd, "Inhaled nanoparticles--a current review," *Int J Pharm*, vol. 356, pp. 239-47, May 22 2008.
- [1.34] D. Bikiaris, "Can nanoparticles really enhance thermal stability of polymers? Part II: An overview on thermal decomposition of polycondensation polymers," *Thermochimica Acta*, vol. 523, pp. 25-45, 2011.
- [1.35] S. K. Sahoo, S. Parveen, and J. J. Panda, "The present and future of nanotechnology in human health care," *Nanomedicine*, vol. 3, pp. 20-31, Mar 2007.
- [1.36] R. Owen and M. Depledge, "Nanotechnology and the environment: risks and rewards," *Mar Pollut Bull*, vol. 50, pp. 609-12, Jun 2005.

- [1.37] T. Fleischer and A. Grunwald, "Making nanotechnology developments sustainable. A role for technology assessment?," *Journal of Cleaner Production*, vol. 16, pp. 889-898, 2008.
- [1.38] G. A. Silva, "Introduction to nanotechnology and its applications to medicine," *Surg Neurol*, vol. 61, pp. 216-20, Mar 2004.
- [1.39] A. P. Dowling, "Development of nanotechnologies," *Materials Today*, vol. 7, pp. 30-35, 2004.
- [1.40] F. Sanchez and K. Sobolev, "Nanotechnology in concrete – A review," *Construction and Building Materials*, vol. 24, pp. 2060-2071, 2010.
- [1.41] M. J. Pitkethly, "Nanomaterials – the driving force," *nanotoday*, vol. 7, pp. 20-29, 2004.
- [1.42] Anon. (2004). *Nanoscience and nanotechnologies: opportunities and uncertainties*. Available: <http://www.nanotec.org.uk/finalReport.htm>
- [1.43] A. Cockburn, R. Bradford, N. Buck, A. Constable, G. Edwards, B. Haber, P. Hepburn, J. Howlett, F. Kampers, C. Klein, M. Radomski, H. Stamm, S. Wijnhoven, and T. Wildemann, "Approaches to the safety assessment of engineered nanomaterials (ENM) in food," *Food Chem Toxicol*, vol. 50, pp. 2224-42, Jun 2012.
- [1.44] J. Y. R. Ying, *Nanostructured Materials*: Academic, 2001.
- [1.45] V. Uskoković, "Nanotechnologies: What we do not know," *Technology in Society*, vol. 29, pp. 43-61, 2007.
- [1.46] R. Feynman, "There's plenty of room at the bottom," *Resonance: Journal of Science Education*, vol. 16, p. 890, 2011.
- [1.47] J. Corbett, P. A. McKeown, G. N. Peggs, and R. Whatmore, "Nanotechnology: International Developments and Emerging Products," *CIRP Annals - Manufacturing Technology*, vol. 49, pp. 523-545, 2000.
- [1.48] V. J. Morris, "Emerging roles of engineered nanomaterials in the food industry," *Trends Biotechnol*, vol. 29, pp. 509-516, 2011.
- [1.49] C. Som, P. Wick, H. Krug, and B. Nowack, "Environmental and health effects of nanomaterials in nanotextiles and façade coatings," *Environment International*, vol. 37, pp. 1131-1142, 2011.
- [1.50] K. Savolainen, L. Pylkkänen, H. Norppa, G. Falck, H. Lindberg, T. Tuomi, M. Vippola, H. Alenius, K. Hämeri, J. Koivisto, D. Brouwer, D. Mark, D. Bard, M. Berges, E. Jankowska, M. Posniak, P. Farmer, R. Singh, F. Krombach, P. Bihari, G. Kasper, and M. Seipenbusch, "Nanotechnologies, engineered nanomaterials and occupational health and safety – A review," *Safety Science*, vol. 48, pp. 957-963, 2010.

- [1.51] A. Nasir, "Nanotechnology and dermatology: part I--potential of nanotechnology," *Clin Dermatol*, vol. 28, pp. 458-66, Jul-Aug 2010.
- [1.52] N. Staggers, T. McCasky, N. Brazelton, and R. Kennedy, "Nanotechnology: the coming revolution and its implications for consumers, clinicians, and informatics," *Nurs Outlook*, vol. 56, pp. 268-74, Sep-Oct 2008.
- [1.53] P. Bordes, E. Pollet, and L. Avérous, "Nano-biocomposites: Biodegradable polyester/nanoclay systems," *Progress in Polymer Science*, vol. 34, pp. 125-155, 2009.
- [1.54] N. Fedullo, E. Sorlier, M. Sclavons, C. Bailly, J.-M. Lefebvre, and J. Devaux, "Polymer-based nanocomposites: Overview, applications and perspectives," *Progress in Organic Coatings*, vol. 58, pp. 87-95, 2007.
- [1.55] H. D. Wagner and R. A. Vaia, "Nanocomposites: issues at the interface," *Materials Today*, vol. 7, pp. 38-42, 2004.
- [1.56] B. Fiedler, F. H. Gojny, M. H. G. Wichmann, M. C. M. Nolte, and K. Schulte, "Fundamental aspects of nano-reinforced composites," *Composites Science and Technology*, vol. 66, pp. 3115-3125, 2006.
- [1.57] Z. L. Wang, Y. Liu, and Z. Zhang, *Materials Systems and Applications II* vol. IV: Kluwer academic / Plenum publishers, 2002.
- [1.58] D. R. Paul and L. M. Robeson, "Polymer nanotechnology: Nanocomposites," *Polymer*, vol. 49, pp. 3187-3204, 2008.
- [1.59] J. Jancar, J. F. Douglas, F. W. Starr, S. K. Kumar, P. Cassagnau, A. J. Lesser, S. S. Sternstein, and M. J. Buehler, "Current issues in research on structure–property relationships in polymer nanocomposites," *Polymer*, vol. 51, pp. 3321-3343, 2010.
- [1.60] T. Nikulainen and C. Palmberg, "Transferring science-based technologies to industry—Does nanotechnology make a difference?," *Technovation*, vol. 30, pp. 3-11, 2010.
- [1.61] K. Aschberger, C. Micheletti, B. Sokull-Kluttgen, and F. M. Christensen, "Analysis of currently available data for characterising the risk of engineered nanomaterials to the environment and human health--lessons learned from four case studies," *Environ Int*, vol. 37, pp. 1143-56, Aug 2011.
- [1.62] V. Carvelli, C. Corazza, and C. Poggi, "Mechanical modelling of monofilament technical textiles," *Computational Materials Science*, vol. 42, pp. 679-691, 2008.
- [1.63] K. Savolainen, H. Alenius, H. Norppa, L. Pylkkanen, T. Tuomi, and G. Kasper, "Risk assessment of engineered nanomaterials and nanotechnologies--a review," *Toxicology*, vol. 269, pp. 92-104, Mar 10 2010.

- [1.64] G. Morose, "The 5 principles of "Design for Safer Nanotechnology", " *Journal of Cleaner Production*, vol. 18, pp. 285-289, 2010.
- [1.65] A. D. Maynard, "Nanotechnology: assessing the risks," *Nano Today*, vol. 1, pp. 22-33, 2006.
- [1.66] C.-F. Chau, S.-H. Wu, and G.-C. Yen, "The development of regulations for food nanotechnology," *Trends in Food Science & Technology*, vol. 18, pp. 269-280, 2007.
- [1.67] D. Parr, "Will nanotechnology make the world a better place?," *Trends Biotechnol*, vol. 23, pp. 395-8, Aug 2005.
- [1.68] V. Türk, C. Kaiser, and S. Schaller, "Invisible but tangible? Societal opportunities and risks of nanotechnologies," *Journal of Cleaner Production*, vol. 16, pp. 1006-1009, 2008.
- [1.69] A. Seaton and K. Donaldson, "Nanoscience, nanotoxicology, and the need to think small," *The Lancet*, vol. 365, pp. 923-924, 2005.
- [1.70] M. Alcoutlabi and G. B. McKenna, "Effects of confinement on material behaviour at the nanometre size scale," *Journal of Physics: Condensed Matter*, vol. 17, pp. R461-R524, 2005.
- [1.71] H. Niu, X. Wang, and T. Lin, "Needle electrospinning: influences of fibre generator geometry," *Journal of the Textile Institute*, pp. 1-8, 2011

Chapter 2 : Nano Fibres and Principles of Electrospinning

2.1 Introduction

The prefix ‘Nano’ is a Greek word meaning ‘dwarf’ and in the scientific content denotes the one billionth part (10^{-9}) of an entity[1, 2]. Nanotechnology is an emerging interdisciplinary technology. The fundamental of nanotechnology lie in the fact that properties of substances changes when their size is reduced to nanometer range [3]. The combination of high specific surface area, flexibility and superior directional strength makes nano fibres of different types suitable for a wide ranging applications from clothing to reinforcement in aerospace structures [4], filters [5], [6], membranes, tissue engineering[7],wound healing, transportation and drug release[8], also in areas of materials science, mechanics, electronics, optics, medicine, plastics, energy, and electronics[7, 9].

2.2 Methods of Producing Nanofibres

It is impracticable to spin nanofibres by conventional polymer spinning methods such as melt, wet, dry or gel spinning. A number of processing techniques such as drawing, template synthesis, phase separation, self-assembly, electrospinning[10] , centrifugal spinning[11] (Force spinning TM)[12, 13] have been used to produce nanofibres in recent years. Electrospinning has attracted much attention recently due to the versatility [10, 14] and ease with which nanometer diameter fibres can be produced from natural and synthetic polymers [14, 15], ceramics[16–22] or composites[10, 22, 23]. The most important methods of producing nano fibres are discussed briefly in Table 2:1 [13], [24–30].

Table 2:1 Comparison of processing techniques for obtaining nano fibres

Process	Technical advantages	Can the process be scaled?	Repeatability	Convenient to process?	Control on fibre dimensions?	Advantages	Disadvantages
Drawing	Laboratory	x	√	√	x	Minimum equipment requirement, vast material selection, simple method	Discontinuous process, low productivity
Template synthesis	Laboratory	x	√	√	√	Fibres of different diameters can be easily achieved by using different templates	Limitation on fibre dimensions and arrangements
Phase separation	Laboratory	x	√	√	x	Minimum equipment requirement. Process can directly fabricate a nanofibre matrix. Batch to batch consistency achieved easily. Mechanical property of the matrix can be tailored by adjusting polymer concentration.	Limited to specific polymer, lack of control on fibre orientation and arrangement

Chapter 2 : Nano Fibres and Principles of Electrospinning

Self-assembly	Laboratory	x	√	x	x	Good for obtaining smaller nanofibres	Complex process, lack of control on fibre orientation and arrangement
Electrospinning	Laboratory (with potential for industrial processing)	√	√	√	√	Cost effective, long continuous nanofibres can be produced, easy setup, vast materials can be spun, versatile	Jet instability, use of high voltage, often toxic solvents are used
Centrifugal spinning	Laboratory (with potential for industrial processing)					Does not require conductive solution as in electrospinning	
Bacterial cellulose						Low cost , high yield	Limited material selection, lack of versatility for functionalization
Extraction						Natural materials	Limited material selection, limited control of fibre diameter and length
Vapour-						Polymer synthesized directly in	limited control of

Chapter 2 : Nano Fibres and Principles of Electrospinning

phase polymerisation						to nanofibres	fibre diameter and length, limited material selection, complicated process
Kinetically controlled solution synthesis							
Chemical Polymerization of Aniline •							

2.2.1 Drawing

In drawing, nano fibres are produced by drawing polymer solutions [30]. A micro pipette with a few micrometres in diameter was dipped into a droplet (Figure 2:1). The

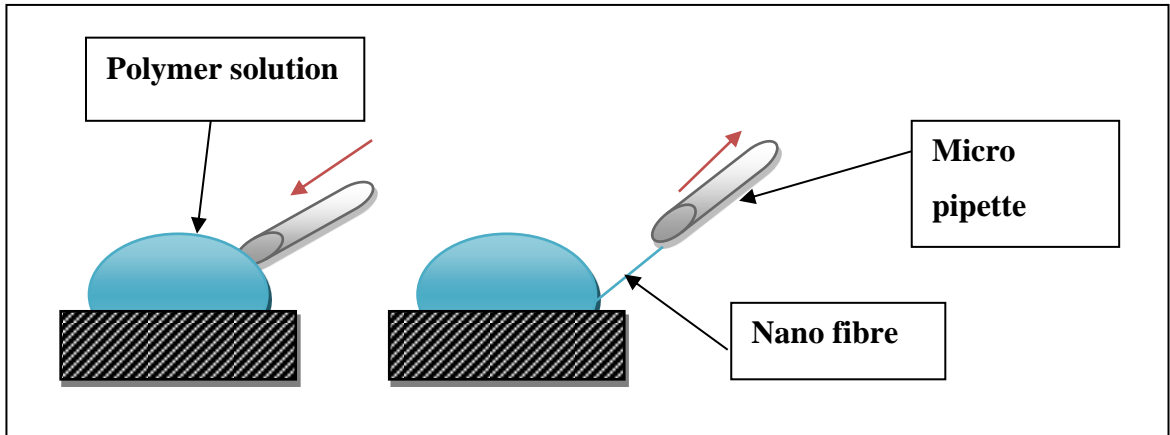


Figure 2:1 Principles of nanofibres by drawing

micro pipette then moved from the liquid at a speed of $1 \times 10^{-4} \text{ ms}^{-1}$, resulting in a nano fibre being pulled. “Drawing a fibre requires a viscoelastic material that can undergo strong deformations while being cohesive enough to support the stresses developed during pulling. The drawing process can be considered as dry spinning at molecular level” [24].

2.2.2 Template Synthesis

In template synthesis polymer solution is extruded by applying pressure on the polymer

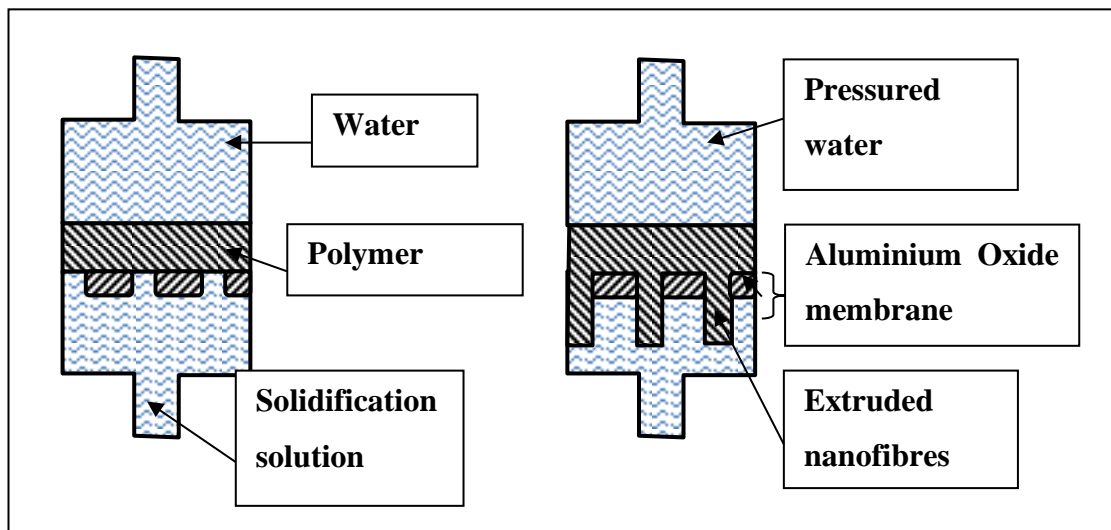


Figure 2:2 Principles of nanofibres by template synthesis

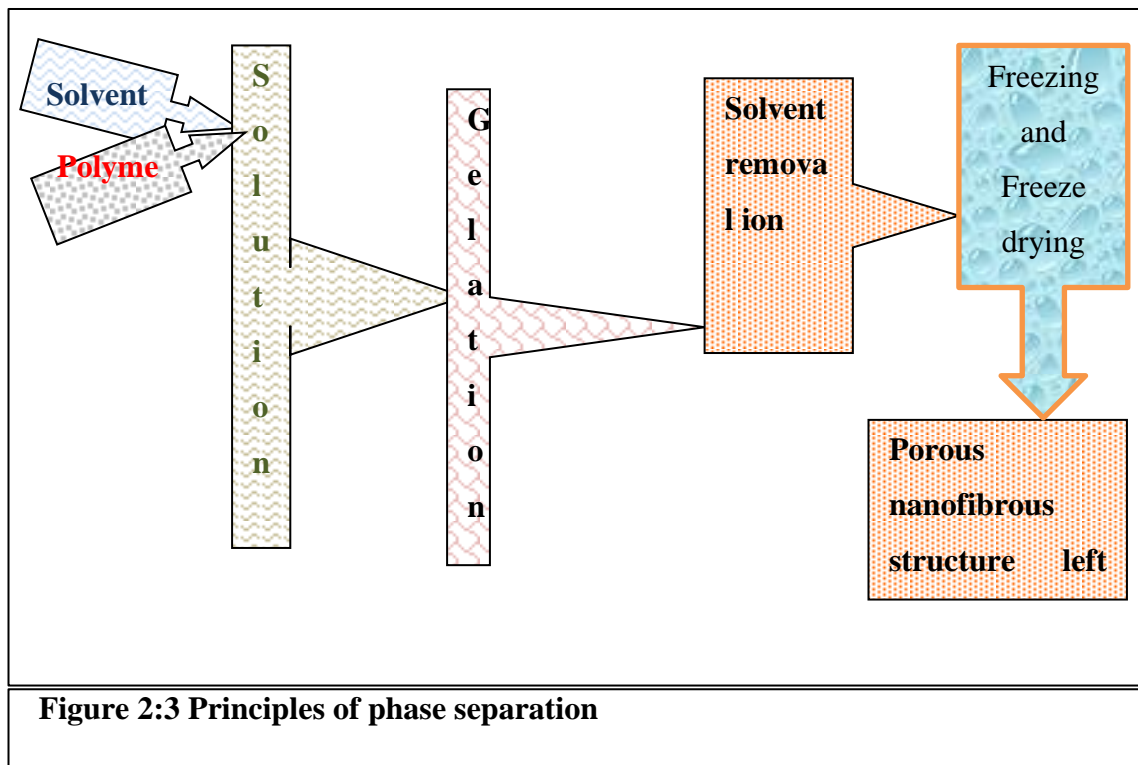
solution. The solution is extruded from template membrane with nanometer sized pores. The polymer solution is forced to extrude through these pores. The extruded solution is exposed to solidifying into nano sized fibres [24] (Figure 2:2).

2.2.3 Self-Assembly

Self-assembly of nano fibres refer to the build-up of nano scale fibres using smaller molecules as basic building blocks. Self-assembly is a process in which individual, pre-existing components organize themselves into an ordered structure required for specific functions without human intervention. The key challenge in self-assembly is to design molecular building blocks that can undergo spontaneous organization into a well-defined pattern that mimic complex biological systems. Self-assembly takes place by non-covalent bonding, which typically includes hydrogen bonding, ionic bonding, water-mediated hydrogen bonding, hydrophilic interaction, and van der Waals interaction. Although each of these forces is rather weak, their collective interactions could produce very stable structure that could closely match the structural features of biological systems through self-assembly [24].

2.2.4 Phase Separation

In phase separation a polymer is firstly mixed with a solvent before undergoing gelation. The main mechanism is the separation of phase due to physical incompatibility. The solvent is then extracted, and the other remaining phase is left behind (Figure 2:3).



In phase separation 5 steps are involved. Raw material dissolution, gelation and phase separation at low freezing temperature, solvent extraction / exchange by immersing in water, freezing, and freeze drying. It takes prolonged time to convert polymer in to nano-fibrous structure. 3D nanostructures without using any sophisticated equipment

can be produced by this method. The scaffold porosity and mechanical properties can be controlled. It is very difficult and perhaps not feasible to maintain fiber orientation [24][30] in phase separation.

2.3 History of Electrospinning

Electrospinning is an old technique. Electric force is an important element of electrospinning, the electric force can accelerate the electrified solution [36]. It was first observed in 1897 by Rayleigh [37], studied in detail by Zeleny (1914) [38, 39] and Sir Taylor in (1964) [37, 40, 41] on electrospraying. Electrospraying and electrospinning are based on the same principle. The solution is charged between the feed mechanism and collector, so the solution is ejected. If the solution has not enough viscoelastic property and chain entanglement, it will be converted into droplets. A jet of low molecular weight breaks up into small droplets, which is a phenomenon termed 'electrospraying' [42-44]. If the solution has enough chain entanglement and viscoelastic properties, it will form a continuous jet. Polymer solution with sufficient chain overlap and entanglements undergoes various instabilities between the capillary tip and the grounded target, which results in thinning of the jet and formation of the submicron scale fibres [45]. This process is known as electrospinning, as already discussed. Critical polymer concentration ' c_{ov} ' can dictate the behavior of electrospraying /electrospinning. This critical concentration is different for each type of polymer – solution. The critical concentration represents the critical chain overlap concentration, where entanglement begins to occur. The polymer concentration ' c ' must be chosen such that a threshold ratio c/c_{ov} is overcome to produce fibres [41]. The process of electrospinning was patented by J.F Cooley [46] in February 1902 and by J. Morton in July 1902 [47]. Further developments toward commercialization were made by Anton Formhals, and described in a sequence of patents from 1934 [48] to 1944[48] for the fabrication of textile yarns. Electrospinning from a melt rather than a solution was patented by C.L Norton in 1936 (U.S. Patent 2,048,651) using an air-blast to assist fibre formation. Sir Geoffrey Ingram Taylor produced the theoretical underpinning of electrospinning; i.e. Taylor Cone [50].

2.4 Theories of The Electrospinning process

The properties of electrospun fibres are due to complex interaction of parameters such as solution rheology, electrical charges, atmospheric parameters and spinning process set up parameters [51]. To understand it properly the process is divided into three stages. Different authors gave different names. e.g. Wang et. al. [52] (2006).

- jet initiation,
- jet elongation with or without branching and/or splitting
- Solidification of jet into nano fibers[53].

Some authors divide it into four stages: [54]

- Base region (the jet emerges)
- Jet region (jet travels)
- Splaying region / Jet thinning region (jet divides in to many jets)
- Collection region

2.4.1 Jet Initiation / Base Region / Taylor Cone Region

The polymer solution/melt always has positive and negative ions. All the ions are in equilibrium, so polymer solutions are electrically neutral. Due to applied voltage (either positive or negative) excessive electrical ions are created (positive or negative depending on applied charge). Once the voltage is applied the ions move between voltage supply and solution. If a negative voltage is applied to the solution, the negative ions will move into solution and a positive charge will move towards voltage supply. In this process excess negative ions will be gathered on the droplet, and the highest charge density will occur at the top of the cone. The Coulombic repulsion among same charged ions increases with higher voltage [51]. With increase in voltage, at a critical voltage V_c the Coulombic repulsions will overcome the surface tension and jet flow initiates.

Figure 2:4 helps to explain the changes in the droplet shape with increase of applied voltage. When the voltage (v) is zero, the solution droplet has a circular shape under the influence of surface tension. The surface tension favours a spherical shape with a smaller surface area. As the voltage is increased, the Coulombic repulsions among solution ions act against surface tension and will charge and change the circular shape of the droplet to a conical shape. The conical shape of the droplet is called “Taylor cone”. Taylor showed that a conical shaped surface, referred to as the Taylor cone, is formed with an angle of 49.3° [50] when a critical potential is reached to disturb the equilibrium of the droplet at the tip of the capillary, that is initiating surface [31] see Figure 2:4. Due to the application of the electric field, a charge is induced on the surface of the droplet. This charge offsets the forces of surface tension and the droplet changes shape from spherical to conical. When the intensity of the electric field (V) attains a certain critical value (V_c), the electrostatic forces overcome the surface tension of the polymer solution and force the ejection of the liquid jet from the tip of the Taylor cone.

The highest charge density is present at the tip of the cone from where the jet is initiated. Taylor showed that V_c (in kilovolts) is given by

$$V_c^2 = 4 (H^2 / L^2) (\ln (2L/R) - 1.5)(0.117 \pi R h)$$

Equation 2:1

Where,

H is the air-gap distance,

L is the length of the capillary tube,

R is the radius of the tube (units: H, L, and R in centimetres) and

h is the surface tension of the fluid (dyne/cm).

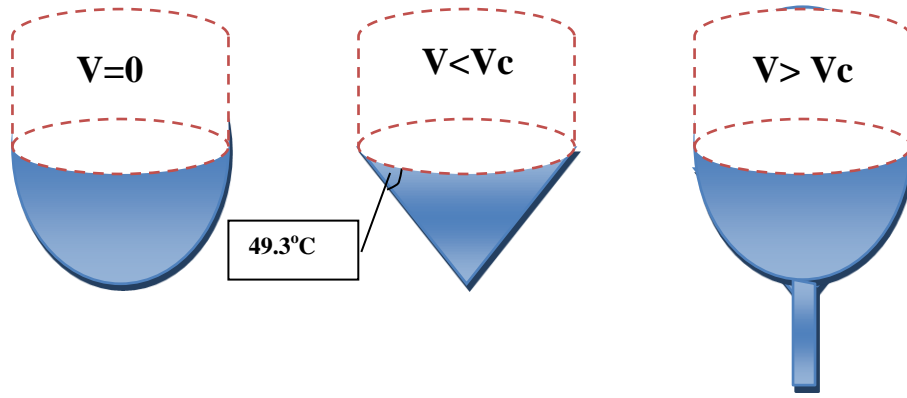


Figure 2:4 Changes in the polymer droplet with applied potential

As can be seen in (Figure 2:4), Taylor predicted the angle of droplet 49.3° , when the jet initiation occurs. There are controversies about the angle of Taylor's cone. As summarized by Teo et al [49] (2011), two independent studies reported 33.5 and 50 degree as the Taylor cone's angle. Taylor has proposed a spheroidal shape for initiating droplet, while Yarin et al (2001) suggested hyperboloid shape for non-self-similar solutions and reported a sharper Taylor Cone for jet initiation. Immediately, after leaving the Taylor cone, the jet follows a straight path, and the jet diameter decreases with distance from tip [51, 53].

Taylor cone can precede the initiation of the jet. The jet follows a path that began with a straight segment. The diameter of the jet, in the straight segment, decreased monotonically with distance from the tip [51].

2.4.2 Jet Thinning / Jet Region and Splaying Region

In this region beyond the base region, the electrical force accelerates and stretches the jet. In this region the jet diameter decreases and its length increases rapidly as it travels down. The jet comes under the influence of bending instability after the straight

segment of the jet. The jet follows a spiral, zigzag path in a region called the envelope cone after the base region. The apex of the envelop cone starts at the end of the straight segment [51]. In this region the amount of mass per unit time passing at any point on the axis remains constant [31]. The electric charge moves as ions with the jet. The jet travels and stretches in the direction of the electric field towards Collector. The solution viscoelastic force of the solution opposes jet stretch. Deitzel et al [55] (2006) explained the relation of jet radius with the following equation, assuming electric jet as a cylindrical geometry.

$$\frac{A}{V} = \frac{2}{R} \quad \text{Equation 2:2}$$

Where

A is the surface area of the cylindrical volume element,

V is the volume and

R is the radius of the jet.

Bigger jet radius will result in lower surface area with the associated specific volume element. The jet radius decays very rapidly if the flow rate is slow. Considering that the polymer solution density and the surface charge density the constant, the charge to mass ratio decreases with increase in jet radius.

$$a = E \left(\frac{q}{m} \right) \quad \text{Equation 2:3}$$

Where

a is acceleration,

E is the electric field strength,

q is the available charge for the given volume element and

m is the mass of a given volume element.

It should be noted that this simplified model of a cylinder was only meant to provide a generalized illustration of the interaction between the solution feed rate, electrospinning voltage, and the charge to mass ratio.

Consequently, as the jet radius increases, the acceleration of the fluid decreases. The polymer acceleration is affected by the viscoelastic properties of the jet. The viscoelastic properties of jet are affected by the occurrence of solvent evaporation.

2.4.3 Jet Instabilities

As the jet accelerates towards the collector, the jet diameter is reduced. The jet thinning can be due to solvent evaporation, splaying and/or stretching of the jet. The jet carries electrical charges with it as it travels. The same electrical charges in the jet generate Coulombic repulsion among solution atoms. The higher applied voltage (Coulombic force i.e. radial force) overcomes surface tension (cohesive forces) in the jet. The Coulombic repulsions act against cohesive forces and solution atoms to go away in the radial directions and stretch the jet in the axial direction. As Coulombic repulsion increases, the jet starts splitting in to same diameter multiple jets with similar electrical charges in multiple directions. This process of splitting is called splaying [56, 57]. Splaying occurs several times until the jet becomes dried into fibre form. After each splitting, the charge redistribution occurs into new size/shape. The jets after splitting carry same charge, so they move away from each other [53]. Due to these repulsions they follow a chaotic path. The jet becomes thinner due to splaying. It is not that only splaying is responsible for jet thinning, since stretching is also responsible for it. The splaying and splitting can occur simultaneously or independently [54].

The jet stretching occurs due to instabilities. The instabilities can cause bending and hence further stretching of the jet. The instabilities can be divided into two main parts varicose and whipping instability. In varicose instability “the centre line remains straight but the jet radius is modulated”.

In whipping instability “the jet radius remains constant but the centre line is modulated” [31, 58]. The varicose instability is known as axisymmetric and whipping instability is known as non-axisymmetric instability. The varicose instability can be divided further into Rayleigh instability and the electric field induced conducting mode axisymmetric instability. Hohman et al. (2001) and Shin et al. (2001) investigated the stability of electrospinning PEO jet and concluded that the possibility for three types of instabilities (Figure 2:5, Figure 2:6, [51]) [31, 32].

- Classic Rayleigh instability (axisymmetric)
- Electric field induced axisymmetric “conducting mode” instability
- Whipping instability (Nonaxisymmetric instability)

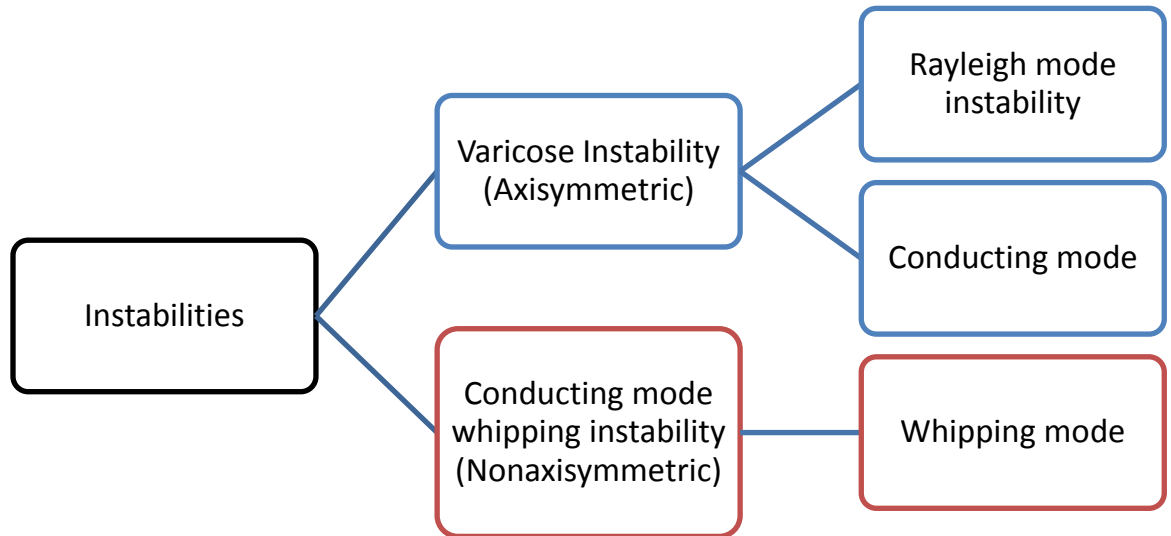


Figure 2:5 Instabilities

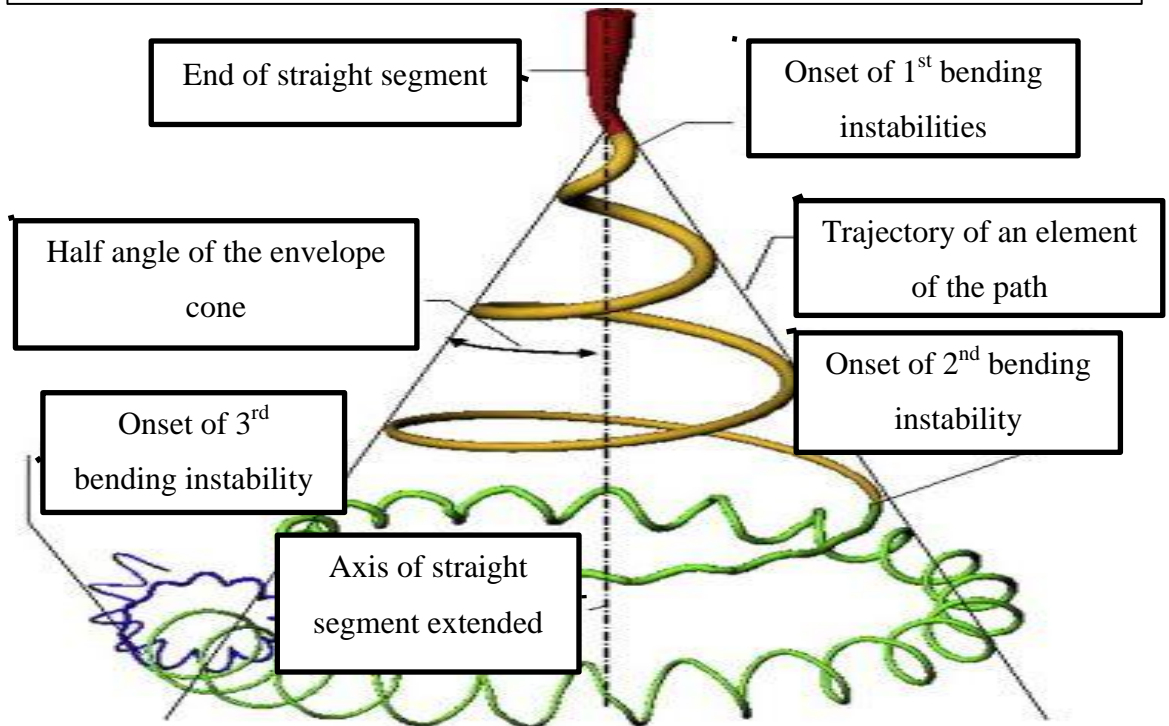


Figure 2:6 Onset development of bending instabilities

The Rayleigh instability occurs due to two opposing forces: Coulombic repulsion and surface tension. The surface tension minimized the total surface area of jet while Coulombic repulsion expands the surface area. The jet with lower viscoelastic properties and with lack of long chain molecules breaks up into droplets with applied voltage. The electrical force breaks the jet. Surface tension creates round shaped droplets. If viscosity of solution is higher with sufficient chain entanglements, the jet will be formed.

2.4.4 Jet Solidification / Collection Region

As the solution jet moves towards collector, it becomes more thin and elongated. Solvent evaporation rate, atmospheric parameters, polymer solution proportion, needle to collector distance etc. affect the process of solidification. The solution jet either gets dried or reaches semi dry. Partially wet fibres get attached at some point with other fibres [51, 53]. This is important for overall mat strength [51]. More wet fibres merge easily and may become flat. Dry fibres do not merge. The solidification rate varies according to solvent.

As the rapidly ‘whipping’ jet moved towards the target maintained at an attractive potential, it continued to expand in to a spiralling and looping path. This continued until the jet became fairly thin and was intercepted by target. As explained earlier the longer the jet travels, the smaller is its diameter. The solidification of the jet results in the deposition of a dry nano fibre on the collector. The solidification rate varies with the polymer concentration, electrostatic field, and gap distance. Yarin et al. (2008) used a quasi-one-dimensional equation to describe the mass decrease and volume variation of the fluid jet due to evaporation and solidification, by assuming that there is no branching or splitting from the primary jet. Conglutination is the process by which partially solidified jets can produce fibres that are attached at points of contact. Strong attachments at crossing points stiffen the mat. This is an important factor in determining the mechanical properties of the nonwoven structure. After the onset of bending instability, the jet may follow a very complicated path and successive loops of coil may touch in flight and form permanent connections [53]. Garlands are nano fibre networks formed when loops of an electrospinning jet conglutinate in flight [51].

2.5 Electrospinning Parameters and Properties of Electrospun Nanofibres

Nano fibre has unique features and properties gifted by its dimension. Nano fibre has more surface area to length ratio, cellular dimensions and hence able to create extracellular type structures, ease of functionalizing them; wide range of morphologies. The diameter of a fiber produced by electrospinning primarily depends on the spinning parameters, solution concentration. It has been found that the morphology such as fibre diameter and its uniformity of the electrospun polymer fibres are dependent upon various parameters listed below. The ideal targets for electrospinning are morphology controllable fibres and mass production. These targets are not easily achievable. Hence, more deeply parametric studies are required. Some of the parameters affecting process /

electrospinnability, productivity, quality, fibre deposition pattern, electrospun mat construction, structure and fibre morphology are as below.

Solution properties: - Solution concentration & viscosity[3, 30, 31, 36, 37, 59–64]; Electrical property of solution[3, 31, 37, 60], Elasticity of solution[60, 65], Surface tension[3, 37, 60, 63], pH[66], Volatility of solvent[3, 31], Evaporation of solvent [67], Solution preparation parameter /method[68, 69], Type of solvent/ Solvent quality [68, 70–73], multicomponent solvent [37, 74–77], additives in solvents[3, 78, 79]

Polymer properties: - Molecular weight of polymer [3, 37, 60, 64, 72, 80–82]; Nature of polymer [83]/ Blend of polymers [84]

Processing conditions:- Applied voltage[3, 31, 36, 37, 60, 64], Distance from needle to collector [3, 31, 37, 60, 64], Volume feed rate [31], Needle / extrusion / capillary tip diameter[37, 60, 69, 85–89] , Spinneret design[3], AC / DC Supply[35, 90], Multi needle/nozzles[3, 91–98], net charge density[63, 99]; Effect of polarity [100–102]

Atmospheric conditions:-Temperature [3, 60, 103–105] , Humidity[3, 31, 60, 67, 85, 104, 106, 107], Air velocity[31, 108]/ Gases / Surrounding air /Vacuum condition[31], Vapour concentration of solvent [67]

External Forces: - vibration [99, 109], Electrical field distribution / Supplementary Electrode / Insulator [31, 99, 110, 111], Magnetic field [31, 99], Gas-assisted effect [99]

Other parameters:-Time of spinning [112], Method of collection [14, 99, 113] , Speed of collector[3, 114–118] , Collector geometry /pattern / arrangement[3, 14, 37, 119–121] combination of some other process with electrospinning (air blowing system) [120–123].

2.5.1 Solution Concentration & Viscosity

Solution concentration and viscosity are related. Viscosity is directly proportional to the concentration [124]. Solution concentration decides the limiting boundaries for the formation of electrospun fibres due to variations in the viscosity and surface tension [31]. As the solution concentrations increases from very low to high, the morphology changes from beads to beads on string to thick and smooth fibres. Lower viscosity solution just spins droplets, while for high viscosity will block the needle and the solution will not be spinnable. Hence, optimum concentration/viscosity is required to electrospin. Lower viscosity solution gives beaded, short and branched thin fibres while higher viscosity solution gives smooth (bead-less) longer and un-branched thick fibres. Lower concentration solution can stretch easily also, if has more tendency of creating multi-jets by splitting compared to higher concentration solution. So,

concentration/viscosity affects fibre morphology. The voltage required to spin viscous solution is higher than at a lower concentration solution [3, 30, 31, 36, 37, 59–64].

2.5.2 Electrical Property/Conductivity of Solution

Doshi and Reneker (1995) [125] defined V_{start} as the voltage required for jet initiation (i.e. voltage required to start a jet from the Taylor cone). They reported that higher voltage is needed by the increased concentration of the solution, which shows that higher force is needed to electrospin as the solution concentration is increased. A few researches have also established the relationship between polymer concentration and viscosity required to electrospin fibres. Koski et al [80] (2004) reported that polyvinyl alcohol (PVA) can be electrospun, if a solution with higher concentration as found with smaller deposition area. Increased concentration resists bending instability. Less bending instability results in less flight path and less spreading, which gives thicker fibre in a smaller deposition area. Viscosity has no direct effect on concentration on fibre formation [24]. Polymer solutions are mostly conductive. The dissolved polymer ions in solvent act as charged ions, when electric force is applied to polymeric solution. During electrospinning these charged ions flow in the polymer solution under the influence of electric force and render the jet to travel towards the collector. Having same charges of charged ions in the polymeric solution, they create Coulombic repulsion, which in turn helps breaking the Taylor cone to initiate the jet as well as splitting the jet further into smaller fibres. Increased conductivity is mainly associated with more stretching of fibre to submicron dimension and also to the splitting of the jet, which also contributes in further thinning of fibres to submicron dimension. Increased conductivity favours mostly bead-less fibres as the beaded jet is stretched to form fibres. Hence, controversies also exists, increased conductivity may attract more solution, if feed rate is higher. In that case, it will favour thicker fibres and may further depend upon the viscoelastic property of the solution which can also favour beaded fibres as [3, 37, 60, 124, 126].

2.5.3 Surface Tension

The polymer solution initially forms droplets at the end of the needle and gets stretched under the influence of electrical force and splits under Coulombic forces. The surface tension holds water as droplets, when the Coulombic force exceed surface tension, a jet emerges and electrospinning starts. Surface tension holds the solution molecules together and has a tendency to reduce the surface area per unit mass of the solution.

Increase in surface tension favours bead formation. A solution with higher surface tension needs more electrical force to initiate electrospinning [24].

2.5.4 pH

The PVA solution conductivity is pH dependent. Increase in pH value gave straighter and finer PVA fibres. It is difficult to electrospin PVA in acidic condition [66].

2.5.5 Volatility of Solvent

The evaporation rate and the drying time depend on solvent vapour pressure. Solvent volatility influenced the phase separation process. Highly volatile solvents create pores along the fibre [3, 31].

2.5.6 Evaporation of Solvent

Fibre diameter became smaller when evaporation and solidification happened more slowly because of the higher vapour concentration of solvent [67].

2.5.7 Solution Preparation Parameter /Method

When the fully hydrolysed PVA is dissolved at high temperature to ensure embryonic crystallites, defect free fibres can be electrospun. PVA/water electrospun fibre morphology is affected by temperature. Chain entanglements of the solution are a function of the dissolution temperatures. At lower temperatures chain entanglement is absent. Solution preparation time is an important parameter for such systems. Longer cooling time results in higher viscosity. The dissolution temperatures and the elapsed time influences fibre morphology [68]. “Decreasing PAN concentration and / or increasing solution temperature result in progressive reduction of fibre diameter” [69].

2.5.8 Type of Solvent / Solvent Quality

The fibre formation mechanism depends on solvent type, inferior solvent fibre formation depends on chain entanglements. The type of solvent plays a vital role in determining chain entanglements. A good solvent will generate enough chain entanglement for spinning and inferior solvent will form no entanglements [68, 70–73].

2.5.9 Multi-component Solvent

Highly porous PLLA fibres were produced by electrospinning using a ternary solvent system of BuOH/DCM/PLLA. Porous fibres were formed with more volatile solvent than with less volatile solvent in the spinning solution. Increasing the ratio of non-solvent/solvent closer to 40/60 generated highly porous electrospun fibres [76]. The small fibres are generated from PCL solutions in a mixture of DCM and DMF than in

the PCL solution in DCM alone [77]. In case of multi component solvent, higher proportion of non-solvent decreases viscosity, so thinner fibres are produced [37, 74–77].

2.5.10 Additives in Solvents

Salt addition makes the solution more conductive because of higher salt ions. Increased salt ions create more self-repulsion of the excess charges on the jet [79]. By the salt addition, fibres with uniform diameter and fewer beads were obtained from PEO, polyacrylic acid (PAA), polyamide, poly-DL-lactic acid (PDLA) and PS solutions. A decrease in PVA fibre diameter is also reported with the higher concentration of NaCl. Finer fibres are reported with smaller ionic additive radii. Larger ions produced coarser fibres. The mobility of smaller radii ions is higher, which resulted in finer fibres due to increased elongation forces [3]. In some cases, higher conductivity due to salt, generated thicker jets under the attraction of the electrical force. After addition of additive salt, coarser fibres are also reported [3, 78, 79].

2.5.11 Molecular Weight of Polymer

Gupta et al. [127] (2005) determined the critical chain overlap concentration (C^*) for different Mw PMMA. They reported a decrease in C^* with an increase in molecular weight. They found reduction in the number of beads and droplets as the molecular weight increased. Uniform fibres at concentration greater than C^* were obtained. Generally the solution viscosity is higher for the higher molecular weight solution. Polymer molecular weight represents the length of the polymer chain. In other words molecular weight determines entanglement of the polymer chain in solvent [24]. Generally higher molecular weight polymers produce thicker and bead-less fibres. Molecular weight also affects the fibre cross-sectional shape, fibre diameter, uniformity, physical properties of fibres and fibre diameter distribution [3, 37, 60, 64, 72, 80–82, 124].

2.5.12 Applied Voltage

Applied voltage is responsible for many phenomena such as initiation of jet, instabilities in jet etc. Electrospinning is known for its spinning process based on electrostatic forces. Applied voltage determines the field strength between collector and solution. Jet initiation occurs when the Coulombic repulsive forces generated in the solution drop let by applied voltage overcomes surface tension. The speed of jet flight and the jet instability are determined by applied voltage. The effect of applied voltage affects fibre

morphology further dependent on feed rate and solution properties. Higher applied voltage creates more Coulombic repulsions in the bead, so multiple jets are generated at a given feed rate which in turn produces thin fibres. As the jet travels, the charge is also transported along with it. This electrified jet travels in a chaotic motion and in a circular instable path. Coulombic forces split the jet into more jets with higher applied voltage. As a result, fibre becomes thinner. Higher applied voltage with relative higher feed rate will increase the flow of material in the jet, which generates thicker fibres. As discussed, applied voltage not only affects fibre size but also to bead formation. Depending on solution properties and other parameters, the beads get larger or smaller with increase in applied voltage. Solution with negligible chain entanglement and higher surface tension generates droplets (i.e. only beads) called electrospraying.

A solution with higher surface tension and chain entanglement will create bead on string structures. In this case as applied voltage increases bead shapes change from round to spindle type and more flatter. It is also reported that increase in applied voltage may generate beads and may reduce beads by elongating the solution with higher entanglement to a flatter fibre shape. Various researchers used external rings or ring electrodes to apply external electric fields. This external electric field created the attraction and repulsion on the jet resulting in changes in the jet path. This technique can be used in controlling the deposition of fibres [3, 31, 36, 37, 60, 64].

2.5.13 Needle to Collector Distance (NTCD)

The electrospun fibre structure and morphology is affected by NTCD, as NTCD affects the deposition time, evaporation rate, electric field strength and whipping or instability interval. Usually less NTCD favours wet and beaded fibres [3]. As NTCD is increased, fibres are elongated due to increase in flight time. An increased distance provides more time for stretching of the beads, which generates less beaded fibre. As fibre travels more they become thinner and expose more surfaces to air, so it also becomes drier too. This is not the case always, in spinning of PVA, gelatine and chitosan for example there is no significant changes in fibre size is observed with increase in NTCD. Some researchers noted increase in fibre diameter with increased NTCD, the reason reported is because of the reduction in the electric field per unit distance. As NTCD increases, electric field per unit distance reduces, less stretching and splitting occurs, which generates thicker fibres [3, 31, 37, 60, 64].

2.5.14 Volume Feed Rate / Polymer Flow Rate

The feed rate of the polymer from the syringe influences the jet velocity and the material feed rate. Generally fibre diameter increases with an increased feed rate. Increased feed rate also creates more beaded morphologies as they do not get enough time to dry before reaching the collector [3]. Low feed rate may block the needle depending on solution properties due to fast evaporation of solution [31].

2.5.15 Needle / Extrusion / Capillary Tip Diameter

Various conclusions can be derived by varying needle size. As needle size increased, the average fibre diameter is either increased, decreased or has no effect. As needle size increases, the material throughput increases. Hence, thicker fibres can be achieved depending on solution property and applied voltage. As fibre diameter increases, the tendency of splitting increases more. In that case smaller diameter fibres are obtained after certain increase in diameters. Few researchers noted no significant changes in average fibre diameters [37, 60, 69, 85–89].

2.5.16 Spinneret Design

Various spinnerets were designed to produce core and sheath, hollow fibres [3].

2.5.17 AC / DC Supply

Polyethylene oxide (PEO) electrospinning has been carried out using both DC and AC driving potentials has been carried out. The AC potential reduced the fibre ‘whipping’ and produced mats with higher degree of fibre alignment [35, 90].

2.5.18 Multi Needles / Nozzles

Multiple needle tips were also used to increase productivity, blends and blend ratios [3, 91–98].

2.5.19 Net Charge Density

The solution charge density on the electropun jet is due to the jet becoming highly unstable in case of high voltage. The solution drips in case of low charge density. Thus, there is an optimum voltage for stable spinning where the electric field and the surface charges on the jet cause jet acceleration towards the collector. Higher charge density on the jet causes greater instability, because the same charges repulsion destabilizes the jet, while tangential stress acting parallel to the flow tends to stabilize it. At a high charge density, the self-repulsion exceeds the stabilizing tangential stress resulting in bending instability [63, 99].

2.5.20 Effect of Polarity

Change of polarity means using negative or positive charge on the collector with the negative opposing charge on the solution droplet. Negative polarity gave larger fibres than positive ions. The cross sections of polyamide 6 fibres are found flat under negative polarity and are found round under positive polarity. When the syringe is positively charged, the time take to spin is less than the time required to spin the same amount of the solution compared to when the syringe is negatively charged. [100–102].

2.5.21 Temperature

When the temperature is increased polyamide 6, cellulose acetate fibres with decreased fibre diameter are produced.

Table 2:1 Effect of humidity on fibre morphology

Humidity	Fibre morphology
<25%	Smooth and pore less
31-38%	Reduced number of uniform and random circular pores
40-45%	Pore shape remained same but they populated heavily
50-59%	Abundant number of pores found surface, leaving little spaces between pores. Pores are not circular in shape but has non-uniform shapes due to merging of pores
60-72%	Larger and non-uniform pores than 50-59%

This reduction in diameter is due to the decrease in solution viscosity at higher temperatures [3, 60, 103, 104, 105].

2.5.22 Humidity

Acrylic fibers spun in relative humidity more than 60% did not dry properly.

Casper et al [106] (2004) studied the effect of different humidity ranges (<25%, 31-38%, 40-45%, 50-59%, 60-72%) on polystyrene fibre morphology by keeping the temperature constant at 24°C. The results are as shown below in Table 2:2:

Polyethylene oxide (PEO) in water produced fibres with smaller diameter decreased with increased RH%. Beaded fibres were formed in the case of thin jet diameter [3, 31, 60, 67, 85, 104, 106, 107].

2.5.23 Air Velocity /Gases / Surrounding Air /Vacuum Condition

The breakdown voltage of the atmospheric gases is said to influence the charge

retaining capacity of the fibres . Pore formation by evaporative cooling is called “breathe figures.” Breathe figures occur on the fiber surfaces due to the imprints of condensed moisture droplets caused by the evaporative cooling of moisture in the air surrounding the spinneret [31].

2.5.24 Vapour Concentration of Solvent / Solvent Evaporation

Evaporation and solidification affects fibre diameter and morphology. Reduction on fibre diameter is reported, when slower evaporation and solidification were performed [67].

2.5.25 Vibration

It has been suggested that the application of vibration technology would lower the viscosity and thus improve electrospinning [99, 109].

2.5.26 Electrical Field Distribution / Supplementary Electrode / Insulator

The polarity and strength of the applied voltage can be altered by auxiliary electrodes. Auxiliary electrodes are used to control the deposition location and area of the electrospun fibre, aligning nano fibres and forming simple patterns [31, 99, 110, 111].

2.5.27 Gas-Assisted Effect

Highly viscous solutions or solutions with high surface tension require higher forces to electrospin. Blow of the jet is used to stretch the fibres along with the electric force. It can be improved further by using heated gases or high temperature air, which in turn reduces solution viscosity. By using flow of air/gas, fibre deposition can also be controlled and finer fibre diameters can also be obtained [99].

2.5.28 Time of Spinning

Aligned PVA fibres were obtained between two collectors for a short time. As the deposition time is increased, fibres start forming bundles binding fibres and forming fibre tows.[112].

2.5.29 Method of Collection

The method of collection can play and control the deposition of fibres. Various collectors have been reported such as knife edge disks, grids, charged needle etc. [99] foil, rotating drums, parallel electrodes etc. try to collect fibre assemblies, which is explained in detail by Teo and Ramakrishna [14, 99, 113].

2.5.30 Speed of Collector

The take up can be stationary or rotating. A rotating take up system has an effect on the molecular structure and on the degree of fibre alignment. Higher speed generates more aligned fibres and thinner fibres [3, 114–118].

2.5.31 Combination of Other Process with Electrospinning (Air Blowing System)

In melt blown electrospinning, combining melt blown with electrospinning is used to produce higher airflow rate at the nozzle which produces smaller diameter fibres [48].

This new process offers the following advantages over the conventional electrospinning process. (1) The air blow assists the electric field to pull the solution; (2) A decrease in the solution viscosity of the jet is achieved by elevating the air temperature and (3) Faster evaporation rate [120–123].

2.6 Electrospinnability

Based on the above parameters electrospinnability [128] is defined. “The amount of fibres collected on the collector was evaluated within a specified time frame at various fluid and process conditions via image analysis and defined as “electrospinnability”, or in short, spinnability”. The higher spinnability implies a greater chance of the polymer solution being spinnable and thus a higher amount of fibre produced within the same period of time.

2.6.1 Advances in Electrospinning

Electrospinning is a versatile and relatively high productivity method among the available methods for nano fibre production. The conventional single needle electrospinning process has low productivity and is not suitable for the industrial scale production. Problems such as needle blocking, limited width of fabric, non-uniform fibre distribution also limits the use of single needle electrospinning for industrial scale. Researchers tried multiple needle spinneret to increase productivity. Problems such as lower productivity and limited fabric width were solved to a certain extent by multiple needle electrospinning. Problems such as needle blocking still exist. Fabric thickness variation along the fabric width is difficult to control in multiple needle electrospinning. The distance between needle has to be adjusted every time a parameter, polymer or solvent is changed because the interaction between the jets gets altered. Apart from that the multiple needle electrospinning has its own inherent problems such as the Coulombic repulsions among the jets. The electrical interferences between the jet due to Coulombic repulsions limits the number of nozzles to be used per unit area. All above

problems diverted research interest towards needle-less electrospinning, with various approaches reported. In needle-less electrospinning researchers tried open bath surface methods.

Table 2:2 Comparison between needle electrospinning and needle-less electrospinning	
Needle Electrospinning	Need-less Elecrosprinng
Needle blocking can stop process	No problems related to needle
Electrical interference between jets	Jets can self-adjust minimum electrical interference
Difficult to maintain cleanliness of needles	No problems related to needle
Difficulty of adjusting space between needle whenever there is change in ay parameters to minimize electrical interference between jets	No problems related to needle
Easy to interpret data as number of jets are known	Not possible to count the jets so hard to interpret jet behaviour/
Solution properties remain same	Solution property may change in case of highly evaporating solvent. Solvent may evaporate from free surface leaving thick solution
Collector can be placed almost in any direction	Mostly collector has to be above the solution
Core sheath, hollow, multicomponent fibres can be fabricated easily	Not possible or with very difficulties
	Increased mechanical activities or noise level due to rotating parts or air bubbles
Difficult to maintain same feed rate through each nozzle	
	More influence of atmospheric conditions

Researchers generated spikes in a solution bath with a magnetic field by attracting the magnetic solution underneath the polymer solution. The generated spikes act as taylor cones to electrospin the solution into fibres. Researchers also tried rotating spiked

rollers disks to generate multiple Taylor cones on spikes. Some researchers also used bubbles by introducing air into a bath to create multiple Taylor cones. The rotating drum concept is industrially accepted for the production of bulk nano fibres for commercial use.

Elmarco designed machine on this principle. Disadvantages of needle blockage, uniformity on the fabric width are overcome by needle-less electrospinning. Jets self-adjust spacing between them to minimize electrical interference from adjacent jets. Table 2:3 represents advantages and disadvantages of needle and needle-less electrospinning.

2.7 Bibliography

- [2.1] D. Eder, "Carbon Nanomaterials: part I," *Department of Materials Science and Metallurgy - university of Cambridge*, 2010. [Online]. Available: http://www.msm.cam.ac.uk/teaching/partIII/courseM6/A-M6_Eder_2010_handout.pdf.
- [2.2] K. Vadodaria, "Nano technology," *Mantra bulletin*, vol. 23, no. 6, pp. 5–7, 2005.
- [2.3] A. Patanaik, R. D. Anandjiwala, R. S. S. Rengasamy, A. Ghosh, and H. Pal, "Nanotechnology in fibrous materials-a new perspective," *Textile Progress*, vol. 39, no. 2, pp. 67 – 120, 2007.
- [2.4] F. K. Ko, "Nanofibre technology : Bridging the Gap between Nano and Macro World," in *Nanoengineered Nanofibrous Materials*, V. Guceri, Selcuk and Gogotsi, Yuri G. and Kuznetsov, Ed. Springer Netherlands, 2004, pp. 1–18.
- [2.5] V. Thavasi, G. Singh, and S. Ramakrishna, "Electrospun nanofibres in energy and environmental applications," *Energy & Environmental Science*, vol. 1, no. 2, p. 205, 2008.
- [2.6] P. P. Tsai, H. Schreuder-gibson, P. Gibson, and H. Schreudergibson, "Different electrostatic methods for making electret filters," *Journal of Electrostatics*, vol. 54, no. 3–4, pp. 333–341, Mar. 2002.
- [2.7] S. Agarwal, J. H. Wendorff, and A. Greiner, "Use of electrospinning technique for biomedical applications," *Polymer*, vol. 49, no. 26, pp. 5603–5621, Dec. 2008.
- [2.8] A. Greiner and J. H. Wendorff, "Electrospinning: a fascinating method for the preparation of ultrathin fibres.," *Angewandte Chemie (International ed. in English)*, vol. 46, no. 30, pp. 5670–703, Jan. 2007.

- [2.9] L. Qian and J. P. Hinestroza, "Application of nanotechnology for high performance textiles," *Journal of textile and apparel technology and management*, vol. 4, no. 1, pp. 1–7, 2004.
- [2.10] Z. Huang, "A review on polymer nanofibres by electrospinning and their applications in nanocomposites," *Composites Science and Technology*, vol. 63, no. 15, pp. 2223–2253, Nov. 2003.
- [2.11] O. Jirsac and D. Stranska, "Nanofibre technologies and nanospider applications," *VDI-Berichte*, no. 1940, pp. 41–44, 2006.
- [2.12] K. Sarkar, C. Gomez, S. Zambrano, M. Ramirez, E. de Hoyos, H. Vasquez, and K. Lozano, "Electrospinning to Forcespinning(TM)," *Materials Today*, vol. 13, no. 11, pp. 12–14, Nov. 2010.
- [2.13] "<http://www.fibreitech.com/forcespinning/>."
- [2.14] W. E. Teo and S. Ramakrishna, "A review on electrospinning design and nanofibre assemblies.," *Nanotechnology*, vol. 17, no. 14, pp. R89–R106, Jul. 2006.
- [2.15] S. Fridrikh, J. Yu, M. Brenner, and G. Rutledge, "Controlling the Fibre Diameter during Electrospinning," *Physical Review Letters*, vol. 90, no. 14, pp. 1–4, Apr. 2003.
- [2.16] T. Mikołajczyk, "Effect of Ceramic Nanoparticles on the Rheological Properties of Spinning Solutions of Polyacrylonitrile in Dimethylformamide," *Europe*, vol. 13, no. 1, pp. 28–31, 2005.
- [2.17] D. Li and Y. Xia, "Direct Fabrication of Composite and Ceramic Hollow Nanofibres by Electrospinning," *Nano Letters*, vol. 4, no. 5, pp. 933–938, May 2004.
- [2.18] D. Li, Y. Wang, and Y. Xia, "Electrospinning of Polymeric and Ceramic Nanofibres as Uniaxially Aligned Arrays," *Nano Letters*, vol. 3, no. 8, pp. 1167–1171, Aug. 2003.
- [2.19] W. Sigmund, J. Yuh, H. Park, V. Maneeratana, G. Pyrgiotakis, A. Daga, J. Taylor, and J. C. Nino, "Processing and Structure Relationships in Electrospinning of Ceramic Fibre Systems," *Journal of the American Ceramic Society*, vol. 89, no. 2, pp. 395–407, Feb. 2006.
- [2.20] R. Ramaseshan, S. Sundarrajan, R. Jose, and S. Ramakrishna, "Nanostructured ceramics by electrospinning," *Journal of Applied Physics*, vol. 102, no. 11, p. 111101, 2007.
- [2.21] J. T. McCann, M. Marquez, and Y. Xia, "Highly porous fibres by electrospinning into a cryogenic liquid.," *Journal of the American Chemical Society*, vol. 128, no. 5, pp. 1436–7, Feb. 2006.

- [2.22] I. Chronakis, "Novel nanocomposites and nanoceramics based on polymer nanofibres using electrospinning process—A review," *Journal of Materials Processing Technology*, vol. 167, no. 2–3, pp. 283–293, Aug. 2005.
- [2.23] H. Schreuder-gibson, K. Senecal, M. Sennett, Z. Huang, J. Wen, W. Li, D. Wang, S. Yang, Y. Tu, Z. Ren, and C. Sung, "Characteristics of electrospun carbon nanotube-polymer composites," pp. 1–11.
- [2.24] S. Ramakrishna, K. Fujihara, W. Teo, and L. Teik-cheng, *An introduction to electrospinning and nanofibres*. World Scientific, 2005, p. 396.
- [2.25] R. Murugan and S. Ramakrishna, "Design strategies of tissue engineering scaffolds with controlled fibre orientation.," *Tissue engineering*, vol. 13, no. 8, pp. 1845–66, Aug. 2007.
- [2.26] K. Jayaraman, M. Kotaki, Y. Zhang, X. Mo, and S. Ramakrishna, "Recent Advances in Polymer Nanofibres," *Journal of Nanoscience and Nanotechnology*, pp. 52–65, Jan. 2004.
- [2.27] S. G. Kumbar, R. James, S. P. Nukavarapu, and C. T. Laurencin, "Electrospun nanofibre scaffolds: engineering soft tissues.," *Biomedical materials (Bristol, England)*, vol. 3, no. 3, p. 034002, Sep. 2008.
- [2.28] E. D. Boland, J. A. Matthews, K. J. Pawlowski, D. G. Simpson, G. E. Wnek, and G. L. Bowlin, "Electrospinning collagen and elastin preliminary vascular tissue engineering," *Frontiers in Bioscience*, vol. 9, pp. 1422–1432, Sep. 2004.
- [2.29] C. P. Barnes, S. a Sell, E. D. Boland, D. G. Simpson, and G. L. Bowlin, "Nanofibre technology: designing the next generation of tissue engineering scaffolds.," *Advanced drug delivery reviews*, vol. 59, no. 14, pp. 1413–33, Dec. 2007.
- [2.30] V. Beachley and X. Wen, "Polymer nanofibrous structures: Fabrication, biofunctionalization, and cell interactions," *Progress in Polymer Science*, vol. 35, no. 7, pp. 868–892, Jul. 2010.
- [2.31] T. Subbiah, G. S. Bhat, R. W. Tock, S. Parameswaran, S. S. Ramkumar, and R. Zufan, "Electrospinning of nanofibres," *Journal of Applied Polymer Science*, vol. 96, no. 2, pp. 557–569, Apr. 2005.
- [2.32] A. Frenot and I. S. Chronakis, "Polymer nanofibres assembled by electrospinning," *Science And Technology*, vol. 8, pp. 64–75, 2003.
- [2.33] D. Li and Y. Xia, "Electrospinning of Nanofibres: Reinventing the Wheel?," *Advanced Materials*, vol. 16, no. 14, pp. 1151–1170, 2004.
- [2.34] K. V. Vadodaria and S. R. Naik, "Electro-spinning," *Mantra Textile Magazine*, vol. 1, no. 2, pp. 4–9, 2006.

- [2.35] R. Kessick, J. Fenn, and G. Tepper, "The use of AC potentials in electrospraying and electrospinning processes," *Polymer*, vol. 45, no. 9, pp. 2981–2984, Apr. 2004.
- [2.36] J. Deitzel, "The effect of processing variables on the morphology of electrospun nanofibres and textiles," *Polymer*, vol. 42, no. 1, pp. 261–272, Jan. 2001.
- [2.37] N. Bhardwaj and S. C. Kundu, "Electrospinning: a fascinating fibre fabrication technique.," *Biotechnology advances*, vol. 28, no. 3, pp. 325–47, 2010.
- [2.38] Y. Ding, P. Zhang, Y. Jiang, F. Xu, J. Yin, and Y. Zuo, "Mechanical properties of nylon-6/SiO₂ nanofibres prepared by electrospinning," *Materials Letters*, vol. 63, no. 1, pp. 34–36, Jan. 2009.
- [2.39] B. Ding, C. Li, Y. Miyauchi, O. Kuwaki, and S. Shiratori, "Formation of novel 2D polymer nanowebs via electrospinning," *Nanotechnology*, vol. 17, no. 15, pp. 3685–3691, Aug. 2006.
- [2.40] J. Zeleny, "The Electrical Discharge from Liquid Points, and a Hydrostatic Method of Measuring the Electric Intensity at Their Surfaces," *Physical Review*, vol. 3, no. 2, pp. 69–91, 1914.
- [2.41] N. Bock, M. a. Woodruff, D. W. Hutmacher, and T. R. Dargaville, "Electrospraying, a Reproducible Method for Production of Polymeric Microspheres for Biomedical Applications," *Polymers*, vol. 3, no. 1, pp. 131–149, Jan. 2011.
- [2.42] a Jaworek and a Sobczyk, "Electrospraying route to nanotechnology: An overview," *Journal of Electrostatics*, vol. 66, no. 3–4, pp. 197–219, Mar. 2008.
- [2.43] a. Jaworek, a. Krupa, M. Lackowski, a. T. Sobczyk, T. Czech, S. Ramakrishna, S. Sundarajan, and D. Pliszka, "Nanocomposite fabric formation by electrospinning and electrospraying technologies," *Journal of Electrostatics*, vol. 67, no. 2–3, pp. 435–438, May 2009.
- [2.44] Y. Wu and R. L. Clark, "Controllable porous polymer particles generated by electrospraying.," *Journal of colloid and interface science*, vol. 310, no. 2, pp. 529–35, Jun. 2007.
- [2.45] M. Mckee, C. Elkins, and T. Long, "Influence of self-complementary hydrogen bonding on solution rheology/electrospinning relationships," *Polymer*, vol. 45, no. 26, pp. 8705–8715, Dec. 2004.
- [2.46] J. F. Cooley, "Apparatus for electrically dispersing fluids (uspatent 692631)," U.S. Patent 6926311902.
- [2.47] W. J. Morton, "Methods of dispersing fluids (US patent 705691)," U.S. Patent 7056911902.

- [2.48] A. Formhals, "Process and apparatus for preparing artificial threads; US patent1975504.pdf," 1934.
- [2.49] C. L. Norton, "Method of and apparatus for producing fibrous or filamentary material -US2048651," U.S. Patent 20486511936.
- [2.50] G. Taylor, L. Series, and P. Sciences, "Electrically driven jets," *Society*, vol. 313, no. 1515, pp. 453–475, 1969.
- [2.51] D. H. Reneker and A. L. Yarin, "Electrospinning jets and polymer nanofibres," *Polymer*, vol. 49, no. 10, pp. 2387–2425, May 2008.
- [2.52] X. Wang, J. Cao, Z. Hu, W. Pan, and Z. Liu, "Jet shaping nanofibres and collection of nanofibre mats in electrospinning," *Journal of material science technology*, vol. 22, no. 4, pp. 536–540, 2006.
- [2.53] K. Garg and G. L. Bowlin, "Electrospinning jets and nanofibrous structures.," *Biomicrofluidics*, vol. 5, no. 1, p. 13403, Jan. 2011.
- [2.54] D. H. Reneker and I. Chun, "Nanometre diameter fibres of polymer , produced by electrospinning," *Solutions*, vol. 7, pp. 216–223, 1996.
- [2.55] J. Deitzel, *Polymeric Nanofibres*, no. v. 918. American Chemical Society, 2006, p. 464.
- [2.56] Y. M. Shin, M. M. Hohman, M. P. Brenner, and G. C. Rutledge, "Electrospinning: A whipping fluid jet generates submicron polymer fibres," *Applied Physics Letters*, vol. 78, no. 8, p. 1149, 2001.
- [2.57] M. M. Hohman, M. Shin, G. Rutledge, and M. P. Brenner, "Electrospinning and electrically forced jets. I. Stability theory," *Physics of Fluids*, vol. 13, no. 8, p. 2201, 2001.
- [2.58] M. M. Hohman, G. Rutledge, M. Shin, and M. P. Brenner, "Electrospinning and electrically forced jets. II. Applications," *Physics of Fluids*, vol. 13, no. 8, p. 2221, 2001.
- [2.59] X. Zong, K. Kim, D. Fang, S. Ran, B. S. Hsiao, and B. Chu, "Structure and process relationship of electrospun bioabsorbable nanofibre membranes," *Source*, vol. 43, pp. 4403–4412, 2002.
- [2.60] S.-H. Tan, R. Inai, M. Kotaki, and S. Ramakrishna, "Systematic parameter study for ultra-fine fibre fabrication via electrospinning process," *Polymer*, vol. 46, no. 16, pp. 6128–6134, Jul. 2005.
- [2.61] S. Theron, "Experimental investigation of the governing parameters in the electrospinning of polymer solutions," *Polymer*, vol. 45, no. 6, pp. 2017–2030, Mar. 2004.

- [2.62] D. H. Reneker, A. L. Yarin, H. Fong, and S. Koombhongse, "Bending instability of electrically charged liquid jets of polymer solutions in electrospinning," *Journal of Applied Physics*, vol. 87, no. 9, p. 4531, 2000.
- [2.63] H. Fong, "Beaded nanofibres formed during electrospinning," *Polymer*, vol. 40, no. 16, pp. 4585–4592, Jul. 1999.
- [2.64] S. S. Ojha, M. Afshari, R. Kotek, and R. E. Gorga, "Morphology of electrospun nylon-6 nanofibres as a function of molecular weight and processing parameters," *Journal of Applied Polymer Science*, vol. 108, no. 1, pp. 308–319, 2008.
- [2.65] J. H. Yu, S. V. Fridrikh, and G. C. Rutledge, "The role of elasticity in the formation of electrospun fibres," *Polymer*, vol. 47, pp. 4789–4797, 2006.
- [2.66] W. Keunson, J. Hoyouk, T. Seunglee, and W. Park, "Effect of pH on electrospinning of poly(vinyl alcohol)," *Materials Letters*, vol. 59, no. 12, pp. 1571–1575, May 2005.
- [2.67] S. Tripatanasuwan, Z. Zhong, and D. H. Reneker, "Effect of evaporation and solidification of the charged jet in electrospinning of poly(ethylene oxide) aqueous solution," *Polymer*, vol. 48, no. 19, pp. 5742–5746, Sep. 2007.
- [2.68] S. Shenoy, W. Bates, and G. Wnek, "Correlations between electrospinnability and physical gelation," *Polymer*, vol. 46, no. 21, pp. 8990–9004, Oct. 2005.
- [2.69] C. Wang, H.-S. Chien, C.-H. Hsu, Y.-C. Wang, C.-T. Wang, and H.-A. Lu, "Electrospinning of Polyacrylonitrile Solutions at Elevated Temperatures," *Macromolecules*, vol. 40, no. 22, pp. 7973–7983, Oct. 2007.
- [2.70] C. J. Luo, M. Nangrejo, and M. Edirisinghe, "A novel method of selecting solvents for polymer electrospinning," *Polymer*, vol. 51, no. 7, pp. 1654–1662, Mar. 2010.
- [2.71] S. Shenoy, W. Bates, H. Frisch, and G. Wnek, "Role of chain entanglements on fibre formation during electrospinning of polymer solutions: good solvent, non-specific polymer / polymer interaction limit," *Polymer*, vol. 46, no. 10, pp. 3372–3384, Apr. 2005.
- [2.72] G. Eda, J. Liu, and S. Shivkumar, "Flight path of electrospun polystyrene solutions: Effects of molecular weight and concentration," *Materials Letters*, vol. 61, no. 7, pp. 1451–1455, Mar. 2007.
- [2.73] G. Eda, J. Liu, and S. Shivkumar, "Solvent effects on jet evolution during electrospinning of semi-dilute polystyrene solutions," *European Polymer Journal*, vol. 43, no. 4, pp. 1154–1167, Apr. 2007.

- [2.74] S. Han, J. Youk, K. Min, Y. Kang, and W. Park, "Electrospinning of cellulose acetate nanofibres using a mixed solvent of acetic acid/water: Effects of solvent composition on the fibre diameter," *Materials Letters*, vol. 62, no. 4–5, pp. 759–762, Feb. 2008.
- [2.75] J. yong Park, sung woo Han, and in hwa Lee, "Preparation of electrospun porous ethyl cellulose fibre by THF/DMAc binary solvent system," *Journal of industrial engineering chemistry*, vol. 13, no. 6, pp. 1002–1008, 2007.
- [2.76] Z. Qi, H. Yu, Y. Chen, and M. Zhu, "Highly porous fibres prepared by electrospinning a ternary system of nonsolvent/solvent/poly(l-lactic acid)," *Materials Letters*, vol. 63, no. 3–4, pp. 415–418, Feb. 2009.
- [2.77] K. H. Lee, H. Y. Kim, M. S. Khil, Y. M. Ra, and D. R. Lee, "Characterization of nano-structured poly(ε-caprolactone) nonwoven mats via electrospinning," *Science*, vol. 44, pp. 1287–1294, 2003.
- [2.78] P. Heikkila, "Electrospinning of polyacrylonitrile (PAN) solution: Effect of conductive additive and filler on the process," *eXPRESS Polymer Letters*, vol. 3, no. 7, pp. 437–445, Jun. 2009.
- [2.79] X.-H. Qin, S.-Y. Wang, T. Sandra, and D. Lukas, "Effect of LiCl on the stability length of electrospinning jet by PAN polymer solution," *Materials Letters*, vol. 59, no. 24–25, pp. 3102–3105, Oct. 2005.
- [2.80] A. Koski, K. Yim, and S. Shivkumar, "Effect of molecular weight on fibrous PVA produced by electrospinning," *Materials Letters*, vol. 58, pp. 493 – 497, 2004.
- [2.81] K. W. Kim, K. H. Lee, M. S. Khil, Y. S. Ho, and H. Y. Kim, "The effect of molecular weight and the linear velocity of drum surface on the properties of electrospun poly(ethylene terephthalate) nonwovens," *Fibres and Polymers*, vol. 5, no. 2, pp. 122–127, Jun. 2004.
- [2.82] H. M. Ji, H. W. Lee, M. R. Karim, I. W. Cheong, E. a. Bae, T. H. Kim, M. S. Islam, B. C. Ji, and J. H. Yeum, "Electrospinning and characterization of medium-molecular-weight poly(vinyl alcohol)/high-molecular-weight poly(vinyl alcohol)/montmorillonite nanofibres," *Colloid and Polymer Science*, vol. 287, no. 7, pp. 751–758, Mar. 2009.
- [2.83] N. K. Sharma, "Nano fibres and nonwovens via electrospinning," *The Indian Textile Journal* <http://www.indiantextilejournal.com/articles/FAdetails.asp?id=616>, no. October, 2007.

- [2.84] J. Gunn and M. Zhang, "Polyblend nanofibres for biomedical applications: perspectives and challenges.," *Trends in biotechnology*, vol. 28, no. 4, pp. 189–97, Apr. 2010.
- [2.85] J. Jeun, Y. Kim, Y. Lim, J. Choi, C. Jung, and P. Kang, "Electrospinning of Poly (L-lactide-co-D , L-lactide)," vol. 13, no. 4, pp. 592–596, 2007.
- [2.86] H. B. Wang, M. E. Mullins, J. M. Cregg, A. Hurtado, M. Oudega, M. T. Trombley, and R. J. Gilbert, "Creation of highly aligned electrospun poly-L-lactic acid fibres for nerve regeneration applications.," *Journal of neural engineering*, vol. 6, no. 1, p. 016001, Mar. 2009.
- [2.87] J. Sutasinpromprae, S. Jitjaicham, M. Nithitanakul, C. Meechaisue, and P. Supaphol, "Preparation and characterization of ultrafine electrospun polyacrylonitrile fibres and their subsequent pyrolysis to carbon fibres," *Polymer International*, vol. 833, no. October 2005, pp. 825–833, 2006.
- [2.88] P. Heikkila and a Harlin, "Parameter study of electrospinning of polyamide-6," *European Polymer Journal*, vol. 44, no. 10, pp. 3067–3079, Oct. 2008.
- [2.89] J. Macossay, A. Marruffo, R. Rincon, T. Eubanks, and A. Kuang, "Effect of needle diameter on nanofibre diameter and thermal properties of electrospun poly (methyl methacrylate)," *Polymers for Advanced Technologies*, vol. 18, no. February, pp. 180–183, 2007.
- [2.90] S. Sarkar, S. Deevi, and G. Tepper, "Biased AC Electrospinning of Aligned Polymer Nanofibres," *Macromolecular Rapid Communications*, vol. 28, no. 9, pp. 1034–1039, May 2007.
- [2.91] S. a. Theron, a. L. Yarin, E. Zussman, and E. Kroll, "Multiple jets in electrospinning: experiment and modeling," *Polymer*, vol. 46, no. 9, pp. 2889–2899, Apr. 2005.
- [2.92] C. S. Kong, S. G. Lee, S. H. Lee, K. H. Lee, N. G. Jo, and H. S. Kim, "Multi-jet ejection and fluctuation in electrospinning of polyvinyl alcohol with various nozzle diameters," *Polymer Engineering & Science*, vol. 49, no. 11, pp. 2286–2292, Nov. 2009.
- [2.93] O. O. Dosunmu, G. G. Chase, W. Kataphinan, and D. H. Reneker, "Electrospinning of polymer nanofibres from multiple jets on a porous tubular surface," *Nanotechnology*, vol. 17, no. 4, pp. 1123–1127, Feb. 2006.
- [2.94] G. Kim, Y. Cho, and W. Kim, "Stability analysis for multi-jets electrospinning process modified with a cylindrical electrode," *European Polymer Journal*, vol. 42, no. 9, pp. 2031–2038, Sep. 2006.

- [2.95] Y. Yang, Z. Jia, Q. Li, L. Hou, and Guan, "Electrospun uniform fibres with a special regular hexagon distributed multi-needle system," *Journal of Physics: Conference Series*, vol. 012027, no. 142, pp. 1–7, 2008.
- [2.96] C. J. Angammana and S. H. Jayaram, "Effects of Electric Field on the Multi-jet Electrospinning Process and Fibre Morphology," pp. 1–4.
- [2.97] W. Tomaszewski, "Investigation of Electrospinning with the Use of a Multi-jet Electrospinning Head," *October*, vol. 13, no. 4, pp. 22–26, 2005.
- [2.98] A. Varesano, R. A. Carletto, and G. Mazzuchetti, "Journal of Materials Processing Technology Experimental investigations on the multi-jet electrospinning process," *Journal of Materials Processing Technology*, vol. 209, pp. 5178–5185, 2009.
- [2.99] W.-E. Teo, R. Inai, and S. Ramakrishna, "Technological advances in electrospinning of nanofibres," *Science and Technology of Advanced Materials*, vol. 12, no. 1, p. 013002, Feb. 2011.
- [2.100] A. Kilic, F. Oruc, and aLi Demir, "Effects of Polarity on Electrospinning Process," *Textile Research Journal*, vol. 78, no. 6, pp. 532–539, Jun. 2008.
- [2.101] P. Supaphol, C. Mit-Uppatham, and M. Nithitanakul, "Ultrafine electrospun polyamide-6 fibres: Effect of emitting electrode polarity on morphology and average fibre diameter," *Journal of Polymer Science Part B: Polymer Physics*, vol. 43, no. 24, pp. 3699–3712, Dec. 2005.
- [2.102] P. Supaphol, C. Mit-uppatham, and M. Nithitanakul, "Ultrafine Electrospun Polyamide-6 Fibres: Effects of Solvent System and Emitting Electrode Polarity on Morphology and Average Fibre Diameter," *Macromolecular Materials and Engineering*, vol. 290, no. 9, pp. 933–942, Sep. 2005.
- [2.103] S. R. Givens, K. H. Gardner, J. F. Rabolt, and D. B. Chase, "High-Temperature Electrospinning of Polyethylene Microfibres from Solution," *Macromolecules*, vol. 40, no. 3, pp. 608–610, Feb. 2007.
- [2.104] S. Vrieze, T. Camp, a. Nelvig, B. Hagström, P. Westbroek, and K. Clerck, "The effect of temperature and humidity on electrospinning," *Journal of Materials Science*, vol. 44, no. 5, pp. 1357–1362, Oct. 2008.
- [2.105] O. Hardick, B. Stevens, and D. G. Bracewell, "Nanofibre fabrication in a temperature and humidity controlled environment for improved fibre consistency," *Journal of Materials Science*, vol. 46, no. 11, pp. 3890–3898, Feb. 2011.
- [2.106] C. L. Casper, J. S. Stephens, N. G. Tassi, D. B. Chase, and J. F. Rabolt, "Controlling Surface Morphology of Electrospun Polystyrene Fibres: Effect of

Humidity and Molecular Weight in the Electrospinning Process,” *Macromolecules*, vol. 37, no. 2, pp. 573–578, Jan. 2004.

[2.107] M. S. Peresin, Y. Habibi, A.-H. Vesterinen, O. J. Rojas, J. J. Pawlak, and J. V. Seppälä, “Effect of moisture on electrospun nanofibre composites of poly(vinyl alcohol) and cellulose nanocrystals,” *Biomacromolecules*, vol. 11, no. 9, pp. 2471–7, Sep. 2010.

[2.108] X. Zhang, M. R. Reagan, and D. L. Kaplan, “Electrospun silk biomaterial scaffolds for regenerative medicine,” *Advanced drug delivery reviews*, vol. 61, no. 12, pp. 988–1006, Oct. 2009.

[2.109] Y. Wan, J. He, J. Yu, and Y. Wu, “Electrospinning of High-Molecule PEO Solution,” *Polymer*, vol. 103, pp. 3840–3843, 2007.

[2.110] Y. Yang, Z. Jia, L. Hou, Q. Li, L. Wang, and Z. Guan, “Controlled Deposition of Electrospinning Jet by Electric Field Distribution from an Insulating Material Surrounding the Barrel of the Polymer Solution,” *IEEE Transactions on Dielectrics and Electrical Insulation*, vol. 15, no. 1, pp. 269–276, 2008.

[2.111] M. V. Kakade, S. Givens, K. Gardner, K. H. Lee, D. B. Chase, and J. F. Rabolt, “Electric field induced orientation of polymer chains in macroscopically aligned electrospun polymer nanofibres,” *Journal of the American Chemical Society*, vol. 129, no. 10, pp. 2777–82, Mar. 2007.

[2.112] S. Chuangchote and P. Supaphol, “Fabrication of aligned poly (vinyl alcohol) nanofibres by electrospinning,” *J Nanosci Nanotechnol.*, vol. 6, no. 1, pp. 125–129, 2006.

[2.113] N. M. Neves, R. Campos, A. Pedro, J. Cunha, F. Macedo, and R. L. Reis, “Patterning of polymer nanofibre meshes by electrospinning for biomedical applications,” *International journal of nanomedicine*, vol. 2, no. 3, pp. 433–48, Jan. 2007.

[2.114] B. Sundararaj, V. Subramanian, T. S. Natarajan, R.-Z. Xiang, C.-C. Chang, and W.-S. Fann, “Electrospinning of continuous aligned polymer fibres,” *Applied Physics Letters*, vol. 84, no. 7, p. 1222, 2004.

[2.115] A. Baji, Y.-W. Mai, S.-C. Wong, M. Abtahi, and P. Chen, “Electrospinning of polymer nanofibres: Effects on oriented morphology, structures and tensile properties,” *Composites Science and Technology*, vol. 70, no. 5, pp. 703–718, May 2010.

[2.116] S. Lee and J. Yoon, “Continuous Nanofibres Manufactured by Electrospinning Technique,” *Notes*, vol. 10, no. 5, pp. 282–285, 2002.

- [2.117] K. H. Lee, H. Y. Kim, M. S. Khil, Y. M. Ra, and D. R. Lee, "Characterization of nano-structured poly([epsilon]-caprolactone) nonwoven mats via electrospinning," *Polymer*, vol. 44, no. 4, pp. 1287–1294, Feb. 2003.
- [2.118] H. Lee, H. Yoon, and G. Kim, "Highly oriented electrospun polycaprolactone micro/nanofibres prepared by a field-controllable electrode and rotating collector," *Applied Physics A: Materials Science & Processing*, vol. 97, no. 3, pp. 559–565.
- [2.119] D. Li, G. Ouyang, J. T. McCann, and Y. Xia, "Collecting electrospun nanofibres with patterned electrodes," *Nano letters*, vol. 5, no. 5, pp. 913–6, May 2005.
- [2.120] A. Varesano, A. Montarsolo, and C. Tonin, "Crimped polymer nanofibres by air-driven electrospinning," *European Polymer Journal*, vol. 43, pp. 2792–2798, 2007.
- [2.121] G. H. Kim and H. Yoon, "A direct-electrospinning process by combined electric field and air-blowing system for nanofibrous wound-dressings," *Applied Physics A*, vol. 90, no. 3, pp. 389–394, Nov. 2007.
- [2.122] Y. Lee, K. Watanabe, T. Nakamura, B. S. Kim, H. Y. Kim, and I. S. Kim, "Development of Melt Blown Electrospinning Apparatus of Isotactic Polypropylene Department of Functional Machinery and Mechanics , Faculty of Textile Science and Technology , Effect of LiCl on Fibre Diameter 3 . 1 Effect of Air Flow Rate At Nozzle on," *System*, vol. 1, pp. 826–829, 2010.
- [2.123] I. C. Um, D. Fang, B. S. Hsiao, A. Okamoto, and B. Chu, "Electro-spinning and electro-blowing of hyaluronic acid," *Biomacromolecules*, vol. 5, no. 4, pp. 1428–36, 2004.
- [2.124] P. Heikkila and a Harlin, "Parameter study of electrospinning of polyamide-6," *European Polymer Journal*, vol. 44, no. 10, pp. 3067–3079, Oct. 2008.
- [2.125] J. Doshi and D. H. Reneker, "Electrospinning process and applications of electrospun fibres," *Journal of Electrostatics*, vol. 35, pp. 151–160, Nov. 1995.
- [2.126] T. Subbiah, G. S. Bhat, R. W. Tock, S. Parameswaran, S. S. Ramkumar, and R. Zufan, "Electrospinning of nanofibres," *Journal of Applied Polymer Science*, vol. 96, no. 2, pp. 557–569, Apr. 2005.
- [2.127] P. Gupta, C. Elkins, T. E. Long, and G. L. Wilkes, "Electrospinning of linear homopolymers of poly(methyl methacrylate): exploring relationships between fibre formation, viscosity, molecular weight and concentration in a good solvent," *Polymer*, vol. 46, no. 13, pp. 4799–4810, Jun. 2005.
- [2.128] C. Pattamaprom, W. Hongrojjanawiwat, P. Koombhongse, P. Supaphol, T. Jarusuwannapoo, and R. Rangkupan, "The Influence of Solvent Properties and

Functionality on the Electrospinnability of Polystyrene Nanofibres,” *Macromolecular Materials and Engineering*, vol. 291, no. 7, pp. 840–847, Jul. 2006.

Chapter 3 : Experimental and Testing Techniques in Detail

The following instruments were used during experimental work and testing. Their principles and methods of operation are described in detail in this chapter.

3.1 Solution Preparation

3.1.1 Ultrasonic Bath

An ultrasonic bath uses ultrasonic energy to dissolve ingredients. Its principle and mechanism are explained below: the ultrasonic waves pass through the solution and create tiny bubbles. This physical process is known as “cavitation”. The produced bubbles are compressed due to cavitation. These bubbles act as micro reactors. They grow, oscillate, split and break due to temperature and pressure generated by cavitation. The collapses of bubbles generate shock waves in the solution and improve mixing. This cavitation process ruptures particles, causes mechanical erosion. It also generates chemical radicals in solutions. The ultrasonic effect depends on different parameters such as sonication time, ultrasonic energy frequency, bath temperature, particle size and the position of sample container (vertical/horizontal) in the bath [1]. The ultrasonic effect creates mechanical effect and increases solvent penetration into the sample matrix. The contact surface area between solid and liquid phase increases due to cavitation and bubble collapse [2].



Figure 3:1 Ultrasonic bath (Decon Ultrasonic – F5 minor)

In the present work, the ultrasonic bath by Decon ultrasonics limited (Figure 3:1) (Model – F5 Minor) was used to dissolve polymers and for making homogenous polymer solutions for electrospinning.

3.2 Solution Testing

3.2.1 Viscosity

Viscosity is an important parameter of any solution, because it affects spinnability as well as fibre morphology in electrospinning. If the viscosity is too low then fibre cannot be formed and only droplets will be formed. If the viscosity is too high then the solution will block the needle, hence; spinning will not be possible.

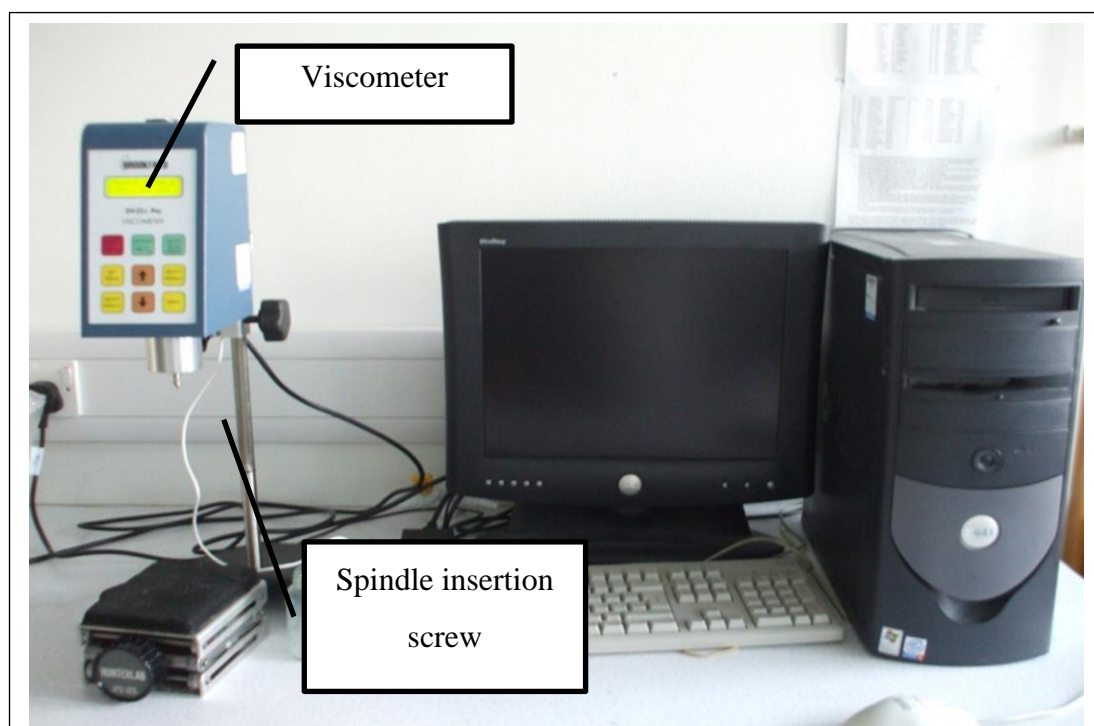
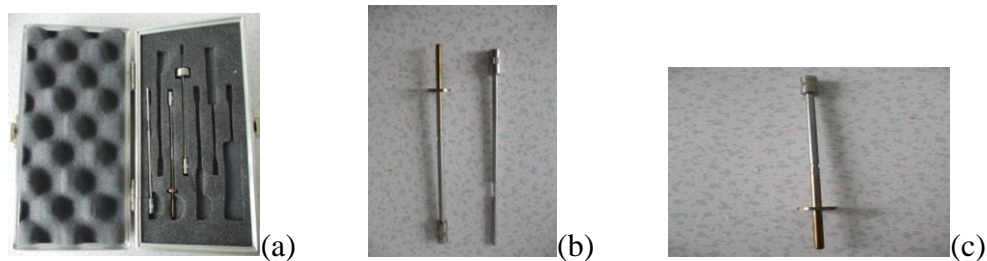


Figure 3:2 Brookfield DV II Pro Viscosimeter



- (a) Box of different size spindles
- (b) Spindle “S63” and “S64” (Left to right)
- (c) Spindle “S64”

Figure 3:3 Viscosimeter spindles (Brookfield DV II Pro viscosimeter)

Generally, lower viscosity spins beaded fibre and high viscosity produces round solid fibres [3],

“Viscosity is a measure of the resistance of a fluid which is being deformed by either shear or tensile stress. In everyday terms (and for fluids only), viscosity is "thickness" or "internal friction". Thus, water is "thin", having a lower viscosity, while honey is "thick", having a higher viscosity. To put it simply, the less viscous the fluid is, the greater its ease of movement (fluidity)” [4].

A viscometer (also called viscosimeter) is an instrument used to measure the viscosity of a fluid. “Viscosity can be determined by measuring a drop between fluid and surface due to relative motion between them the fluid remains stationary and an object moves through it, or the object is stationary and the fluid moves past it ” [4].

In the present work, viscosities of polymer solutions were measured with a Brookfield DV-II Pro (Figure 3:2) rotational viscometer. In a rotational viscometer, the spindle is rotated in the solution. The torque required to turn the spindle in the solution is converted into viscosity of that solution. Solution samples were placed in beaker. Different spindles are used to measure viscosity of different solutions. All spindles have spindle numbers on them for ease of identification. The change in viscosity and shear stress with change in shear rate is measured. All samples were placed in the same beaker, to get the viscosity of the solutions, spindles “S63” and “S64” (Figure 3:3) were used. Factors such as beaker size, spindle size, spindle RPM/shear rate, temperature, time, pressure, previous history, solution composition and additives also need to be determined. [4].

3.2.2 Surface Tension

Surface Tension is an important solution property, affecting electro-spinnability as well as fibre morphology. Surface tension is a property of the surface of a liquid that allows it to resist external forces, for example, as in floating of some insects on the surface of water (e.g. water striders). “This property is caused by cohesion of similar molecules, and is responsible for many of the behaviours of liquids” [7]. “Interactions occur between the molecules of a liquid and those of any liquid or gaseous substance which is not soluble in the liquid; these result in the formation of an interface. Energy is required to change the form of this interface or surface. The work required to change the shape of a given surface is known as the interfacial or surface tension” [7].

To electrospin fibres from solution droplet at the tip of the needle, critical voltage V_c is required. The solution forms round droplet at the end of needle/spinneret due to surface tension. As the voltage is applied and increased between droplet and collector, the droplet shape changes from round to conical. This elongated form of droplet is called

“Taylor cone” [5]. The charges generated between the atoms of the solution due to electric charge generate repulsions between them. The droplet becomes elongated. When the applied voltage overcomes the surface tension of the solution at a critical voltage (V_c), a the jet emerges from the droplet [6]. Surface tension holds the solution into a round shape during spinning. A solution with low viscoelastic force and high surface tension will form beads [6].

In the present work, the Kruss K6 surface tension meter (Figure 3:6) was used. It follows the ring method. In the ring method, the ring is dipped in the solution. The solution is raised as the ring (Figure 3:5, Table 3:1) is raised from the solution. The ring forms a film with the solution sample. The solution is then lowered until the liquid film (Figure 3:4) is stretched. As the film is stretched the force is recorded. At only a precise maximum force the film will be broken. The reading of this maximum force is recorded. At the maximum, the force vector is exactly parallel to the direction of motion and the contact angle θ is 0° .

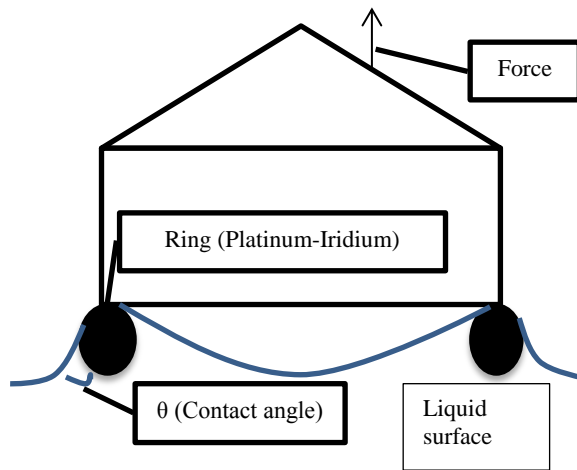
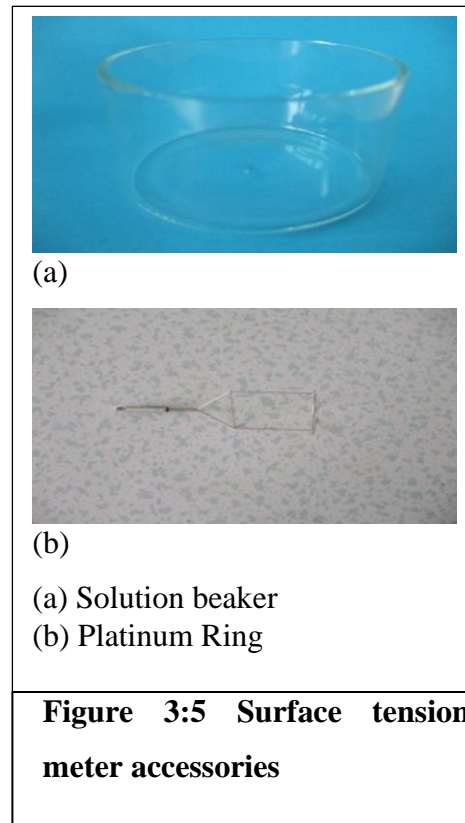


Figure 3:4 Schematic diagram of the ring methods



The maximum force is only determined precisely on the return movement of the ring and used to calculate the tension.

The calculation is made according to the following equation:

$$\sigma = \frac{F_{max} - F_v}{L \cdot \cos \theta}$$

(σ =surface or interfacial tension; F_{max} =maximum force; F_v =weight of volume of liquid lifted; L =wetted length, θ =contact angle)

The contact angle θ decreases, with increased extension. The θ has 0° value at the point of maximum force, so, $\cos\theta$ will be 1[7].

Surface tension has the dimension of force per unit length or energy per unit area.

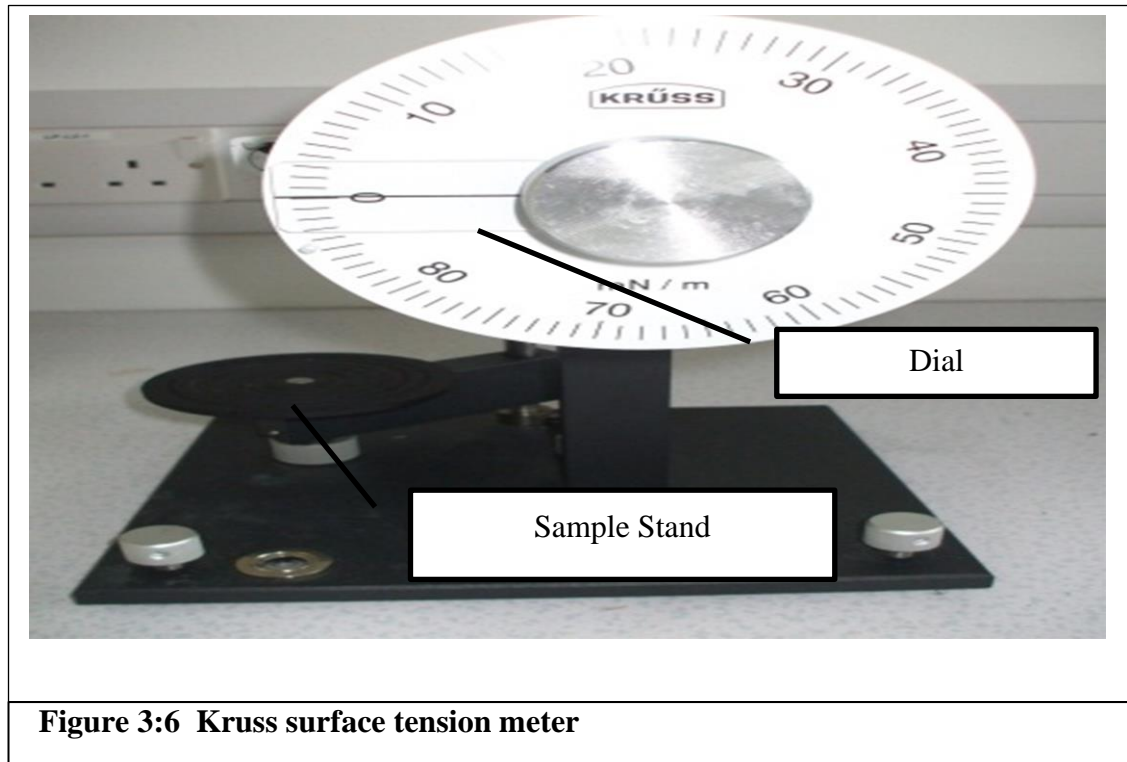


Figure 3:6 Krüss surface tension meter

Table 3:1 Specifications of ring (Krüss K6)

Ring material	Platinum-Iridium
Wetted length	119.95mm
Circumference	59.97mm
Ring radius	9.545mm
Wire radius	0.185mm
R/r	51.6

3.2.3 Conductivity of Solution

In the electrospinning process, the electric charge is transferred from the electrode to the spinning droplet at the needle tip. Solvent conductivity is very important for the transfer of electric field to the solution. Solutions with zero conductivity cannot be electrospun. Generally, the solution conductivity is found higher compared to solvents, due to free

ions of solutes (polymer and impurities). The polymer itself has ionic functionalities as with polyelectrolyte. The electrical conductivity of a solution is due to free ions available and ionic mobility. Higher polymer concentration in a solution may reduce electrical conductivity due to restricting ionic movements, due to many ions.



Figure 3:7 Oakton CON 110 conductivity meter

Conductivity is the ability of a material to conduct electric current. “The conductivity (or specific conductance) of an electrolyte solution is a measure of its ability to conduct electricity. Conductivity is traditionally determined by measuring the AC resistance of the solution between two electrodes” [8].

The basic principle of conductivity measurement is simple. Two electrode plates are placed in the sample to apply electric potential, and the current is then measured according to:

$$G = I/R = I (\text{amps}) / E (\text{volts}) \quad (3.1)$$

Where G = Conductivity, R = Resistivity, I = Current, E= Voltage

The basic unit of conductivity is the Siemens (S), formerly called the mho. The standardized measurements are expressed in Siemens/cm (S/cm) to compensate with any electrode dimension variations.

$$C = G \times (L/A) \quad (3.2)$$

Where, C = Specific conductivity; G = measured conductivity and L/A = electrode cell constant, where L is the length of the column of liquid between the electrode and A is

the area of the electrodes. Most conductivity meters have a two-electrode cell with the electrode surface made up of platinum, titanium, gold-plated nickel, or graphite.

We used Oakton hand held CON 110 conductivity meter to measure solution conductivity (Figure 3:7). Con 110 is microprocessor based conductivity meter with LCD display. The meter has a conductivity electrode (ECCONSEN91, electro constant =1) with built in temperature sensor. The temperature sensor used for auto temperature compensation because, the conductivity meter is affected by temperature. The conductivity meter is calibrated with calibration solution and then the electrode is immersed in the solution to measure the conductivity[9].

3.2.4 Ultra Violet-Visible Spectroscopy (UV-vis)

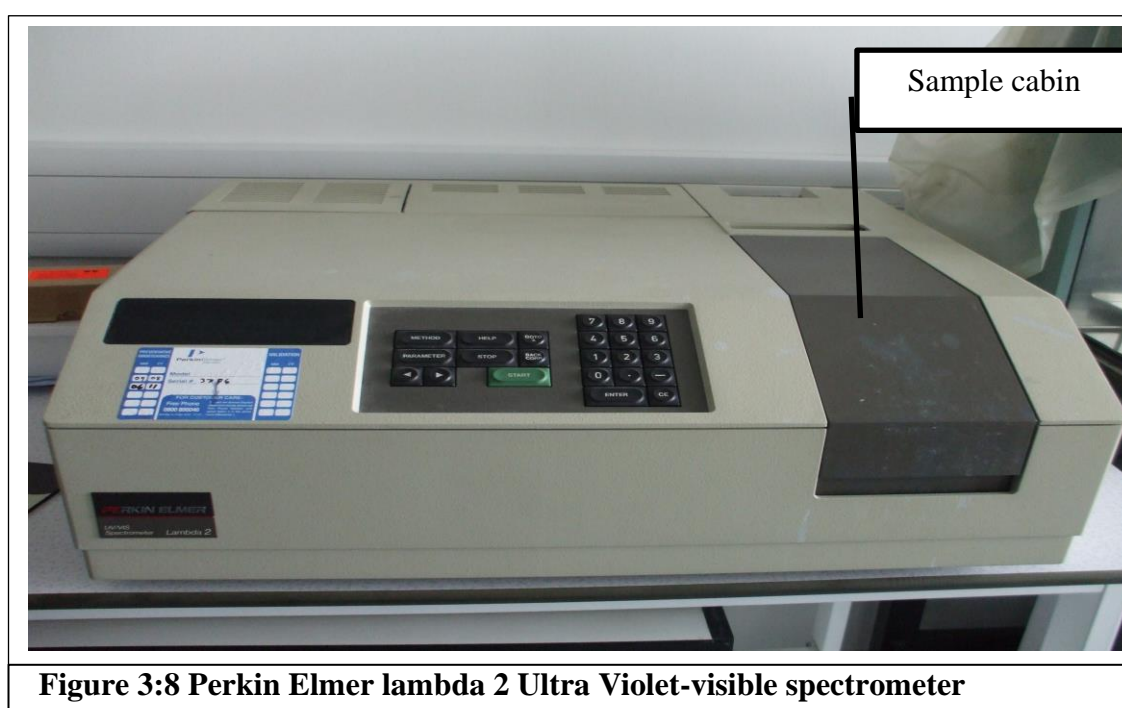


Figure 3:8 Perkin Elmer lambda 2 Ultra Violet-visible spectrometer

The visible range of electromagnetic waves is restricted part of the total spectrum. The ultra violet (UV) region starts at the violet colour visible range. With any further decrease in wavelength from violet the electromagnetic waves fall in the UV region.

The visible spectrum is considered between 380-770nm and the ultra violet region is normally considered from 200-380nm. A wavelength is the distance between adjacent peaks (or trough) and can be measured in meters, cm or nanometres.

The UV or visible light wave passes through a compound. The wave promotes the energy level of the electron from a ground level to a higher energy excited level in the compound molecules. The electron absorbs energy, when it is promoted to higher energy level. For a smaller electron jump less energy will be required compared to a big jump. Depending on the required energy, the electron will absorb the light wave. These energies can be measured. Wavelength of maximum absorption and absorption intensity

depends on molecular structure. UV-Visible regions are not specific enough to identify unknown samples. This data can be useful to confirm sample details. In UV-Visible absorption spectrum, the vertical axis shows absorbance (amount of light at a particular wavelength that light is absorbed more). In the present study, absorption peak of all the solutions were studied in UV-visible range using Perkin Elmer lambda 2 UV-visible spectrometer (Figure 3:8). Different amount of light is absorbed at each wavelength. Each spectrum can be used to identify chemicals.

3.3 Polymer and Nano Fibre and Mat Testing

3.3.1 Cold Field Emission Scanning Electron Microscope

Principle of Electron Microscope

The electron microscope uses a beam of electrons to illuminate the specimen and produces a magnified image. The ordinary non confocal light microscope can magnify an image up to 2000x and is limited by diffraction to about 200nm resolution. An Electron microscope uses electrons, which have 1,00,000 times shorter wavelength compared to visible light (photons). SEM can achieve resolution up to 50pm (picometer) and magnification up to 10,00,000x [10].

The ordinary light microscope magnifies images by glass lenses to focus light on or through the specimen. In electron microscope (EM) electrostatic and electromagnetic controls act as lense to focus an electron beam on the image. The electron beam is initially diffracted in transmission. Then the electron beam is refocused by the EM. The magnified image (from hundreds to many hundred thousands) of the focused area can be seen on a screen or film [10].

The electron microscope uses electrostatic and electromagnetic "lenses" to control the electron beam and focus it to form an image. These lenses are analogous to, but different from the glass lenses of an optical microscope that forms a magnified image by focusing light on or through the specimen. In transmission, the electron beam is first diffracted by the specimen, and then, the electron microscope "lenses" re-focus the beam into a Fourier-transformed image of the diffraction pattern for the selected area of investigation. The real image thus formed is magnified by a factor ranging from a few hundred to many hundred thousand times, and can be viewed on a detecting screen or

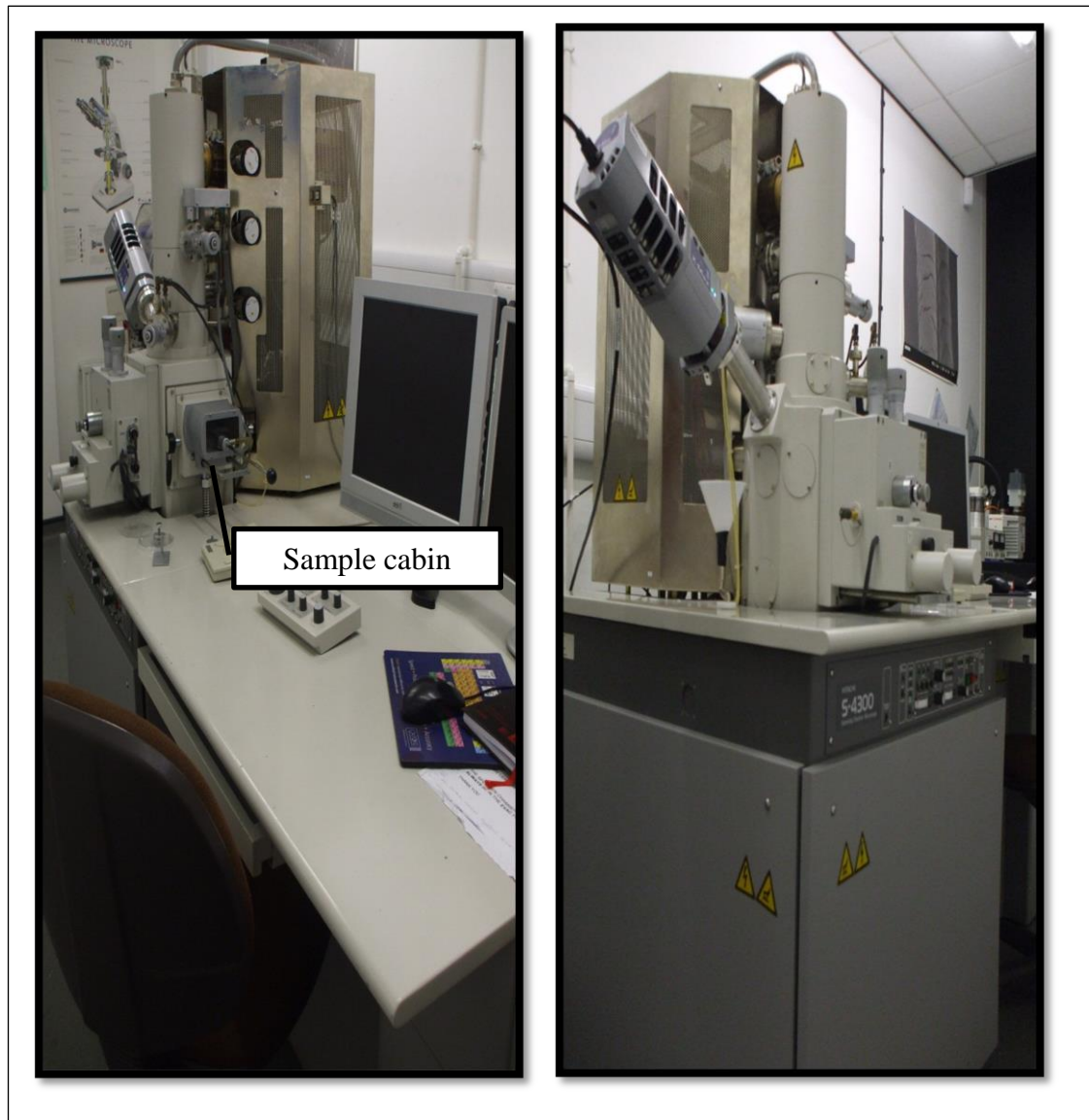


Figure 3:9 Cold Field Emission Scanning microscope Hitachi S-4300

recorded using photographic film or plates or with a digital camera [10].

Scanning Electron microscope

In scanning electron microscope (SEM) the images of sample are scanned with a high-energy beam of electrons in a raster scan pattern. The electrons interact with the atoms of the sample and generate signals containing sample surface topography information. The SEM uses secondary electrons, back-scattered electrons (BSE), characteristic X-rays, light (cathodoluminescence), specimen current and transmitted electrons to create images.

A wide range of magnifications is possible, from about 10 times (about equivalent to that of a powerful hand-lense) to more than 500,000 times, about 250 times the magnification limit of the best light microscopes. Back-scattered electrons (BSE) are reflected beam electrons from the sample by elastic scattering. BSE are based on the

characteristic X-ray spectra. The BSE signal intensity is strongly related to the spectrum atomic number (Z). BSE images can provide different sample element distribution. The emitted characteristic X-rays are used to identify the composition and measure the abundance of elements in the sample [11].

FE-SEM (Field Emission Scanning Electron Microscope)

The FESEM are high vacuum instruments (less than 1×10^{-7} Pa in the gun zone). The vacuum allows electron movement along the column without scattering and helps prevent discharges inside the gun zone.

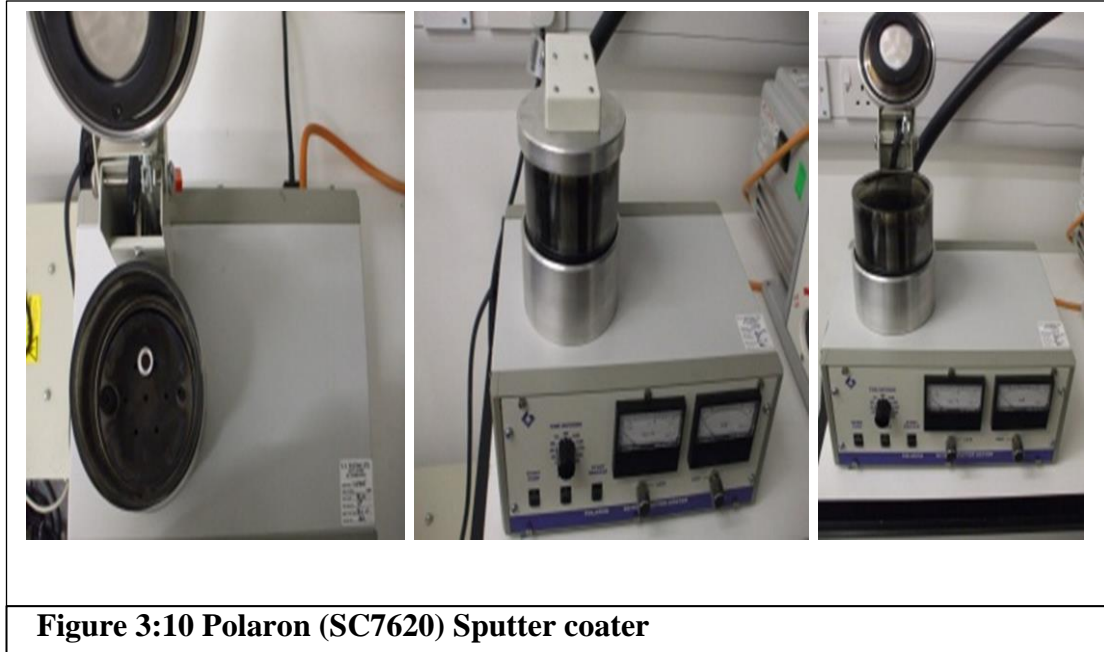


Figure 3:10 Polaron (SC7620) Sputter coater

The electron gun provides a large and stable current in a small beam. The type of emitters (thermionic emitter and field emitter) makes difference between the Scanning Electron Microscope (SEM) and the Field Emission Scanning Electron Microscope (FESEM). Thermionic emitters in SEM use electrical current to heat up a filament. The two most common thermo-emitter filaments are Tungsten (W) and Lanthanum Hexaboride (LaB6). Field Emission in FESEM generates electrons and avoids heating. A Field Emission Gun (FEG) (cold cathode field emitter) does not heat the filament. The emission is initiated by placing the small tip tungsten filament in a huge electrical potential gradient. An electric field can be concentrated to very high level due to the small tip radius (100nm). FESEM produces a cleaner image, less electrostatic distortions and spatial resolution $< 2\text{nm}$ (that means 3 or 6 times better than an SEM) due to using a field emission gun.

In the present work, a Hitachi S-4300 CFE-SEM (Figure 3:9) was used to investigate fibre morphology. All samples were placed on SEM stubs. Sample images were

obtained after coating with gold palladium. Different accelerating voltage (Usually 1kV), and current of 10 μ A were used.

Sample preparation for SEM

All samples in the present work were coated with gold-palladium for 45 or 60 seconds at 18mA. All samples on stub were coated by Polaron Sc7620 (Figure 3:10), Quorum technologies Ltd, UK). The coating was performed under an Argon gas environment. Due to nonconductive nature of the electrospun fibres, a conductive coating is needed for a better image in SEM. The electron beam can interact with the conductive coating, which is needed for SEM images.

3.3.2 X-Ray Diffraction (XRD)

X-rays are electromagnetic radiation with wavelengths between about 0.02 Å and 100 Å (1Å = 10⁻¹⁰ meters). Our eyes are sensitive to the different wavelengths of visible light in the electromagnetic spectrum which appear to us as different colours. X-ray wavelengths are similar to atoms size and they are useful to explore crystals.

X-rays have smaller wavelength than visible, which is higher in energy. X-rays with high energy can penetrate in to the matter more easily than visible light.

X-ray Diffraction and Bragg's Law

X-ray diffraction (XRD) is a non-destructive tool to analyse all kinds of matter ranging from fluids, to powders and crystals. XRD is used in research, production and engineering for material characterization and quality control. X-ray crystallography is the study of crystal structures through X-ray diffraction techniques. X-ray crystallography leads to understand the material and their molecular structure of the substance. The x-ray beam on a crystalline lattice in a given orientation is scattered in a definite manner depending on the atomic structure of the lattice. Solid matter can have distinct states according to molecular/atomic arrangements: crystalline and amorphous.

Crystalline: The atoms are arranged in a regular pattern, and there is the smallest volume element that by repetition in three dimensions describes the crystal.

Amorphous: the atoms are arranged in a random way similar to the disorder we find in a liquid. [12]“....every crystalline substance gives a pattern; the same substance always gives the same pattern; and in a mixture of substances each produces its pattern independently of the others.” [13]

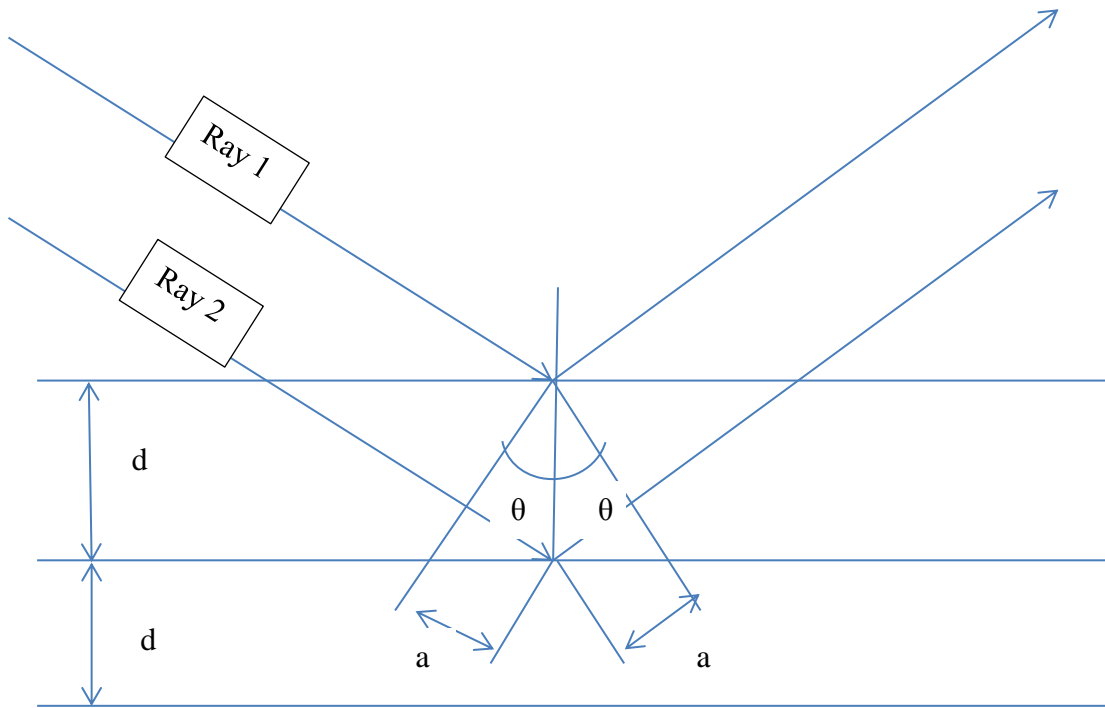


Figure 3:11 Bragg's Law

When X-ray hits a solid atom, each atom acts as a source of radiation. The electron gains energy and starts oscillating at the same frequency as the incoming X-ray energy field. If the atoms in the crystals are arranged in a regular pattern, the energy leaving the solid will be in constructive interference in few directions. If the atoms are not arranged in a pattern, destructive interference will occur. The energy leaving the atom will reduce or there will be no energy. The constructive interference and destructive interference provide a diffraction pattern.

If troughs and crests of the waves are in phase with each other (i.e.; trough facing trough and crest facing crest), their amplitude will be added. The resultant wave will have higher amplitude compared to the incident wave, this is called constructive interference. If the troughs and crests are not in phase with each other (i.e. displaced and not facing each other), their resultant amplitude will decrease, this is called destructive interference. When troughs and crests are out of phase with each other (i.e., troughs facing crests and crests facing troughs) their resultant amplitude will be zero. The resultant wave will be completely destroyed. Figure 3:11 shows two parallel X-rays (Ray 1 and Ray 2) hitting two planes. The distance between the planes is d . Ray 1 is reflected back from the upper atomic plane and Ray 2 is reflected back from the bottom atomic plane at an angle " θ ". Ray 2 has to travel " $2a$ " distance more than Ray 1.

Where

$$a = d \sin \theta$$

$$2a = 2d \sin \theta$$

Now if “nl” represents wavelength number then:

$$2a = nl$$

$$nl = 2d\sin\theta$$

$2a \neq$ integral number: Ray 1 and Ray 2 are not in phase. That will lead to destructive interference

$2a =$ integral number: Ray 1 and Ray 2 are in phase. That will lead to constructive interference

This is referred to as Bragg's Law for X-ray diffraction.

From the X-ray wavelength (λ) angle (θ) can be measured and the spacing (d) between the atomic planes.

$$d = \lambda / 2 \sin \theta$$

By reorienting crystals, the atomic plane will be exposed to X-rays. The d-spacing between all atomic planes in a crystal can be measured. Hence, the crystal structure and the size of a unit cell can be determined. XRD peaks (Figure 3:12) are very important/unique for every substance. The peak position, peak width and peak intensity are important and unique parameters for every substance [14]

The X-ray Powder Method

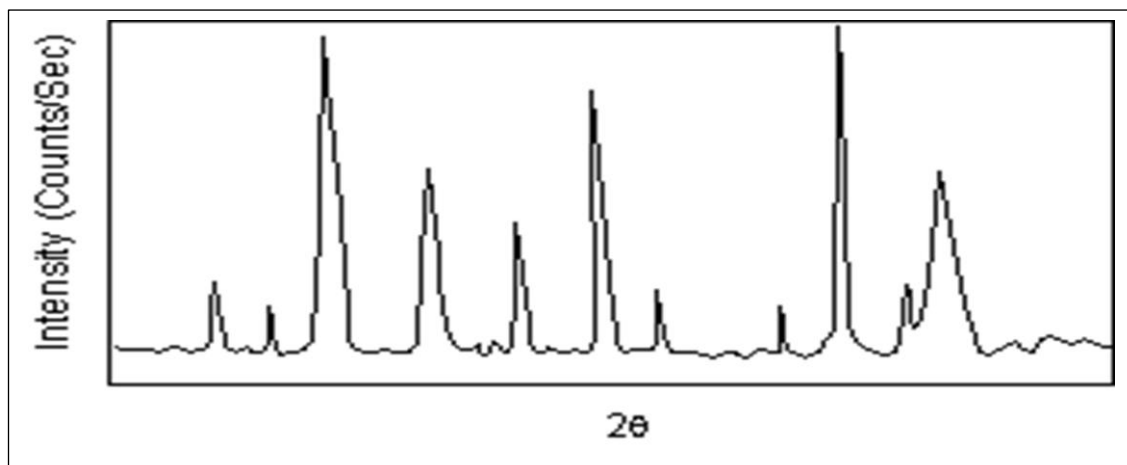


Figure 3:12 Typical X-Ray diffraction graph

In order to determine d spacing for all atomic planes, it would be time consuming to reorient the crystal to measure the angle θ . A powder method is used in XRD. The substance in powder form will have number of randomly oriented atomic planes. At the angle of incident θ from 0° to 90° , almost all the angles of diffraction can be recorded hence different atomic spacing can be detected. An electronic detector detects X-rays from the sample on the opposite side on the X-ray tube at different angles between 0° to 90° .

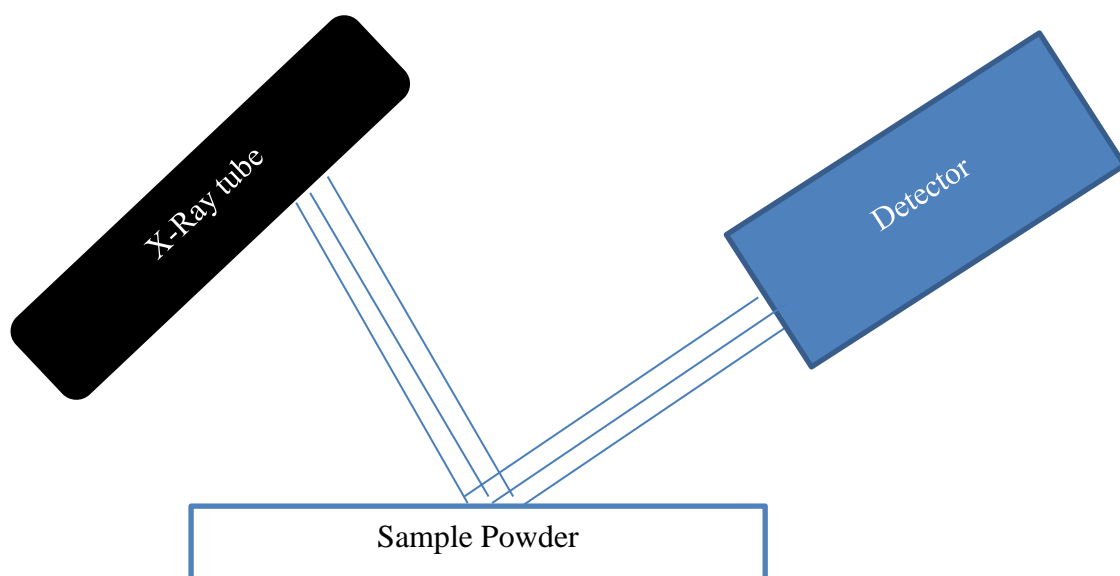


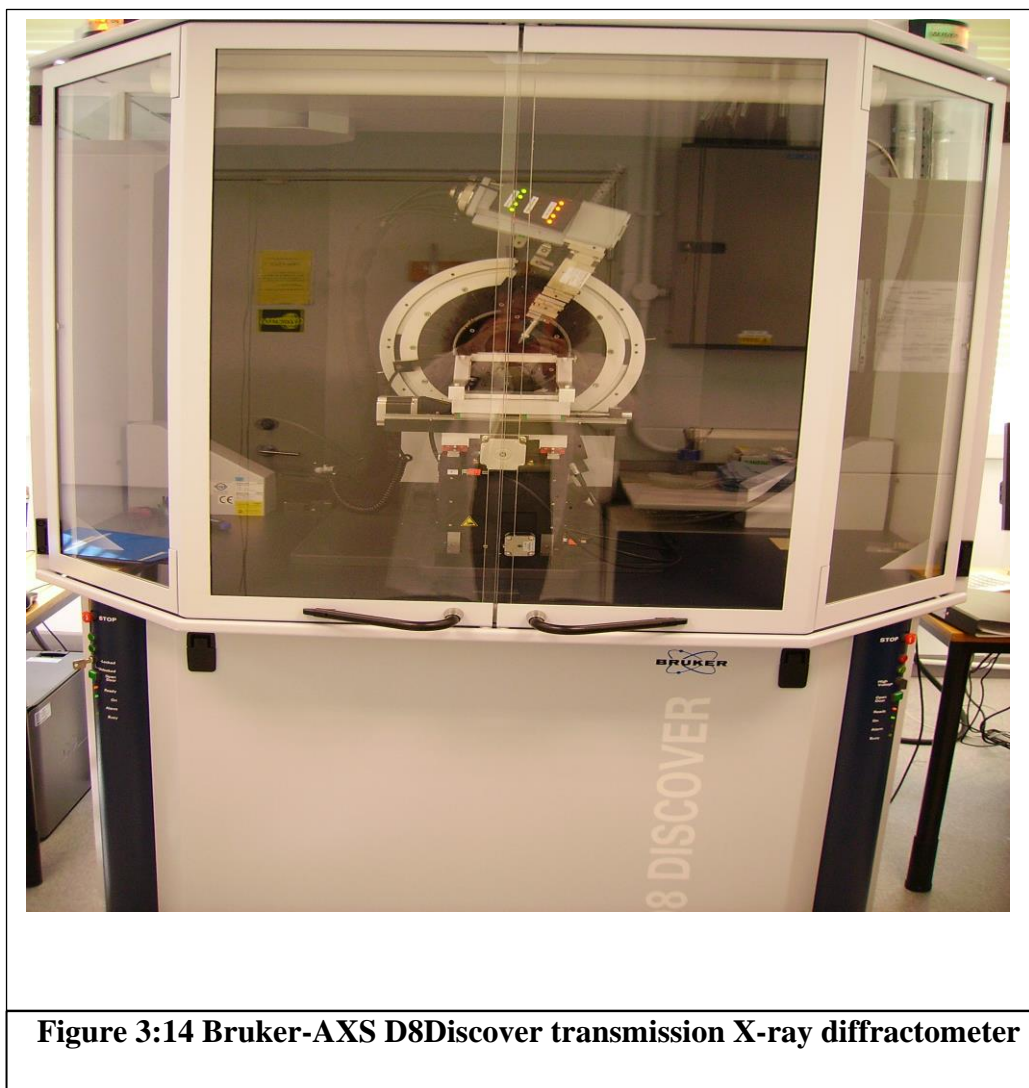
Figure 3:13 Schematic diagram of XRD

The instrument called goniometer, which rotates both X-ray tube and detector. It keeps track of the angle q (Figure 3:13). A computer keeps record of angle q and the X-ray intensity is detected. The Graph of X-ray intensity against $2q$ is plotted and d-spacing is also calculated using Bragg's equation [14, 15].

The XRD can be used for various analytical studies. The end uses are as below:

1. Identification of material: By matching peaks with a database or by comparing diffraction patterns with the chemical structure.
2. Polymer crystallinity: Higher crystallinity causes brittleness of polymers. So it is important to know the crystallinity. The crystalline part of a polymer gives a sharp narrow peak and an amorphous region gives very broad (halo) peak.
3. Residual stress: Any process such as mechanical, chemical or thermal generates a residual stress. So, by measuring the d spacing, the stress distribution can be determined.
4. Texture analysis: The preferred orientation of the crystallites in polycrystalline aggregates.

In the present study, X-ray diffraction patterns were obtained using a Bruker-AXS D8Discover transmission (Figure 3:14) X-ray diffractometer under a scanning range 3 to 85 2θ and step size of 0.202 which means 4061 steps at 5 seconds/step. The total scan time is 35 mins 16 secs; Using a Cu kAlpha source, Lambda 1.5406 angstroms; and scanned at 40kV, 40mA.

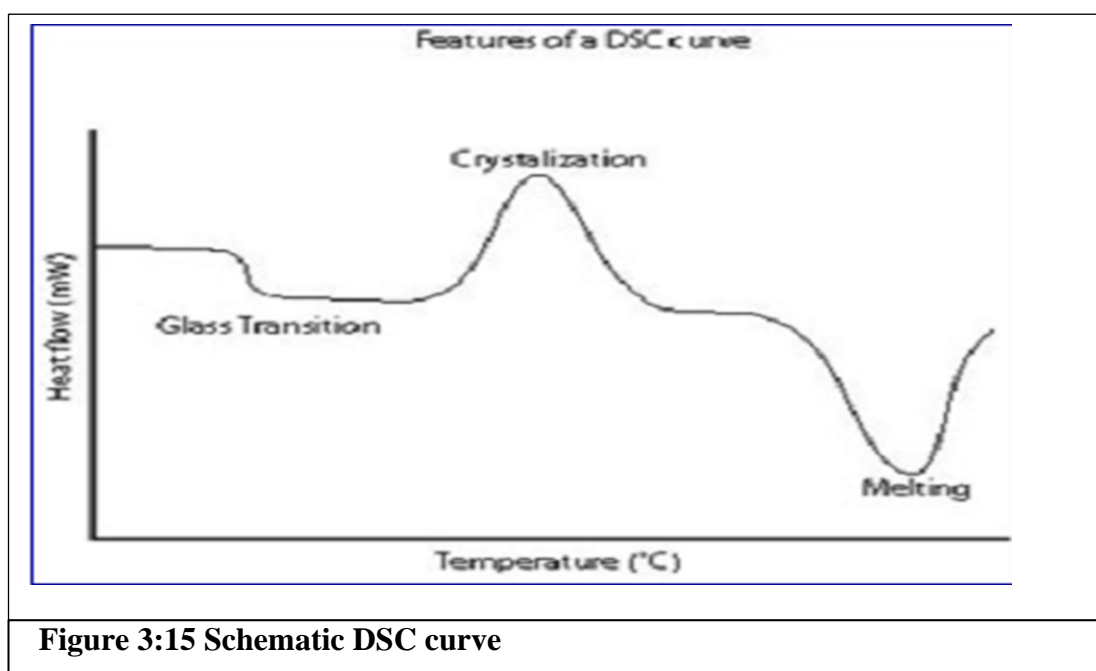


3.3.3 Differential Scanning Calorimetry

DSC measures the overall heat flow and temperature associated with phase transition as the function of the time and temperature of a solution. DSC is a thermo analytical technique to characterize the melting behavior, crystallization, solid-solid transitions, solid-liquid transition, chemical reaction of a solution [16]. With the help of DSC, different phase changes can be studied, which are not visible to the eye. Every material changes its state when heated or cooled for e.g. water becomes ice, when cooled and vapor when heated. The molecules gain energy as a material is heated. Hence, when liquid heated to vapor, the molecules get enough energy to escape from a rigid liquid structure to less restricted vapor structure. Here the material gains energy, hence, it is endothermic transition. The energy/ unit mass is called latent heat. Here the energy supplied does not change or changes very little until a phase change is completed.

As a material is heated, it shows different thermal phenomena as a DSC curve. Glass transition (T_g) occurs in an amorphous material at T_g the heat capacity of the material is increased with more mobility of molecules.

Crystallization occurs, when a material is heated beyond T_g . Here the material becomes more ordered. The crystallization process is exothermic; hence, the thermal energy is released. Material releases energy, while changing from amorphous to a crystalline state. A melting peak T_m occurs when the material melts. A material cannot melt unless it is in a crystalline form. Melting is an endothermic process as the material absorbs energy to melt.



In DSC the difference in the amount of heat required to increase the temperature of a sample compared to reference is measured as a function of temperature. Usually an empty pan is used for reference. The sample and reference are kept at the same temperature during the whole experiment.

The temperature program maintains the $\Delta T/\Delta t$ (heating rate) constant, but the heat flow ($\Delta Q/\Delta t$) changes. The pan with sample in it heat up at different temperature than the empty pan, in spite of the same heat rate applied to both. Because the heat capacity of any material is different than air, so in order to maintain the same heat, higher/less heat flow will need to be supplied at the same heat rate. A computer keeps record of the temperature, heat rate and heat flow. The heat flow can be measured as an endothermic or exothermic peak. Heat flowing to the sample depends on whether the process is exothermic or endothermic.

Some measurements can be done from the DSC data, are as given below. A typical DSC curve is shown in Figure 3:15.

- Glass Transitions
- Melting and Boiling Points
- Crystallisation time and temperature
- Percent Crystallinity
- Heats of Fusion and Reactions
- Specific Heat and Heat Capacity
- Oxidative Stability
- Rate and Degree of Cure
- Reaction Kinetics
- Percent Purity
- Thermal Stability

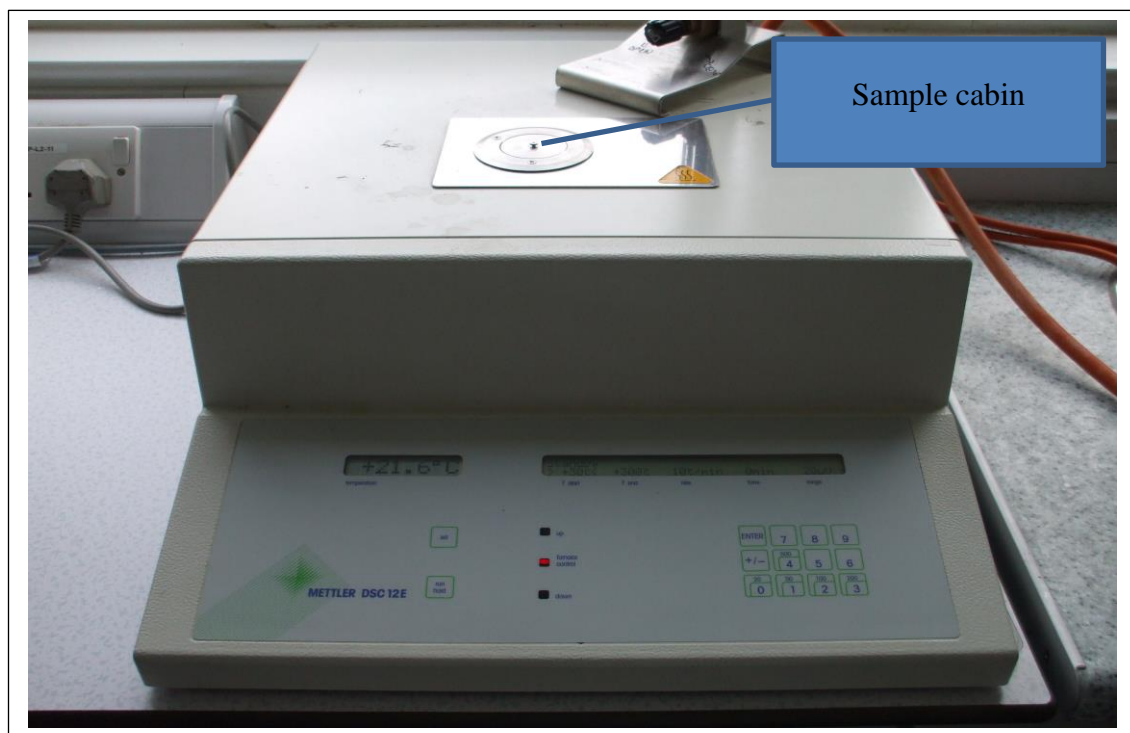


Figure 3:16 METTLER-TA instrument DSC12E

Sample Preparation

Thermal analyses of samples were done by a METTLER-TA instrument DSC12E (Figure 3:16). TOLEDO-TA89 E software was used to obtain DSC curves.

Samples are kept in an aluminium pans with lid. The lid is fixed in the DSC sampler, and 4-5 grams of sample is weighed into an aluminium pan (Figure 3:17). A small hole is created on the top of the lid to allow air or any gas medium to enter in to aluminium

pan. The aluminium pan with the sample in it is kept in to DSC together with the empty aluminium pan. Factors such as scan rate, pan type, gas type, heating rate, sample weight can affect DSC results.



Figure 3:17 DSC Sampler

3.3.4 Fourier Transform Infrared (FTIR) Spectrometry

IR radiation excites molecules into higher energy state. As IR is passed through a sample, some of the IR is absorbed by the sample and some passes through it. As a result, the IR patterns of molecular absorption and transmission unique to the tested sample are generated. IR is like a fingerprint for every particular type of material. The chemical bonds oscillations can be in any of the forms such as vibration, stretching, bonding, rocking, wagging. The vibration occurs at a specific frequency according to bonds present between atoms. According to the molecular structure, the IR radiation wavelength is absorbed. The wavelength absorbed by a particular molecule is decided by the energy difference between rest and excited vibrational states.

The absorption wavelength is proportional to initiate intra molecular oscillations. There are different regions allotted to IR waves. 14000cm^{-1} to 4000cm^{-1} for near infrared (NIR), 4000cm^{-1} to 400cm^{-1} for mid infrared (MIR) and 400cm^{-1} to 10cm^{-1} for far infrared (FIR). FTIR is the data processing technique for infrared raw data converted to understandable data/graphs. FTIR is useful for identifying any organic or inorganic chemicals in solid, liquid or gas form. It is useful to identify functional groups in chemical bonds [17, 18].

The molecular motions can be associated with functional group oscillations, which are always at the same location of the IR spectra irrespective of the substance. Any IR

absorption pattern can be easily differentiated for each compounds and can be used as a fingerprint for that specific substance [18, 19].

Higher to lower energy electromagnetic waves in the visible range appears as different colours.

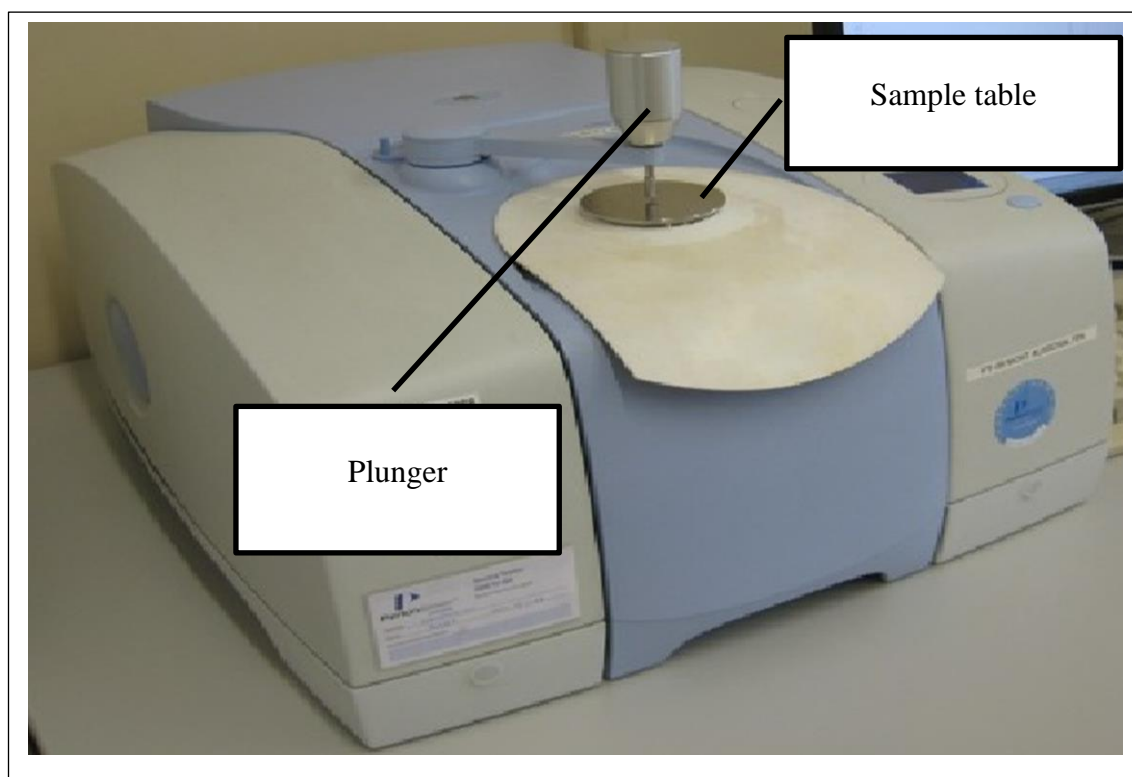


Figure 3:18 ATR-FTIR Perkin-Elmer Spectrum 100 FT-IR

On the lower end of the visible range the infrared zone starts. Infrared waves have lower frequency and longer wavelength compared to visible range electromagnetic waves.

IR spectra can be used for compound specific detection and identification. According to Beer's law, the IR spectra can also be used for quantitative analysis. The intensity or the amplitude of the absorbance (i.e. peak height) is proportional to the concentration of compounds [19].

$$A = a.b.c$$

Where, A =absorbance, a = absorbance, b = path length, c= sample concentration

The FTIR is an analytical technique for IR spectroscopy and it converts IR data into useful quantitative as well as qualitative form. The mathematical technique called Fourier transformation and it is used to decode IR data.

The FTIR spectrometer plots a graph of absorbance (or % transmittance) vs energy in the form of wave number cm^{-1} . The IR wavenumber range depends upon the detector

but usually the $500\text{-}4000\text{cm}^{-1}$ range is studied. The FTIR spectrometer can be divided into two regions. $1600\text{-}4000\text{cm}^{-1}$ is called “functional group region” and $500\text{-}1600\text{cm}^{-1}$ is called “fingerprint region”. The functional group region shows peaks related to stretching motions of the functional groups. The peaks are easily identifiable for groups such as alcohols, amines, aromatics, amides, aliphatic, alkenes, acids, esters and acrylonitrile. In the fingerprint region the peaks are complex and overlap with each other. The pattern of peak in this region is very important; it can be used as fingerprint for a particular compound [19].

Sample Preparation

Sample preparation is a very important part of conventional FTIR. In conventional FTIR the solid sample has to be in a thin film form. It is not possible to convert all chemical components in thin films on their own. Few substances such as KBr, BaF₂, AgCl, have no peaks or minimum identifiable impact on IR spectra. Such substances can be used as matrices to form thin films of the chemical compounds for IR study. The matrix material should be chosen such that it should not react with the chemical compound. The process of making film is time consuming. A new technique called “Attenuated total Reflection” with nil or very small sample proportion is now used. In ATR, the IR beam is passed through an optically dense crystal with higher reflective index at a certain angle. The fraction of the incident beam reflected and the wave extends beyond the crystal surface into sample held on the crystal. The wave only penetrates 0.5μ to 5μ beyond the crystal into the sample. So, the sample and crystal must be in good contact. The ATR method is a versatile method for any shape, configuration, thickness, liquids, solids and powders can be analysed [19].

There are a number of crystal materials available. Zinc selenide (ZnSe) and Germanium crystal are widely used.

Infrared spectra were obtained on the Perkin-Elmer Spectrum 100 FT-IR (Figure 3:18). The universal ATR sampling accessory, deposited neatly onto a diamond/ZnSe plate. The scans were carried out between 650 and 4000cm^{-1} at the resolution of 4cm^{-1} .

3.3.5 Tensile Test

In the present study tensile tests were done to characterize and compare the mechanical properties of samples. The Instron tensile strength tester used is working on constant rate of extension principle.

The CRE machine has two clamps. One is stationary and the other is moved at a constant speed throughout the test. For yarn and electrospun mat tensile testing,

specimens of specific dimensions were taken and extended at a constant rate until they broke. The maximum force and elongation at maximum force were recorded. The tensile tests were carried out on an Instron tester (Model 3345) (Figure 3:19).

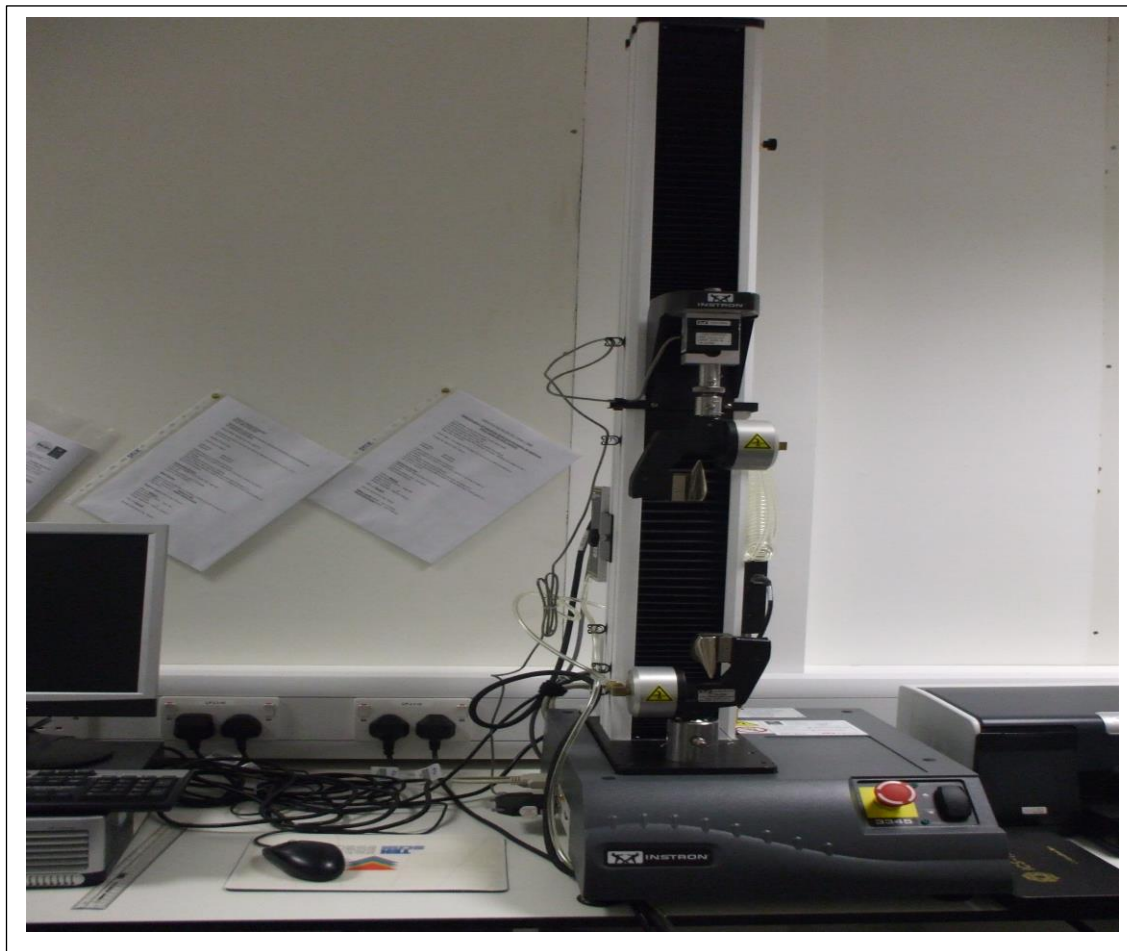


Figure 3:19 Instron Tensile tester (Model 3345)

3.3.6 Antibacterial Test

Gram-positive *Staphylococcus aureus* and Gram-negative *Pseudomonas aeruginosa* bacteria were used to study the antibacterial properties of electrospun Manuka honey mats. The micro-organisms (cultured from NCTC) were purchased from TCS biosciences ltd., U.K. The micro-organisms were received in 1mm solid domed freeze dried pellets forms in small vials. The discs were removed from the vials by sterile forceps. Oxoid nutrient broth prepared media in bijoux without salt and with 7.5% salt were purchased from fisher scientific, UK. The freeze dried discs were placed in the nutrient broth between two flames to maintain sterile atmosphere. The *Staphylococcus aureus* and the *Pseudomonas aeruginosa* discs were placed in nutrient broth. The freeze dried discs were readily soluble in nutrient broth. The broth solutions were gently shaken to dissolve the discs completely. The broth bottles were kept in an incubator at

37°C for 24 hours. The broth solutions turned turbid due to growth of micro-organisms, and were spread on nutrient agar plates with “L shaped” sterile spreader between flames. Ready prepared Oxoid nutrient agar plates (90mm) were purchased from Fisher scientific, UK. The electrospun mats (15PEO, 50MHPEO, 65MHPEO) were cut into round discs, the 15PEO and 100% MH solutions were placed on 6mm filter disc. All samples were placed on nutrient agar plates and subsequently in an incubator at 37°C for 24 hours. All nutrient agar plates were investigated for antibacterial activities.

3.4 Bibliography

- [3.1] H. M. Santos and J. L. Capelo, "Trends in ultrasonic-based equipment for analytical sample treatment," *Talanta*, vol. 73, pp. 795-802, 2007.
- [3.2] M. A. Rostagno, M. Palma, and C. G. Barroso, "Ultrasound-assisted extraction of soy isoflavones," *Journal of Chromatography A*, vol. 1012, pp. 119-128, 2003.
- [3.3] P. Heikkila, "Electrospinning of polyacrylonitrile (PAN) solution: Effect of conductive additive and filler on the process," *eXPRESS Polymer Letters*, vol. 3, pp. 437-445, 2009.
- [3.4] Anon, "More solutions to sticky problems - A guide to getting more from your brookfield viscometer," B. E. Labs, Ed., ed. USA: Brookfield Engineering Labs, 2005.
- [3.5] K. Garg and G. L. Bowlin, "Electrospinning jets and nanofibrous structures," *Biomicrofluidics*, vol. 5, p. 13403, 2011.
- [3.6] A. Patanaik, R. D. Anandjiwala, R. S. Rengasamy, A. Ghosh, and H. Pal, "Nanotechnology in fibrous materials—a new perspective," *Textile Progress*, vol. 39, pp. 67-120, 2007.
- [3.7] Anon. *Surface tension*. Available: http://en.wikipedia.org/wiki/Surface_tension
- [3.8] Anon. *Conductivity (electrolytic)*. Available: http://en.wikipedia.org/wiki/Solution_conductivity
- [3.9] Anon. (2003). *Instruction Manual Oakton con11 & 110 Handheld Conductivity/TDS/Temperature/RS232C Meter*. Available: http://www.specmeters.com/assets/1/22/2220-Full_Manual.pdf
- [3.10] Anon. *Electron microscope*. Available: http://en.wikipedia.org/wiki/Electron_microscope
- [3.11] Anon. *Scanning electron microscope*. Available: http://en.wikipedia.org/wiki/Scanning_electron_microscope

- [3.12] C. J. Garvey, I. H. Parker, and G. P. Simon, "On the Interpretation of X-Ray Diffraction Powder Patterns in Terms of the Nanostructure of Cellulose I Fibres," *Macromolecular Chemistry and Physics*, vol. 206, pp. 1568-1575, 2005.
- [3.13] A. W. Hull, "A new method of chemical analysis," *J Am Chem Soc*, vol. 41, pp. 1168-1175, 1919/08/01 1919.
- [3.14] S. A. Nelson. (2011). *X-Ray Crystallography*. Available:
<http://www.tulane.edu/~sanelson/eens211/x-ray.htm>
- [3.15] Anon. (1999). *Basics of X-ray Diffraction*. Available:
<http://epswww.unm.edu/xrd/xrdbasics.pdf>
- [3.16] S. Roy, A. T. Riga, and K. S. Alexander, "Experimental design aids the development of a differential scanning calorimetry standard test procedure for pharmaceuticals," *Thermochimica Acta*, vol. 392–393, pp. 399-404, 2002.
- [3.17] J. Coates, "Interpretation of Infrared Spectra , A Practical Approach," *Encyclopedia of Analytical Chemistry*, pp. 1-23, 2000.
- [3.18] M. Gallignani and R. Brunetto Mdel, "Infrared detection in flow analysis - developments and trends (review)," *Talanta*, vol. 64, pp. 1127-46, Dec 15 2004.
- [3.19] M. Poliskie and J. O. Clevenger, "Fourier transform infrared (FTIR) spectroscopy for coating characterization and failure analysis," *Metal Finishing*, vol. 106, pp. 44-47, 2008.

Chapter 4 : Investigating, Formation and Characterisation of Manuka Honey Nanofibres and its Antibacterial Properties for Wound Healing

4.1 Introduction

Honey is a wound healing remedy that was used by ancient civilizations [1, 2]. It is mentioned as a healing substance in the Bible, the Koran, and the Torah [3, 4]. Honey is most commonly consumed in its unpreserved state, i.e. liquid, crystallized or in the comb. It is eaten as a food, used as a flavouring agent, food preservative[5, 6], sweetener[7], humectant[8, 9], in skin care and beauty therapy products[10, 11] also in wound care products, in various cosmetics such as hand lotions and moisturizers to soap bars and bubble baths, cleansers, creams, shampoos and conditioners. It is also used as medicine (i.e. for wound treatment, ulcers, burns etc.) either by ingestion or by topical application [3]. Honey has long been known to possess a broad spectrum of activity against a wide range of bacteria such as pathogenic as well food-spoiling aerobes and anaerobes, gram-positives and gram-negatives of around 60 species [2, 4, 7, 12-15] including MRSA [16]. Other benefits of honey include antioxidant, anti-tumour, antiinflammatory, antimutagenic and antiviral properties [6]. The predominant acid found in honey is gluconic acid. Some of the components (carbohydrates, water, and traces of organic acids, enzymes, amino acids, pigments, pollen and wax) are due to maturation of the honey, some are added by the bees and some of them are derived from the plants[17].

The definition of honey depends upon who defines it. Most people think of honey as a food, but some others consider it as an elixir, and still some as medicine[15]. The factors responsible for the bactericidal activity of this honey are the high sugar concentration, H_2O_2 , the 1,2-dicarbonyl compound methylglyoxal (MGO), the cationic antimicrobial peptide bee defensin-1 and the low pH[12, 18], high osmolality[16, 19] and some physical properties such as high viscosity, acidic pH (3.2 to 4.5) [20] is said to be inhibitory to many animal pathogens.

Active Manuka honey is regarded as a special honey derived from the Manuka tree (*Leptospermum scoparium*) [21] often exhibits antibacterial activity called the unique Manuka factor (UMF) [5, 21, 22] that is unrelated to the content of hydrogen peroxide, which is responsible for the antibacterial activity of other honeys. This unique activity

of Manuka honey is due to the presence of methyl glyoxal [22]. Although very low levels of MGO are found in most honey, the high level of MGO in Manuka honey is unique. The UMF is rated from 0 (low efficacy) to 20 (high efficacy) and over, with the higher rating indicating higher antibacterial potency. UMF rating is based on a well diffusion assay where the area of exclusion of bacterial growth that the honey causes relative to the phenol control is measured [28]. For example, a UMF rating of 10 has equivalent antimicrobial potency to a 10% phenol solution [6]. Active Manuka honey, with its non-peroxide, antibacterial activity, is more effective than honey with hydrogen peroxide against some types of bacteria [23].

Electrospinning is a fibre-forming technology that uses electrostatic force to draw a polymer solution into fine jets, producing fibres with a diameter ranging from tens of nanometers to several micrometres. These ultrathin fibres have been explored for use in applications such as drug delivery, high-performance filters, wound dressing, artificial tissue, and protective clothing and as food-related additions as for example in aiding digestion.

4.1.1 Electrospinning Of Manuka Honey

Electrospinning of various Manuka honey aqueous solutions with concentrations ranging from 10 to 60 w/w % were investigated in preliminary research. It was observed that droplets fell down from the spinneret and no continuous jets formed, because the Manuka honey solutions did not have sufficient viscoelasticity to form a continuous stream in the spinning process. In order to electrospin and enhance the potential biocompatibility of the electrospun Manuka honey fibres, all-aqueous process for electrospinning of Manuka honey is done in combination with PEO. PEO is well-documented as a biocompatible polymer and has been successfully blended with collagen in electrospinning[24]. A few groups of researchers claimed that biopolymers, including collagen, silk, casein, chitosan did not electrospin from aqueous solutions, but can be successfully electrospun by blending with PEO [25, 26]. The principles of electrospinning are explained in chapter 1, Fig 1:6. The fibre morphology depends on various parameters such as solution property, process parameters, atmospheric conditions. The present study was conducted to electrospin MHPEO fibres and to study the effect of various parameters on fibre properties. Various studies such as DSC, mechanical strength, antibacterial property were also investigated.

4.2 Material and Methods

4.2.1 Materials

Polyethylene oxide (PEO) with an average molecular weight 3,00,000 was purchased from Sigma Aldrich, UK. Manuka honey (MH) (UMF 25+) was purchased from Holland and Barrat, U.K. All solutions were stored at room temperature and used without further purification.

4.2.2 Solution Preparation

15% (w/w) PEO solution was prepared in deionised-sterile water. Polyethylene oxide powder was added to water at room temperature and dissolved by a mechanical stirrer for 2 days. In order to make Manuka honey solution in PEO (MHPEO), Manuka honey was added and stirred well for 3 hours to mix well with PEO. Two solutions with MH to PEO solution ratio of 10% (w/w) (10MHPEO) and 15 % (w/w) (15MHPEO) were prepared.

4.2.3 Solvent and Solution Properties (Viscosity, Surface Tension and Conductivity)

The viscosities of all solutions were measured with a Brookfield DV-II Pro using an S63 spindle. Surface Tension was measured by a Kruss surface tension meter (model K6). Conductivity was measured with an Oakton con 110 handheld conductivity meter.

4.2.4 Ultra Violet - Visible Spectroscopy

Absorption peak of all the solutions were studied in UV-visible range using a Perkin Elmer lambda 2 UV-Visible spectrometer. A different amount of light is absorbed at each wavelength, so each spectrum can be used to identify different chemical compositions.

4.2.5 Visual Observation

Photos were taken to see changes in miscibility of MH in PEO by Fuji film finepix A805 camera.

4.2.6 Electrospinning

The homogeneous PEO and MHPEO solutions were delivered from a 5 mL syringe. The solution was fed to a vertically orientated (16 gauge) blunt ended metal needle via Teflon tubing. The volume feed rate was digitally controlled by a positive displacement

microprocessor syringe pump (M22 PHD 2000, Harvard Apparatus, Eden bridge Kent, United Kingdom). The needle was connected to one electrode of a high voltage direct-current power supply (MK35P2.0-22, Glassman, New Jersey, USA), and the collector was connected to earth, to create an electric field between needle and collector.

4.2.7 Scanning Electron Microscopic (SEM) Studies

The surface morphology of electrospun mats were recorded with cold field emission Hitachi Scanning Electron Microscope (Model: S-4300, Japan). Samples were mounted on aluminium stubs by using double-sided adhesive tape, then placed in a sputter coater unit (Polaron SC7620) with gold-palladium coating for 60 seconds. Finally, the stubs were placed into the SEM for observation at 1 kV accelerating voltage and 10µamps current.

4.2.8 Differential Scanning Calorimetry (DSC) Studies

Thermal analysis was performed using Mettler DSC 12 E. All 5gms samples were weighed and placed in to aluminium pans. The lids of all the pans were pierced for air circulation. The samples were heated at a scanning rate of 10°C/min. All samples were heated with an empty aluminium pan in atmospheric air..

4.2.9 Fourier Transform Infrared Red Spectroscopy (FTIR)

A Perkin Elmer Spectrum 100 ATR-FTIR Spectrophotometer was used to study the FTIR spectrum.

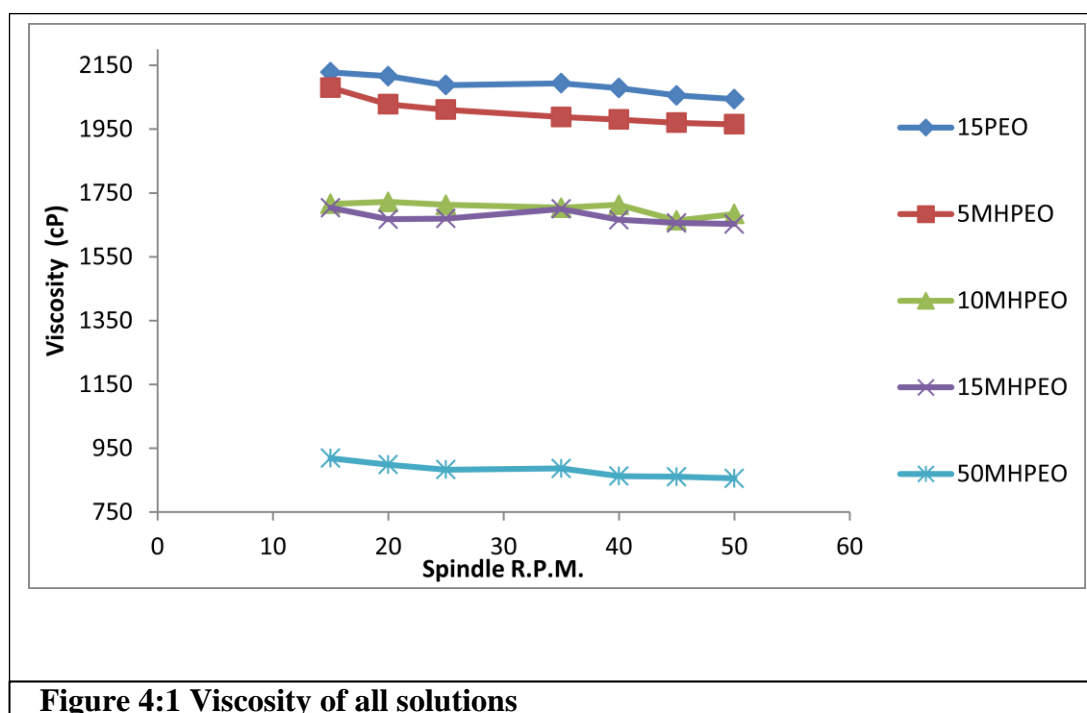
4.2.10 Antibacterial Test

In the present study, Gram-positive *Staphylococcus aureus* and Gram-negative *Pseudomonas aeruginosa* bacteria were used to study the antibacterial properties of electrospun mats. The method is explained in chapter 3, topic 3.3.6

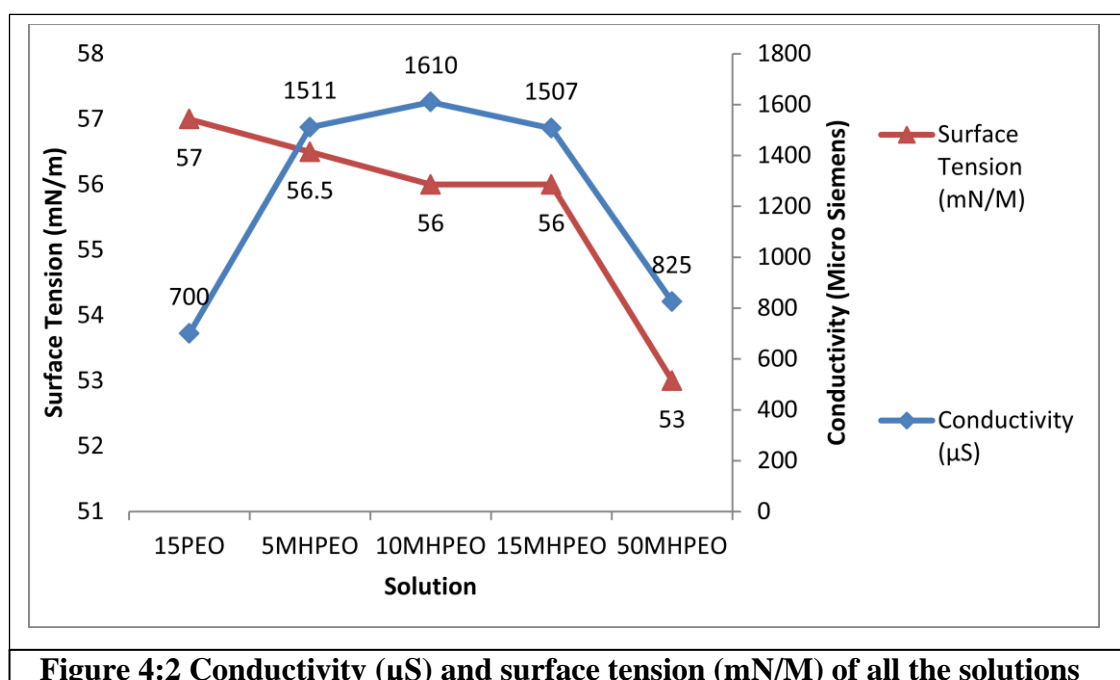
4.3 Results and Discussion

4.3.1 Viscosity, Surface Tension and Conductivity

As can be seen in Figure 4:1, the viscosity of the solution decreased with the addition of MH from 15PEO to 5MHPEO, 10MHPEO, 15MHPEO and 50MHPEO.



The reason is the increase in water content with addition of MH, addition of honey increased overall the water content. Honey is hygroscopic and humectant by nature [7, 28-31].



Considering sugar and other molecules of the solution, water in honey increased the distance between all molecules. Higher water content in honey, generated hydrogen with MH molecules. The bonds between MH molecules weakened [32] as referred to [33]. The above two reasons contributed in reducing MHPEO viscosity with higher MH content.

The conductivity (Figure 4:2) increased from 15PEO, 5MHPEO to 10MHPEO. Conductivity is reduced with any further increase in MH content from 15MHPEO to 50MHPEO (Table 4:1).

The conductivity of the solution depends on ionic concentration and ionic mobility. Initially with addition of MH from 15PEO, 5MHPEO to 10MHPEO; the conductivity increased due to increase in MH ions. However, with further increase in MH content, from 10MHPEO upwards the ionic mobility was reduced due to higher MH concentration. So conductivity was reduced from 10MHPEO to 15MHPEO and then 50MHPEO.

A similar result was reported by Aquarone et al (2007) with pure honey [34]. The surface tension of all solutions was reduced from 15PEO to 5MHPEO, 10MHPEO, 15MHPEO and 50MHPEO proportionally (Figure 4:2) and (Table 4:1).

4.3.2 Photographs of Honey

Photographs of the PEO solution and (10 and 15) MHPEO solutions are shown in Figure 4:5.

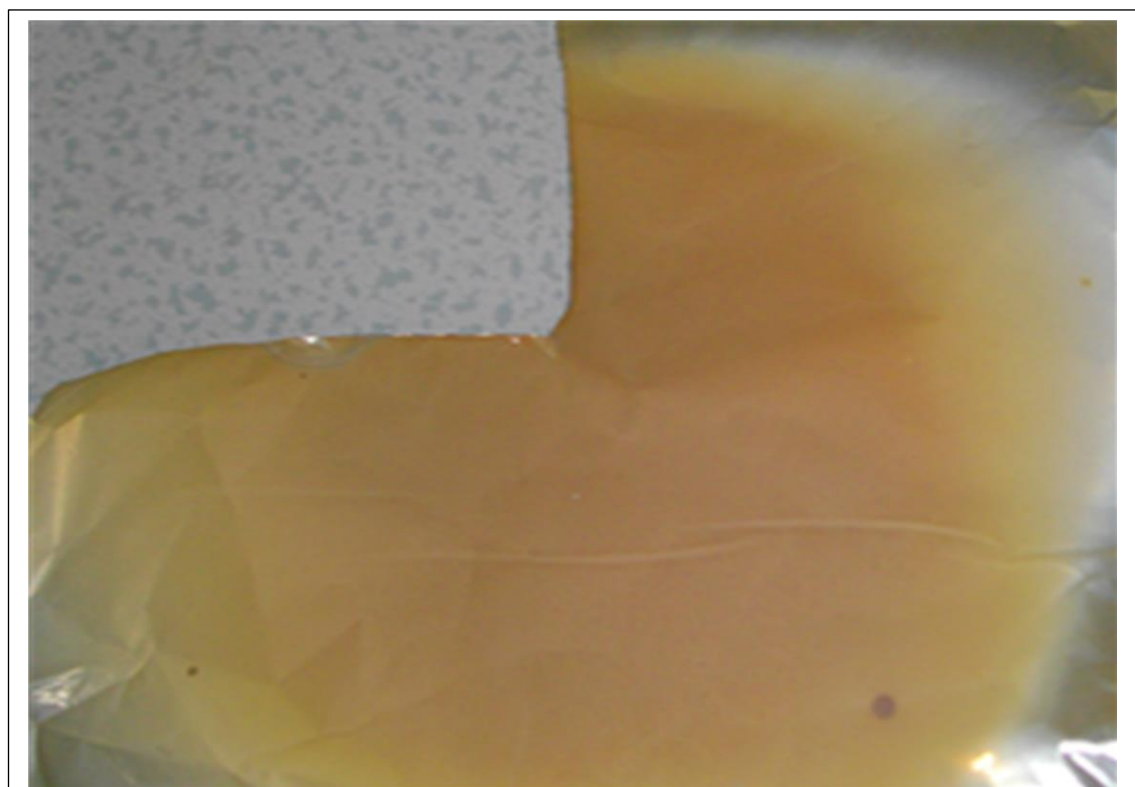


Figure 4:3 Electrospun mat 15MHPEO

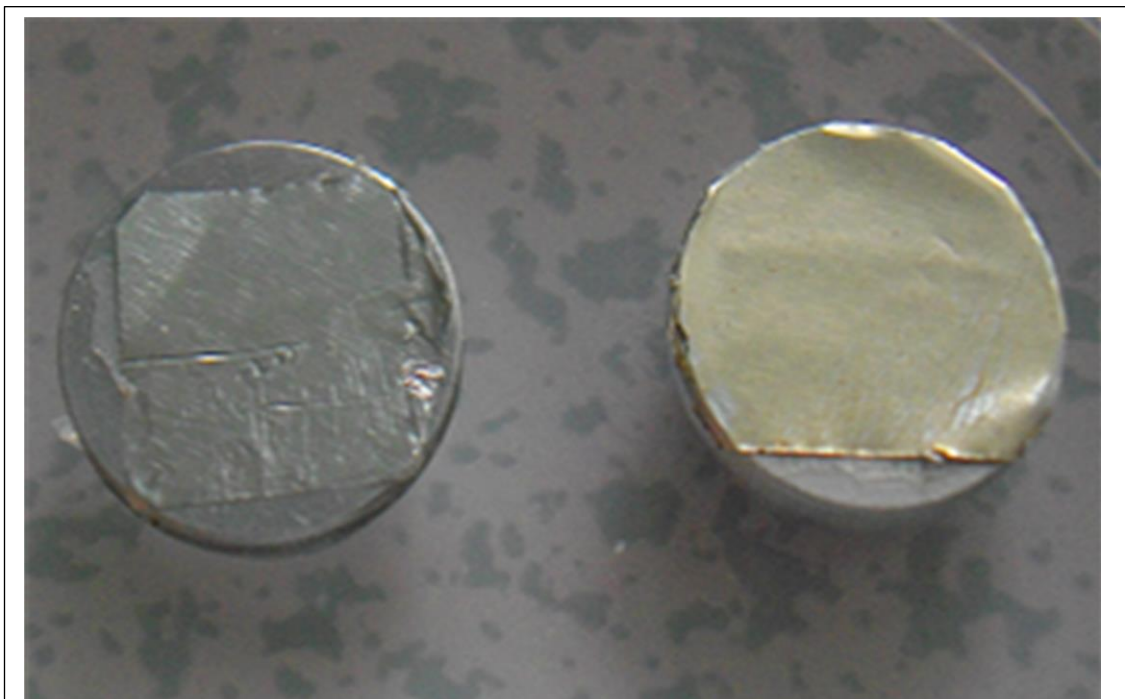


Figure 4:4 SEM stubs of electrospun mats of (Left) 15PEO and 15MHPEO (Right)



Figure 4:5 Solutions of 15PEO, 10MHPEO, 15MHPEO (Left to right)

As can be seen MH is mixed with PEO and also as the concentration of honey increases from 10% to 15%, the solution colour becomes more honey-like.

Table 4:1 Conductivity (micro Siemens), surface tension (mN/m) and UV-visible absorption peak (nm)

Solution	Conductivity (micro Siemens)	Surface Tension (mN/m)	UV- Visible Absorption spectra (nm)
15PEO	700	57	No Peak
5MHPEO	1511	56.5	251
10MHPEO	1610	56	261
15MHPEO	1507	56	561
50MHPEO	825	53	275

A white electrospun mat of PEO on an SEM stub can be seen in Figure 4:4 and honey-like colour electrospun mat of MH-PEO can be seen in Figure 4:3 .

4.3.3 Ultra Violet-Visible Spectroscopy (Uv-visible spectra)

As can be seen in Figure 4:6, Table 4:1, the Uv-visible spectra of 15PEO did not show any peak but it showed a slope.

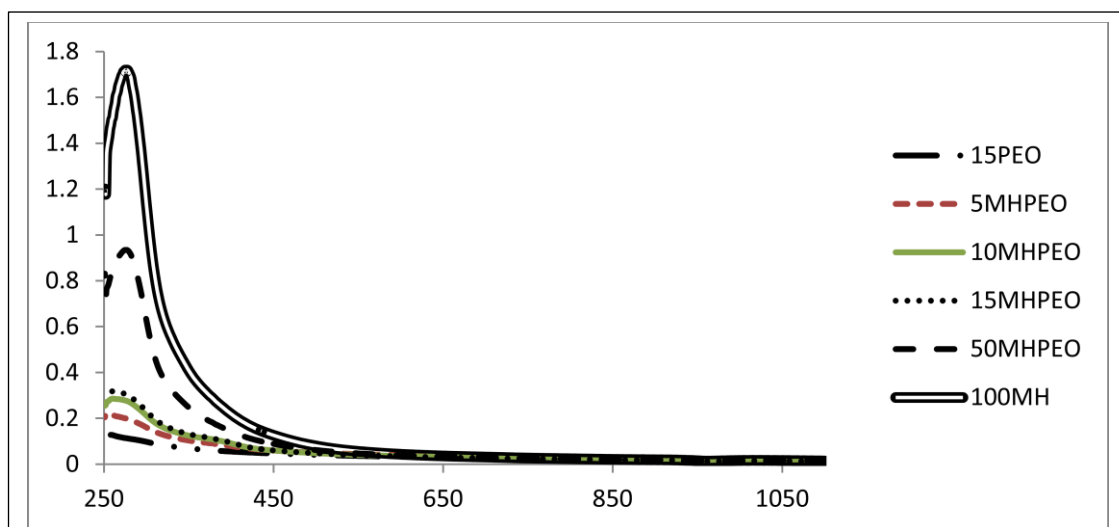


Figure 4:6 UV-Visible spectra

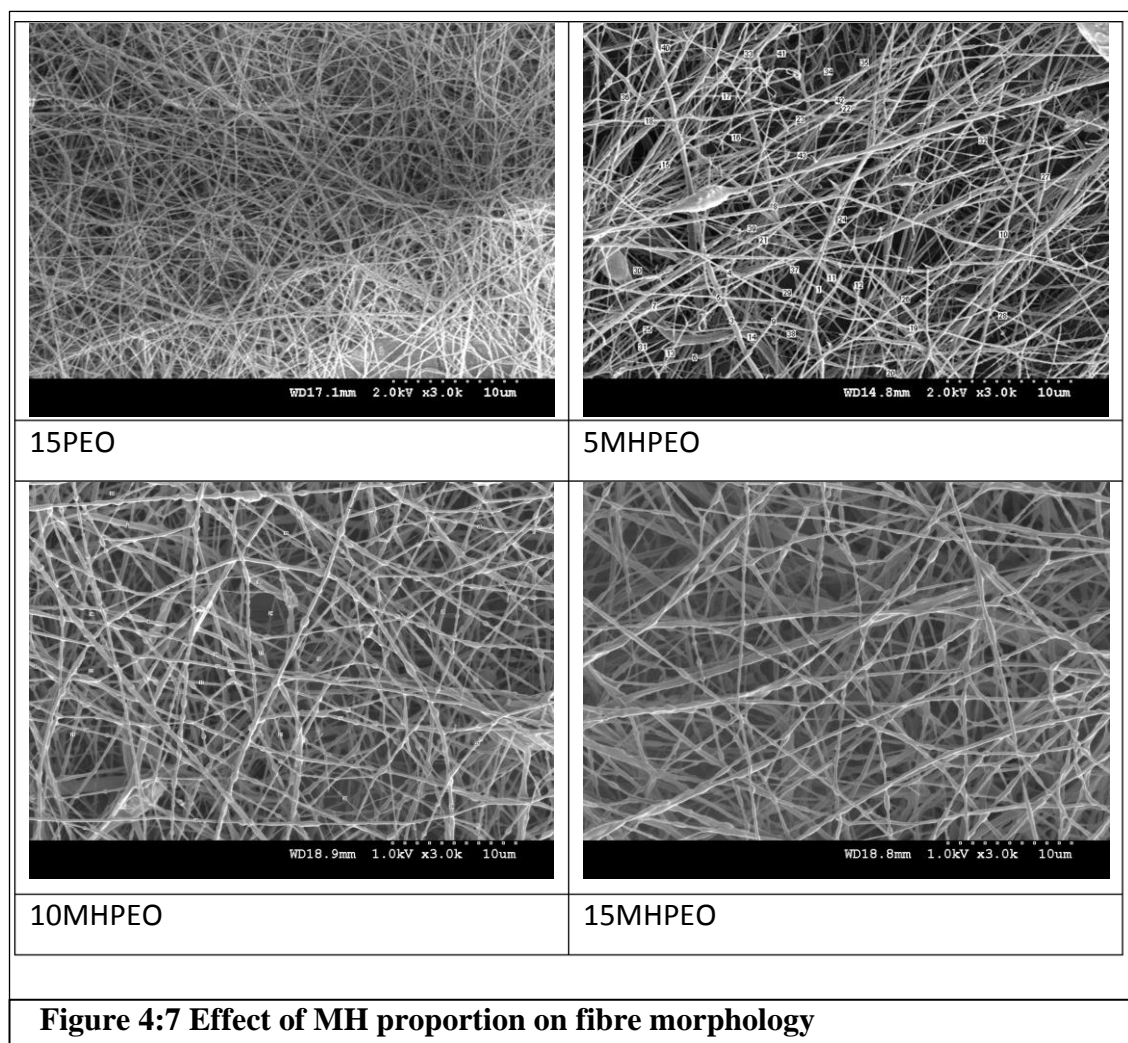
The absorption peak of all MHPEO solutions is shifted towards a higher value with the addition of MH. 100% MH showed very broad peak between 310nm and 350nm which disappears in solutions at lower MH content

In this work, PEO and MHPEO solutions were electrospun into micro-nano fibres. Manuka honey concentration had a measurable effect on the final fibre morphology.

4.3.4 Influence of MH:PEO Ratio on Fibre Properties

As discussed earlier, the effect of addition of MH in PEO was measurable..

All MHPEO solution viscosities and surface tensions decreased and the conductivity increased with the increase of the proportion of MH compared to PEO solution (Table 4:1, Figure 4:1, Figure 4:2). In electrospinning, higher viscosity favours the formation of thicker fibres without beads [35, 36] but higher surface tension and lower conductivity favours bead formation [37, 38]



In the present work, all the processing parameters were maintained at the same level (Applied voltage =13 kV, Feed rate= 1.5 ml/hr, needle diameter= 16G and NTCD = 30cm) , only the MH proportion was changed in the solutions. Fibres obtained from 15PEO were almost circular, less-merged and thinner compared to any MHPEO fibres (Figure 4:7, Figure 4:8). With increasing the MH concentration, the fibre became flatter, thicker and sticky (merged).

The MHPEO produced fibres were wet compared to 15PEO fibres. MH is hygroscopic and humectant by nature, so the MHPEO jet does not dry fully. Therefore, when it

strikes the collector fast, the fibres became flatter. The stickiness could be due to residual water content in the MHPEO blend, so fibres became merged at their contact points. The average 15PEO diameter was 0.139 μ m. The fibre diameters for 5MHPEO, 10MHPEO, 15MHPEO were 0.198 μ m, 0.237 μ m and 0.34 μ m respectively.

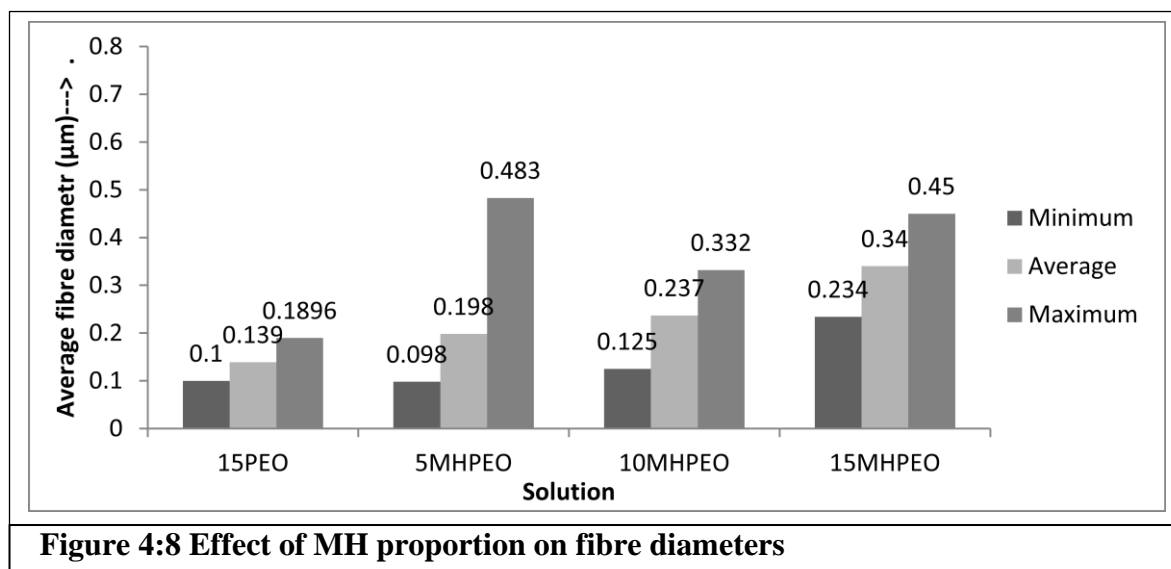


Figure 4:8 Effect of MH proportion on fibre diameters

4.3.5 Influence of Applied Voltage on Fibre Properties

Zong et al (2005) [36] reported increased solution flow rate with increase in electrical force. The effect of applied voltage varies depending on the solution and process parameters. Generally, an increase in applied voltage generates thinner fibres. Increased voltage increases coulombic repulsions and electrical force, so, fibres get stretched and split in to more fibres. As a result, thinner fibres are generated [39].

In order to study the effect of applied voltage on fibre morphology, only the applied voltage was changed and all other parameters were kept same. As voltage is increased, the 15MHPEO fibre diameter is reduced (Figure 4:9, Figure 4:10). As discussed previously, higher applied voltage generated more coulombic repulsions into solution molecules; so the solution jets started splitting. Higher applied voltage generated more electrical force, stretching the fibres more. Overall, thinner fibres generated with higher voltage, and dried faster, so fibres at higher voltage dried faster.

Dry fibres have low residual solvent content, so they merge less compared to wet fibres. Hence, 15MHPEO fibres at higher voltage were less merged, less flat shaped and thinner compared to fibres generated at lower applied voltage. The fibre diameter was reduced from 0.582 μ m, 0.34 μ m, 0.293 μ m, 0.216 μ m at 9kV, 13kV, 21kV and 25kV, respectively.

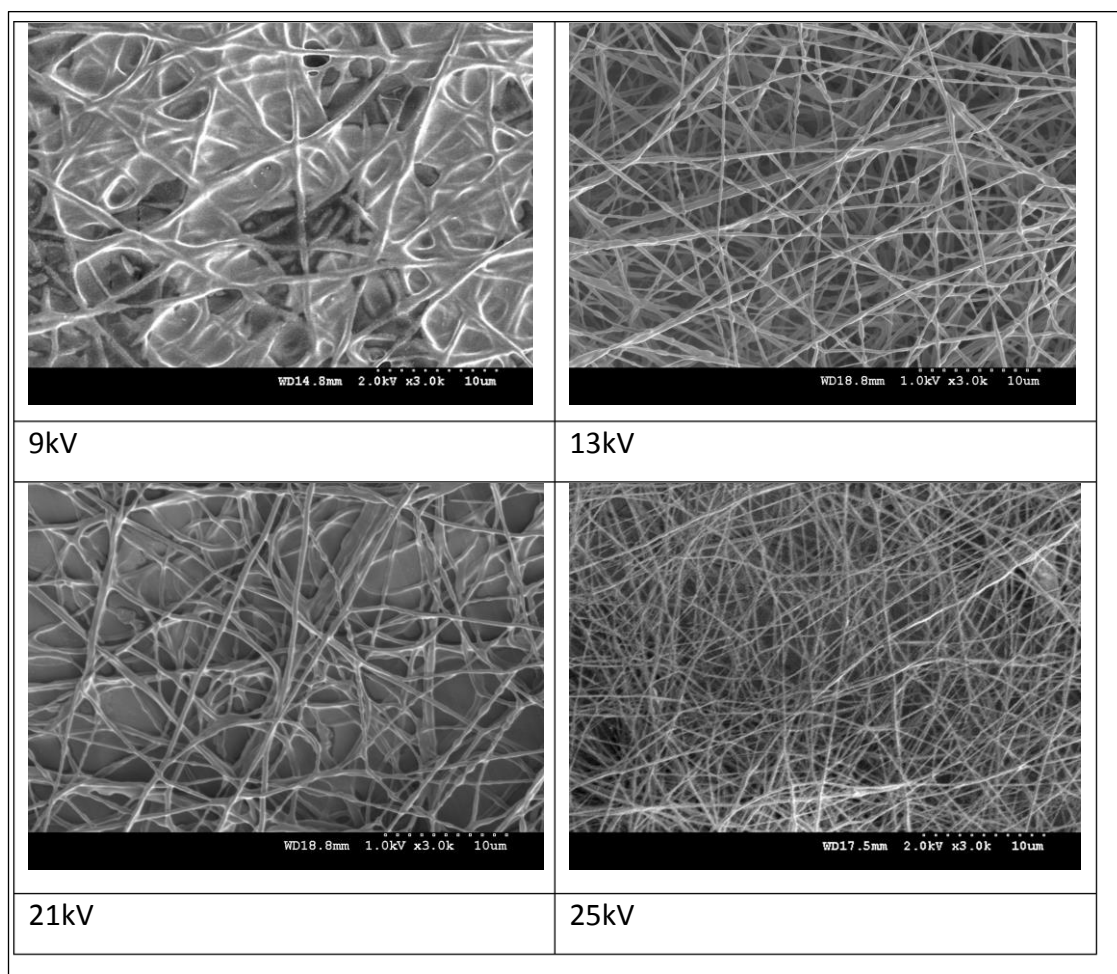


Figure 4:9 Effect of applied voltage on fibre morphology

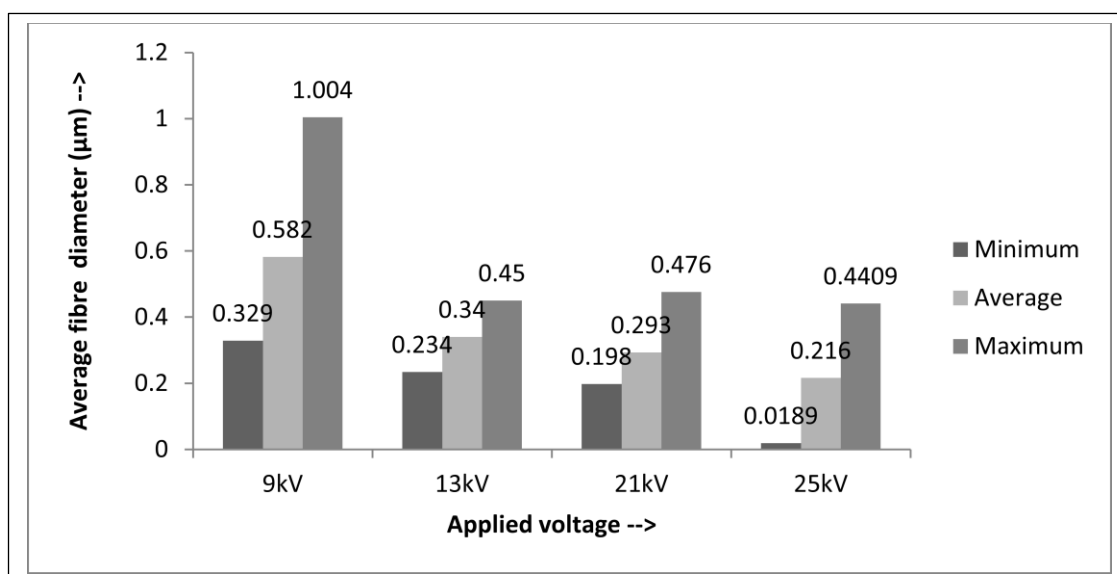


Figure 4:10 Effect of applied voltage on fibre diameters

4.3.6 Influence of Needle to Collector Distance (NTCD) on Fibre Properties

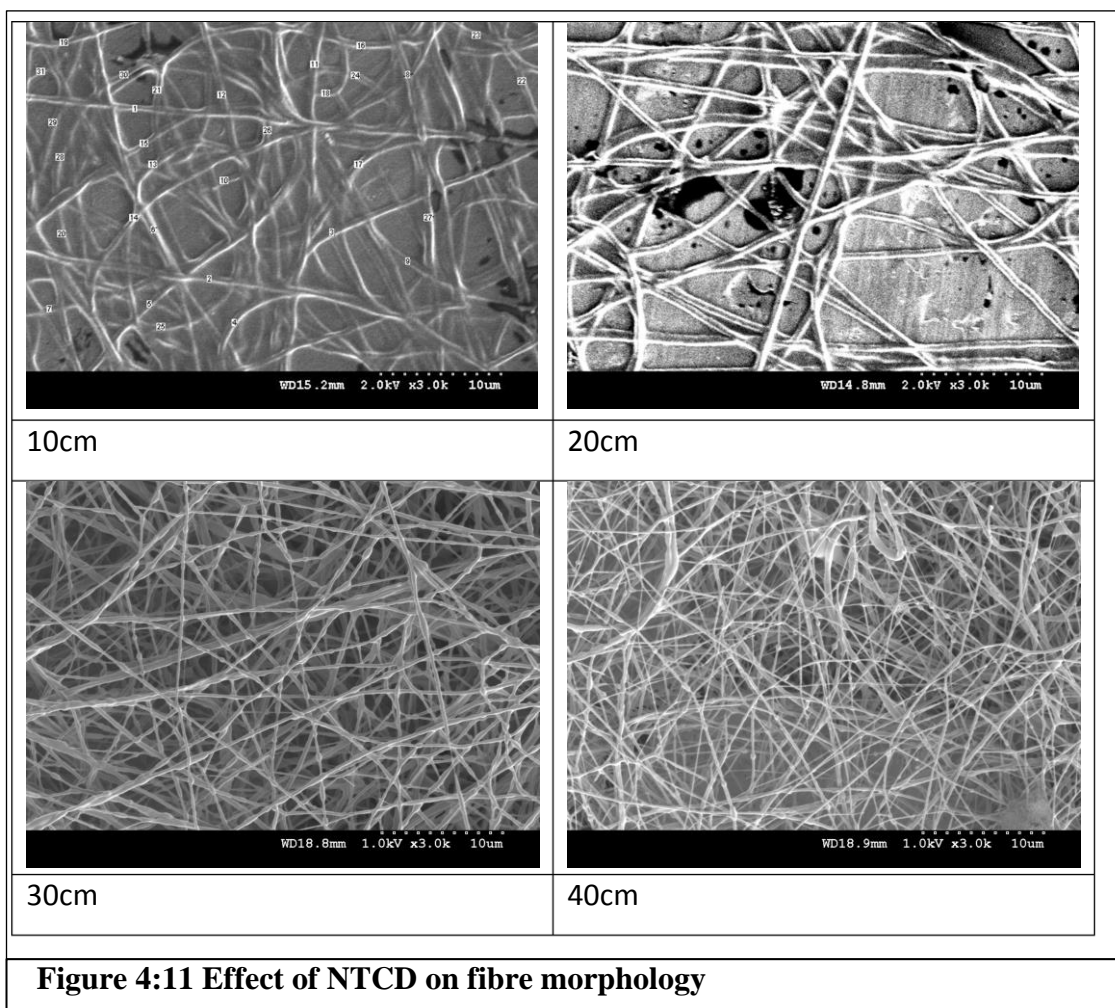


Figure 4:11 Effect of NTCD on fibre morphology

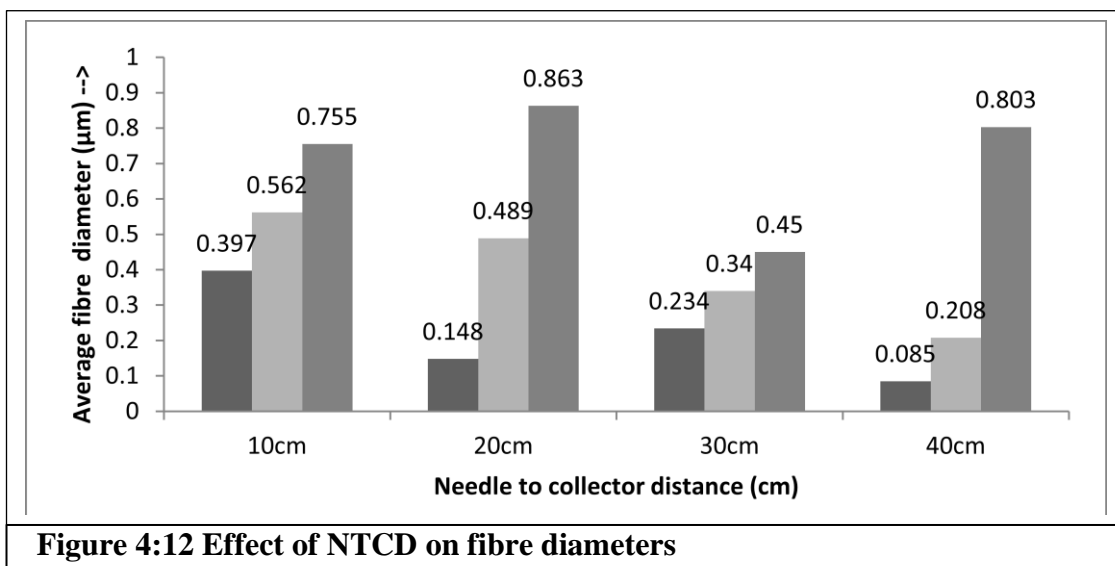


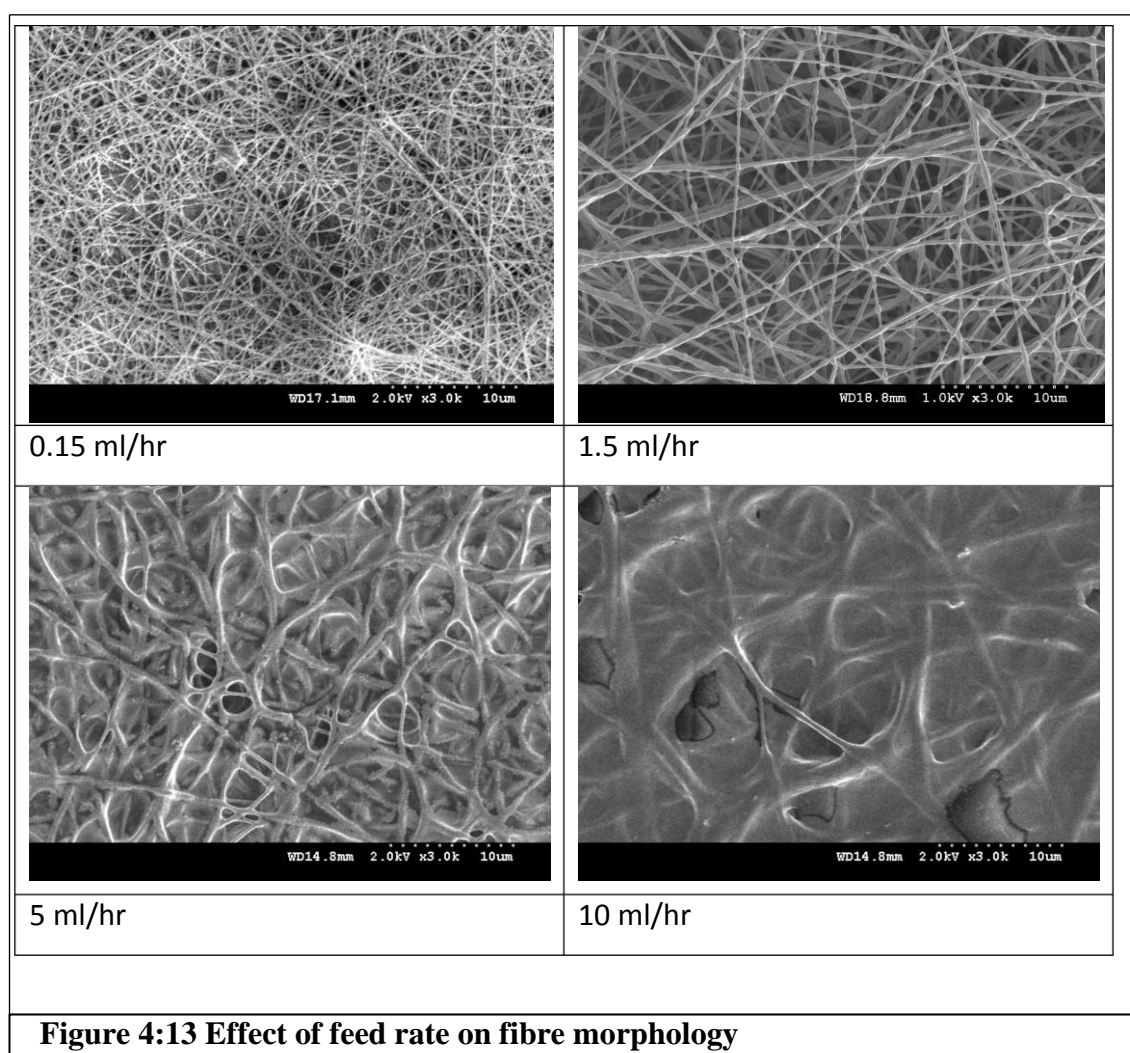
Figure 4:12 Effect of NTCD on fibre diameters

In the present study, the average 15MHPEO fibre diameter decreased from 0.562µm, 0.489 µm, 0.34 µm, 0.208 µm with increase in NTCD from 10cm, 20cm, 30cm, and 40cm respectively (Figure 4:11, Figure 4:12). 15MHPEO fibres were flatter, thicker and merged at lower NTCD compared to higher NTCD.

This could be because the longer the distance offers longer flight time for the solution to stretch and split [39]. As NTCD increased the fibres became drier. Dry fibres do not merge and consequently do not get flat as they hit the target collector compared to wet fibres.

4.3.7 Influence of Feed Rate on Fibre Property

The amount of solution for electrospinning is controlled by its feed rate using a feed control pump mechanism. As the feed rate increased, more solution is present for electrospinning. Generally, with higher feed rate, thicker fibres are generated, so establishing an optimum feed rate is desirable. As higher feed rate can generate droplets and lower feed rate can block the needle for highly volatile solvents.



In the present study, all the parameters were kept the same except for the feed rate. The feed rate varied to study the effect of feed rate on 15MHPEO fibre. The 15MHPEO fibre diameter increased with higher feed rate. Thicker fibres did not dry well and wet fibres became merged and flat, on reaching the collector. 15MHPEO fibres became flatter, thicker and merged with higher the feed rate (Figure 4:13, Figure 4:14). The

fibre diameter increased from 0.203 μm , 0.34 μm , 0.706 μm to 0.924 μm with respect of feed rates 0.15ml/hr, 1.5 ml/hr, 5 ml/hr and 10 ml/hr.

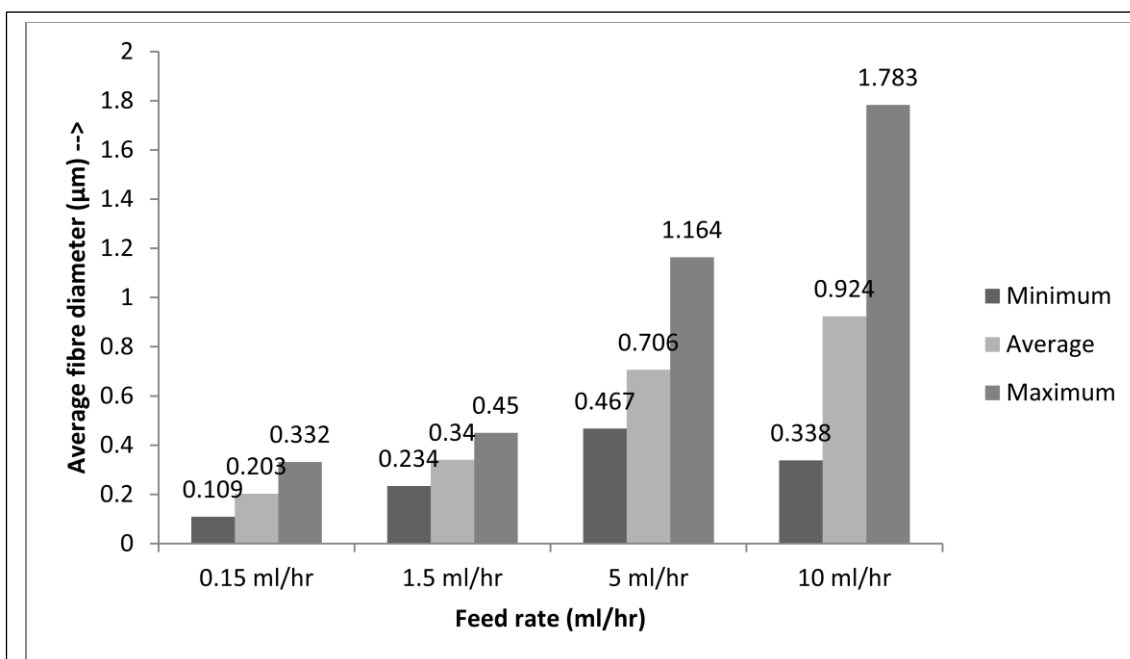


Figure 4:14 Effect of feed rate on fibre diameters

4.3.8 Differential Scanning Calorimetry

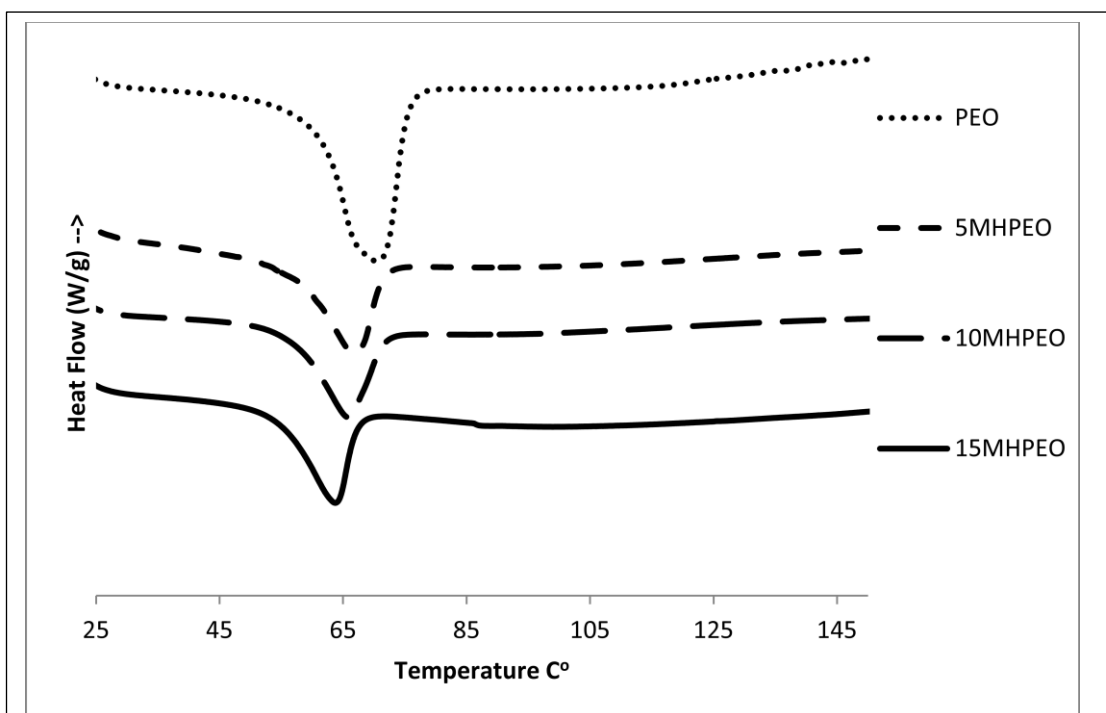


Figure 4:15 DSC curves of electrospun mats

DSC thermograms provide information on phase change of the material with applied temperature. In the present study, DSC thermograms (Figure 4:15) were taken to study the thermal behaviour of 15PEO and all MHPEO mats.

The 15PEO mat showed an endothermic melting peak at 67.4°C. All MHPEO mats also showed a sharp endothermic peak. The endothermic peak in all MHPEO mixtures is due to PEO. As the MH content increased the endothermic peak shifted towards a lower temperature. The area under the melting peak was reduced as the MH content increased. The area under the peak is known as melting enthalpy. The reduction in melting temperature and melting enthalpy suggests reduction in the crystallinity of MHPEO mats with higher MH content. The melting temperature was reduced from 64.3°C, 63.3°C, and 61.1°C for 5MHPEO, 10MHPEO and 15MHPEO respectively.

4.3.9 FTIR

The FTIR spectrum of pure polyethylene oxide (PEO) is shown in Figure 4:16. The characteristic peaks of PEO can be seen at 2879.70cm⁻¹, (CH stretching mode), 1466.51cm⁻¹ (CH₂ scissoring mode), 1094.08 cm⁻¹ (C-O-C stretching mode), 960.76 cm⁻¹ (CH₂ twisting mode) and the characteristic band at 840.99 cm⁻¹. The band assignments of pure PEO are in agreement with other researchers [40-43].

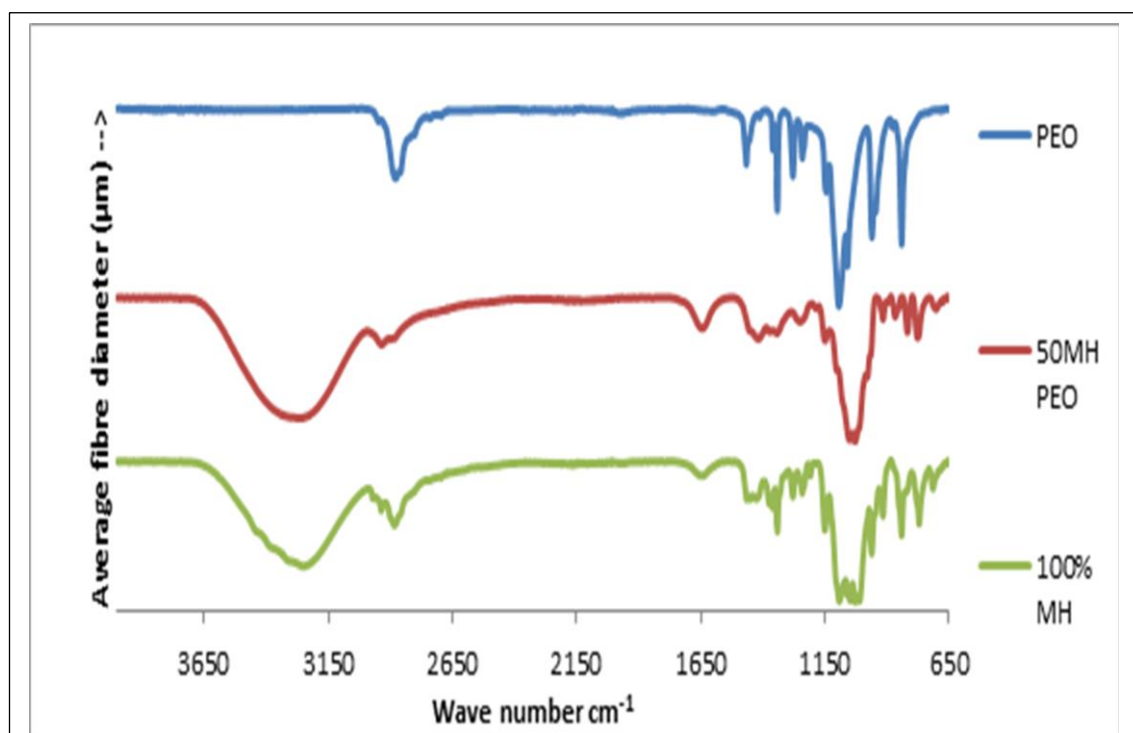


Figure 4:16 FTIR of electrospun mats

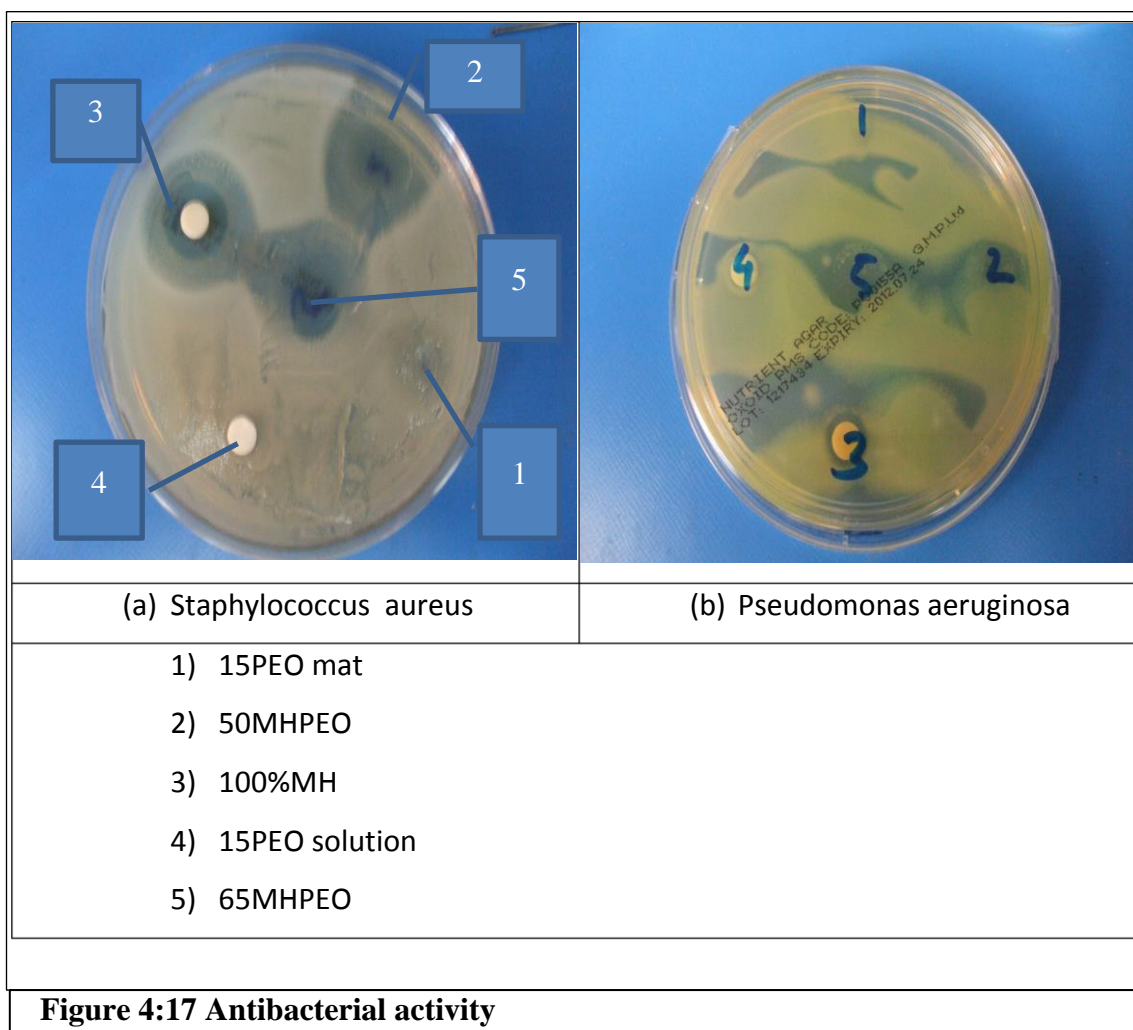
In the FTIR spectrum of honey (Figure 4:16), the peak at 915.80cm⁻¹ is due to C-H bending of carbohydrate, whereas the peak observed at 1049.99cm⁻¹ and 1249.65cm⁻¹ corresponds to C-O stretch in the C-OH group as well as the C-C stretch in the carbohydrate structure. The small shoulder peak at around 1100cm⁻¹ could be related to stretching of the C-O band of C-O-C linkage. The C-O-C is present in the sucrose as a glycoside bond. The peak present around 1342.17cm⁻¹ is due to O-H bending of C-O-

H group and the band at 1417.28 cm^{-1} is a combination of O–H bending of the C–OH group and C–H bending of the alkenes. The broad band at 3269.93 cm^{-1} can be due to O–H group. The band at 2935.39 cm^{-1} could denote the C–H stretching of carboxylic acids and NH_3^+ stretching band of free amino acids, which are present in honey at low concentrations. Similar results were observed by T. Gallardo-Veldzquez et al (2009)[44] and Tewari et al(2005) [45].

The presence of PEO can be confirmed from the FTIR diagram (Figure 4:16). In PEO-Manuka honey blend is observed by the triplet peak of C–O–C stretching vibration at 1150.02 cm^{-1} , 1091.95 cm^{-1} and the small shoulder peak at around 1053 cm^{-1} . Corresponding peaks in PEO can be seen in Figure 4:16 at 1047.24 cm^{-1} , 1143.63 cm^{-1} , 1094.08 cm^{-1} and 1059.32 cm^{-1} with a maximum at 1094.08 cm^{-1} . Tonin et al (2007)[40] observed similar peak in PEO at 1150.02 cm^{-1} , 1091.95 cm^{-1} and a shoulder peak around 1059 cm^{-1} . A peak at 1047.24 cm^{-1} , 1028.09 cm^{-1} , 2936.79 cm^{-1} , 3249.23 cm^{-1} etc. in PEO Manuka honey blend corresponds to the peak at 1049.99 cm^{-1} and 1028.09 cm^{-1} , 2935.39 cm^{-1} and 3269.93 cm^{-1} in Manuka honey, shown in Figure 4:16. All observation clearly demonstrates a mix of PEO and Manuka honey.

4.3.10 Antibacterial Activity

In this work, antimicrobial activity of the 100% MH, 15 PEO solution, 15PEO mat 50, 65 MHPEO mats were tested for *Staphylococcus aureus* and *Pseudomonas aeruginosa*. Initial tests showed that the 15MHPEO mat do not possess any antibacterial activity and was suppressed by PEO in 15MHPEO. Fibres with higher MH concentration, such as 50MHPEO and 65MHPEO mats were produced to increase MH proportion. It can be seen in Figure 4:17, the 100% MH, 50MHPEO and 65MHPEO showed antibacterial activity against both species. The zone of inhibition is visible in both cases. The 15PEO solution and 15PEO mat did not show any antibacterial activity. It can be concluded that at higher MH concentration the MHPEO mats exhibit antibacterial activity.



4.4 Conclusion

Electrospinning of Manuka honey has been investigated and successfully produced. Manuka honey alone cannot be electrospun from aqueous solution. The processability of Manuka honey can be improved by blending with PEO. Changes in solution properties, FTIR and photographic observation show interactions between Manuka honey and PEO. It is found that various parameters affected MHPEO fibre morphology. Higher feed rate, higher MH content produced thicker, merged and flatter MHPEO fibres. By varying the MH proportion from 5MHPEO to 15MHPEO fibres with diameter 0.198 μ m to 0.34 μ m were obtained. Changing feed rate from 0.15ml/hr to 10ml/hr produced fibres from 0.203 μ m to 0.924 μ m respectively. Longer NTCD and higher applied voltage produced thinner less merged and more round shaped fibres. 0.562 μ m to 0.208 μ m diameter fibres were obtained by varying NTCD from 10cm to 40cm respectively. Lower voltage at 9kV generated 0.582 μ m and higher voltage at 25kV generated 0.216 μ m diameter fibre. DSC curves suggested that the crystallinity of MHPEO fibres is less than the crystallinity of 15PEO fibres. The higher the MH

proportion the less is the melting temperature for MHPEO mats. The FTIR results of 50MHPEO showed relevant peaks of both PEO and MH. Antibacterial tests suggested that MHPEO fibres are effective at higher MH proportion (in our case 50MHPEO and more).

4.5 Bibliography

- [4.1] P. C. Molan. (26-Jul-2011). *Manuka honey as a medicine*. Available: <http://bio.waikato.ac.nz/pdfs/honeyresearch/bioactives.pdf>
- [4.2] R. Cooper, "Honey modulates biofilms of *Pseudomonas aeruginosa* in a time and dose dependent manner," *Journal of ApiProduct and ApiMedical Science*, vol. 1, pp. 6-10, 2009.
- [4.3] A. Werner and O. Laccourreye, "Honey in otorhinolaryngology: when, why and how?," *Eur Ann Otorhinolaryngol Head Neck Dis*, vol. 128, pp. 133-7, Jun 2011.
- [4.4] N. Namias, "Honey in the management of infections," *Surgical Infections*, vol. 4, pp. 219-226, 2003 Summer July, 2003.
- [4.5] P. E. Lusby, A. L. Coombes, and J. M. Wilkinson, "Bactericidal activity of different honeys against pathogenic bacteria," *Arch Med Res*, vol. 36, pp. 464-7, Sep-Oct 2005.
- [4.6] A. Wallace, S. Eady, M. Miles, H. Martin, A. McLachlan, M. Rodier, J. Willis, R. Scott, and J. Sutherland, "Demonstrating the safety of manuka honey UMF 20+ in a human clinical trial with healthy individuals," *British journal of nutrition*, vol. 103, pp. 1-6, 2009.
- [4.7] P. B. Olaitan, O. E. Adeleke, and I. O. Ola, "Honey: a reservoir for microorganisms and an inhibitory agent for microbes," *African Health Sciences*, vol. 7, pp. 159-165, September 2007.
- [4.8] O. Y. Oumeish, "The cultural and philosophical concepts of cosmetics in beauty and art through the medical history of mankind," *Clinics in Dermatology*, vol. 19, pp. 375-386, 2001.
- [4.9] M. Ramos-E-Silva and S. Coelho Da Silva Carneiro, "cosmetics for the elderly," *Clinics in Dermatology*, vol. 19, pp. 413-423, 2001.
- [4.10] A. P. Saikia, V. K. Ryakala, P. Sharma, P. Goswami, and U. Bora, "Ethnobotany of medicinal plants used by Assamese people for various skin ailments and cosmetics," *J Ethnopharmacol*, vol. 106, pp. 149-57, Jun 30 2006.
- [4.11] A. Pieroni, C. L. Quave, M. L. Villanelli, P. Mangino, G. Sabbatini, L. Santini, T. Boccetti, M. Profili, T. Ciccioli, L. G. Rampa, G. Antonini, C. Girolamini, M.

Cecchi, and M. Tomasi, "Ethnopharmacognostic survey on the natural ingredients used in folk cosmetics, cosmeceuticals and remedies for healing skin diseases in the inland Marches, Central-Eastern Italy," *J Ethnopharmacol*, vol. 91, pp. 331-44, Apr 2004.

[4.12] J. Jervis-Bardy, A. Foreman, S. Bray, L. Tan, and P. J. Wormald, "Methylglyoxal-infused honey mimics the anti-Staphylococcus aureus biofilm activity of manuka honey: potential implication in chronic rhinosinusitis," *Laryngoscope*, vol. 121, pp. 1104-7, May 2011.

[4.13] R. A. Cooper, E. Halas, and P. C. Molan, "The efficacy of honey in inhibiting strains of *Pseudomonas aeruginosa* from infected burns," *J Burn Care Rehabil*, vol. 23, pp. 366-70, Nov-Dec 2002.

[4.14] L. Boukraa, "Additive Activity of Royal Jelly and honey against *pseudomonas aeruginosa*," *Alternative Medicine Review*, vol. 13, pp. 330-333, 2008.

[4.15] A. A. Al-Jabri, "Honey, milk and antibiotics," *African Journal of Biotechnology* vol. 4, pp. 1580-1587, December-2005.

[4.16] P. H. Kwakman, A. A. Te Velde, L. de Boer, C. M. Vandenbroucke-Grauls, and S. A. Zaat, "Two major medicinal honeys have different mechanisms of bactericidal activity," *PLoS One*, vol. 6, p. e17709, 2011.

[4.17] E. Anklam, "A review of the analytical methods to determine the geographical and botanical origin of honey," *Food Chemistry*, vol. 63, pp. 549-562, 1998.

[4.18] M. Subrahmanyam, A. R. Hemmady, and S. G. Pawar. (June 2003, 09/04/2010). The sensitivity to honey of multidrug – resistant *pseudomonas aeruginosa* from infected burns. *Annals of Burns and Fire Disasters XVI*(2), 1-5.

[4.19] P. H. Kwakman, A. A. te Velde, L. de Boer, D. Speijer, C. M. Vandenbroucke-Grauls, and S. A. Zaat, "How honey kills bacteria," *FASEB J*, vol. 24, pp. 2576-82, Jul 2010.

[4.20] A. E. Jeffrey and C. M. Echazarreta, "Medical uses of honey," *Rev Biomed*, vol. 7, pp. 43-49, 1996.

[4.21] C. J. Adams, C. H. Boulton, B. J. Deadman, J. M. Farr, M. N. Grainger, M. Manley-Harris, and M. J. Snow, "Isolation by HPLC and characterisation of the bioactive fraction of New Zealand manuka (*Leptospermum scoparium*) honey," *Carbohydr Res*, vol. 343, pp. 651-9, Mar 17 2008.

[4.22] C. J. Adams, M. Manley-Harris, and P. C. Molan, "The origin of methylglyoxal in New Zealand manuka (*Leptospermum scoparium*) honey," *Carbohydr Res*, vol. 344, pp. 1050-3, May 26 2009.

- [4.23] Anon. (2009, 28/01/2009). *What's special about active manuka honey?* Available: <http://bio.waikato.ac.nz/honey/special.shtml>
- [4.24] H. H.-J. Jin, S. V. Fridrikh, G. C. Rutledge, and D. L. Kaplan, "Electrospinning Bombyx mori Silk with Poly(ethylene oxide)," *Biomacromolecules*, vol. 3, pp. 1233-1239, 2002.
- [4.25] J. Lu, Y. Zhu, Z. Guo, P. Hu, and J. Yu, "Electrospinning of sodium alginate with poly(ethylene oxide)," *Polymer*, vol. 47, pp. 8026-8031, 2006.
- [4.26] S. Alborzi, L. T. Lim, and Y. Kakuda, "Electrospinning of sodium alginate-pectin ultrafine fibres," *J Food Sci*, vol. 75, pp. C100-7, Jan-Feb 2010.
- [4.27] Y.-F. Qian, Y. Su, X.-Q. Li, H.-S. Wang, and C.-L. He, "Electrospinning of Polymethyl Methacrylate Nanofibres in Different Solvents," *Iranian Polymer Journal*, vol. 19, pp. 123-129, 2010.
- [4.28] M. T. Sanford. (1986, Moisture In Honey. *ENY130*, 1-6. Available: <https://edis.ifas.ufl.edu/pdf/files/AA/AA24900.pdf>
- [4.29] S. Singh, R. S. Gill, and P. P. Singh, "Desiccant honey dehydrator," *International Journal of Ambient Energy*, vol. 32, pp. 62-69, 2011.
- [4.30] A. Lazaridou, C. G. Biliaderis, N. Bacandritsos, and A. G. Sabatini, "Composition, thermal and rheological behaviour of selected Greek honeys," *Journal of Food Engineering*, vol. 64, pp. 9-21, 2004.
- [4.31] O. M. Atrooz, M. A. Al-Sabayleh, and S. Y. Al-Abbadi, "Studies on Physical and Chemical Analysis of various Honey Samples and Their Antioxidant Activities," *Journal of Biological Sciences*, vol. 8, pp. 1338-1342, 2008.
- [4.32] Z. Ren, X. Bian, L. Lin, Y. Bai, and W. Wang, "Viscosity and melt fragility in honey–water mixtures," *Journal of Food Engineering*, vol. 100, pp. 705-710, 2010.
- [4.33] S. H. Zhou, L. R. Tao, and B. L. Liu, "Glass transition temperature and its implication for drying and stability of dried foods," *Vacuum & Cryogenics*, vol. 8, pp. 46-50, 2002.
- [4.34] C. Acquarone, P. Buera, and B. Elizalde, "Pattern of pH and electrical conductivity upon honey dilution as a complementary tool for discriminating geographical origin of honeys," *Food Chemistry*, vol. 101, pp. 695-703, 2007.
- [4.35] C. Huang, S. Chen, C. Lai, D. H. Reneker, H. Qiu, Y. Ye, and H. Hou, "Electrospun polymer nanofibres with small diameters," *Nanotechnology*, vol. 17, pp. 1558-1563, 2006.

- [4.36] X. Zong, K. Kim, D. Fang, S. Ran, B. S. Hsiao, and B. Chu, "Structure and process relationship of electrospun bioabsorbable nanofibre membranes," *Polymer*, vol. 43, pp. 4403-4412, 2002.
- [4.37] H. Fong, "Beaded nanofibres formed during electrospinning," *Polymer*, vol. 40, pp. 4585-4592, 1999.
- [4.38] W. Zhang, E. Yan, Z. Huang, C. Wang, Y. Xin, Q. Zhao, and Y. Tong, "Preparation and study of PPV/PVA nanofibres via electrospinning PPV precursor alcohol solution," *European Polymer Journal*, vol. 43, pp. 802-807, 2007.
- [4.39] S. Ramakrishna, K. Fujihara, W.-E. Teo, T.-C. Lim, and Z. Ma, *An Introduction to Electrospinning And Nanofibres*: World Scientific Publishing Company, Singapore, 2005.
- [4.40] C. Tonin, A. Aluigi, C. Vineis, A. Varesano, A. Montarsolo, and F. Ferrero, "Thermal and structural characterization of poly(ethylene-oxide)/keratin blend films," *Journal of Thermal Analysis and Calorimetry*, vol. 89, pp. 601-608, 2007.
- [4.41] S. Ramesh, T. F. Yuen, and C. J. Shen, "Conductivity and FTIR studies on PEO-LiX [X: CF₃SO₃(-), SO₄(2-)] polymer electrolytes," *Spectrochim Acta A Mol Biomol Spectrosc*, vol. 69, pp. 670-5, Feb 2008.
- [4.42] T. Çaykara, S. Demirci, M. S. Eroğlu, and O. Güven, "Poly(ethylene oxide) and its blends with sodium alginate," *Polymer*, vol. 46, pp. 10750-10757, 2005.
- [4.43] A. G. B. Pereira, A. T. Paulino, C. V. Nakamura, E. A. Britta, A. F. Rubira, and E. C. Muniz, "Effect of starch type on miscibility in poly(ethylene oxide) (PEO)/starch blends and cytotoxicity assays," *Materials Science and Engineering: C*, vol. 31, pp. 443-451, 2011.
- [4.44] T. Gallardo-Velázquez, G. Osorio-Revilla, M. Z.-d. Loa, and Y. Rivera-Espinoza, "Application of FTIR-HATR spectroscopy and multivariate analysis to the quantification of adulterants in Mexican honeys," *Food Research International*, vol. 42, pp. 313-318, 2009.
- [4.45] J. C. Tewari and J. M. K. Irudayaraj, "Floral Classification of Honey Using Mid-Infrared Spectroscopy and Surface Acoustic Wave Based z-Nose Sensor," *J.Agric.FoodChem.*, vol. 53, pp. 6955-6966, 2005.

Chapter 5 : Investigating the Electrospinning of Ethylcellulose

5.1 Introduction

Cellulose is the most abundant and widely used organic material [1]. A number of environmentally friendly and biocompatible products can be produced from cellulose [2].

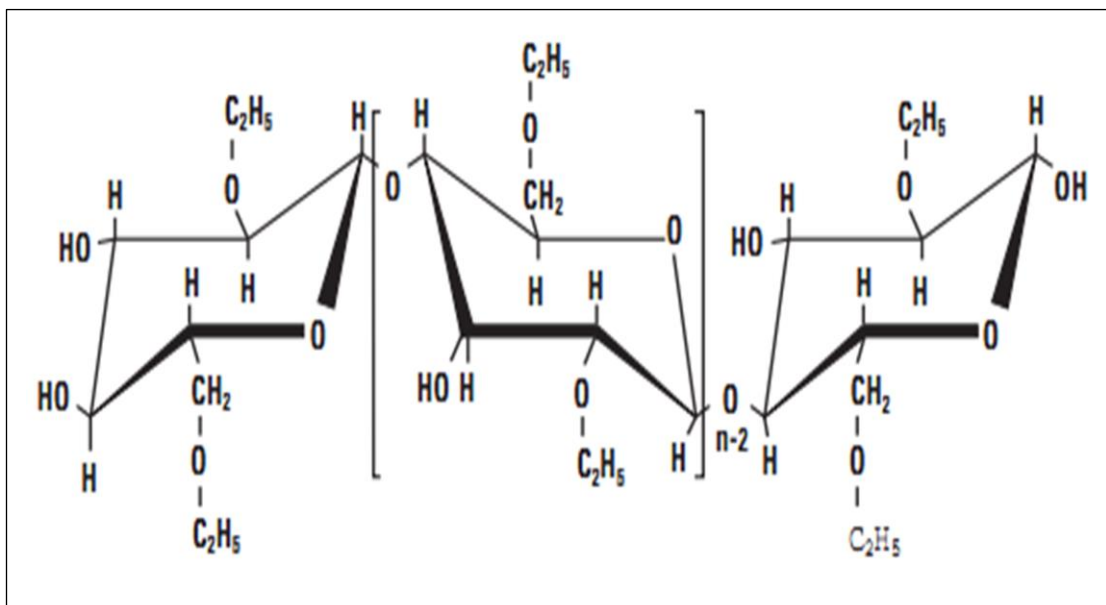


Figure 5:1 Chemical structure of Ethylcellulose

Cellulose can be converted or functionalised to a range of derivatives by various processes (for e.g. etherification, esterification etc.) [3, 4]. Different types of cellulosic ethers can be obtained by etherification [5] for e.g. carboxymethylcellulose (CMC), cyanoethylcellulose (CEC), ethylcellulose (EC), methylcellulose (MC), hydroxyethylcellulose (HEC), hydroxypropylcellulose (HPC), and mixed ethers such as hydroxy-propylmethylcellulose (HPMC), carboxymethyl- hydroxyethylcellulose (CMHEC), and hydroxyl- methylcellulose (HEMC). EC (Figure 5:1) is degradable but not biodegradable or biocompatible [6-8] but it is nevertheless widely used in pharmaceuticals, food, personal /beauty care, ceramics, pastes, printing inks, coatings etc [2, 9]. EC can function as a binder; a tough/ flexible film former; a time-release agent, water barrier, and rheology modifier, to name a few. In food EC is used for binding as a gelling agent (organogelator) [10, 11], film former and flavour fixatives, [12]. EC is colourless, odourless, tasteless, and noncaloric, thermoplastic and film forming [2]. EC is the most widely used water-insoluble polymer for controlled release in pharmaceuticals [13] and being semi synthetic it degrades to nontoxic and readily

excreted products [14], it is also widely used in oral and topical formulation[15]. The structure of EC is shown in Figure 5:1.

Electrospinning is a versatile method for producing nano fibres from cellulose and its derivatives. There are few research articles reporting on fibre from cellulose and its derivatives produced by the electrospinning method for e.g. electrospinning of cellulose acetate [16-27]; ethyl cellulose [28-31]. Cellulose [32-34] and hydroxyethyl cellulose[35]. Various authors mentioned the principle of electrospinning [36-38]. The principle of electrospinning is described in details in chapter 1, Fig 1:6.

The abundance and biodegradability of cellulose make cellulose fibre useful in a wide range of areas such as filtration, biomedical applications and protective clothing, as already stated. Electrospun mats have larger specific surface areas and smaller pore size compared to commercially non-woven fabrics. Cellulosic nanofibres are of interest in a wide variety of applications including semipermeable membranes, nano composites, filters, protection clothing and biomedical applications such as wound dressings, tissue engineering scaffolds and drug delivery systems [39, 40].

In this work, we have systematically evaluated the effects of different solvent systems not previously investigated. The main objective of the present work was to widen the selection of the solvent systems that could be used to electrospun EC fibres. This will allow some applications such as carriers for drug delivery to wider selection of the solvent system so that the electrospinnable spinning solutions of EC is optimised (compatible) with the active ingredient(s) of the end use.

5.2 Materials and Experimental Methods

5.2.1 Materials

Ethanol was purchased from Fisher scientific, Toluene from Rathburn and EC (Ethoxyl content 48%, 45cP of 5% EC in 60:40 toluene: ethanol at 25° C) was purchased from Aldrich. All the chemicals were used without further purification.

5.2.2 Solution Preparation

15% (w/w) EC solution was prepared by dissolving EC powder in different proportion of ethanol and toluene mixtures (0:100, 40:60, 50:50, 60:40, 100:0). All solutions were kept in air tight bottles in ultrasonic bath for 1day to properly dissolve the EC. The 15% (w/w) EC in 100% toluene is referred as 15EC100To, the 15%EC (w/w) in 60:40 ethanol: toluene) is referred as 15EC60Et and the 15 %(w/w) in 60:40 (Toluene:

Ethanol) is referred as 15EC60, further in the study. All solutions were kept at room temperature before being filled in a 5ml syringe and spun into nano fibres.

5.2.3 Electrospinning Setup

The homogeneous EC solutions were fed from a 5 ml syringe to a vertically orientated (15 gauge) blunt ended metal needle ‘spinneret’ via Teflon tubing. The volume feed rate was digitally controlled by a positive displacement microprocessor syringe pump (M22 PHD 2000, Harvard Apparatus, Eden bridge Kent, United Kingdom). The needle was connected to one electrode of a high voltage direct-current power supply (MK35P2.0-22, Glassman, New Jersey, USA). The effects of different processing parameters on fibre property were studied. The processing parameters such as solvent ratios (ethanol: toluene), applied voltage and needle to collector distance (NTCD) were studied. A grounded stationary rectangular metal collector covered by a piece of aluminium foil was used as target for the nanofibre deposition. The complete electrospinning apparatus was enclosed in a glass box and the electrospinning was carried out at room temperature.

5.2.4 Solvent and Solution Properties (Viscosity, Surface Tension and Conductivity)

The viscosities of all solutions were measured by a Brookfield DV-II Pro viscometer with a S63 spindle and the surface tension was measured by a Kruss surface tension meter model K6. Conductivity was measured by Oakton con 110 handheld conductivity meter.

5.2.5 Visual Observation

Photos were taken to see changes in turbidity of EC solutions in different solvent mixtures by a Fuji film finepix A805 camera.

5.2.6 Scanning Electron Microscopic (SEM) Studies

The surface morphologies were recorded with a Hitachi Scanning Electron Microscope (Model: S-4300, Japan). The electrospun webs were mounted on an aluminium stub using a double-sided adhesive tape. Fibrous mats on stubs were coated in a sputter coater unit (Polaron SC7620) with gold-palladium coating for 60 seconds. Prepared samples were finally placed into the SEM and observed at accelerating voltage of 1 kV and 10 μ Amps current.

5.2.7 FTIR (Fourier Transform Infrared Spectroscopy)

A Perkin Elmer Spectrum 100 ATR-FTIR Spectrophotometer was used to get the FTIR spectra. The IR spectra were taken from 650cm^{-1} to 4000cm^{-1} using a ZnSe diamond ATR device, the ATR device was set to base value with air.

5.2.8 Differential Scanning Calorimetry (DSC) Studies

Thermal analysis was performed using Mettler DSC 12 E. All samples were kept in aluminium pans with pierced lids. The reference sample was kept in empty aluminium pan with pierced lid. The samples were heated at a scanning rate of $10^{\circ}\text{C}/\text{min}$ in atmospheric air and all samples were weighed up to 5mg.

5.3 Results and Discussions

5.3.1 Solvent and Viscosity

Polymer-solvent interaction plays very important role in solution viscosity [41]. The polymer-solvent and polymer-polymer interactions were also investigated by other researchers [38, 42]. Generally, a good solvent gives higher viscosity whilst a poor solvent low viscosity. Polymer molecules interact with each other strongly then with the solvent if in poor state.

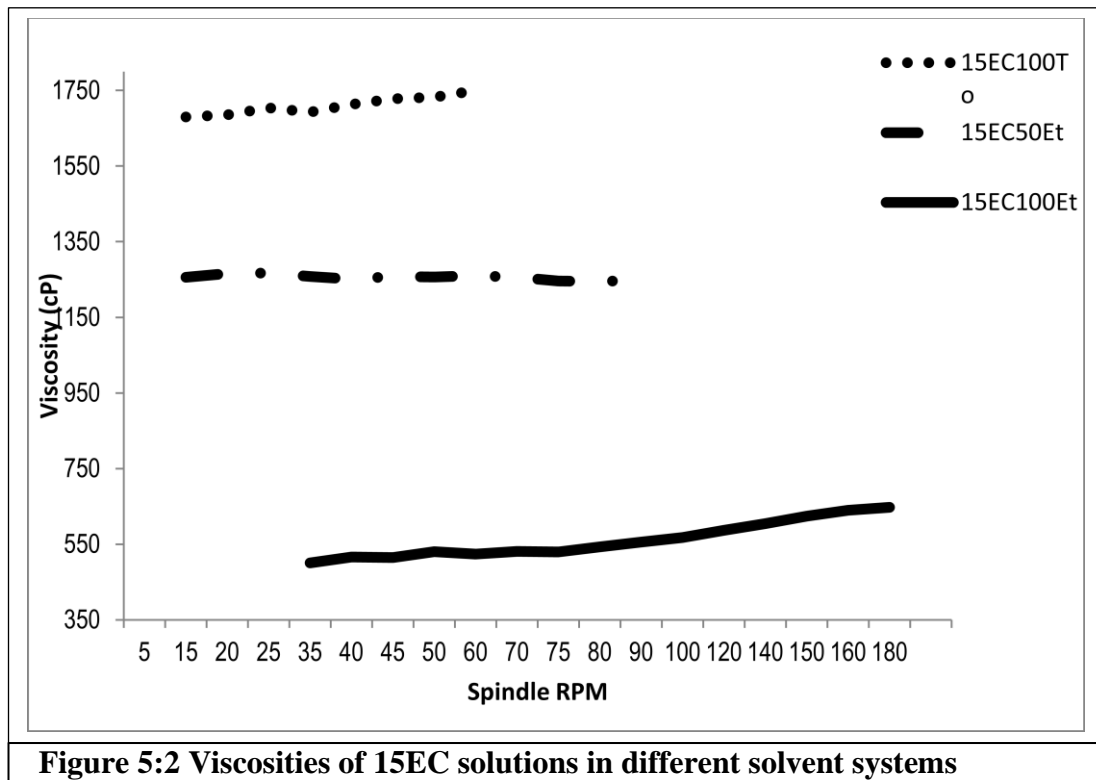


Figure 5:2 Viscosities of 15EC solutions in different solvent systems

Polymer molecules squeeze out the solvent between them in the case of a poor solvent, furthermore the polymer chains collapse and adopt curled configurations in the poor solvent. In case of good solvent, the polymer-solvent interaction increases. The long

chain polymer molecules are surrounded by solvent molecules and reduce polymer-polymer interaction. So, the polymer will adopt an uncurled configuration. The intrinsic viscosity of a polymer solution with good solvent is higher compared to a poor solvent. A good solvent allows higher concentration, along with maintaining a stable fluid form, while a poor solvent will lead to gelation with more polymer addition due to more polymer-polymer interactions.

Figure 5:2 shows the viscosity of 15EC solutions in different solvent systems. Viscosity of 15EC100Et was the lowest. The viscosity increased as the proportion of toluene increased in solution. The 15EC100To had highest viscosity.

Arwidsson et al. (1951)[43] correlated a good solvent with steep rise in viscosity at high polymer concentrations compared to a poor solvent.

Hence, increased viscosity of EC in toluene compared to ethanol proves that toluene is a good solvent compared to ethanol for the EC.

5.3.2 Conductivity and Surface Tension

Surface tension and solution conductivity are important parameters affecting fibre morphology [38].

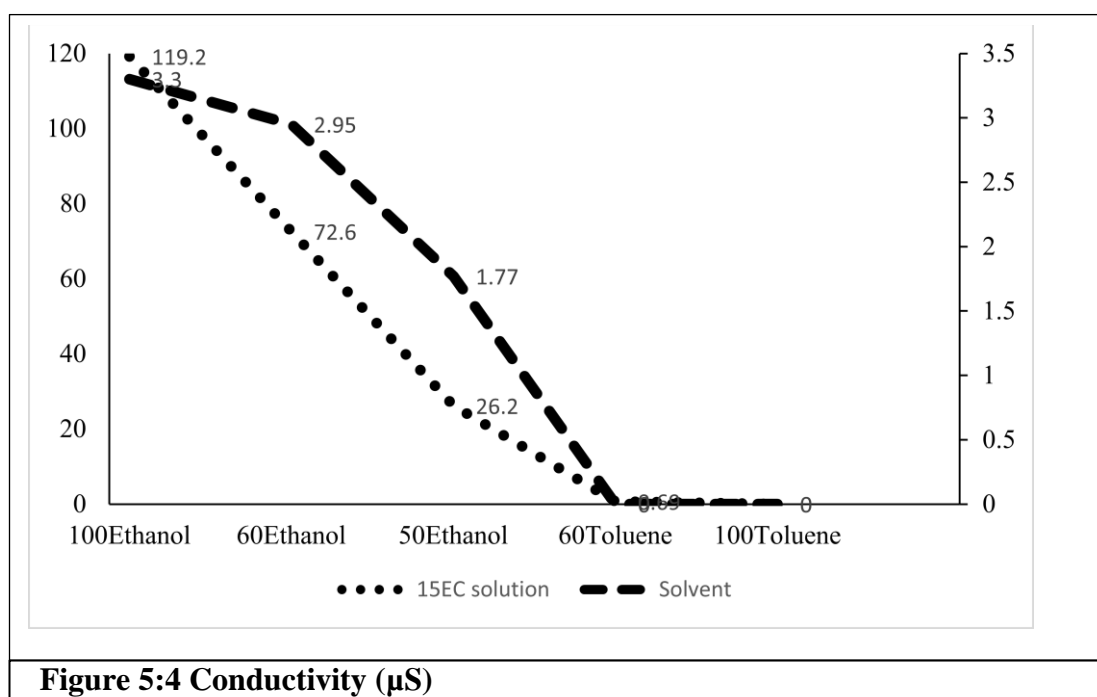
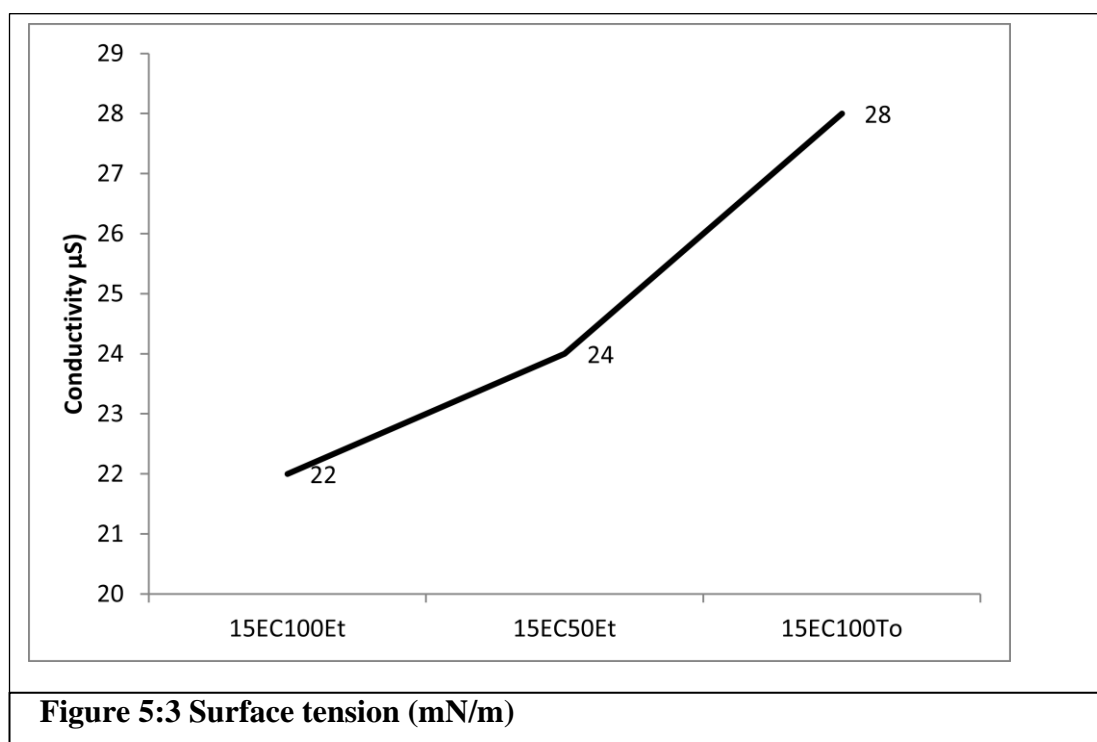
Table 5:1 Conductivity of EC solvents

No	Solvent		Solution	
	Ethanol: Toluene	Conductivity (μ S)		Conductivity (μ S)
1	100:0	0	15EC100Et	0
2	60:40	0	15EC60Et	0.69
3	50:50	1.77	15EC50Et	29.2
4	40:60	2.95	15EC60To	72.6
5	0:100	3.30	15EC100To	119.2

In the present work, (Figure 5:4 and Table 5:1), the conductivity of solvent decreased as the ratio of toluene/ethanol increased (from 0% to 100%) and vice versa.

The conductivity of 100% toluene was found to be zero. Similar trends were seen in corresponding solutions with conductivity decreasing from 15EC100Et to 15EC100To with increase in toluene proportion of the conductivity of 15EC100To was found to be zero. It can be seen that the solution conductivity is much higher compared to solvent conductivity in case of ethanol as one part of the solvent. This can be explained by the fact that addition of EC in solvent increased the overall solution conductivity due to EC

ions. In case of 100% toluene this was not the case. Solvent (toluene) and 15EC100To both showed zero conductivity.



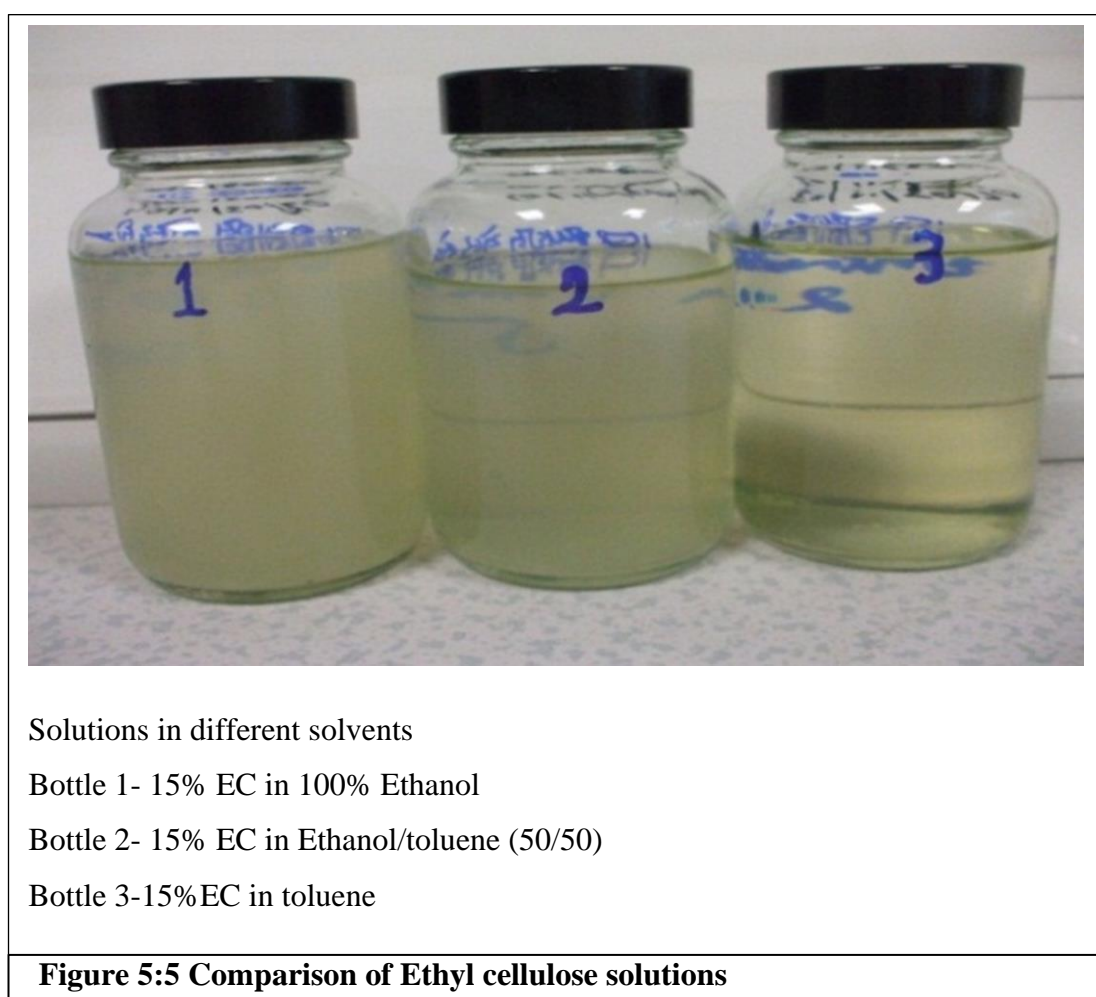
Surface tensions of ethyl cellulose solutions are given in Figure 5:3. The result shows rise in surface tension from 15EC100Et to 15EC100To as the toluene proportion increased.

5.3.3 Visual Observation

Photographs of EC solutions are shown in Figure 5:5. The turbidity of 15EC solutions increased as the ethanol proportion increased with the highest turbidity of 15EC 100Et. As discussed earlier the viscosity also decreased with higher proportion of ethanol.

Jullander et al.(1955)[44] reported viscosity and turbidity as important physical characteristics of solutions. They assumed decreased viscosity and increased turbidity as decreased “solubility”, i.e. a smaller portion of the material mass molecularly dispersed.[44].

Similar trends were observed in the present work. The solution of 15EC100Et had more turbidity and less viscosity. The reason might be because EC is partially/ not soluble in Ethanol compared to toluene.



Films were casted (Figure 5:6) at room temperature by drying EC solutions on glasses. Film made from 15EC100Et was found brittle and fragile. As the toluene/ethanol ratio increased, the films became more flexible (Table 5:2).

Table 5:2 Ethyl cellulose solution and film visual property

No.	Film detail	Solution appearance	Film appearance	Film Flexibility
1	15EC100Et	More cloudy (Not transparent)	Film with more white dots	Fragile & rigid
2	15EC50Et	Less cloudy (Semi-transparent)	Film with less white dots	semi fragile & rigid
3	15EC100To	Clear (transparent)	Clear film	Pliable & flexible



EC films in different solvents (Left to right)

Left: - 15% EC in ethanol

Middle:-15% EC in ethanol/toluene (50/50)

Right:-15%EC in toluene

Figure 5:6 Comparison of Ethyl cellulose films from different solvent systems

The 15EC100To film had highest flexibility. This characteristic of EC films lies in the polymer-solvent interaction. Toluene is a more nonpolar solvent compared to ethanol, which is more polar. According to literature [43, 45, 46], the mechanical properties of film were dependant on the solvent used for casting. Hass et al. (1952) [45] also noted that films of cellulose derivatives were more brittle when casted from polar solvents; this was resulted from a larger degree of crystallinity. The Hercules Powder Co. (2002) [46] brochure on ethyl cellulose recognized that flexible films of maximum strength were obtained when nonpolar solvents which had little or no affinity for water constituted a major portion of the solvent. Arwidssons et al. (1991) [43] noted that water presence at low concentrations in (e.g. ethanol), should be avoided in solvents for

EC. The water accumulates in the solution during evaporation. The resulting film had a spongy structure and poor mechanical properties.

5.3.4 Effect of Solvent on Ethylcellulose Electrospinning

Electrospun fibres may consist of beads, beaded-fibres, or fibres, depending on the solution properties or process conditions. Lee et al (2005)[47] reported viscosity, surface tension and solution conductivity as the main factors for bead formation. Surface tension, conductivity and viscosity plays major role in deciding the final fibre property [48]. Eda et al (2007)[49] reported that the rheological property of the solution affects bead to fibre morphology. Liu et al (2002)[50] noticed that surface tension is affected by solvent composition and viscosity is affected by polymer concentration.

Park et al. (2007) [28] reported surface tension as one of the parameters affecting bead formation and fibre length. Higher surface tension creates beads [51] . Beads disappear with reduction in surface tension [52].

Fong et al (1999)[52] noticed bead formation increases with distance between beads, and spherical to spindle like shape change of the bead with increased solution viscosity [51]. The solution viscosity is directly correlated to polymer molecular weight, solution concentration, polymer structure, polymer-solvent interaction [51, 53]. The average distance between the beads increases with higher viscosity [51]. With higher viscosity more uniform fibre are formed and very high solution viscosity blocks the needle from spinning and very low viscosity produces only droplets due to lack of entanglement [53-55].

Entanglement analysis shows that solution viscosity plays a very important role in making bead-fibre structure [56]. At least one entanglement per polymer chain is needed to form a fibre [49]. Viscosity and electrical conductivity affects jet elongation and fibre diameter [28]. Beads became smaller and spindle shaped with increased electric charge. Beads disappear and smaller fibres are formed with higher conductivity [51].

As can be seen from the SEM images (Figure 5:7), there is a large effect of the solvents used on fibre morphology. All the 15EC solutions in different ethanol: toluene mixtures were spun at the same electrospinning parameters. The feed rate was kept at 1.5 ml/hr. The applied voltage was 21kV, the NTCD was 20cm and needle gauge was 16.G 15EC100Et produced beads on strings in the structure. 15EC100Et produced fibres with irregular and round shaped beads. The boiling point of Et is low (approx. 78°C). Ethanol evaporation dried the fibre surface faster, followed by the evaporation of the solvent

inside the bead. The faster evaporation of the solvent bead generated an uneven surface, also the EC100Et has round shaped bead in the fibre structure.

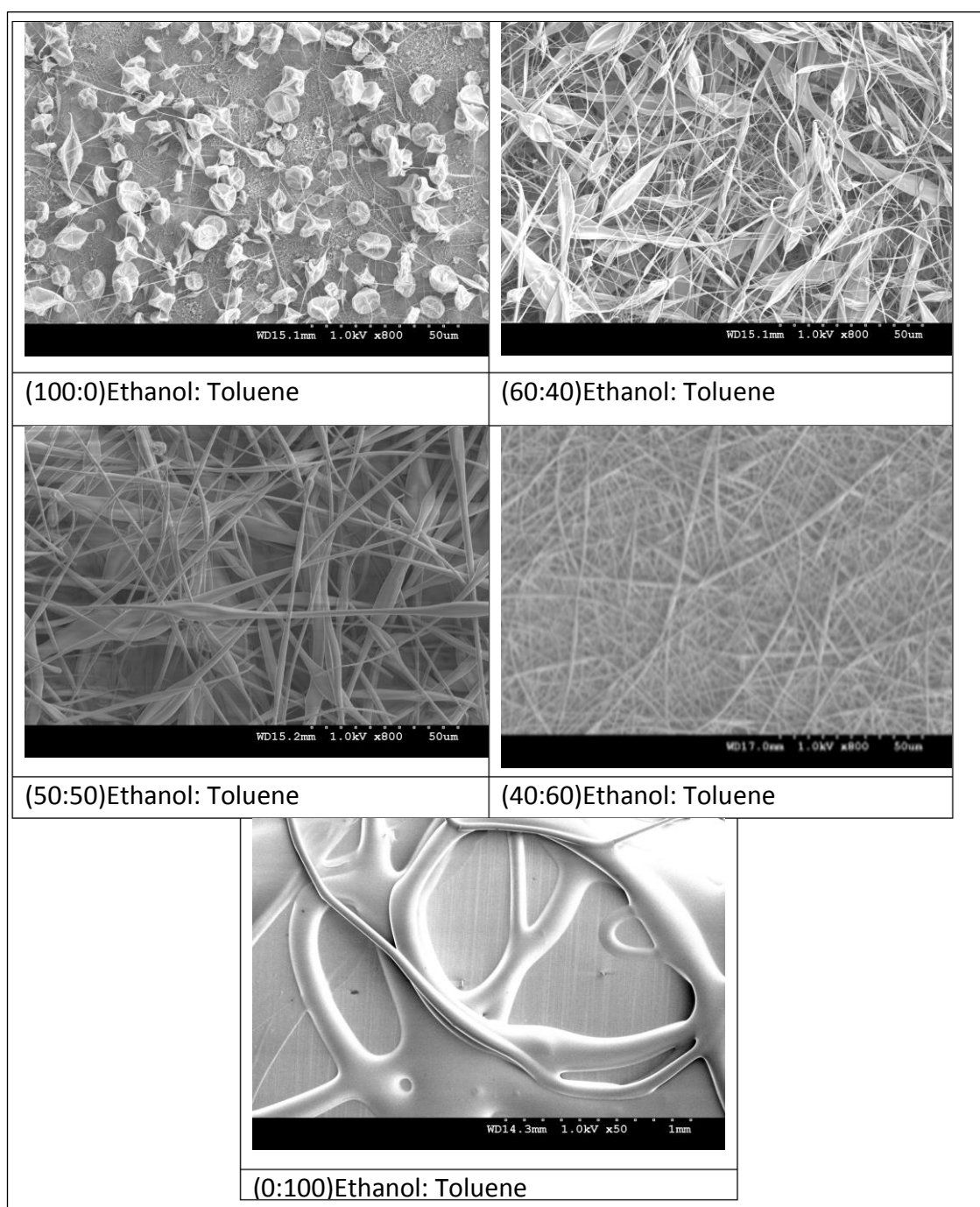


Figure 5:7 Effect of solvent proportion on fibre morphology

The viscosity of EC100Et is lower than any other EC solutions in the present study. Lower viscosity means, the EC100Et solution has not enough chain entanglement to generate bead-less fibres. So, the jet started producing droplets at some intervals. Surface tension of EC100Et produced round shaped beads. In case of EC100Et the surface tension is lower compared to any other EC solutions. Theoretically, lower surface tension should favour fewer beads. The effect of surface tension overcomes the






effect of viscosity and higher conductivity for producing beaded fibres. The surface tension was high enough to generate round shaped beads.

The EC100Et viscosity is not too low and hence it did not produce only beads but it produced beads on fibre due to some chain entanglements in the solutions.

Addition of toluene into EC reduced solution conductivity and increased solution viscosity as well as surface tension.

As discussed earlier, higher solution viscosity favours bead-less fibres, but higher surface tension and lower conductivity favours beaded fibres. In case of 15EC60Et, beads on string structure were produced (Table 5:3). The beads were more elongated than the beads of 15EC100Et. Viscosity and surface tension increased from 15EC100Et to 15EC60Et. Surface tension created beads in the fibre, but increased viscosity resisted the formation of beads. Bead became more elongated. Again due to a higher proportion of ethanol, the solvent evaporation was faster. Collapsed and irregular shaped beads were formed. With further increase in toluene, the beads became more elongated and solid. In 15EC50Et, fibres were produced with beads.

Table 5:3 Effect of solvent on ethyl cellulose electrospinning

Solvents (Ethanol: Toluene) ratio	Shape	Remark
100:0		Irregular / collapsed round bead on string
60:40		Irregular / collapsed elongated bead on string
50:50		Regular / solid elongated bead on string
40:60		Fibres
0:100		Thick fibres

The beads were not collapsed but were more solid. Bead formation was due to surface tension, but increasing the viscosity of 15Ec50Et resisted the formation of full beads (round shaped). Hence, elongated beads were formed. The evaporation of the solvent

was not as fast as in the case of 15EC100Et and 15EC60Et. Toluene has higher boiling point (approx. 110°C), so it evaporates slowly and allow to dry fibres slowly, which generated solid beads. With further increase in toluene proportion in solvent, the solution viscosity increased further. Higher viscosity overcomes surface tension at this stage, and no beads were formed, only fibres were formed in the case of 15EC60To. The average fibre diameters were 0.568 μm .

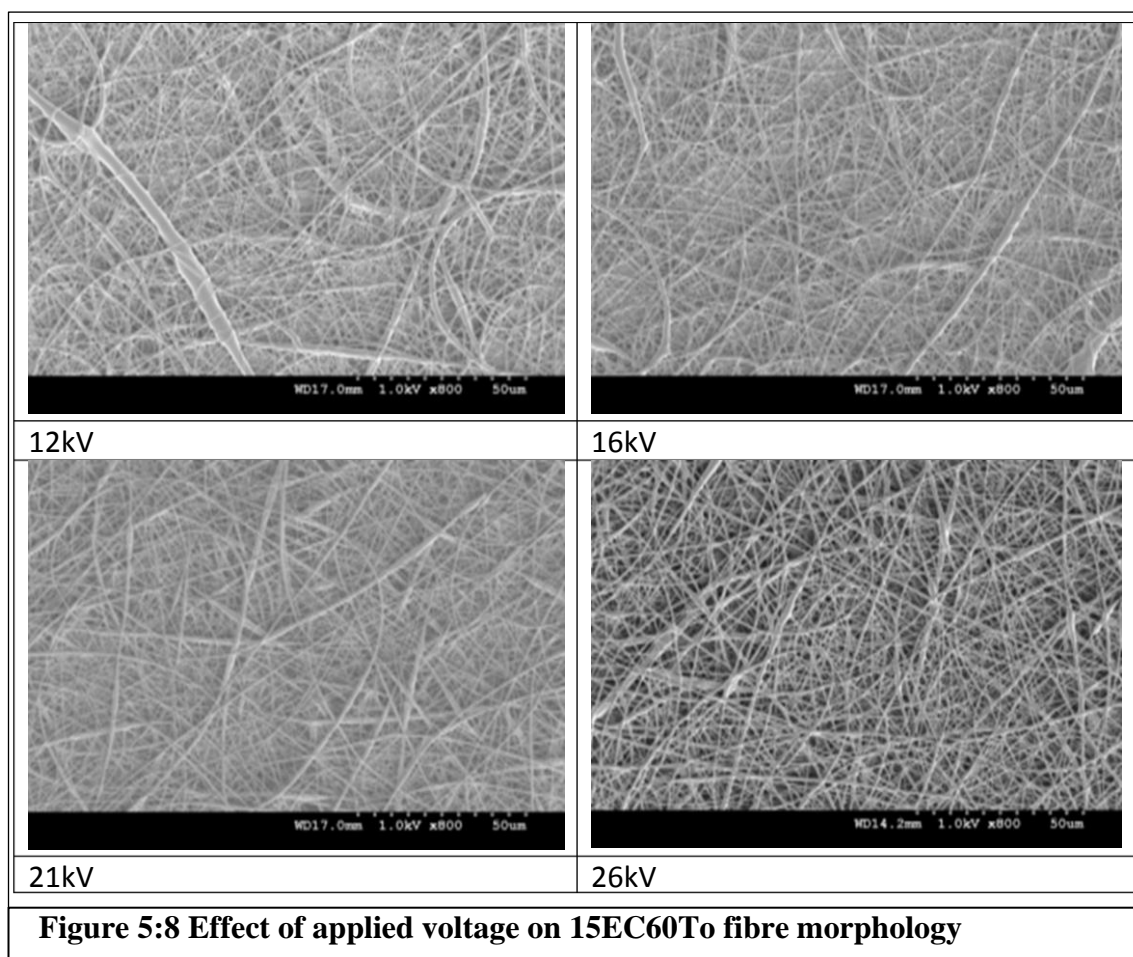
As discussed earlier, with the addition of toluene in ethanol (40, 50, 60) % wt., smooth and nearly bead-less fibres are produced. This might be due to increased viscosity with the addition of toluene into ethanol. 15EC100To produced thicker, bead-less fibres. The measured conductivity of 15EC100To was zero, but in spite of zero conductivity, stretch was observed on the 15EC100To solution droplets at higher voltage. This means still negligible conductivity existed in the 15EC100To solution, which was not measured by the conductivity meter. Unlike in the use of 15EC100Et, the 15EC100To spinning created larger droplets before spinning. Supaphol et al (2004) [57] observed similar increase in the fibre diameter with increasing m-cresol content. M-cresol increased the viscosity of the PA-6 solution and decreasing spinning conductivity. The increased viscoelastic force with reduction in coulombic repulsive force and in pulling electrical force, the fibre diameter increased. Previously reported work [51] also showed that high solution viscosity favoured the formation of thicker fibres without beads. Electrospinning using a concentrated nylon-4.6 solution produced smooth bead free nanofibres with thicker diameters. Although the surface tension, which was one of the main factors that influenced the formation of beaded fibres increased as the nylon concentration increased in the electrospinning solution, the viscosity increased more rapidly and was the main factor influencing the character of electrospun nanofibres. Similar effects can be seen in the present study. An addition of Toluene in the EC solutions increased with viscosity and surface tension. The effect of viscosity was found dominant and EC100To produced thicker bead-less fibres in spite of the increased surface tension.

5.3.5 Effect of Applied Voltage on Fibre Morphology

In electrospinning, the electrical potential applied to the polymer solution plays very important role in determining the size and shape of the fibre. The effect of field strength or applied voltage is one of the most studied parameters among the process variables of electrospinning [56-60]. Electrical forces are important in electrospinning.

Electrospinning starts, when coulombic repulsions and the electrical force overcome solution surface tension [37].

Higher applied voltage means higher coulombic repulsions and higher electrical force between needle and collector. Coulombic forces in the jet encourages splitting of jet and electrical forces encourages stretching of jets. Higher electrical force generally produces finer fibres. It varies depending upon the polymer-solution property, and the processing parameters. Higher electrical force pulls more solution, which generates a thicker jet. Higher applied voltage accelerates the jet giving less time for stretching / splitting of jet, hence coarser fibres are generated [38]. In electrospinning, the electrical charge is transported with the flow of the polymer jet. The change in the spinning current changes the shape of the jet initiating point, and hence it affects the properties of the electrospun fibres. Megelski et al.(2006) found reduced average fibre diameter with increase in voltage of 5kV to 12kV[51].



In the present work, 15EC60To fibres spun at the feed rate of 1.5ml/hr, at 20cm NTCD using 16G needle. In order to study the effect of applied voltage on fibre properties, the electrospinning is done at different voltages from 12kV, 16kV, 21kV and 25kV. All samples were observed in CFE-SEM. The average diameters were calculated by randomly selecting fibres from different areas of the SEM sample images. As can be

seen in (Figure 5:8, Figure 5:9) the average fibre diameter is reduced from 0.617 microns to 0.596 microns, 0.568 microns and 0.556 microns for increase in voltage from 12kV, 16kV, 21kV to 25kV, respectively.

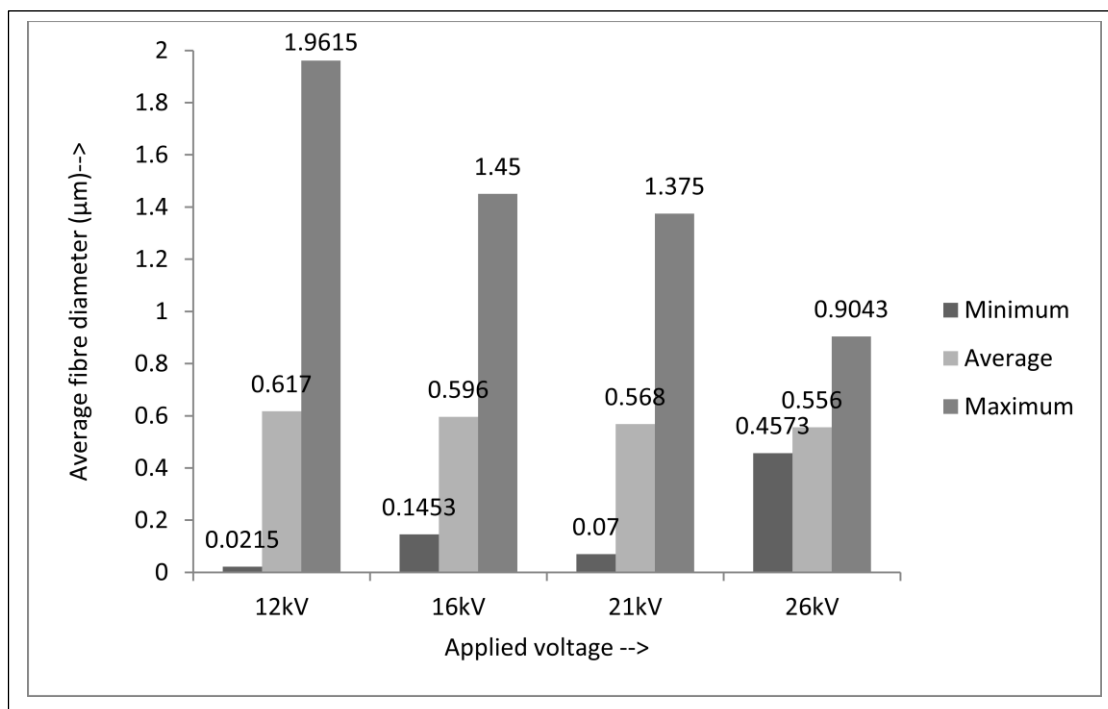


Figure 5:9 Effect of applied voltage on 15EC60To fibre diameter

5.3.6 Effect of Needle to Collector Distance on Fibre Morphology

NTCD affects the structure and morphology of the electrospun fibres. The change in NTCD affects the deposition time, evaporation rate, and whipping or instability interval [51]. The higher NTCD means more time for jet to travel, so more stretching and splitting during spinning, so, thinner fibres can be generated. Thinner fibres have more surface exposed for drying, at the same time the jet gets more flight time in higher NTCD. Generally drier and thinner fibres are generated at higher NTCD. In some cases increase in diameter of the fibres were also reported at higher NTCD [61], the reason for this was due to a reduced voltage per unit distance at higher NTCD. As NTCD increased the distribution of electric field per unit distance weakens, so, the stretching electrical force and splitting coulombic repulsions are being reduced, this in turn generates thicker fibres at higher NTCD.

In the case of 15EC60To the NTCD changed keeping other parameters the same at applied voltage-21kV, feed rate-1.5ml/hr and 16G needle. The NTCD changed from 10cm, 20cm to 30cm for studying the effect of NTCD on the morphology and shape of the fibre.

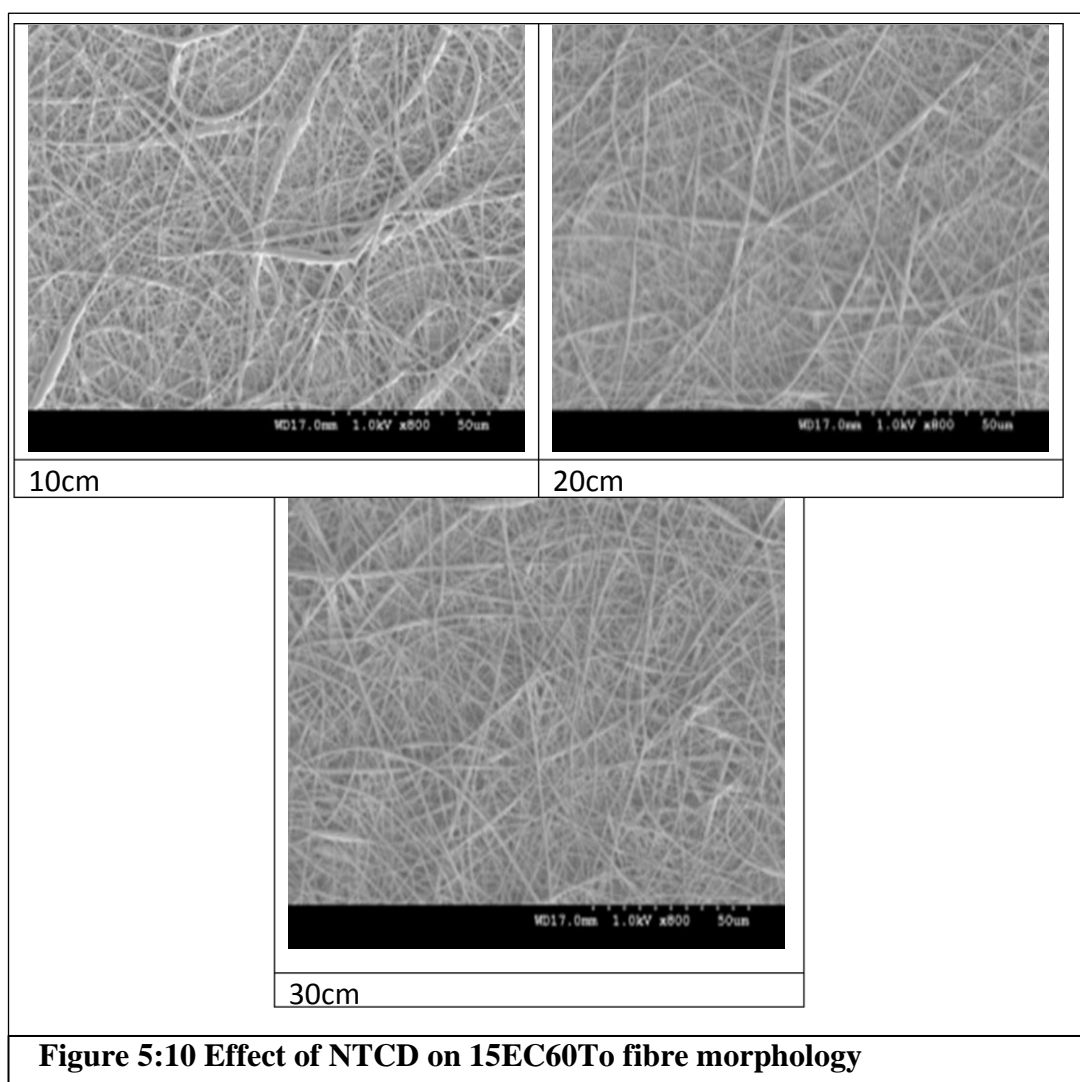


Figure 5:10 Effect of NTCD on 15EC60To fibre morphology

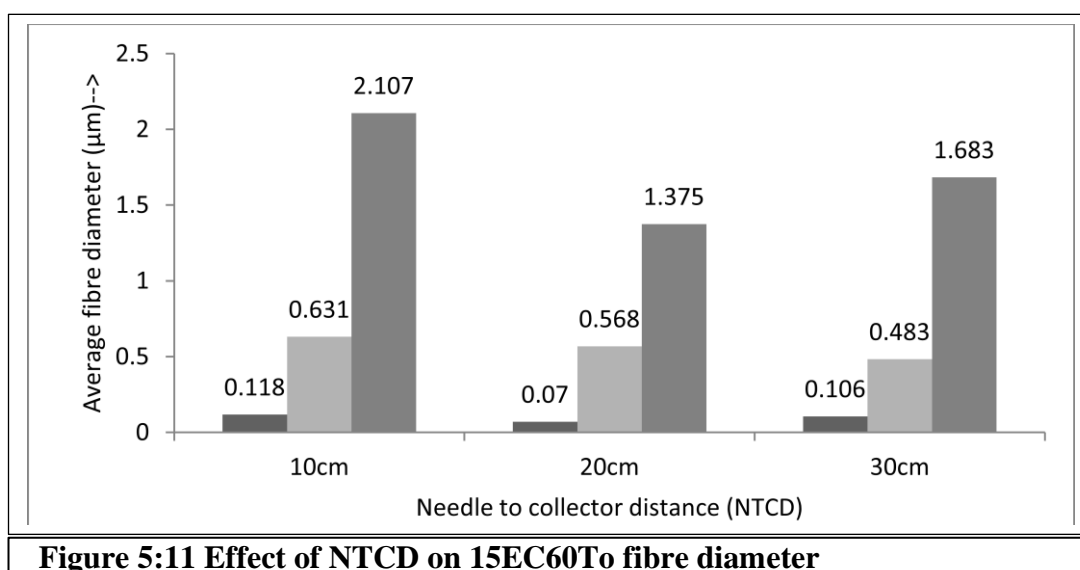


Figure 5:11 Effect of NTCD on 15EC60To fibre diameter

The fibre diameter is reduced with higher NTCD, the average diameter of the fibres reduced from 0.631microns to 0.568microns and 0.483microns at 10cm, 20cm and 30cm NTCD respectively (Figure 5:10, Figure 5:11).

5.3.7 FTIR (Fourier Transform Infrared Spectroscopy)

The FTIR spectrum of EC solutions with different solvent ratios are shown in (Figure 5:12, Figure 5:13, Figure 5:14).

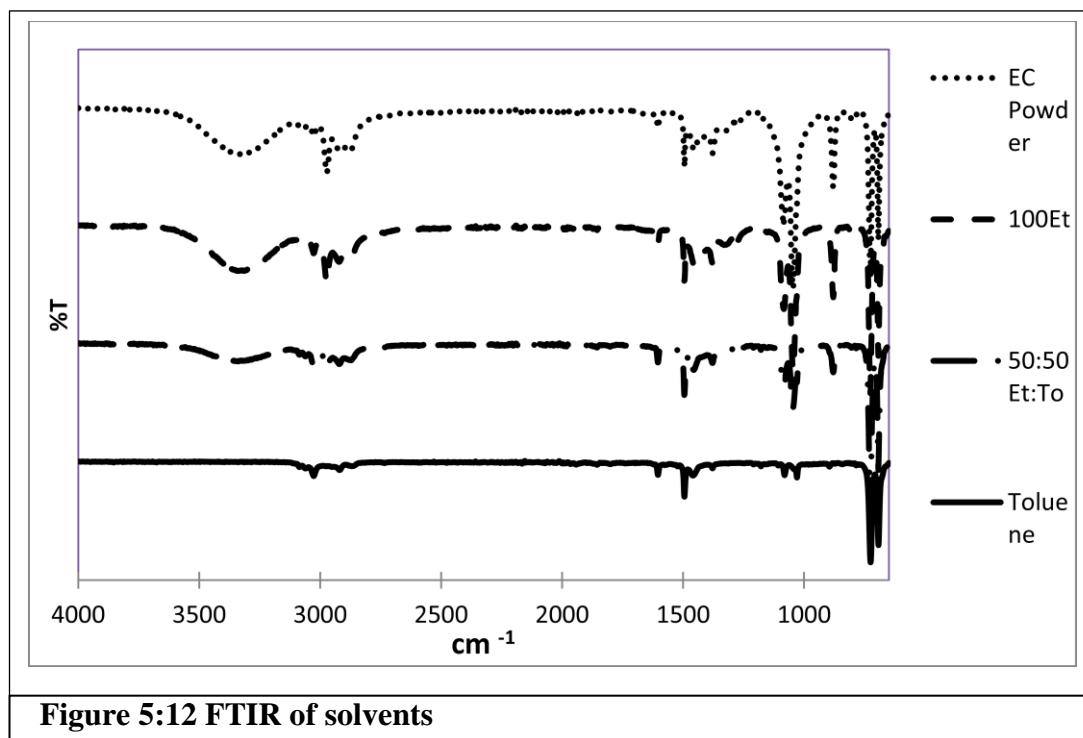


Figure 5:12 FTIR of solvents

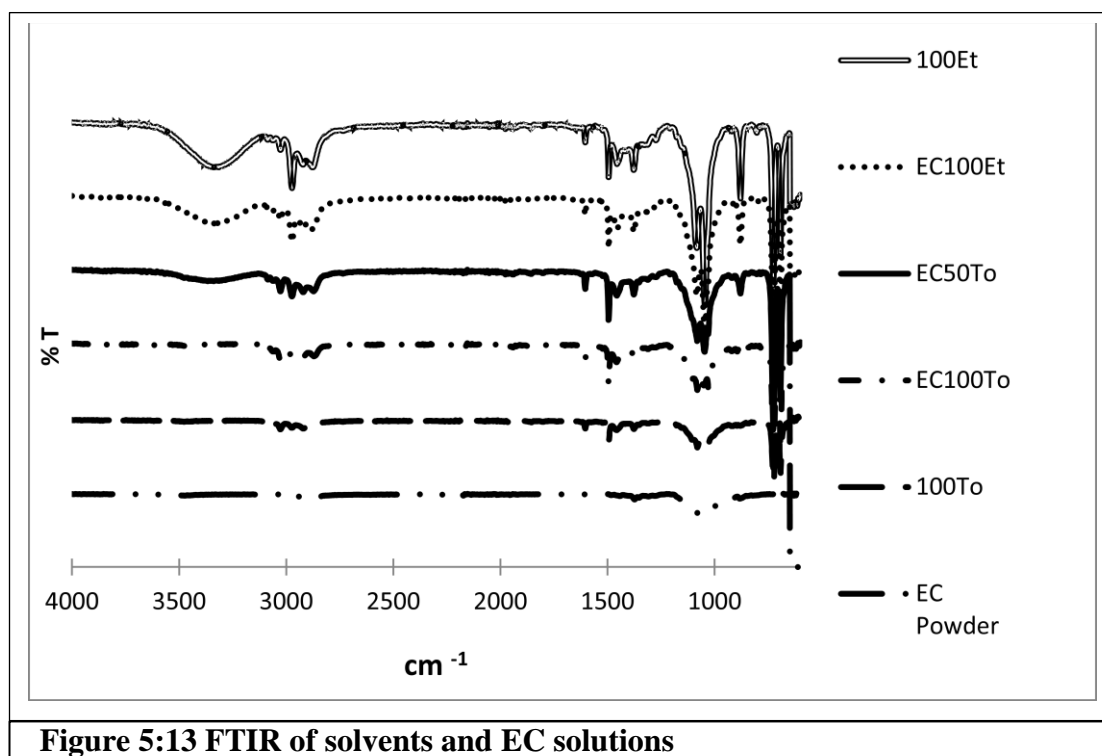


Figure 5:13 FTIR of solvents and EC solutions

A band at 3476 cm^{-1} was attributed to -OH stretching vibration in the EC powder present on the closed ring structure of the polymer repeating units. The spectrum of EC shows characteristic absorption bands for -C-O-C- stretching vibration at 1052.21 cm^{-1} and C-H stretching bands at 2871.36 cm^{-1} and 2973.29 cm^{-1} .

The absorption at 1374.54 cm^{-1} corresponds to C–H bending. Toluene FTIR shows, (the =C–H stretches of aromatics (3087.22, 3062.88, 3027.49) and the –C–H stretches of the alkyl (methyl) group (2920.13). The carbon-carbon stretches in the aromatic ring (1604.54, 1495.45, 1459.48), the in-plane C–H bending (1082.14, 1030.07), and the C–H oop (725.43).

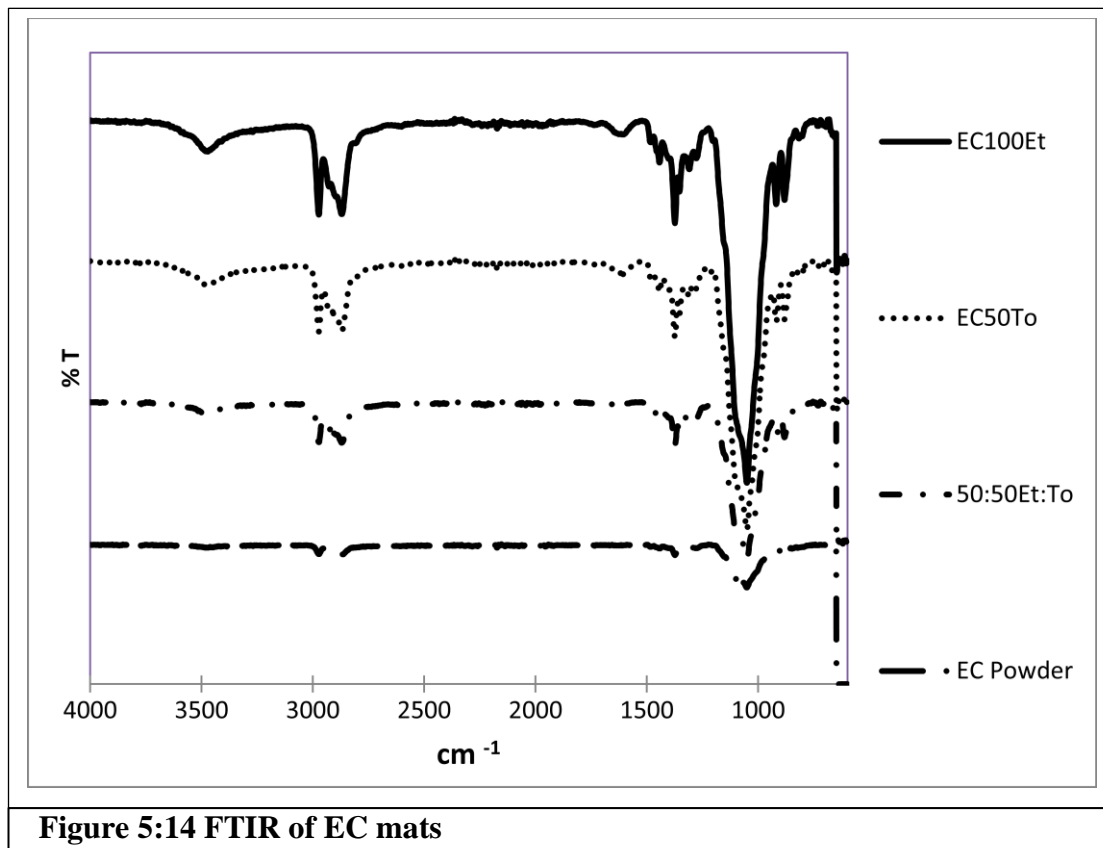


Figure 5:14 FTIR of EC mats

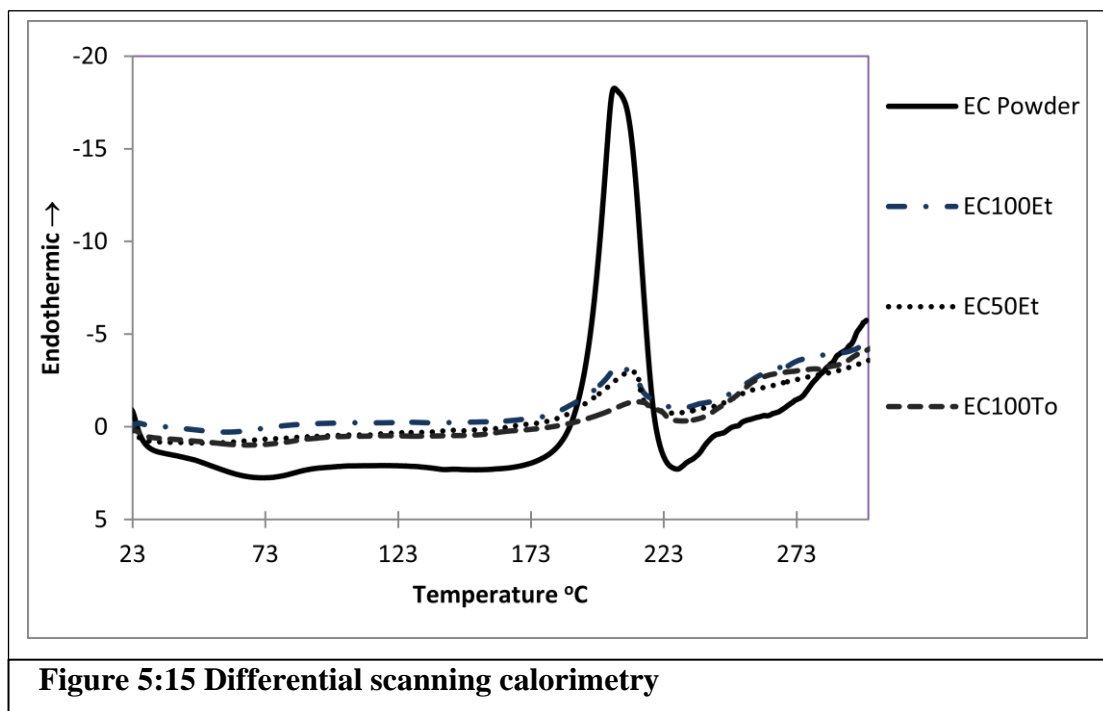
Ethanol FTIR shows, O–H band at 3325.09 cm^{-1} , C–H band at (2973.59 , 2924.94 , 2879.54) cm^{-1} , C=C band at 1648.14 cm^{-1} , CH₂ band at (1453.75 , 1417.34 , 1379.81 , 1328.67 , 1274.89) cm^{-1} , C–O band at (1087.70 , 1045.41) cm^{-1}

FTIR of all ethyl cellulose solutions have shown the effect of ethyl cellulose and relevant solvent systems on the corresponding bands in the FTIR chart. For example, as can be seen wide –O–H stretch at 3325.09 cm^{-1} in ethanol appears at 3331.54 cm^{-1} in the ethyl cellulose solution with 100% ethanol, it gets smaller in the 50:50 mixture of ethanol: toluene at 3350.34 cm^{-1} and it disappears in ethyl cellulose solution with 100% toluene.

FTIR in all films made from all solvent systems after drying, showed identical charts as in the case of the ethyl cellulose powder. After solvent evaporation, there are not many changes in the ethyl cellulose structure.

5.3.8 Differential Scanning Calorimetry

The DSC thermograms for EC powder and EC fibres prepared from different mixture of ethanol:toluene ratios. EC100Et, EC50Et50To and EC100To mats were cut into 5mg of samples (Figure 5:15). The DSC curve of the EC powder showed an exothermic transition peak at temperature of 69.7°C and a sharp endothermic melting peak at 203.6°C , the DSC curve for EC100Et showed an exothermic transition at 56.1°C and endotherm at 206°C .



The EC100To DSC curve showed exothermic transition at 63.3°C and endotherm at 211.5°C and the EC50Et50To DSC curve showed exothermic transition at 53.1°C and endotherm at 208.9°C . The melting temperature, crystallinity depends on the solvent and polymer interaction [62, 63].

5.4 Conclusion

EC was successfully electrospun with different solvent systems from bead on string structure to smooth, bead-less, fibrous film structure. Characterization of the electrospun nanofibres shows that solution viscosity, net charge density carried by the electrospinning jet and by the surface tension of the solution is the main factors influencing fibre morphology. Beaded fibres were formed due to low viscosity of the solution of ethylcellulose in ethanol. As discussed, low viscosity favours beaded fibres. In the case of ethanol: toluene (50:50), due to higher viscosity. Smooth bead-less fibres were formed compared to ethanol in which higher surface tension and lower conductivity beaded fibres were formed. In case of toluene as a solvent, in spite of higher surface tension and negligible conductivity (which favours beaded fibres),

smooth and coarse fibres were formed due to higher viscosity compared to the other two cases. Therefore in EC, viscosity plays a much significant effect more than the surface tension and the conductivity of the solution. As viscosity depends on solution concentration and on the type of solvent system. Although all ethyl cellulose solutions were prepared with the same concentration, their viscosities were different due to different solvent systems. This indicates that the selection of solvent plays very important role on fibre morphology of ethyl cellulose. This finding can aid in the optimisation of the formation of EC fibres and their effective functionality for a variety of end uses.

5.5 Bibliography

- [5.1] C. R. Carere, R. Sparling, N. Cicek, and D. B. Levin, "Third generation biofuels via direct cellulose fermentation," *Int J Mol Sci*, vol. 9, pp. 1342-60, Jun 2008.
- [5.2] Anon. (2005, 16/09/2012). *ETHOCEL-Ethylcellulose Polymers Technical Handbook*. Available:
http://msdssearch.dow.com/PublishedLiteratureDOWCOM/dh_004f/0901b8038004fb7c.pdf?filepath=ethocel/pdfs/noreg/192-00818.pdf&fromPage=GetDoc
- [5.3] R. F. Conaway, "Chemistry of Cellulose Derivatives," *Industrial & Engineering Chemistry*, vol. 30, pp. 516-523, 1938/05/01 1938.
- [5.4] M. Bonet, C. Quijada, and F. Cases, "Characterization of Ethylcellulose with Different Degrees of Substitution (DS): A Diffuse-Reflectance Infrared Study," *Canadian Journal Of Analytical Sciences And Spectroscopy*, vol. 49, pp. 234-239, 2004.
- [5.5] S. C. Fox, B. Li, D. Xu, and K. J. Edgar, "Regioselective esterification and etherification of cellulose: a review," *Biomacromolecules*, vol. 12, pp. 1956-72, Jun 13 2011.
- [5.6] O. Pillai and R. Panchagnula, "Polymers in drug delivery," *Curr Opin Chem Biol*, vol. 5, pp. 447-451, 2001.
- [5.7] W. Yuan, J. Yuan, F. Zhang, and X. Xie, "Syntheses, Characterization, and in Vitro Degradation of Ethyl Cellulose-graft-poly(ϵ -caprolactone)-block-poly(l-lactide) Copolymers by Sequential Ring-Opening Polymerization," *Biomacromolecules*, vol. 8, pp. 1101-1108, 2007/04/01 2007.
- [5.8] M. Li, O. Rouaud, and D. Poncelet, "Microencapsulation by solvent evaporation: State of the art for process engineering approaches," *International Journal of Pharmaceutics*, vol. 363, pp. 26-39, 2008.

- [5.9] Anon, "Product Safety Assessment: ETHOCEL™ Ethylcellulose Polymers," ed: The Dow Chemical Company, 2008, pp. 1-8.
- [5.10] A. J. Gravelle, S. Barbut, and A. G. Marangoni, "Ethylcellulose oleogels: Manufacturing considerations and effects of oil oxidation," *Food Research International*, vol. 48, pp. 578-583, 2012.
- [5.11] A. K. Zetzi, A. G. Marangoni, and S. Barbut, "Mechanical properties of ethylcellulose oleogels and their potential for saturated fat reduction in frankfurters," *Food Funct*, vol. 3, pp. 327-37, Mar 2012.
- [5.12] T. A. L. Do, J. R. Mitchell, B. Wolf, and J. Vieira, "Use of ethylcellulose polymers as stabilizer in fat-based food suspensions examined on the example of model reduced-fat chocolate," *Reactive and Functional Polymers*, vol. 70, pp. 856-862, 2010.
- [5.13] N. Grattard, M. Pernin, B. Marty, G. Roudaut, D. Champion, and M. Le Meste, "Study of release kinetics of small and high molecular weight substances dispersed into spray-dried ethylcellulose microspheres," *Journal of Controlled Release*, vol. 84, pp. 125-135, 2002.
- [5.14] G. B. Avanço and M. L. Bruschi, "Preparation and characterisation of ethylcellulose microparticles containing propolis," *Rev. Ciênc. Farm. Básica Apl.*, vol. 29, pp. 129-134, 2008.
- [5.15] O. A. Cavalcanti, B. Petenuc, A. C. Bedin, E. A. G. Pineda, and A. A. W. Hechenleitner, "Characterisation of Ethylcellulose Films containing Natural Polysaccharides by Thermal Analysis and FTIR Spectroscopy," *Acta. Farm. Bonaerense*, vol. 23, pp. 53-7, 2004.
- [5.16] D. Han and P.-I. Gouma, "Electrospun bioscaffolds that mimic the topology of extracellular matrix," *Nanomedicine*, vol. 2, pp. 37-41, 2006.
- [5.17] P. Taepaiboon, U. Rungsardthong, and P. Supaphol, "Vitamin-loaded electrospun cellulose acetate nanofibre mats as transdermal and dermal therapeutic agents of vitamin A acid and vitamin E," *Eur J Pharm Biopharm*, vol. 67, pp. 387-97, Sep 2007.
- [5.18] B. Ding, C. Li, Y. Hotta, J. Kim, O. Kuwaki, and S. Shiratori, "Conversion of an electrospun nanofibrous cellulose acetate mat from a super-hydrophilic to super-hydrophobic surface," *Nanotechnology*, vol. 17, pp. 4332-4339, 2006.
- [5.19] W. Son, J. Youk, and W. Park, "Antimicrobial cellulose acetate nanofibres containing silver nanoparticles," *Carbohydrate Polymers*, vol. 65, pp. 430-434, 2006.

- [5.20] Y. Tian, M. Wu, R. Liu, Y. Li, D. Wang, J. Tan, R. Wu, and Y. Huang, "Electrospun membrane of cellulose acetate for heavy metal ion adsorption in water treatment," *Carbohydrate Polymers*, vol. 83, pp. 743-748, 2011.
- [5.21] S. Tungprapa, T. Puangparn, M. Weerasombut, I. Jangchud, P. Fakum, S. Semongkhon, C. Meechaisue, and P. Supaphol, "Electrospun cellulose acetate fibres: effect of solvent system on morphology and fibre diameter," *Cellulose*, vol. 14, pp. 563-575, 2007.
- [5.22] S. O. Han, J. H. Youk, K. D. Min, Y. O. Kang, and W. H. Park, "Electrospinning of cellulose acetate nanofibres using a mixed solvent of acetic acid/water: Effects of solvent composition on the fibre diameter," *Materials Letters*, vol. 62, pp. 759-762, 2008.
- [5.23] W. K. Son, J. H. Youk, T. S. Lee, and W. H. Park, "Electrospinning of ultrafine cellulose acetate fibres: Studies of a new solvent system and deacetylation of ultrafine cellulose acetate fibres," *Journal of Polymer Science Part B: Polymer Physics*, vol. 42, pp. 5-11, 2004.
- [5.24] O. Suwantong, P. Opanasopit, U. Ruktanonchai, and P. Supaphol, "Electrospun cellulose acetate fibre mats containing curcumin and release characteristic of the herbal substance," *Polymer*, vol. 48, pp. 7546-7557, 2007.
- [5.25] O. Suwantong, U. Ruktanonchai, and P. Supaphol, "In vitro biological evaluation of electrospun cellulose acetate fibre mats containing asiaticoside or curcumin," *J Biomed Mater Res A*, vol. 94, pp. 1216-25, Sep 15 2010.
- [5.26] O. Suwantong, U. Ruktanonchai, and P. Supaphol, "Electrospun cellulose acetate fibre mats containing asiaticoside or Centella asiatica crude extract and the release characteristics of asiaticoside," *Polymer*, vol. 49, pp. 4239-4247, 2008.
- [5.27] D. Haas, S. Heinrich, and P. Greil, "Solvent control of cellulose acetate nanofibre felt structure produced by electrospinning," *Journal of Materials Science*, vol. 45, pp. 1299-1306, 2010.
- [5.28] J. Y. Park, S. W. Han, and I. H. Lee, "Preparation of Electrospun Porous Ethyl Cellulose Fibre by THF/DMAc binary solvent system," *Journal of industrial engineering chemistry*, vol. 13, pp. 1002-1008, 2007.
- [5.29] X. Wu, L. Wang, H. Yu, and Y. Huang, "Effect of solvent on morphology of electrospinning ethyl cellulose fibres," *Journal of Applied Polymer Science*, vol. 97, pp. 1292-1297, 2005.

- [5.30] J. P. Jeun, Y. M. Lim, J. H. Choi, H. S. La, P. H. Kang, and Y. C. Nho, "Preparation of Ethyl-Cellulose Nanofibres via An Electrospinning," *Solid State Phenomena*, vol. 119, pp. 255-258, 2007.
- [5.31] T. Lei, Z. Zhan, W. Zuo, W. Cheng, B. Xu, Y. Su, and D. Sun, "Electrospinning PVDF/EC fibre from a binary solvent system," *International Journal of Nanomanufacturing*, vol. 8, pp. 294-305, 2012.
- [5.32] Y.-M. Lim, H.-J. Gwon, J. P. Jeun, and Y.-C. Nho. (2010, 12 Dec. 2011). *Preparation of cellulose based nanofibres using electrospinning*. Available: <http://www.intechopen.com/books/nanofibres/preparation-of-cellulose-based-nanofibres-using-electrospinning>
- [5.33] C.-W. Kim, D.-S. Kim, S.-Y. Kang, M. Marquez, and Y. L. Joo, "Structural studies of electrospun cellulose nanofibres," *Polymer*, vol. 47, pp. 5097-5107, 2006.
- [5.34] M. W. Frey, "Electrospinning Cellulose and Cellulose Derivatives," *Polymer Reviews*, vol. 48, pp. 378-391, 2008.
- [5.35] H. Zhang, H. Nie, S. Li, C. J. B. White, and L. Zhu, "Crosslinking of electrospun polyacrylonitrile/hydroxyethyl cellulose composite nanofibres," *Materials Letters*, vol. 63, pp. 1199-1202, 2009.
- [5.36] N. Bhardwaj and S. C. Kundu, "Electrospinning: a fascinating fibre fabrication technique," *Biotechnology advances*, vol. 28, pp. 325-47, 2010.
- [5.37] A. Patanaik, R. D. Anandjiwala, R. S. Rengasamy, A. Ghosh, and H. Pal, "Nanotechnology in fibrous materials—a new perspective," *Textile Progress*, vol. 39, pp. 67-120, 2007.
- [5.38] S. Ramakrishna, K. Fujihara, W.-E. Teo, T.-C. Lim, and Z. Ma, *An Introduction to Electrospinning And Nanofibres*: World Scientific Publishing Company, Singapore, 2005.
- [5.39] Z. Ma, M. Kotaki, and S. Ramakrishna, "Surface modified nonwoven polysulphone (PSU) fibre mesh by electrospinning: A novel affinity membrane," *Journal of Membrane Science*, vol. 272, pp. 179-187, 2006.
- [5.40] S. H. Tan, R. Inai, M. Kotaki, and S. Ramakrishna, "Systematic parameter study for ultra-fine fibre fabrication via electrospinning process," *Polymer*, vol. 46, pp. 6128-6134, 2005.
- [5.41] V. Suthar, A. Pratap, and H. Raval, "Studies on poly (hydroxy alkanoates)/(ethylcellulose) blends," *Bulletin of Materials Science*, vol. 23, pp. 215-219, 2000.

- [5.42] R. Lalani and L. Liu, "Synthesis, characterization, and electrospinning of zwitterionic poly(sulfobetaine methacrylate)," *Polymer*, vol. 52, pp. 5344-5354, 2011.
- [5.43] H. Arwidsson and B. Johansson, "Application of intrinsic viscosity and interaction constant as a formulation tool for film coating. III. Mechanical studies on free ethyl cellulose films, cast from organic solvents," *International Journal of Pharmaceutics*, vol. 76, pp. 91-97, 1991.
- [5.44] I. Jullander and K. Pääbo, "Solubility Properties of Non-ionic Water-soluble Cellulose Ethers in Mixtures of Water and Alcohol," *Acta Chemica Scandinavica*, vol. 9, pp. 1620-1633, 1955.
- [5.45] H. C. Haas, L. Farney, and C. Valle Jr, "Some properties of ethyl cellulose films," *Journal of colloid science*, vol. 7, pp. 584-599, 1952.
- [5.46] Anon. (2002, 12 Dec. 2011). *AQUALON Ethylcellulose (EC) Physical and Chemical Properties*. Available:
http://www.ashland.com/Ashland/Static/Documents/AAFI/PRO_250-42A_Aqualon_EC.pdf
- [5.47] K. H. Lee, H. Y. Kim, H. J. Bang, Y. H. Jung, and S. G. Lee, "The change of bead morphology formed on electrospun polystyrene fibres," *Polymer*, vol. 44, pp. 4029-4034, 2003.
- [5.48] C. Tekmen, A. Suslu, and U. Cocen, "Titania nanofibres prepared by electrospinning," *Materials Letters*, vol. 62, pp. 4470-4472, 2008.
- [5.49] G. Eda, J. Liu, and S. Shivkumar, "Flight path of electrospun polystyrene solutions: Effects of molecular weight and concentration," *Materials Letters*, vol. 61, pp. 1451-1455, 2007.
- [5.50] H. Liu and Y.-L. Hsieh, "Ultrafine fibrous cellulose membranes from electrospinning of cellulose acetate," *Journal of Polymer Science Part B: Polymer Physics*, vol. 40, pp. 2119-2129, 2002.
- [5.51] C. Huang, S. Chen, C. Lai, D. H. Reneker, H. Qiu, Y. Ye, and H. Hou, "Electrospun polymer nanofibres with small diameters," *Nanotechnology*, vol. 17, pp. 1558-1563, 2006.
- [5.52] I. C. H. Fong, D.H. Reneker, "Beaded nanofibres formed during electrospinning," *Polymer*, vol. 40, pp. 4585-4592, 1999.
- [5.53] K. Ziani, C. Henrist, C. Jérôme, A. Aqil, J. I. Maté, and R. Cloots, "Effect of nonionic surfactant and acidity on chitosan nanofibres with different molecular weights," *Carbohydrate Polymers*, vol. 83, pp. 470-476, 2011.

- [5.54] P. Heikkila, "Electrospinning of polyacrylonitrile (PAN) solution: Effect of conductive additive and filler on the process," *eXPRESS Polymer Letters*, vol. 3, pp. 437-445, 2009.
- [5.55] M. Chowdhury and G. K. Stylios, "Analysis of the effect of experimental parameters on the morphology of electrospun polyethylene oxide nanofibres and on their thermal properties," *Journal of the Textile Institute*, vol. 103, pp. 124-138, 2012.
- [5.56] M. M. Munir, A. B. Suryamas, F. Iskandar, and K. Okuyama, "Scaling law on particle-to-fibre formation during electrospinning," *Polymer*, vol. 50, pp. 4935-4943, 2009.
- [5.57] C. Mit-uppatham, M. Nithitanakul, and P. Supaphol, "Ultrafine Electrospun Polyamide-6 Fibres: Effect of Solution Conditions on Morphology and Average Fibre Diameter," *Macromolecular Chemistry and Physics*, vol. 205, pp. 2327-2338, 2004.
- [5.58] X. Zong, K. Kim, D. Fang, S. Ran, B. S. Hsiao, and B. Chu, "Structure and process relationship of electrospun bioabsorbable nanofibre membranes," *Polymer*, vol. 43, pp. 4403-4412, 2002.
- [5.59] T. Subbiah, G. S. Bhat, R. W. Tock, S. Parameswaran, and S. S. Ramkumar, "Electrospinning of nanofibres," *Journal of Applied Polymer Science*, vol. 96, pp. 557-569, 2005.
- [5.60] J. M. Deitzel, J. D. Kleinmeyer, D. Harris, and N. C. Beck Tan, "The effect of processing variables on the morphology of electrospun nanofibres and textiles," *Polymer*, vol. 42, pp. 261-272, 2001.
- [5.61] Y. Ahn, S. Park, G. Kim, Y. Hwang, C. Lee, H. Shin, and J. Lee, "Development of high efficiency nanofilters made of nanofibres," *Current Applied Physics*, vol. 6, pp. 1030-1035, 2006.
- [5.62] S. Pattnaik, K. Swain, S. Mallick, and Z. Lin, "Effect of casting solvent on crystallinity of ondansetron in transdermal films," *Int J Pharm*, vol. 406, pp. 106-10, Mar 15 2011.
- [5.63] J. L. McPeak, "Solvent – induced crystallization of poly (ether ether ketone)," Doctor of Philosophy, Virginia Polytechnic Institute and State University, Virginia Polytechnic Institute and State University, Blacksburg, Virginia, 1999.

Chapter 6 : The Case of Bubble Electrospinning of Ethylcellulose Ultrafine Fibres

6.1 Introduction

Ethylcellulose (EC) is one of the most stable cellulose ether [1]. EC is widely used in pharmaceuticals, food and plastic industries due to its unique properties such as biocompatibility, hydrophobicity, nontoxicity, non-biodegradability and thermoplasticity. EC is colourless, odourless, non-caloric and a tasteless biopolymer [2-6]. EC is electrospun by various researchers to make ultrafine micro-nano fibres [7-11] using needle electrospinning. Nanofibres have unique properties promoted by its dimension compared to its micro/macros. High surface area to volume ratio, cellular dimensions, more active surface due to high surface area and hence more active fibres make them interest to many researchers [12]. Various methods are available for nanofibre production, among them electrospinning is practical and successful. In needle electrospinning the polymer solution/melt is stretched / split into fibres by high electric field [13, 14]. Polymer solution/melt is pumped to the needle tip. The solution forms droplet at needle tip. Opposite voltage is applied on both needle i.e. solution droplet and collector. The coulombic repulsions are generated in the solutions due to same applied voltage charge on all ions in the droplet. The solution forms circular shaped droplets due to surface tension. However, as voltage increases, the repulsions cause ions to move apart from each other and the droplet shape changes from circular to conical. This conical shaped droplet is known as “Taylor Cone”. At critical voltage (V_c), the repulsive force overcomes the surface tension. The Taylor cone splits into jets at a critical voltage. The split jet is attracted towards the collector due to the opposing charge in the collector. During the flight towards the collector, jet takes various chaotic zigzag paths to minimize the effect of all forces. The jet travels a longer path and not at a straight path. Sometimes jets also split due to repulsive forces in the jet. The jet undergoes more splitting , stretching. Jet becomes thinner, of the micro-nano dimension [12, 15]. Various parameters affect fibre morphology such as; feed rate, nozzle to collector distance (NTCD), applied voltage, solution viscosity and surface tension, atmospheric conditions etc. [12, 16, 17].

Based on the above principle, single needle eletrospinning (SNE) and/or multiple needle electrospinning (MNE) were reported by various researchers [18-20]. SNE is simple when only one needle is used. There are negative points/limitations of SNE.

Productivity is not viable for industrial scale production due to use of single spinneret. Problems such as needle blocking may occur in SNE depending on solvent used. In addition, width size of produced mat is limited in SNE. In order to overcome lower productivity, researchers tried MNE. In case of MNE though productivity increases, it has its own problems. In MNE, apart from needle blocking, problems of jet repulsions occur due to like charges in all jets. In MNE, the distance between needle also needed to be adjusted to get uniform thickness across the fabric width [18-20]. Productivity is still limited and depends on number of needle used compared to needle-less systems described later.

All above negative points increased researchers' interest towards needle-less systems. Needle-less electrospinning offers benefits particularly higher productivity due to unlimited jets, unlimited jets offer more grams/unit time. Needle electrospinning can be used for productivity at industrial scale.

A roller based needle-less system, developed by Jirsak, was commercialized by Elmarco under the brand name "nano spider" [21]. The different concepts developed for needle-less electrospinning are as follow: Centrifugal electrospinning system [22, 23]/Rotary Jet-Spinning/ Forcespinning [24, 25], roller electrostatic spinner[26, 27], ferromagnetic suspension [28], electriferous rotating cone [29], conical wire coil [30], circular and tipped surface cylindrical spinneret [31], cylinder with rounded rim, disc and ball were used as spinnerets [21] free surface of a spherical liquid layer [32] , Wire Electrode [33] and bubble electrospinning (BE) [34-44].

BE is a needle-less electrospinning method invented in 2007 [37]. In BE, bubbles are generated by compressed air /gas. The principle of BE is explained in chapter 1, Figure 1.7. 'In contrast to the classical electrospinning, of which the electrospinnability mainly depends on solution properties, bubble-electrospinning's depends on the geometric sizes of the produced bubbles' [37]. Needle-less electrospinning offers benefits such as more productivity due to unlimited jets. Unlimited jets offer more grams/unit time. Needle-less electrospinning can be used for industrial scale productivity.

6.2 Materials and Experimental Methods

6.2.1 Materials

Ethanol (96%) was purchased from Fisher scientific and Toluene from Rathburn, Scotland and used as a solvent. Ethyl cellulose (Ethoxyl content 48%) was purchased from Aldrich. All chemicals were used without further purification.

6.2.2 Solution Preparation

Ethylcellulose powder was mixed with Toluene: Ethanol (60:40) and kept in ultrasonic bath for 24 hours to prepare a 15% (w/w) EC solution. The 15% EC solution was used for BE and SNE.

6.2.3 Solvent and Solution Properties (Viscosity, Surface Tension and Conductivity)

The viscosity of the solution was measured by Brookfield DV-II Pro. Surface Tension was measured by Kruss surface tension meter and conductivity was measured by Oakton con 110 handheld conductivity meter.

6.2.4 Bubble Electrospinning Setup and Parameters

In BE electrospinning air bubbles were generated by compressed air (0.7 bar pressure). A compressor (B100SEC, Charles Austen Pumps Ltd.) was connected to a 15% EC solution reservoir by a 0.8mm inner diameter tube. A high voltage supply (Glassman, MK35P2.0-22 and U.S.A.) was connected to the 15% EC solution. The potential difference between bubble and collector generated multiple jets / fibres formed as explained earlier.

6.2.5 Scanning Electron Microscopic (SEM) Studies

In order to study fibre morphology, the electrospun fibres were observed under a Hitachi CFE-SEM (Model: S-4300, Japan). The gold-palladium sputter coater unit (Polaron SC7620) was used to coat fibres to enable samples to be studied at an accelerating voltage of 1 kV and current of 10 μ Amps in SEM.

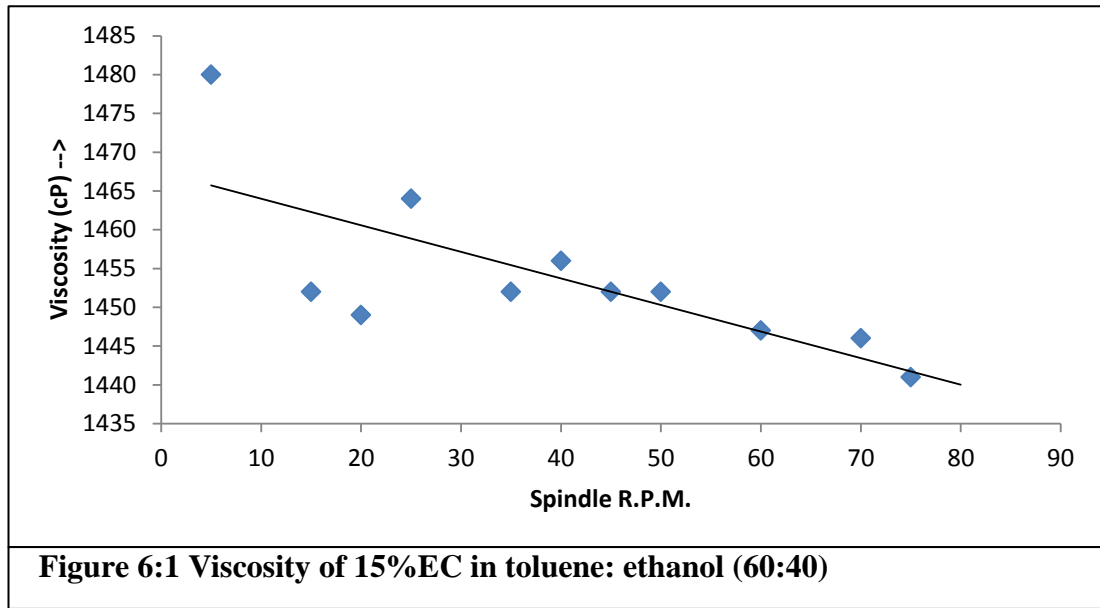
6.2.6 FTIR (Fourier Transform Infrared Spectroscopy)

FTIR is most useful for identifying chemicals that are either organic or inorganic. It can be utilized to quantitate some components of the unknown mixture. It can be applied to the analysis of solids, liquids, and gasses. Infrared spectra were obtained on a Perkin-Elmer Spectrum 100 FT-IR Universal ATR Sampling Accessory, deposited neatly to a diamond/ZnSe plate. The FTIR was used with 4cm⁻¹ resolution to record FTIR spectra between the 4000cm⁻¹ and 600cm⁻¹

6.3 Results and Discussions

6.3.1 Viscosity

Solution viscosity (Figure 6:1), surface tension and conductivity affect the electrospun fibre morphology [45].



‘In contrast to the classical electrospinning, of which the electrospinnability mainly depends on solution properties, bubble electrospinning depends geometrically on sizes of produced bubbles’ [37].

The equations shown below explain the surface tension of the solution and the bubble as given in [46].

$$\sigma_s = A e^{-B/\eta} \quad \text{(Equation 6.1)}$$

Where, σ_s is the surface tension of the polymer solution, A and B are constants, η is the viscosity (η is proportional to M_w^α , M_w is the molecular weight and α is the scaling exponent and value of α lying between 1/3 and 1) .

$$\sigma_B = \frac{1}{4} r (P_i - P_o) \quad \text{(Equation 6.2)}$$

Where, σ_B is the surface tension of bubble, P_i is the air pressure inside and P_o is the air pressure outside the bubble and r is the radius of the bubble.

‘Generally, the number and size of bubbles depend on the gas pressure and the solution property (such as surface tension and viscosity)’ [39], the surface tension of bubbles is independent of properties of the solution, such as viscosity’ [47] but depends on its size and temperature [46].

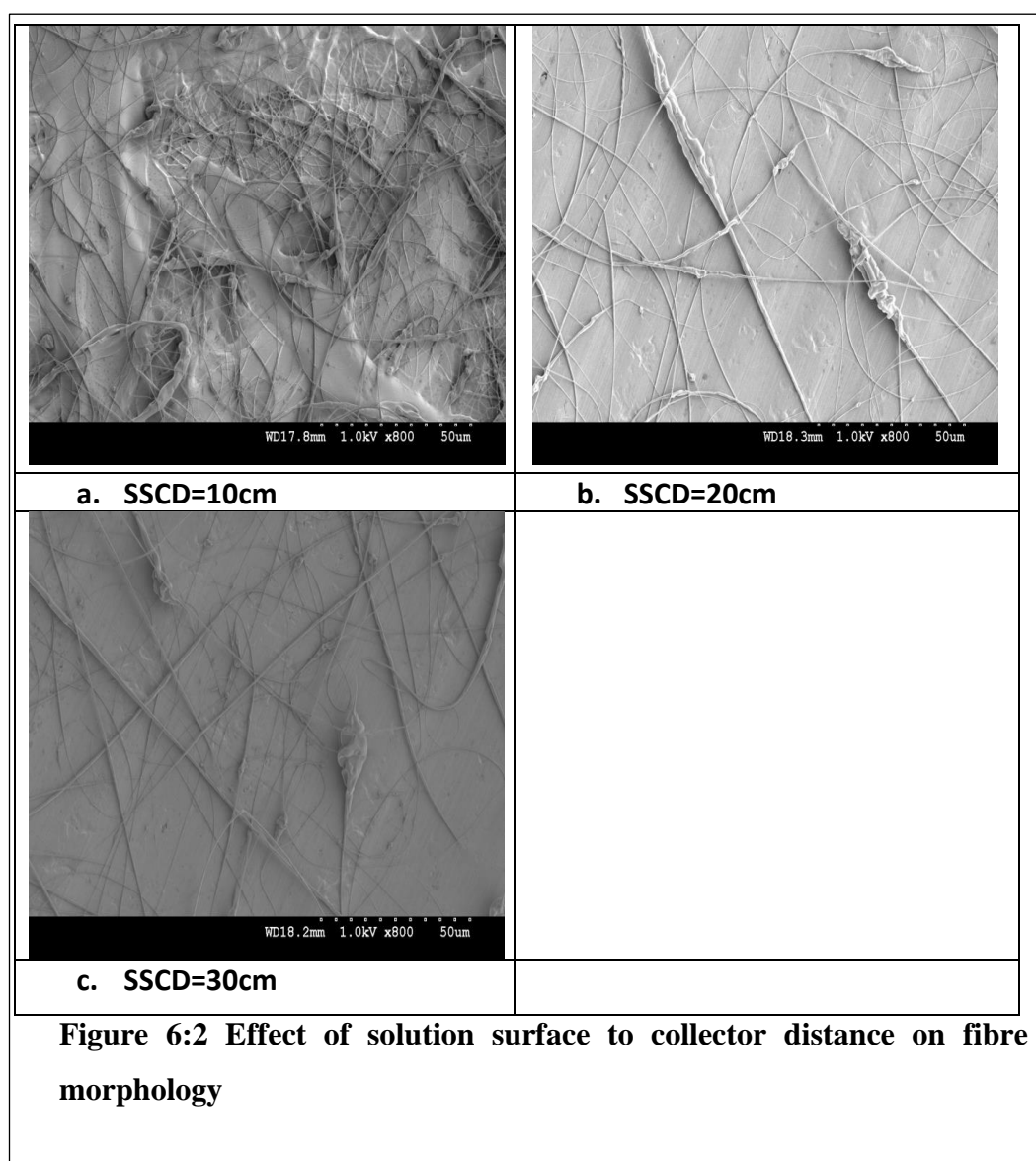
Hence, it is important to know the properties of the solution also. Viscosity of 15% EC solution (60:40/toluene: ethanol) can be seen in Figure 6:1, surface tension was 24mN/m and the conductivity of the solution was 29.5 μ s.

6.3.2 Effect of Solution Surface to Collector Distance on Fibre Property

In SNE, the effect of NTCD on fibre morphology varies with solution property and electric field strength [45].

NTCD not only affect the flight time but it also affects electric field strength between needle and collector. [17, 48]. NTCD affects jet flight distance, which affects time available for solvent evaporation and time for fibre / jet stretching and splitting. Instead of NTCD in SNE, solution to surface distance (SSCD) can be used as a parameter.

In the present study, (Figure 6:2, Figure 6:3) the 15% EC fibre diameter increased with increase in SSCD.



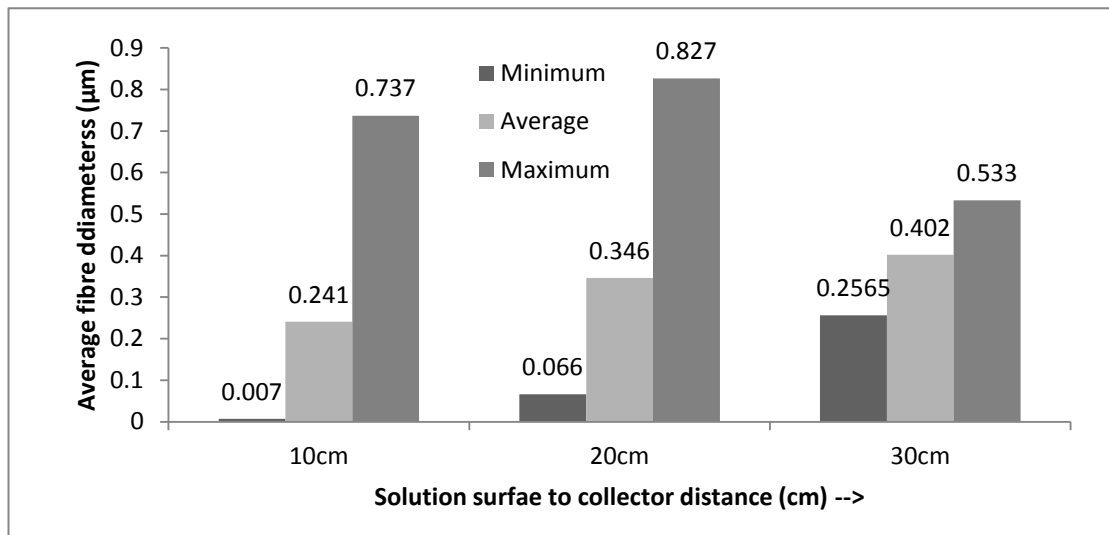
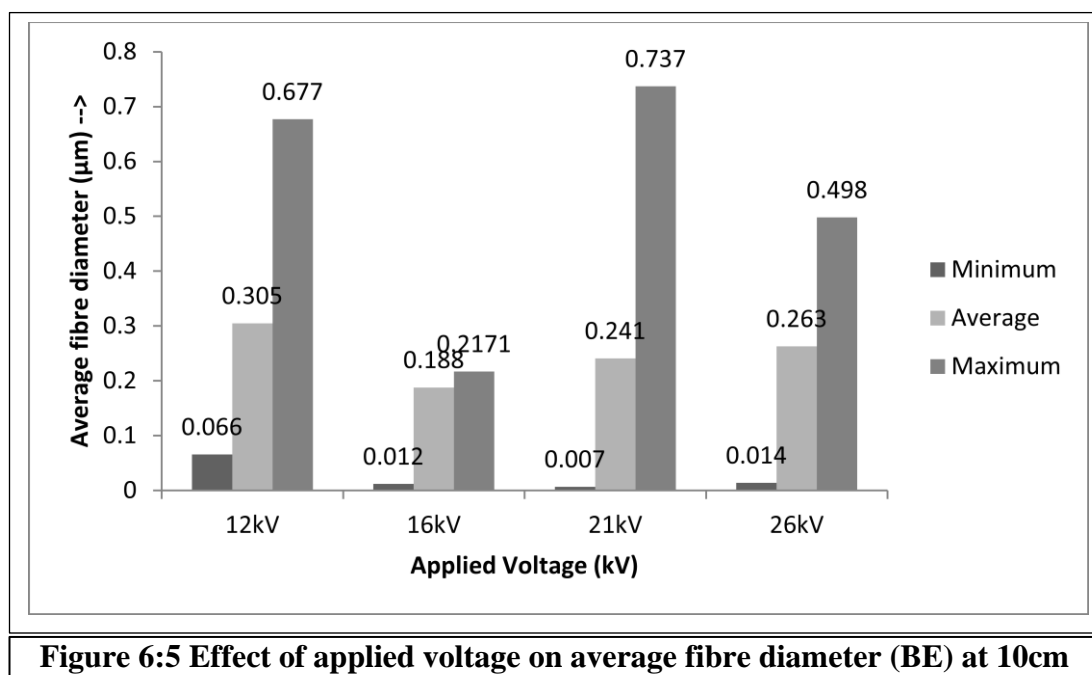
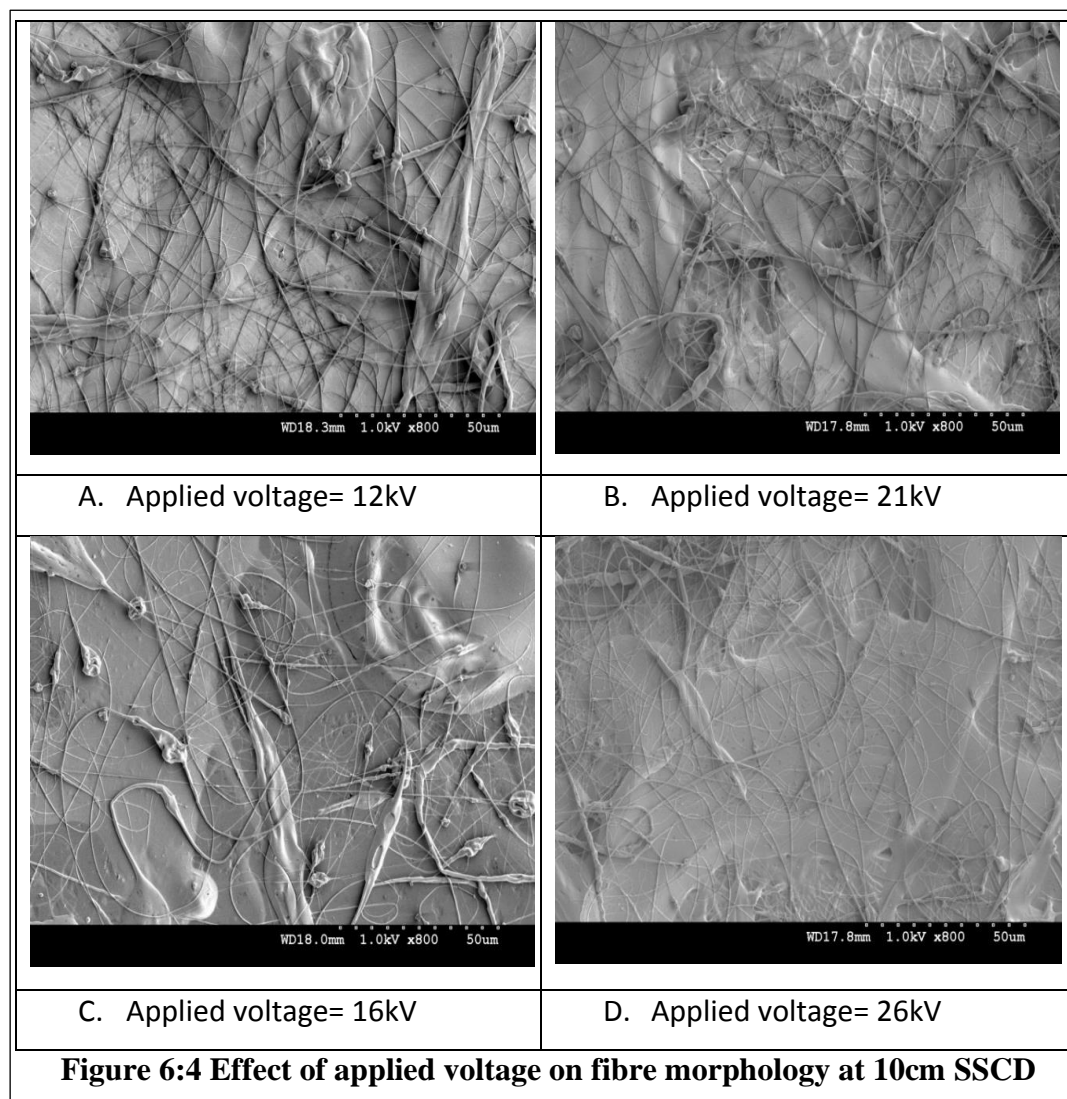


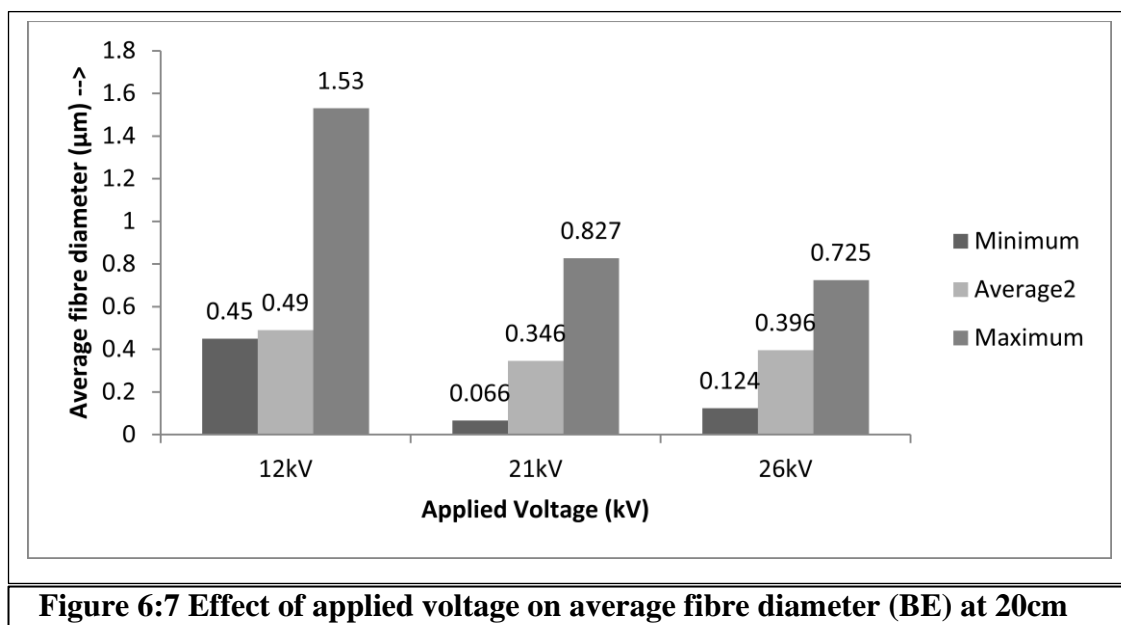
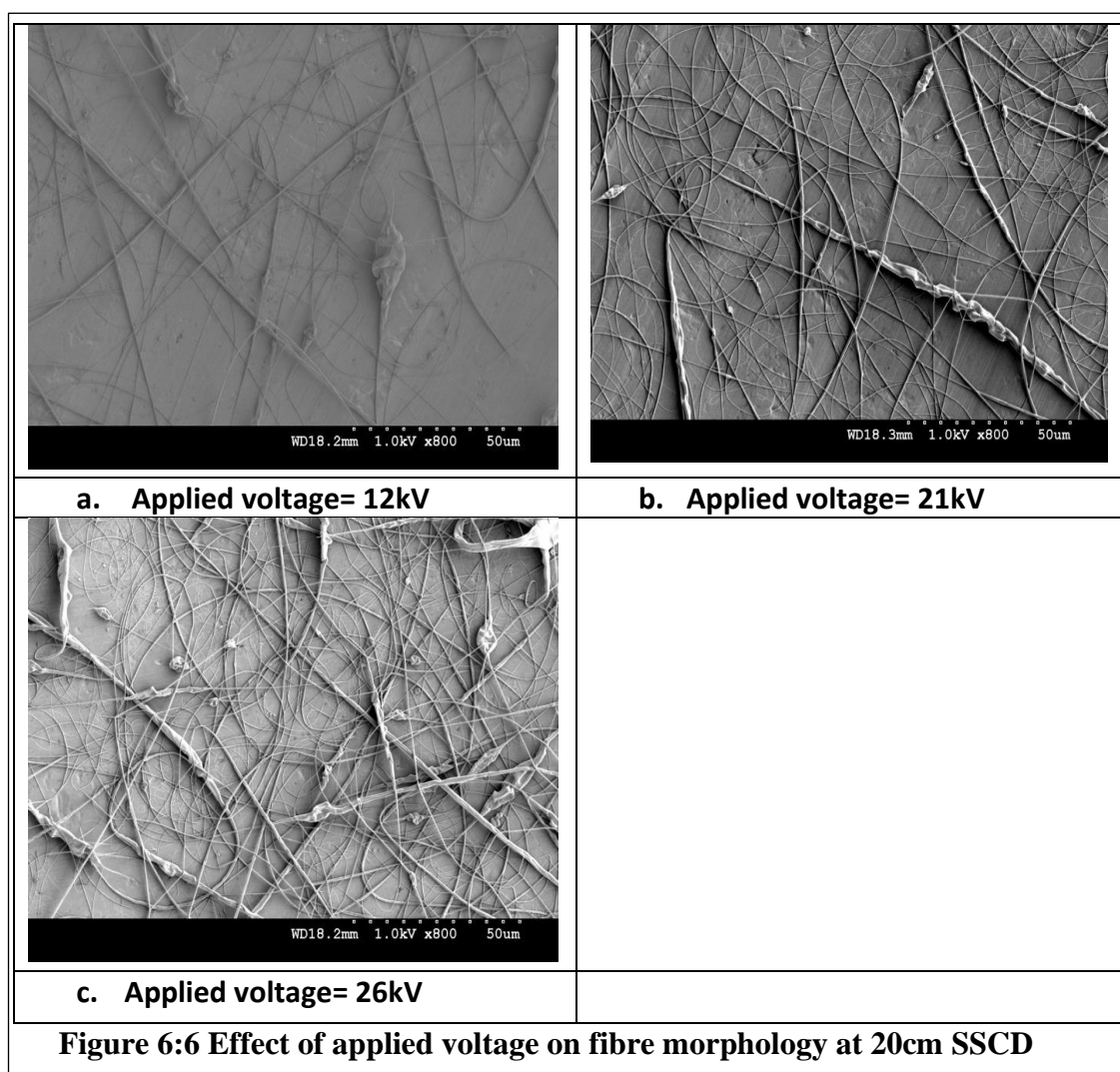
Figure 6:3 Effect of solution surface to collector distance on average fibre diameter

The diameter for SSCD at 10cm, 20cm, 30cm were 0.241μm, 0.346μm and 0.409μm respectively. In bubble electrospinning, jets emerge from bubble, so viscoelastic property of solution in the bubble affects fibre morphology. The solution in the bubble gets stretched as the applied voltage increased. The jet emerged from the bubbles will try to be relaxed from the stresses of the bubble solution. The jet gets relaxed and contracted during its flight. As SSCD increased, jet gets more time to get relaxed, which creates thicker fibres. At the same time, the solvent is evaporated from the open surface solution, which generates thicker jet from viscous solution. Air circulation around the jets due to bubble bursting also evaporated more solvent and creating thicker jet with increasing of the viscous solution. Increase in the viscosity makes the solution thicker and it resists splitting. Overall thicker fibres were generated with increased SSCD.

6.3.3 Effect of Applied Voltage on Fibre Morphology

Combinations of various process parameters decide final fibre morphology and properties in electrospinning. Applied voltage is one of the important parameters responsible for coulombic repulsions, jet initiation, jet instabilities and jet stretching/splitting. Applied voltage has not always the same effect on fibre morphology.





As the applied voltage increases, the coulombic repulsion increases in the Taylor cone. Increase in repulsions, repel the solution ions from each other at critical voltage V_c the Taylor cone splits into jets. As voltage increases more splitting occurs. Applied voltage stretches the jet due to the opposing electric charges on the solution and collector [45].

Depending on feed rate and other parameters, increases in fibre diameter are also reported with increase in applied voltage. Increased applied voltage attracts more solution, which results in increased fibre diameter at 10 cm SSCD (Figure 6:4 and Figure 6:5).

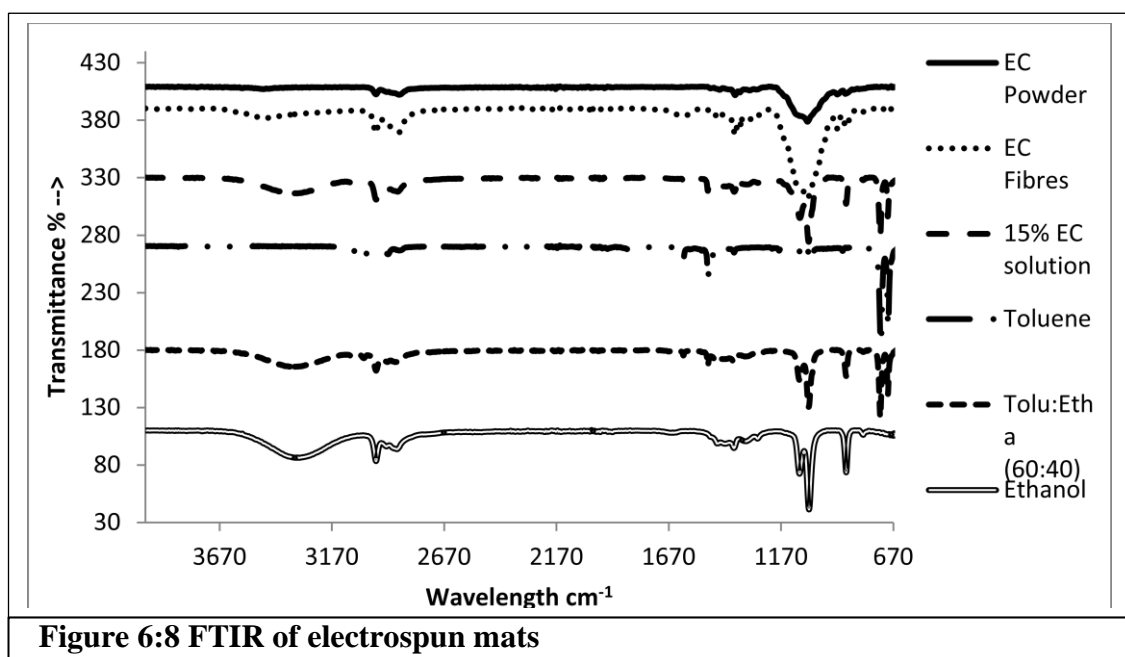
Average fibre diameter is reduced initially from 0.375 μm to 0.188 μm with increased voltage from 12kV to 16kV respectively. Then the fibre diameter increased from 0.188 μm to 0.241 μm and 0.263 μm with increase in applied voltage from 16kV, 23kV to 26kV. The same trend was found at 20 cm SSCD (Figure 6:6 and Figure 6:7). Initially fibre diameter is reduced from 0.490 μm to 0.346 μm then increased to 0.396 μm with increase in applied voltage from 12kV, 16kV to 21kV. In BE, the bubble surface tension holds solution in bubble shape. Whilst applied voltage works opposite to bubble surface tension, as applied voltage is increased, the solution get stretched into jets, so jet initiation interplay between these two forces.

Here, the bubble surface tension is high enough to hold the solution from 12kV to 16kV initially.

Therefore, jets were stretched and diameter reduced. As the applied voltage increased, the electrostatic force overcome the effect of bubble surface tension. Hence, more solution was pulled and thicker fibres were generated. It is also noted that all fibre diameters at 20cm SSCD were coarser than at 10cm SSCD. This supports the phenomenon of increase in SSCD, due to stress reduction solvent evaporation as explained earlier.

6.3.4 FTIR (Fourier Transform Infrared Spectroscopy)

The FTIR spectrum of EC powder, EC electrospun fibre and EC solution in toluene:ethanol (60:40), are as shown in (Table 6:1, Table 6:2, Table 6:3, Figure 6:8). The EC solution showed the effect of EC and the relevant solvent system on corresponding bands in FTIR chart. For example, as can be seen, wide -O-H stretch at 3325.09 cm^{-1} in ethanol appears at 3331.54 cm^{-1} in EC solution with 100% ethanol and gets smaller in 60:40 mixture of ethanol: toluene at 3350.34 cm^{-1} .

**Table 6:1 FTIR bands for Ethanol**

FTIR band at cm^{-1}	Possible assignments
3325.09	O-H stretch
2973.59, 2924.94, 2879.54	C-H stretch
1648.14	C=C band
1453.75, 1417.34, 1379.81, 1328.67, 1274.89	CH_2 band
1087.70, 1045.41	C-O stretch

Table 6:2 FTIR bands for Toluene

FTIR band at cm^{-1}	Possible assignments
3087.22, 3062.88, 3027.49	=C-H stretches of aromatics
2920.13	-C-H stretches of the alkyl (methyl) group
1604.54, 1495.45, 1459.48	carbon-carbon stretches in the aromatic ring
1081.24, 1030.07	in-plane C-H bending
725.43	Out of plane C-H bending

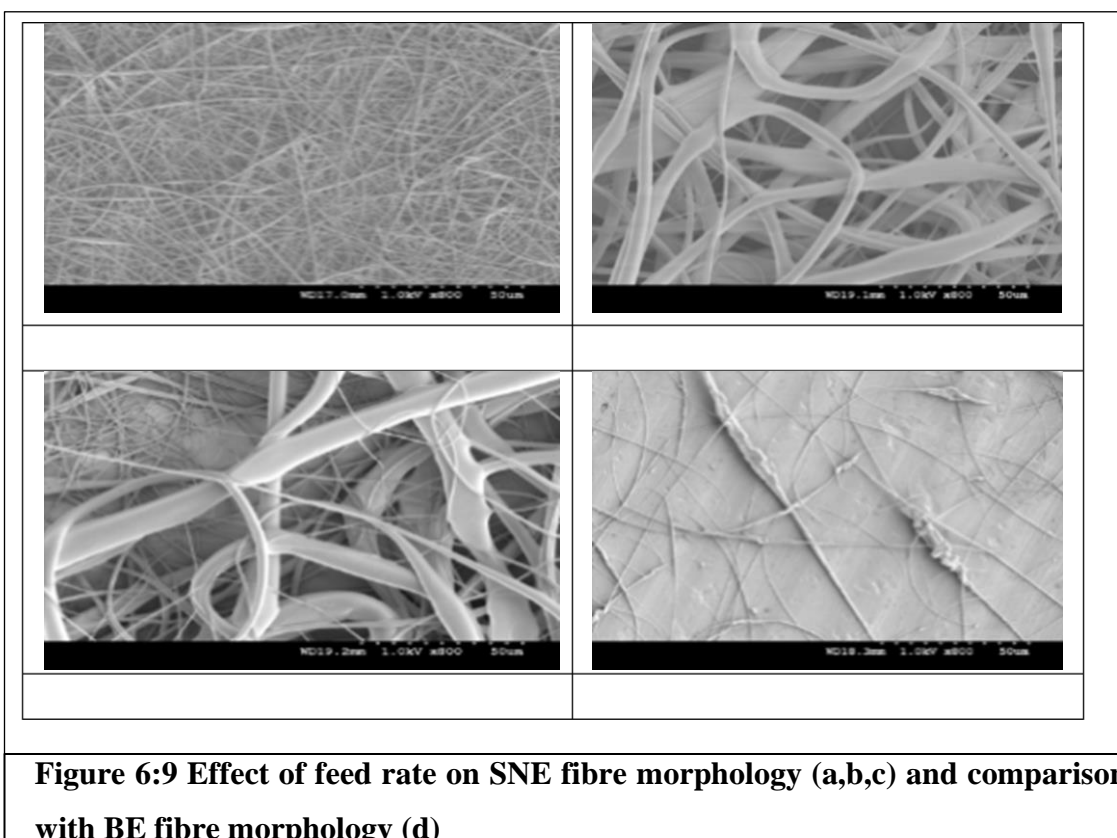
Table 6:3 FTIR bands of etylcellulose

FTIR band at cm^{-1}	Possible assignment
3476	-OH stretching vibration on the closed ring structure of the EC repeating units
1052.21	-C-O-C- stretching vibration
2871.36 and 2973.29	C-H stretching bands
1374.54	C-H bending

FTIR of fibres after drying have showed the same chart as the EC powder. Therefore, after solvent evaporation, there are not many changes in ethyl cellulose structure.

6.4 Comparison between needle electrospinning and bubble electrospinning

6.4.1 Effect of Feed Rate.



In EC electrospinning by SNE, the feed rate was controlled by pump. In BE of EC the feed rate was not controllable, as it was dependant on number of bubbles. In case of SNE and BE the main difference is feeding mechanism. In order to compare SNE and BE results, the EC fibres were produced at different feed rates using SNE and compared with BE result(Figure 6:9 , Figure 6:10).

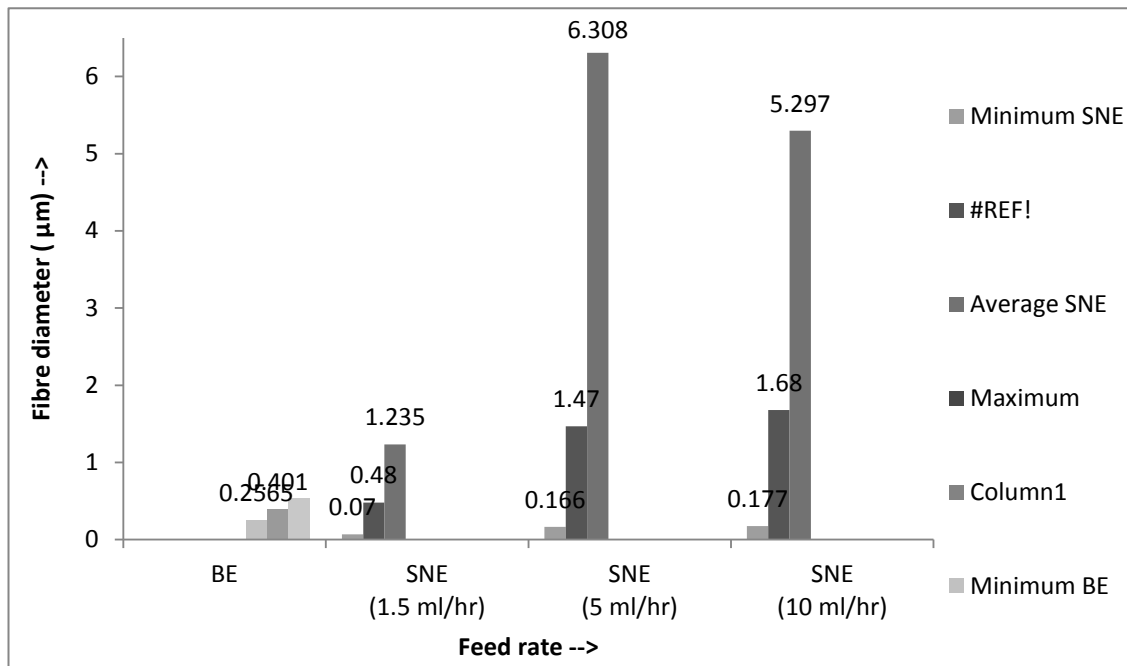


Figure 6:10 Effect of feed rate on SNE average fibre diameter and comparison with BE average fibre diameter

In SNE, feed rate were changed from 1.5ml/hr, 5ml/hr and 10ml/hr keeping other parameters same at 30cm NTCD, 21kV power supply and 16G needle. The average fibre diameters were found 0.483µm at 1.5 ml/hr, 1.472µm at 5ml/hr and 1.681µm at 10ml/hr. The avg. fibre diameter of BE fibres at 30 cm and 21kV was 0.401µm, where the suction pump capacity was 0.7bar. The results of the fibre diameters in SNE at 1.5ml/hr feed rate is comparable with the BE results (suction pump capacity 0.7bar) with the other parameters same. It is interesting to know that the fibre morphologies were different inspite of comparable fibre diameter values. BE fibres found beaded and the SNE fibres were found bead-less. Formation of beads in the BE fibres could be due to surface tension of the bubbles.

6.4.2 Effect of Needle / Solution Surface to Collector Distance on Fibre Morphology.

In SNE (Chapter 5), the effects of different NTCD (10cm, 20cm, and 30cm) on the fibre size and shape were investigated by keeping other parameters same at 21kV applied voltage, 16G needle diameter, 1.5ml/hr feed rate. The average fibre diameters were reduced with longer NTCD. The avg. fibre diameters reduced from 0.631µm, 0.568µm, to 0.483µm, when the NTCD increased from 10cms, 20cms to 30cms. Longer NTCD gives more time for the jet to be stretched before it reaches the target. At the same time the solvent evaporates faster from stretched fibre due to exposure of new stretched surface in the air. Smaller diameter fibres are produced with longer NTCD. In

case of BE (Figure 6:3, Figure 6:2), the EC fibre diameter increased from 0.241 μm for 10cms SSCD to 0.346 μm for 20cm SSCD and to 0.402 μm for 30cm SSCD. In BE; the bubble properties (shape, size and viscoelasticity) affects fibre morphology. In the SNE, the solution properties (surface tension, viscoelasticity) affect the fibre morphologies. In the present study, the bubbles and the solution in the bubbles came under stress with higher applied voltage. As the bubbles burst the stresses in the jet are relieved as the fibre jets contracts. The longer SSCD gave more flight time for the jet relaxation and hence thicker fibres are generated. At the same time, the solvent evaporation might also have occurred due to continuous compressed air flow in the EC bath. The solution became more viscous with the time and produced thicker fibres. Bubbles release the air, when they burst. Air circulation around these fibres might also evaporate some solvent from the jets causing jet solution to become more viscous and resistant to split or stretched. In addition, This may also contributed in quick solvent evaporation.

6.4.3 Effect of Applied Voltage on Fibre Morphology

In SNE (Chapter 5) smaller fibres are produced with higher applied voltages at 20cm NTCD. The fibre diameters were found 0.617, 0.596, 0.568 to 0.556 μm with respect to the applied voltages 12kV, 16kV, 21kV to 26kV respectively.

The effect of applied voltage on BE fibre morphology at 10cm STCD can be seen in Figure 6:4, Figure 6:5. The average fibre diameter changed from 0.305 μm at 12kV, 0.188 μm at 16kV, 0.241 μm at 21kV to 0.263 μm at 26kV at 10cm SSCD in BE. At 20cm SSCD (Figure 6:6, Figure 6:7), the avg. fibre diameter was 0.490 μm , 0.346 μm and 0.396 μm at 12kV; 21kV and 26kV respectively.

The jets in BE are influenced by the bubble surface tension (solution holding force) and the electrostatic force (solution stretching force). As the voltage increased from 12kV to 16kV, the bubble surface tension was greater compared to the electrostatic force. Therefore, the jet was stretched easily and EC fibre diameter reduced. The higher voltage generated more electrostatic force, which generates attraction for the solution. More solution produced thicker fibres.

Fibre diameters at 20cm SSCD became coarser compared to fibre diameters at 10cms at all the voltages in the experiment. Therefore, the stress relaxation and solvent evaporation at longer SSCD is more, as explained earlier.

6.5 Conclusion

Needle electrospinning systems (single or multiple) are not suitable for industrial scale production due to their limitations as explained earlier, such as needle blocking.

Therefore, new needle-less systems were developed based on different feeding systems. BE is one of new needle-less concepts developed. Much more work is done on design of SNE parameters on optimizing electrospun fibre, but needle-less electrospinning methods still lack optimization of parameters [21]. In order to understand morphological changes in EC electrospun fibres, we studied the effect of applied voltage and solution surface to collector SSCD in BE. This increase in diameter can be attributed to the solvent evaporation due to airflow as well as bubble bursts and due to jet relaxation during flight. In BE as applied voltage increased initially, fibre diameter decreased but then started increasing with increase in applied voltage. Initial decrease in fibre diameter was due to higher surface tension influence in the jet. With increase in applied voltage, the applied voltage suppressed the surface tension and pulled more solution, which produced thicker fibres.

Comparisons of the effect of the different process parameters on BE and SNE fibre morphologies were done. Main difference between BE and SNE is feed mechanism. 1.5 ml/hr feed rate is considered as optimum parameter for comparison with BE fibres after comparing fibre diameters of both methods. The morphology of fibre morphologies was found different by both methods. The average SNE fibre diameters become bigger with the higher feed rate. The average fibre diameter reduced in SNE as the NTCD increased. The average fibre diameter increased in case of BE with higher SSCD. Average fibre size reduced with higher applied voltage in SNE. In BE, the average fibre size reduced initially and started increasing as the voltage increased.

6.6 Bibliography

- [6.1] R. F. Conaway, "Chemistry of Cellulose Derivatives," *Industrial & Engineering Chemistry*, vol. 30, pp. 516-523, 1938/05/01 1938.
- [6.2] G. Murtaza, M. Ahamd, N. Akhtar, and F. Rasool, "A comparative study of various microencapsulation techniques: effect of polymer viscosity on microcapsule characteristics," *Pakistan journal of pharmaceutical sciences*, vol. 22, pp. 291-300, 2009.
- [6.3] A. M. Agrawal, S. H. Neau, and P. L. Bonate, "Wet Granulation Fine Particle Ethylcellulose Tablets: Effect of Production Variables and Mathematical Modeling of Drug Release," *AAPS PharmSciTech*, vol. 5, pp. 1-13, 2003.
- [6.4] O. A. Cavalcanti, B. Petenuc, A. C. Bedin, E. A. G. Pineda, and A. A. W. Hechenleitner, "Characterisation of Ethylcellulose Films containing Natural

Polysaccharides by Thermal Analysis and FTIR Spectroscopy," *Acta. Farm. Bonaerense*, vol. 23, pp. 53-7, 2004.

[6.5] R. Badulescu, V. Vivod, D. Jausovec, and B. Voncina, "Grafting of ethylcellulose microcapsules onto cotton fibres," *Carbohydrate Polymers*, vol. 71, pp. 85-91, 2008.

[6.6] Hercules, Incorporated. (12 Dec. 2011). *AQUALON Ethylcellulose (EC) Physical and Chemical Properties*. Available:
http://www.ashland.com/Ashland/Static/Documents/AAFI/PRO_250-42A_Aqualon_EC.pdf

[6.7] X. Wu, L. Wang, H. Yu, and Y. Huang, "Effect of solvent on morphology of electrospinning ethyl cellulose fibres," *Journal of Applied Polymer Science*, vol. 97, pp. 1292-1297, 2005.

[6.8] J. Y. Park, S. W. Han, and I. H. Lee, "Preparation of Electrospun Porous Ethyl Cellulose Fibre by THF/DMAc binary solvent system," *Journal of industrial engineering chemistry*, vol. 13, pp. 1002-1008, 2007.

[6.9] J. P. Jeun, Y. M. Lim, J. H. Choi, H. S. La, P. H. Kang, and Y. C. Nho, "Preparation of Ethyl-Cellulose Nanofibres via An Electrospinning," *Solid State Phenomena*, vol. 119, pp. 255-258, 2007.

[6.10] S. Aydogdu, K. Ertekin, A. Suslu, M. Ozdemir, E. Celik, and U. Cocen, "Optical CO₂ sensing with ionic liquid doped electrospun nanofibres," *J Fluoresc*, vol. 21, pp. 607-13, Mar 2011.

[6.11] S. Kacmaz, K. Ertekin, A. Suslu, Y. Ergun, E. Celik, and U. Cocen, "Sub-nanomolar sensing of ionic mercury with polymeric electrospun nanofibres," *Materials Chemistry and Physics*, vol. 133, pp. 547-552, 2012.

[6.12] Z. Huang, "A review on polymer nanofibres by electrospinning and their applications in nanocomposites," *Composites Science and Technology*, vol. 63, pp. 2223-2253, 2003.

[6.13] P. Gupta, C. Elkins, T. E. Long, and G. L. Wilkes, "Electrospinning of linear homopolymers of poly(methyl methacrylate): exploring relationships between fibre formation, viscosity, molecular weight and concentration in a good solvent," *Polymer*, vol. 46, pp. 4799-4810, 2005.

[6.14] S. Ramakrishna, K. Fujihara, W.-e. Teo, and L. Teik-cheng, *An Introduction to Electrospinning and Nanofibres*: World Scientific Publishing Company, 2005.

[6.15] J. Deitzel, "The effect of processing variables on the morphology of electrospun nanofibres and textiles," *Polymer*, vol. 42, pp. 261-272, 2001.

- [6.16] A. Greiner and J. H. Wendorff, "Electrospinning: a fascinating method for the preparation of ultrathin fibres," *Angewandte Chemie (International ed. in English)*, vol. 46, pp. 5670-703, 2007.
- [6.17] S. H. Tan, R. Inai, M. Kotaki, and S. Ramakrishna, "Systematic parameter study for ultra-fine fibre fabrication via electrospinning process," *Polymer*, vol. 46, pp. 6128-6134, 2005.
- [6.18] S. A. Theron, A. L. Yarin, E. Zussman, and E. Kroll, "Multiple jets in electrospinning: experiment and modeling," *Polymer*, vol. 46, pp. 2889-2899, 2005.
- [6.19] O. O. Dosunmu, G. G. Chase, W. Kataphinan, and D. H. Reneker, "Electrospinning of polymer nanofibres from multiple jets on a porous tubular surface," *Nanotechnology*, vol. 17, pp. 1123-1127, 2006.
- [6.20] Y. Qiu, J. Yu, J. Rafique, J. Yin, X. Bai, and E. Wang, "Large-Scale Production of Aligned Long Boron Nitride Nanofibres by Multijet/ Multicollector Electrospinning," *The Journal of Physical Chemistry C*, vol. 113, pp. 11228-234, 2009.
- [6.21] H. Niu, X. Wang, and T. Lin, "Needle-less electrospinning: influences of fibre generator geometry," *Journal of the Textile Institute*, pp. 1-8, 2011.
- [6.22] F. Dabirian, S. A. Hosseini Ravandi, A. R. Pishavar, and R. A. Abuzade, "A comparative study of jet formation and nanofibre alignment in electrospinning and electrocentrifugal spinning systems," *Journal of Electrostatics*, vol. 69, pp. 540-546, 2011.
- [6.23] L. Wang, J. Shi, L. Liu, E. Secret, and Y. Chen, "Fabrication of polymer fibre scaffolds by centrifugal spinning for cell culture studies," *Microelectronic Engineering*, vol. 88, pp. 1718-1721, 2011.
- [6.24] M. R. Badrossamay, H. A. McIlwee, J. A. Goss, and K. K. Parker, "Nanofibre assembly by rotary jet-spinning," *Nano Lett*, vol. 10, pp. 2257-61, Jun 9 2010.
- [6.25] K. Sarkar, C. Gomez, S. Zambrano, M. Ramirez, E. de Hoyos, H. Vasquez, and K. Lozano, "Electrospinning to Forcespinning™," *Materials Today*, vol. 13, pp. 12-14, 2010.
- [6.26] O. Jirsak, P. Sysel, F. Sanetrik, J. Hruza, and J. Chaloupek, "Polyamic Acid Nanofibres Produced by Needle-less Electrospinning," *Journal of Nanomaterials*, vol. 2010, pp. 1-6, 2010.
- [6.27] E. Kostakova, L. Meszaros, and J. Gregr, "Composite nanofibres produced by modified needle-less electrospinning," *Materials Letters*, vol. 63, pp. 2419-2422, 2009.
- [6.28] A. L. Yarin and E. Zussman, "Upward needle-less electrospinning of multiple nanofibres," *Polymer*, vol. 45, pp. 2977-2980, 2004.

- [6.29] B. Lu, Y. Wang, Y. Liu, H. Duan, J. Zhou, Z. Zhang, Y. Wang, X. Li, W. Wang, W. Lan, and E. Xie, "Superhigh-Throughput Needle-less Electrospinning Using a Rotary Cone as Spinneret," *Small*, vol. 6, pp. 1612-1616, 2010.
- [6.30] X. Wang, H. Niu, T. Lin, and X. Wang, "Needle-less electrospinning of nanofibres with a conical wire coil," *Polymer Engineering & Science*, vol. 49, pp. 1582-1586, 2009.
- [6.31] X. Huang, D. Wu, Y. Zhu, and D. Sun, "Needle-less Electrospinning of Multiple Nanofibres," in *Proceedings of the 7th IEEE International Conference on Nanotechnology*, Hong Kong, 2007, pp. 823-826.
- [6.32] T. Miloh, B. Spivak, and A. L. Yarin, "Needle-less electrospinning: Electrically driven instability and multiple jetting from the free surface of a spherical liquid layer," *Journal of Applied Physics*, vol. 106, p. 114910, 2009.
- [6.33] K. M. Forward and G. C. Rutledge, "Free surface electrospinning from a wire electrode," *Chemical Engineering Journal*, vol. 183, pp. 492-503, 2012.
- [6.34] J. S. Varabhasa, S. Tripatanasuwanb, G. G. Chasea, and D. H. Reneker, "Electrospun jets launched from polymeric bubbles," *Journal of Engineered Fibres and Fabrics*, vol. 4, pp. 46-50, 2009.
- [6.35] Y. Liu and J.-H. He, "Bubble Electrospinning for Mass Production of Nanofibres," *International Journal of Nonlinear Sciences and Numerical Simulation*, vol. 8, pp. 393-96, 2007.
- [6.36] Q. Yang, J.-H. He, and L.-F. Mo, "Bubble-electrospinning for Polyacrylonitrile(PAN) Nanofibres," *International Journal of Nonlinear Sciences & Numerical Simulation*, vol. 11, pp. 165-169, 2010.
- [6.37] R. Yang, J. He, L. Xu, and J. Yu, "Bubble-electrospinning for fabricating nanofibres," *Polymer*, vol. 50, pp. 5846-5850, 2009.
- [6.38] Y. Liu, Z. F. Ren, and J. H. He, "Bubble electrospinning method for preparation of aligned nanofibre mat," *Materials Science and Technology*, vol. 26, pp. 1309-1312, 2010.
- [6.39] Y. Liu, J. H. He, and J. Y. Yu, "Bubble-electrospinning: a novel method for making nanofibres," *Journal of Physics: Conference Series*, vol. 96, p. 012001, 2008.
- [6.40] Y. Liu, L. Dong, J. Fan, R. Wang, and J.-Y. Yu, "Effect of applied voltage on diameter and morphology of ultrafine fibres in bubble electrospinning," *Journal of Applied Polymer Science*, vol. 120, pp. 592-598, 2011.

- [6.41] R. R. Yang, J. H. He, L. Xu, and J. Y. Yu, "Effect of solution concentration on diameter and morphology of PVA nanofibres in bubble electrospinning process," *Materials Science and Technology*, vol. 26, pp. 1313-1316, 2010.
- [6.42] J.-H. He, "From spider spinning to bubble electrospinning and from the wool structure to carbon super-nanotubes," *Materials Science and Technology*, vol. 26, pp. 1273-1274, 2010.
- [6.43] Z.-F. Ren and J.-H. He, "Single polymeric bubble for the preparation of multiple micro/nano fibres," *Journal of Applied Polymer Science*, vol. 119, pp. 1161-1165, 2011.
- [6.44] J.-H. He, "The Smaller, the Better: From the Spider-Spinning to Bubble-Electrospinning," in *Proceedings of the International Congress on Advances in Applied Physics and Materials Science*, Antalya, 2012, pp. 254-256.
- [6.45] S. Ramakrishna, K. Fujihara, W. E. Teo, T. C. Lim, and Z. Ma, *An Introduction to Electrospinning and Nano fibres*. : World Scientific Publishing Company, 2005.
- [6.46] J.-H. He, "Effect of temperature on surface tension of a bubble and hierarchical ruptured bubbles for nanofibre fabrication," *Thermal Science*, pp. 1-4, 30 Nov 2011 2011.
- [6.47] J.-h. He, Y. Liu, L. Xu, J.-y. Yu, and G. Sun, "BioMimic fabrication of electrospun nanofibres with high-throughput," *Chaos, Solitons & Fractals*, vol. 37, pp. 643-651, 2008.
- [6.48] N. Bhardwaj and S. C. Kundu, "Electrospinning: a fascinating fibre fabrication technique," *Biotechnol Adv*, vol. 28, pp. 325-47, May-Jun 2010.

Chapter 7 : Development and Characterisation of Thermochromic Polypropylene Filament Yarn

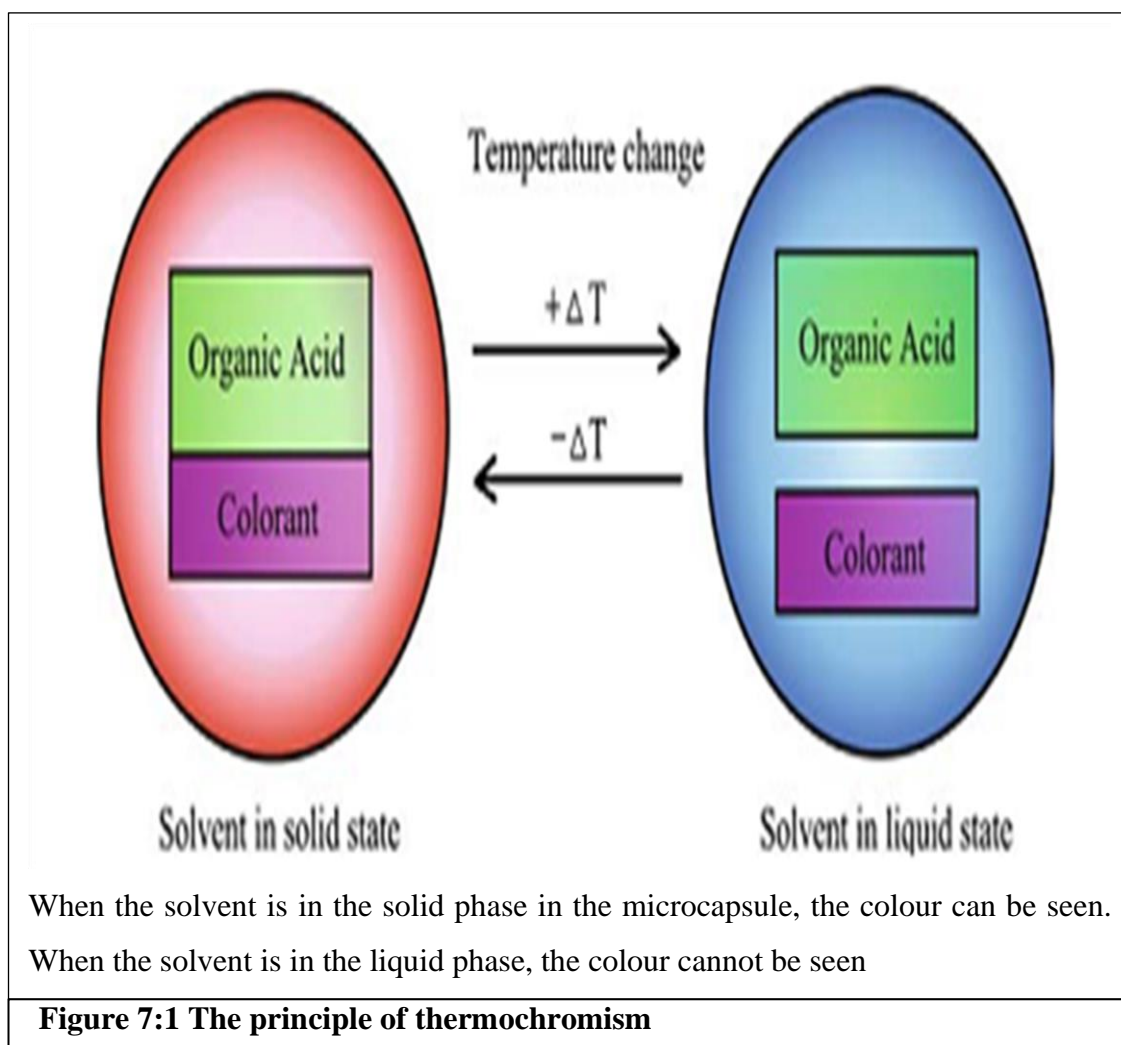
7.1 Introduction

“Smart materials are intelligent materials with capability to sense and respond to their surrounding environment in a predictable and useful manner” [1]. These materials are invented by research in various interdisciplinary fields [1]. Since 1930s the intelligent/smart metal alloys based on s based on Ni-Ti and on Cu, such as Cu-Zn-Al and CuAl-Ni etc. were reported and was commercialised in 1965. In 1975, it was discovered that small change in temperature or concentration of solvent caused swelling of polymeric gels much more than their original dimension. This led to further research in the field of the effect of various external parameters as stimuli on the properties (shape, phase, optical, mechanical) of various materials. Temperature, humidity, pressure, electromagnetic spectrum, radio waves, microwaves, UV light, electric fields, magnetic fields, stress strain etc. are physical parameters which can affect material/polymer properties. Fungi, bacteria, algi and viruses are some examples of biological parameters, whilst electrolytes, salts and pH are known chemical parameters. All the above physical, biological, chemical parameters, which can affect material properties, are called external stimuli [2-4]. Many fibrous materials also show stimuli sensitive responses [2], such materials can be used in sensing activation, logic and control [5]. The materials which change their properties (in most cases optical) in response to external stimuli are called chromogenic [5, 6]. Depending on external stimuli these materials are known as “Electrophoretic” (changes with electric voltage or charge), “Thermochromic” (changes with temperature), “Photochromic” (changes with UV radiation) or “Gasochromic” (changes with reducing/oxidizing effect of gases) [6]. Properties such as the chromogenic property of the above material can be used for fashion, comfort, energy harvesting, energy efficiency, defence, protection etc. [7, 8]. Materials which change their colour with change in temperature are called thermochromic materials [9]. Thermochromism has been defined by several authors [10-12]. According to Dawson et al. (2010) thermochromism is an easily noticeable reversible colour change in the temperature range limited by the boiling point of the solvent in the case of solution or the melting point for solids. [12]. Thermochromic materials vary their colour, intensity or transparency either reversibly or irreversibly

with change in temperature. Various polymers, polymer blends, gels, inorganic, organic compounds show thermochromic behaviour [13-16]. Thermochromic materials can mainly be divided into three types; such as conjugated oligomer [17], leuco dye and liquid crystal [18]. Usually leuco dyes show a single colour change while liquid crystals show several colour changes [19]. The liquid crystal system is well explained in the literature [18]. The leuco dye thermochromism is seen as a result of interaction between three components; a colour former (the leuco dye), an acid (activator) and a low melting point solvent [11, 14, 20].

7.2 The Principle of Leuco Dye Based Thermochromism

The principle of leuco dye thermochromism is well explained in literatures [11, 14, 20]. Figure 7:1 [14] shows the reversible colour mechanism. The heat indicator material is coloured when the temperature is below the melting point of the solvent.



The solvent is in solid phase and the components which form the colour (organic acid and colorant) are in contact. The colour can be seen due to the electron interactions. If the temperature is over the melting point of the solvent or the in the liquid phase, the colour-forming components are not in contact and the colour cannot be seen. The

electrons cannot interact. The colour change is reversible because the colour returns, when the temperature is decreased. The leuco dye system works on encapsulated tri-component system- a colour former, an activator and a low melting solvent. The melting point of the solvent system decides the final temperature for colour loss. The coloured or colourless status can be due to electron interaction between the colour former and the colour activator. When the microcapsules are heated above the solvent melting temperature, naturally the solvent melts. So, the colour former and the colour developer get separated. No electron interaction occurs and the microcapsule becomes colourless. When the micro capsules are cooled, the solvent melting temperature, the colour former and colour developers come much closer. As a result, electron interaction between colour former and developer provide colour. Activation temperature is the temperature where the colour changes, which occurs in a specific temperature interval. Although colour developers referred as ‘catalyst’ or ‘electron acceptors’ in most cases, they in fact act as ‘proton donors’ by being the hydrogen bonding source with the colour forming dye.

Leuco dye based thermochromic effect can be coloured to colourless or vice versa with increase in temperature. The temperature and direction of process can be controlled by selecting the solvent and colour developer system. Depending on composition the colour change occurs over a 5°C temperature range with some thermal hysteresis [11]. Hence while heating colour disappears at a higher temperature than the temperature at which the colour appears while cooling [21], sometimes coloured solids remain even after the melting temperature is reached and become colourless at higher temperature [20].

Thermochromic materials have been widely used in plastics, ceramics and textiles (coating). Thermochromic materials are available as ink, dye, powder, dispersion with many colours and at various activation temperatures. Generally, thermochromic materials contain only 2% dye by mass prior to encapsulation and only around 1% in the final product. Colour strength of the thermochromic composition remains low. Thermochromic micro capsules are applied to textiles either by coating the textiles fibres or printing with thermochromic pigments [14]. These methods require yarn/fabric treatment after they are made. They require pastes or binders to be applied along with thermochromic pigments, which may affect overall fabric properties and handle. Marinkovic et al. (1998) [22] used a thermochromic complex in phase change materials for green house agriculture, which acted as auto regulating shading protection from overheating with increase in temperature. In summer, thermochromic black pigment

textile membranes for building coverings showed reduction by 7.7% in thermal flux [23].

In the present work, thermochromic polypropylene monofilament was melt spun, whilst dope dyeing it with thermochromic pigments. As the pigments are embedded into the filament, there is no need of after treatment such as coating/printing to the yarn/fabric. The advantage of this method is that it is more efficient and effective because it saves cost and time whilst maintaining quality as no change occurs to final filament/fabric properties, and as it is dope dyed, it has excellent colour fastness.

Polyolefin fibres are spun from polymers or copolymers of ethylene and propylene. Polypropylene is converted into textiles via various processes such as melt spinning, ribbon yarns by film making, spun bonding or melt bonding processes [24]. Properties such as excellent chemical resistance, easy processibility [25, 26], sufficient strength and low density expand its usage from plastics into textiles. Out of three structures of polypropylene- isotactic, atactic and syndiotactic, isotactic is more suitable to be converted in to fibre form [25]. Polypropylene is available in monofilament, multifilament, staple fibre, non-woven, fibrillated yarn etc. [27]. Polypropylene monofilaments are used in fishing nets (which floats on water due to having lower density than water), tarpaulins etc. [28]. Polypropylene is also widely used in medical textiles, automotive textiles, industrial textiles, geo textiles, carpeting [25]and moderately in conventional textiles [24].

Polypropylene lacks dyeability because of its nonpolar high crystallinity and lack of functional groups to hold dye molecules [29] (Figure 7:2). Lack of dyeability is one of the main limitations of Polypropylene, which is due to absence of dye site [30]. This problem can be overcome if polypropylene is modified by the addition of dyes prior to melt spinning (dope dying) or by the use of hydrophobic dyes with accelerators, carriers or fibre swelling agents [25, 27].

In melt spinning, the polymer melt is extruded through a spinneret to a cooling or quench zone, where the filament is solidified. During this process, temperature and pressure is applied to melt the polymer in the melting zone, hence spinneret configuration, temperature of cooling zone or medium of cooling (air or any solution or gas) parameters affect fibre morphology (as crystallinity orientation) [25]and properties (tensile).

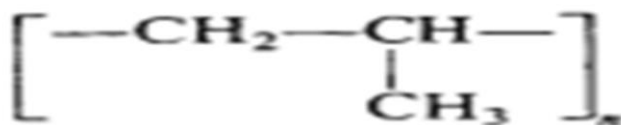


Figure 7:2 Structure of Polypropylene

It is very important to mix and distribute the pigment colours while melt spinning. As it not only affects final appearance of filament, but also affects properties (eg. tensile properties, drawability etc.). Pigment particles may act as nucleation agents (acts as nucleus and lamella grows around it) [25] and affect crystallization behaviour. Pigments may interfere in extrusion and cooling as well, so, processing of polymer with other additives needs trial and error to optimize parameters [25]. The fibre morphology depends on composition, compatibility or miscibility of components [31].

7.3 Materials and Methods

7.3.1 Materials

Thermochromic pigment UMB Blue 31 C was supplied by New prismatic Enterprises Co. Ltd; Taiwan.

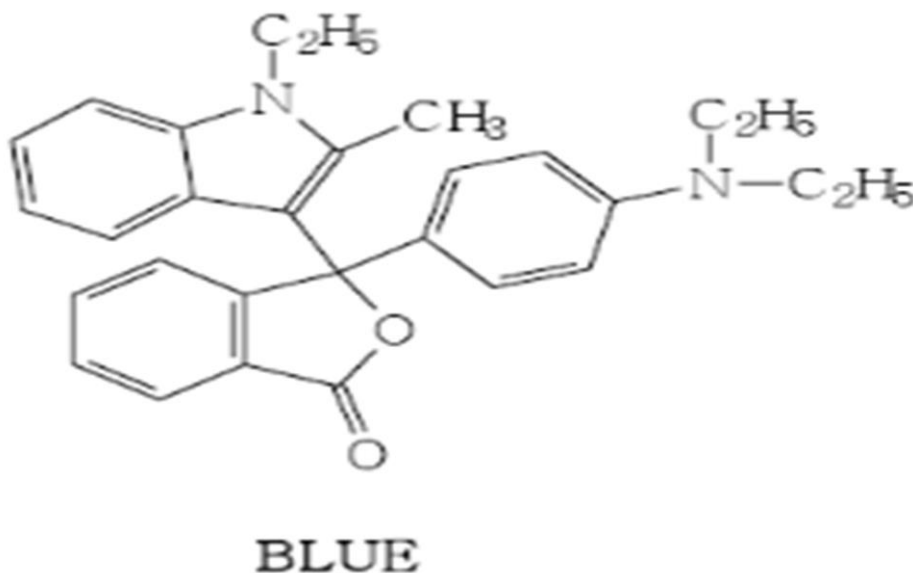


Figure 7:3 UMB Blue structure

The core components of the dye are leuco colour developer and temperature controller (solvent). UMB Blue 31 C contains, 3-(4-Dimethylaminophenyl)-3-(1-ethyl-2, methyl – indnl-3yl) phthalide (2-10%) as a leuco dye. Bisphenol A (5-15%) acts as a colour developer and methyl stearate (50-80%) as a solvent system. The chemical structure

(coloured) of 3-(4-Dimethylaminophenyl)-3-(1-ethyl-2, methyl – indnl-3yl) phthalide dye is in Figure 7:3. When temperature rose, colour change occurs between 30°C to 35°C and as the temperature goes higher, it becomes colourless. The colour changes are reversible. With reducing the temperature, pigments again become coloured. Polypropylene was supplied by Bassell, UK. All materials were used without any purification or changes.

7.3.2 Melt Spinning Setup

Polypropylene and thermochromic polypropylene filaments were extruded through a bench top screw extruder; Extrusion system limited, U.K. The principle and layout of the melt spinning is explained in chapter 1, Figure 1:2. For polypropylene filament, polypropylene chips were fed. For thermochromic polypropylene both the thermochromic pigment (35%) and the polypropylene (65%) chips were fed together. The molten polymer is forced through a single hole spinneret as a jet with speed adjusted by the metering pump. The extruded hot polymer jet was cooled into a water bath and passed through guiding rollers to the Leeson winding unit. Both polypropylene and thermochromic polypropylene filaments were spun with the same parameters. Initially the thermochromic hot jet from die head was found colourless, but it became coloured as it cooled in a water bath.

35% of UMB Blue and 65% polypropylene mixed homogeneously by a single screw extruder to the metering pump and die head system. The single screw zone was heated by three temperature zones T1=201°C, T2=210°C and T3=220°C respectively. The melting pump temperature was set as T4 at 230°C. The two die head zones were set at T5=246°C and T6=240°C temperatures respectively. All heating zones were electrically heated and controlled independently by a panel. The metering pump was initially set to 6.5 rpm but it was giving higher breakage at the spinneret, so after trial and error 4 rpm was found the most suitable with nearly no breakage. The extruder speed was set to 13.2 rpm.

7.3.3 Visual Observation

Photos were taken to see thermochromic effects by a fuji A805 camera.

7.3.4 Scanning Electron Microscopic (SEM) Studies

The surface morphology of the film was recorded with a Hitachi Scanning Electron Microscope (Model: S-4300, Japan). The samples were mounted on an aluminium stub by using a double-sided adhesive tape. Then it was placed in a sputter coater unit

(Polaron SC7620) for gold-palladium coating. Then samples were placed into SEM and observed at an accelerating voltage of 1 kV and current of 10 μ Amps.

7.3.5 Tensile Testing of the Yarns

The tensile tests of polypropylene and thermochromic polypropylene were carried out on an Instron tester (Model 3345) with a 100N load cell. Specimens of 50 mm long by 5 mm wide were tested with a gage length of 25 mm at an extension rate of 10 mm/min. 5 specimens were tested for each sample under the following conditions. Gauge length 25mm, load cell 5000N, transverse speed 1000 mm/min, RH-60% and temperature 20°C.

7.3.6 Fourier Transform Infrared Spectroscopy

FTIR is most useful for identifying chemicals that are either organic or inorganic. It can be utilized to quantify some components of an unknown mixture. It can be applied to the analysis of solids, liquids, and gasses. Infrared spectra were obtained on the Perkin-Elmer Spectrum 100 FTIR Universal ATR Sampling Accessory, deposited neatly onto a diamond/ZnSe plate. The scans were done between 650 and 4000cm⁻¹ at the resolution of 4cm⁻¹.

7.3.7 DSC Test:

Thermal analyses of samples were done by a METLER-TA instrument DSC12E. TOLEDO-TA89 E software was used to obtain DSC curves. Samples of up to 5mg weight of polypropylene bead, UMB Blue bead, polypropylene filament were measured. Thermochromic filaments were placed in sealed aluminium pans, all the aluminium pans lids were pierced by a pin to create a hole. All experiments were performed in a normal atmospheric air. The samples were heated from 20 °C to 300 °C at the rate of 10°C/min. The results are plotted in temperature vs heat flow graphs showing endothermic and exothermic peaks. The melting points were determined from these graphs.

7.3.8 X-ray Diffraction

X-ray diffraction patterns of polypropylene and thermochromic polypropylene bead were obtained using Bruker-AXS D8Discover transmission X-ray diffractometer; scanning range 3 to 85 2theta; step size 0.202 which = 4061 steps @ 5 seconds/step; Total scan time is 35mins 16secs; Using a Cu kAlpha source, Lambda 1.5406 angstroms, scanned at 40kV, 40mA.

7.4 Results and Discussion

7.4.1 Thermochromic Effect

Figure 7:4 shows the thermochromic effect by a very simple demonstration. Two hands were placed on the filament bobbin (Figure 7:4(A)).

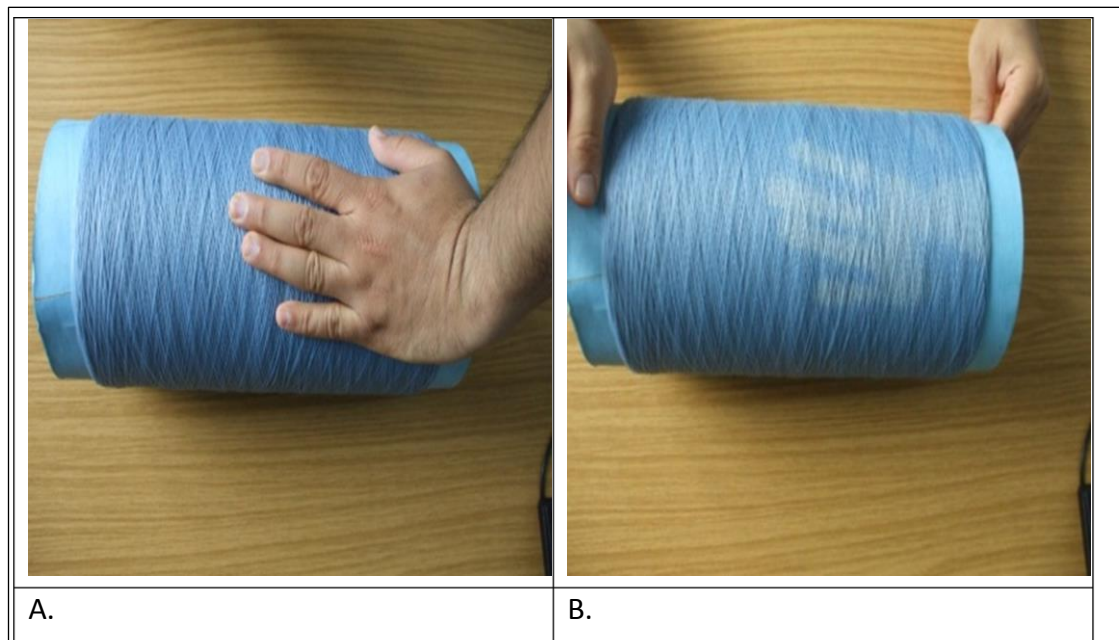


Figure 7:4 Thermochromic effect by body temperature

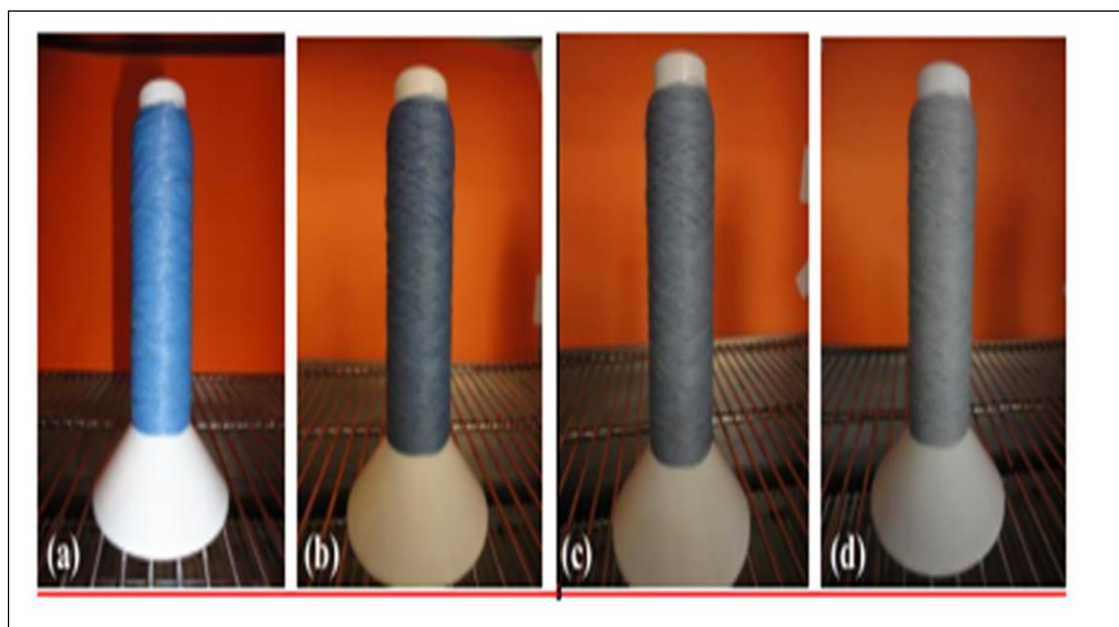
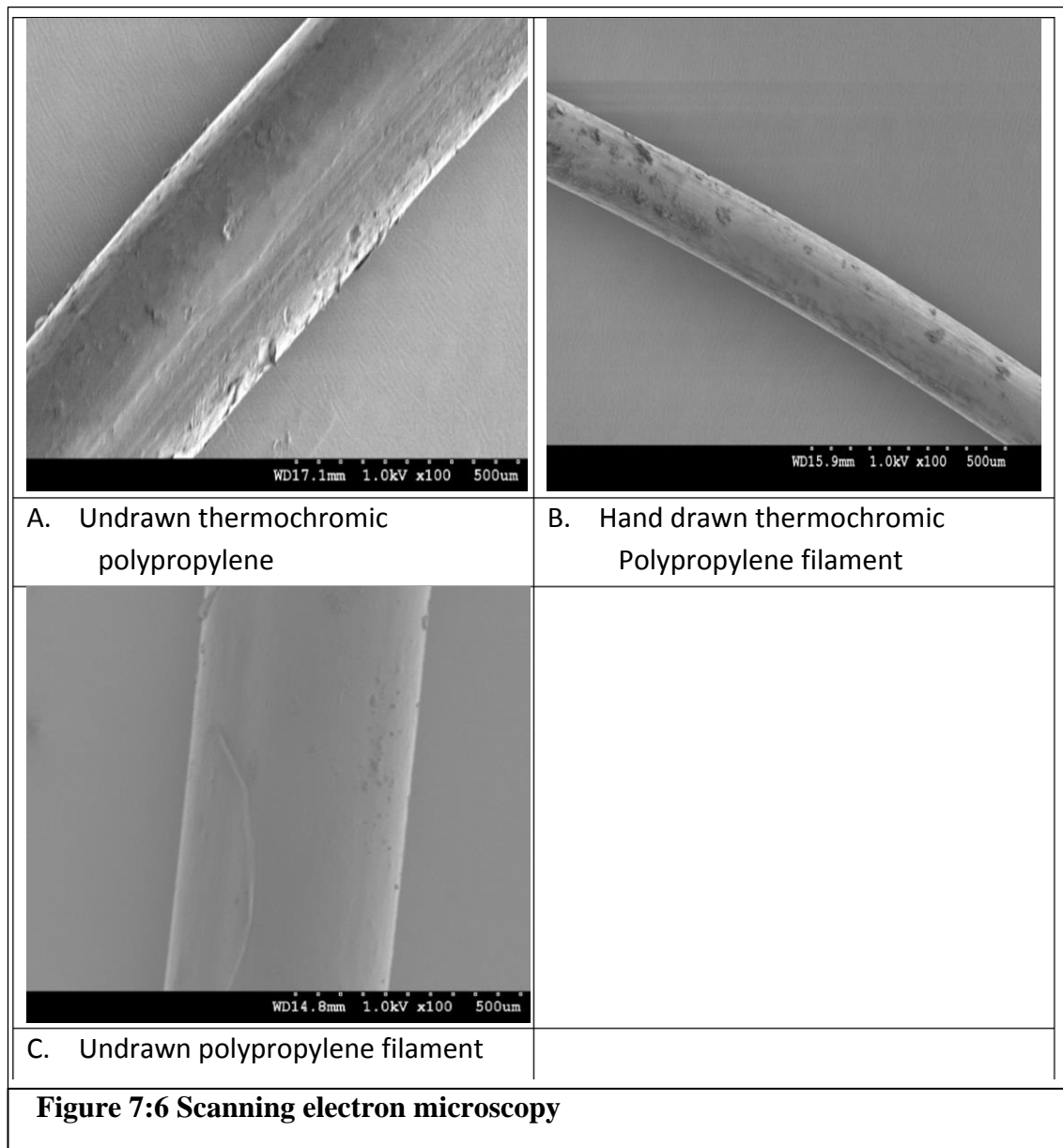


Figure 7:5 Developed thermochromic filament under the temperature of (a) 17°C (b) 25°C (c) 32°C (d) 38°C

After 2 minutes, hand was taken away. From (Figure 7:4(B)), the effect of hand temperatures can be seen. Thermochromic polypropylene became colourless due to body heat. As this is a reversible thermochromic filament, after 2-3 minutes the yarn

again became coloured. Furthermore a thermochromic sample was kept in an oven to accurately assess the effect of different temperatures on the thermochromic filament. The photographs were taken at 17°C, 25°C, 32°C and 38°, Figure 7:5. It can be seen that the thermochromic filament colour is reduced to colourless with increase in temperature.

7.4.2 Scanning Electron Microscopy Analysis



In (Figure 7:6C) the SEM images of undrawn polypropylene filament, in (Figure 7:6A) SEM image of undrawn thermochromic filament and in (Figure 7:6B) a hand drawn thermochromic filaments are shown. Here, all samples were magnified 100 times at 1kV. The image shows roughness on both drawn and undrawn thermochromic polypropylene. Polypropylene filament is smoother compared to thermochromic

polypropylene filament images, which shows clusters of thermochromic pigments in polypropylene.

7.4.3 Tensile Properties

The final properties of melt spun filament depend on the melt spinning process parameters. The polymer/filament exhibits changes in temperature, in die zones, cooling zone and drawing zone. The polymer/filament also exhibit various stresses/stress relaxation during the pressure build up by screw, solidification at the cooling zone and the winding process.

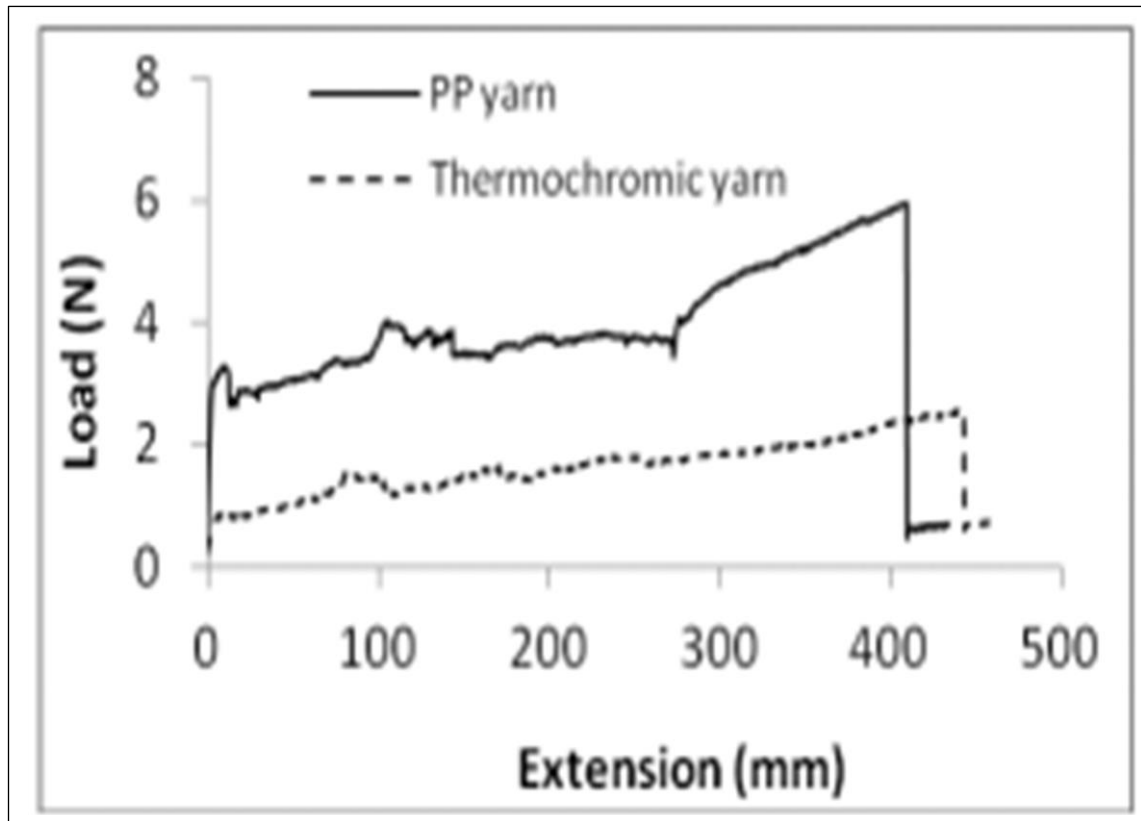


Figure 7:7 Tensile test (Polypropylene and Thermochromic polypropylene)

All above parameters affect the final filament property at molecular (polymer orientation, degree of crystallinity etc.) and the structural level (diameter, morphology etc.) [32, 33]. “When Polypropylene is formed, its crystal formation changes according to the heat treatment temperature and the conditions of the cooling process. These changes create differences in strength, heat resistance and pressure bonding properties” [10]. In spite of using all same parameters for polypropylene and thermochromic polypropylene, their count values were different. The count of the polypropylene was 86tex and the count of the thermochromic polypropylene was 90tex. Tensile testing results of neat polypropylene and thermochromic-polypropylene filaments are shown in Figure 7:7. Neat polypropylene tenacity was found higher than that of thermochromic

polypropylene. Thermochromic polypropylene has higher elongation compared to neat polypropylene. The addition of a thermochromic material has influenced the mechanical properties. The reduction in mechanical property of thermochromic filament can be due to the size, distribution and morphology of thermochromic pigments, a similar result was also observed by Tavanai et al [25] (2005).

7.4.4 FTIR Characterisation

The ATR-FTIR spectra of the neat PP and thermochromic polypropylene are shown in Figure 7:8. Polypropylene filament spectra show the absorption peak at 2918.25 cm^{-1} , which represents the CH_2 group vibration in the main PP polymer chain.

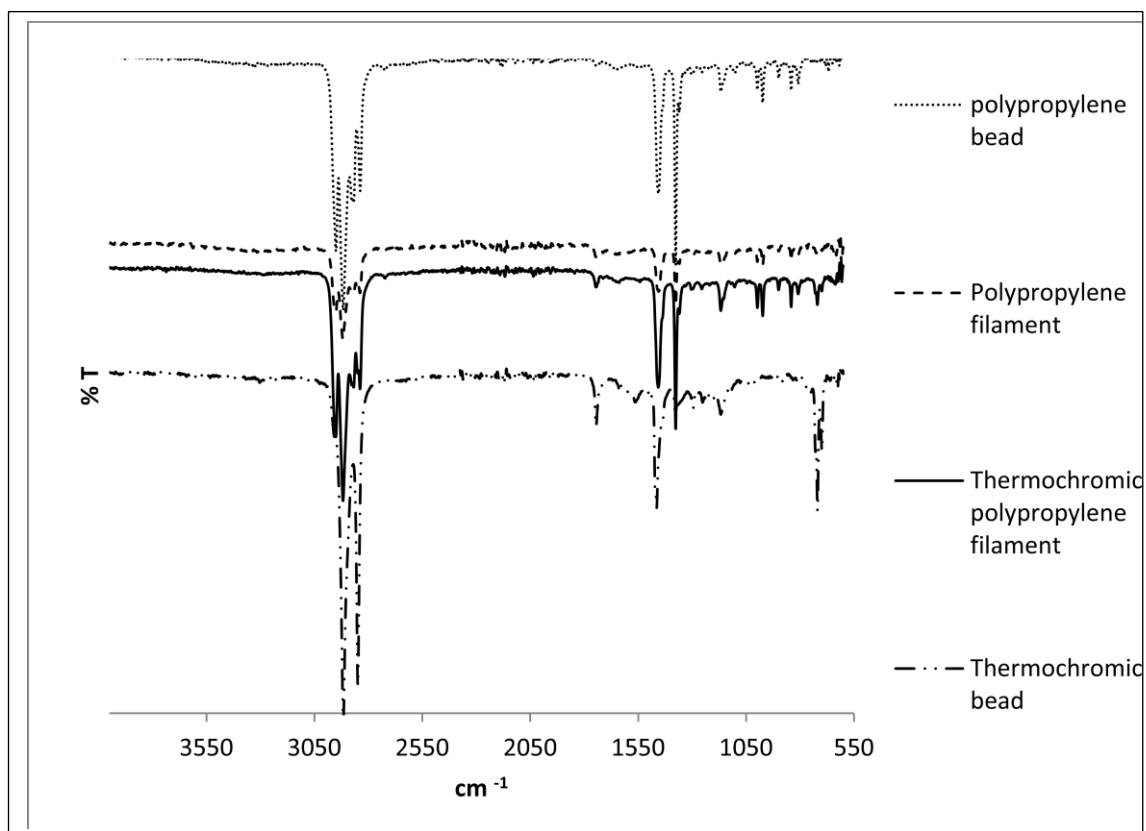


Figure 7:8 FTIR curves

The ATR-FTIR spectrum of the PP shows four large peaks in the wavenumber range $3000\text{--}2800\text{ cm}^{-1}$: the peaks at 2951.27 and 2868.25 cm^{-1} can be attributed to CH_3 asymmetric and symmetric stretching vibrations respectively, while the peaks at 2918.25 and 2833.75 cm^{-1} are due to CH_2 asymmetric and symmetric stretching vibrations respectively. The ATR-FTIR spectrum also shows two intense peaks at 1455.16 and 1376.38 cm^{-1} : The peak at 1455.16 cm^{-1} is caused by CH_3 asymmetric deformation vibrations or CH_2 scissor vibrations, while the peak at 1376.38 cm^{-1} is due to CH_3 symmetry deformation vibrations. The ATR-FTIR spectrum of the neat PP filament also shows numerous small peaks in the $1200\text{--}750\text{ cm}^{-1}$ wavenumber range. The

peak at 1167.82cm^{-1} can be attributed to C-C asymmetric stretching, CH_3 asymmetric rocking and C-H wagging vibrations, while the peak at 997.75cm^{-1} can be attributed to CH_3 asymmetric rocking and C-C asymmetric stretching vibrations, while the peak at 897.39cm^{-1} is due to CH_3 asymmetric rocking and C-C asymmetric and symmetric stretching vibrations. The peaks at 841.25 and 806.35cm^{-1} are due to CH_2 rocking vibrations. Similar peaks were found in polypropylene bead also (with little displacement). All above values match those observed by Morent et al also [34] (2008). The peaks in UMB blue thermochromic bead were found at 2916.83 , 2848.89 , 1464.37 , 1377.61 , 1167.47 , 719.27 cm^{-1} . Most UMB blue peaks are coinciding with polypropylene bead except peak at the 719.27 cm^{-1} . The thermochromic polypropylene filament peaks due to polypropylene were found at 2950.92 , 2917.59 , 2868.31 , 2838.55 , 1456.82 , 1376.39 and 1167.52 cm^{-1} . We did not get full information about the chemical constitution of the binder of the thermochromic beads from the manufacturer.. Peak at 719.76cm^{-1} can be considered due to thermochromic bead in the thermochromic filament. This indicates good mixing of UMB blue (thermochromic material) and polypropylene.

7.4.5 DSC Measurement

Every solid state material when continuously heated will come to a point where it changes phase. “As a material is heated, the atoms and/or molecules gain more energy. At the solid to liquid transition temperature, the atoms/molecules have enough energy to break away from their rigid structure to a less restricted state which is the liquid state. The energy supplied simply goes into converting the solid to liquid, that is , the energy is spent in breaking down the rigid solid structure into the much less rigid liquid state, leading to gain in energy of the material (an endothermic transition)” .[12]. DSC allows to measure thermal transition such as melting boiling points as well as other transition temperatures such a s glass transition temperature (T_G), and crystallization temperature (T_c) etc.[12].

Figure 7:9 shows the DSC thermograms of neat polypropylene and dyed (thermochromic) polypropylene fibres. Polypropylene bead showed endothermic melting peak at 149.1°C . The thermochromic UMB Blue bead curve has showed two endothermic peaks at 37.5°C and 109.1°C . Peak at 37.5°C is due to the melting of the methyl stearate.

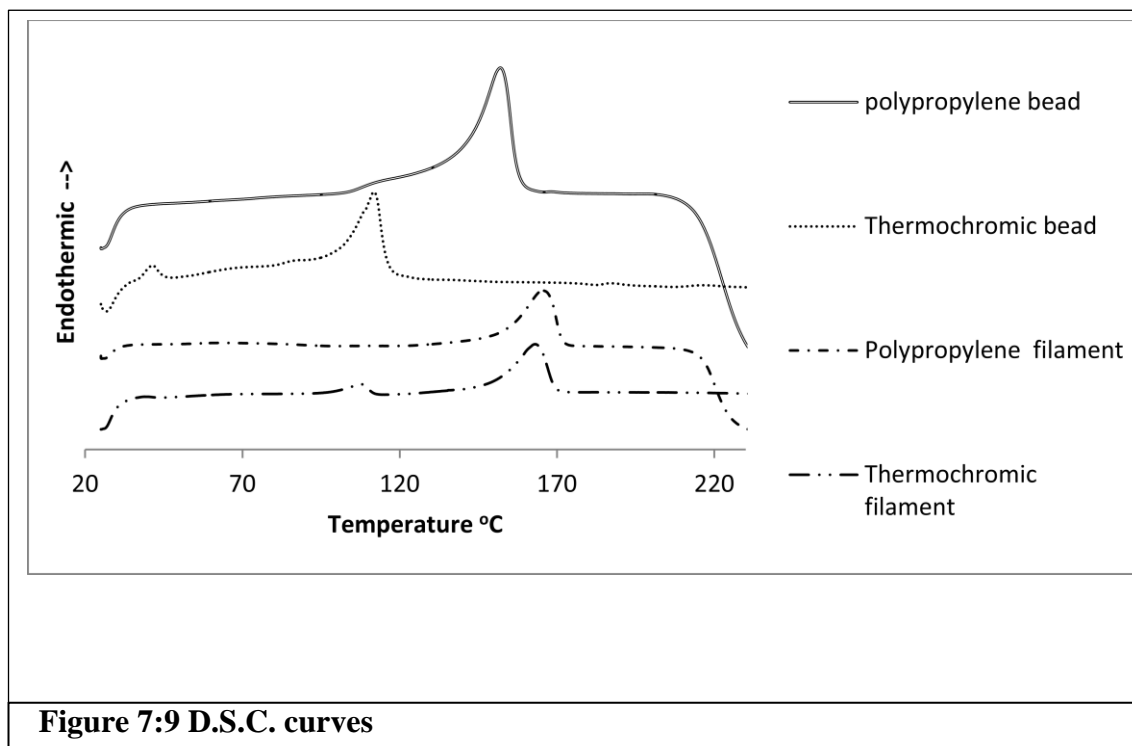


Figure 7:9 D.S.C. curves

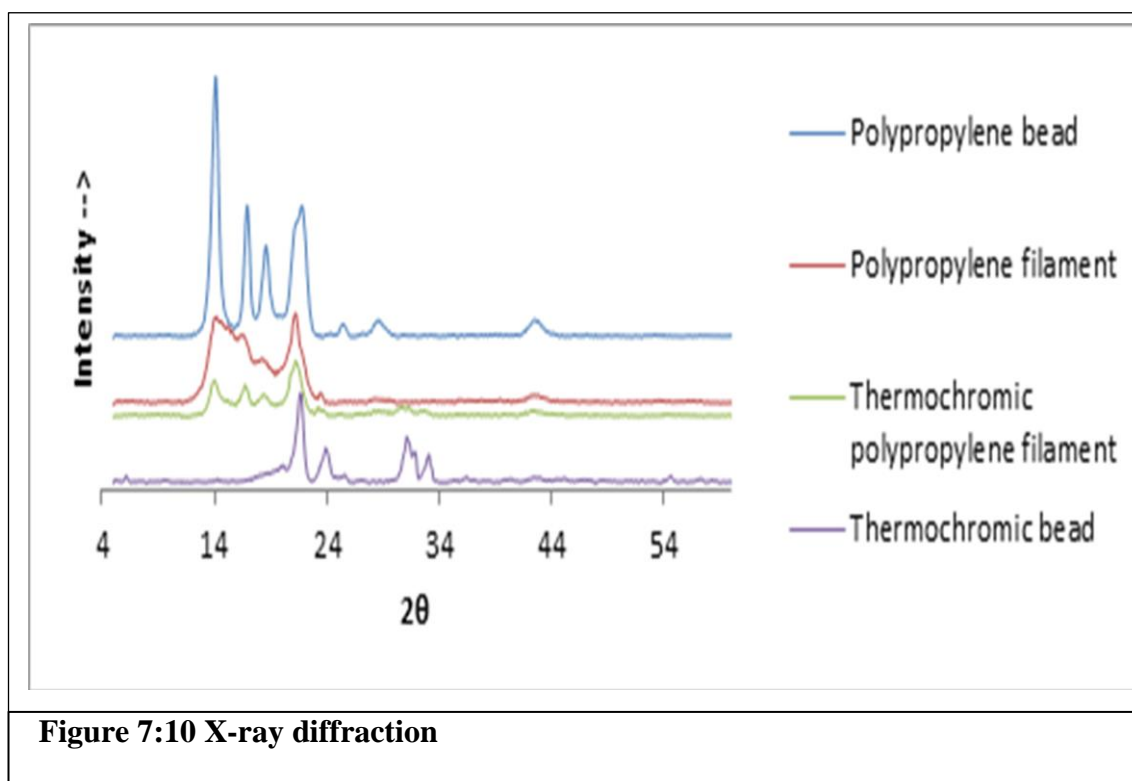


Figure 7:10 X-ray diffraction

The melting point range of methyl stearate is 30.5°C to 39°C [35]. Another peak at 109.1°C is due to an unknown binder, as the supplier did not provide any chemical structural information. After melt spinning, the polypropylene curve showed shift of endothermic peak from 149.1°C to 159.2°C. The thermochromic polypropylene yarn curve has shown an endothermic peak at 36.6°C and has shown another endothermic peak at 101.6°C. A peak at 146.6°C is also due to polypropylene and can be seen in the

thermochromic polypropylene. Reduction in melting temperature in the thermochromic filament suggests reduced crystallinity.

7.4.6 X-Ray Diffraction

Figure 7:10 illustrates the X-Ray diffraction pattern of pure polypropylene bead, thermochromic bead and thermochromic filament (undrawn).

The characteristic diffraction peaks of the polypropylene beads was found at 2θ values = 14.1(110), 16.91 (40), 18.57 (130) [36] and 21.16 (111)[37], 25.39, 28.508, 42.46. In polypropylene filament diffraction peaks were found at 2θ =13.97, 16.66, 18.39, 21.22, 23.486, 28.52, 42.46 etc. In thermochromic bead the peaks were at 2θ = 21.66, 23.90, 25.576, 31.11, 31.824, 33.061, 33.291. In thermochromic polypropylene filament peak were found at 2θ =13.994, 16.715, 18.38, 20.813, 21.218, 23.209, 23.698, 30.54, 31.9, 33, 33.2, 42.52. The diffraction pattern of the thermochromic filament shows peaks of the both polypropylene and thermochromic bead also.

7.5 Conclusion

In the present work, thermochromic polypropylene mono filament was melt spun using a Labspin Screw Extruder with water cooling. Pure polypropylene and thermochromic polypropylene filaments were produced with the same parameters. Both the filaments were studied and compared at various properties. Visual observation suggests uniform distribution of pigments in the polypropylene matrix. The colour change was gradual from blue to colourless above approximately 39°C. When cooled, the colour reversed back again to the original colour. SEM images suggest smoother surface of polypropylene compared to thermochromic polypropylene. The thermochromic pigments contributed in the formulation of rougher thermochromic filament surface. The maximum load value was found higher in polypropylene, and the elongation value was found higher in the thermochromic filament. The results suggest that thermochromic filament is poorer than the pure neat polypropylene, due to size, shape and distribution of the thermochromic pigment in the polypropylene. The DSC results showed two endothermic peaks for the thermochromic bead. The lower endothermic peak suggests activation temperature. The thermochromic filament showed three endothermic peaks, the third endothermic peak is due to polypropylene. The XRD results have found all peaks of polypropylene and also the peak of the thermochromic pigment.

7.6 Bibliography

- [7.1] A. Schwarz, L. Van Langenhove, P. Guernonprez, and D. Deguillemont, "A roadmap on smart textiles," *Textile Progress*, vol. 42, pp. 99-180, 2010.
- [7.2] T. L. Vigo, "Intelligent Fibrous Materials," *Journal of the Textile Institute*, vol. 90, pp. 1-13, 1999.
- [7.3] A. K. Maji and I. Negret, "Smart Prestressing with Shape-Memory Alloy," *J. Eng. Mech.*, vol. 124, pp. 1121-1128, 1998.
- [7.4] L. G. Machado and M. A. Savi, "Medical applications of shape memory alloys," *Brazilian Journal of Medical and Biological Research*, vol. 36, pp. 683-691, 2003.
- [7.5] I. Malherbe, R. D. Sanderson, and E. Smit, "Reversibly thermochromic micro-fibres by coaxial electrospinning," *Polymer*, vol. 51, pp. 5037-5043, 2010.
- [7.6] C. G. Granqvist, P. C. Lansåker, N. R. Mlyuka, G. A. Niklasson, and E. Avendaño, "Progress in chromogenics: New results for electrochromic and thermochromic materials and devices," *Solar Energy Materials and Solar Cells*, vol. 93, pp. 2032-2039, 2009.
- [7.7] S. Yutaka, N. Norikazu, I. Hiroshi, K. Tutomu, O. Masaharu, M. Nobuaki, N. Katuyuki, and F. Katuyuki, "Thermochromic textile material," 1987.
- [7.8] C. G. Granqvist, "Transparent conductors as solar energy materials: A panoramic review," *Solar Energy Materials and Solar Cells*, vol. 91, pp. 1529-1598, 2007.
- [7.9] R. Kulčar, M. Friškovec, N. Hauptman, A. Vesel, and M. K. Gunde, "Colorimetric properties of reversible thermochromic printing inks," *Dyes and Pigments*, vol. 86, pp. 271-277, 2010.
- [7.10] J. Mutanen, T. Jaaskelainen, and J. P. S. Parkkinen, "Thermochromism of fluorescent colors," *Color Research & Application*, vol. 30, pp. 163-171, 2005.
- [7.11] S. Lakio, J. Heinämäki, and J. Yliruusi, "Colorful Drying," *AAPS PharmSciTech*, vol. 11, pp. 46-53, 2010.
- [7.12] T. L. Dawson, "Changing colours: now you see them, now you don't," *Coloration Technology*, vol. 126, pp. 177-188, 2010.
- [7.13] A. Seeboth and D. Löttsch, "Thermochromic Polymers," in *Encyclopedia of Polymer Science and Technology*, ed: John Wiley & Sons, Inc., 2002.
- [7.14] D. Aitken, S. M. Burkinshaw, J. Griffiths, and A. D. Towns, "Textile applications of thermochromic systems," *Review of Progress in Coloration and Related Topics*, vol. 26, pp. 1-8, 1996.

- [7.15] D. Aitken, S. M. Burkinshaw, J. Griffiths, and A. D. Towns, "Textile applications of thennochromic systems," *Review of Progress in Coloration and Related Topics*, vol. 26, pp. 1-8, 1996.
- [7.16] C. Canal Barnils, S. Villeger, P. Erra Serrabasa, and A. Richard, "Study of irreversible thermochromic ink application on textiles," *Tekstil*, vol. 58, pp. 105-111, 2009.
- [7.17] P. Kiri, G. Hyett, and R. Binions, "Solid state thermochromic materials," *Advanced Materials Letters*, vol. 1, pp. 86-105, 2010.
- [7.18] R. M. Christie, S. Sara Robertson, and S. Taylor, "Design Concepts for a Temperature Sensitive Environment using Thermochromic Colour Change," *Colour: Design & Creativity*, vol. 1(1), pp. 1-11, 2007.
- [7.19] S. L. P. Tang and G. K. Stylios, "An overview of smart technologies for clothing design and engineering," *International Journal of Clothing Science and Technology*, vol. 18, pp. 108-128, 2006.
- [7.20] S. M. Burkinshaw, J. Griffiths, and A. D. Towns, "Reversibly thermochromic systems based on pH-sensitive functional dyes," *Journal of Materials Chemistry*, vol. 8, pp. 2677-2683, 1998.
- [7.21] Anon. (2012, July 2012). *Principle of thermochromism* Available: <http://www.chromazone.co.uk/Thermochromism.htm>
- [7.22] M. Marinković, R. Nikolić, J. Savović, S. Gadžurić, and I. Zsigrai, "Thermochromic complex compounds in phase change materials: Possible application in an agricultural greenhouse," *Solar Energy Materials and Solar Cells*, vol. 51, pp. 401-411, 1998.
- [7.23] T. Karlessi, M. Santamouris, K. Apostolakis, A. Synnefa, and I. Livada, "Development and testing of thermochromic coatings for buildings and urban structures," *Solar Energy*, vol. 83, pp. 538-551, 2009.
- [7.24] M. Wishman and G. E. Hagler, "Polypropylene Fibres," in *Handbook of Fibre Chemistry 2nd edition*, ed. by Lewin, M. and Pearce, E.M. Marcel Dekker, New York, NY, M. Lewin and E. M. Pearce, Eds., 2 ed The state of america marcel dekker inc., 270 Madison Avenue, New York, New York 10016, <http://www.dekker.com>, 1998, pp. 161-277.
- [7.25] H. Tavanai, M. Morshed, M. Zarebini, and A. Salehi Rezve, "A Study of the Nucleation Effect of Pigment Dyes on the Microstructure of Mass Dyed Bulked Continuous Filament Polypropylene," *Iranian polymer journal*, vol. 14, pp. 267-276, 2005.

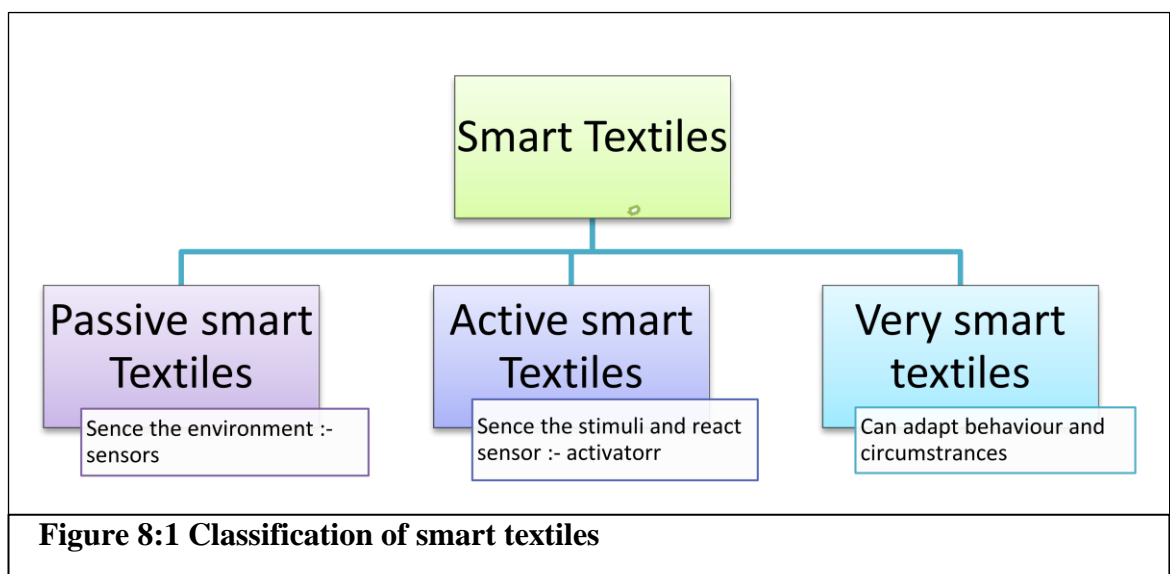
- [7.26] A. F. Vargas, V. H. Orozco, F. Rault, S. Giraud, E. Devaux, and B. L. López, "Influence of fibre-like nanofillers on the rheological, mechanical, thermal and fire properties of polypropylene: An application to multifilament yarn," *Composites Part A: Applied Science and Manufacturing*, vol. 41, pp. 1797-1806, 2010.
- [7.27] S. M. Burkinshaw, P. E. Froehling, and M. Mignanelli, "The effect of hyperbranched polymers on the dyeing of polypropylene fibres," *Dyes and Pigments*, vol. 53, pp. 229-235, 2002.
- [7.28] J. A. Kent, "Kent and Riegel's Handbook of Industrial Chemistry and Biotechnology, Volumes 1 & 2 (11th Edition)," ed: Springer - Verlag.
- [7.29] S. C. O. Ugbolue, *Polyolefin Fibres: Industrial and Medical Applications*: Woodhead Pub., 2009.
- [7.30] J. Akrman and M. Kaplanova, "The coloration of polypropylene fibres with acid dyes," *Journal of the Society of Dyers and Colourists*, vol. 111, pp. 159-163, 1995.
- [7.31] A. Marcinčin, "Modification of fibre-forming polymers by additives," *Progress in Polymer Science*, vol. 27, pp. 853-913, 2002.
- [7.32] Y.-P. Jeon and C. L. Cox, "Simulation of Multifilament Semicrystalline Polymer Fibre Melt-Spinning," *Journal of Engineered Fibres and Fabrics*, vol. 4, pp. 34-43, 2009.
- [7.33] A. G. Kravtsov, H. Brünig, and S. F. Zhandarov, "Analysis of the polarization state of melt-spun polypropylene fibres," *Journal of Materials Processing Technology*, vol. 124, pp. 160-165, 2002.
- [7.34] R. Morent, N. De Geyter, C. Leys, L. Gengembre, and E. Payen, "Comparison between XPS- and FTIR-analysis of plasma-treated polypropylene film surfaces," *Surface and Interface Analysis*, vol. 40, pp. 597-600, 2008.
- [7.35] G. Knothe, A. C. Matheaus, and T. W. Ryan Iii, "Cetane numbers of branched and straight-chain fatty esters determined in an ignition quality tester☆," *Fuel*, vol. 82, pp. 971-975, 2003.
- [7.36] I. Karacan and H. Belni, "An X-Ray diffraction study for isotactic polypropylene fibres produced with take-up speeds of 2500-4250 m/min," *Tekstil Ve Konfeksiyon*, pp. 201-209, 2011.
- [7.37] A. R. Bhattacharyya, T. V. Sreekumar, T. Liu, S. Kumar, L. M. Ericson, R. H. Hauge, and R. E. Smalley, "Crystallization and orientation studies in polypropylene/single wall carbon nanotube composite," *Polymer*, vol. 44, pp. 2373-2377, 2003.

Chapter 8 : End Uses and Further Work

8.1 Introduction

It is very important to engineer the size, shape and functionality of any product when considering end uses, its cost and productivity in today's material market. After selection of the material from a vast range of materials, it is important to choose a proper material processing technique(s). Textile grade polymers are processed in to different forms such as fibres, yarns or fabric for many industrial, medical and domestic end uses.

Textiles are an inseparable part of modern life of modern human in the form of clothing, upholstery, filtration, medical, aerospace and many more. Development of functional, smart and structural textiles revolutionized modern human life and comfort [1]. Smart textiles are “textiles that are able to sense stimuli from the environment to react to them and adapt to them by integration of functionalities in the textile structure. Stimuli and response can have an electrical, thermal, chemical, magnetic or other origin” [2].



Smart textiles can be divided into three groups (Figure 8:1), and can be developed by incorporating or coating functional or smart material [3, 4] in to textiles. Depending on the smart material used, the behaviour of the textile changed. Shape memory materials (returns to a preprogramed shape with any stimuli [3]); phase change materials (absorb, store and release heat as required in order to keep the wearer at optimum temperature [3]), chromatic materials (changes colour with change in external stimuli [3]. are a few examples of smart materials.

Functional clothing includes all the clothing those are specifically engineered to deliver predetermined performance of functionality to user over and above its normal functions.

They can be classified as protective textiles, sport textiles, medical textiles etc.

In the present thesis, different polymers were processed using different methods to generate functional, smart and structural fibrous morphologies / textiles. Synthetic polymers can be processed into fibre by conventional spinning method such as melt spinning, wet spinning or dry spinning. In this work, conventional melt spinning was used to produce “smart” thermochromic polypropylene. Melt spinning is mainly used to process thermoplastic polymers into textile fibres. Nanofibres cannot be produced by a conventional spinning methods such as melt, dry or wet spinning [6]. Electrospinning is one of the most versatile and industrially viable methods to produce nanofibres.

Engineering the nanofibre morphology depends on complex interactions of various solutions, atmospheric, polymeric and process parameters during electrospinning. Nano dimension adds new properties to the fibres itself. There are several benefits of nano dimensions.

- The nano dimension means large surface area to volume or mass ratio.
- Nanofibres can be easily functionalized by adding additives for any chemical, biological end use. Ease of blending with different materials make it easy to adjust the blend of composition.
- Higher surface area gives more surface(s) for interactions. This may increase the processing speed and may reduce the total material requirement by reducing wastage of unused material in the fibre body.
- The nanofibres have very small dimension up to a cellular level, so it can interact easily at that dimension.
- Nano fibre mats can have interconnected pores, smaller pores and higher pore space to material ratios. They can be used for hi-end filtration applications.
- Flexibility of changing various electrospinning parameters to produce different size and various nano fibrous morphologies for example beaded or bead-less, porous fibres, coiled or uncoiled fibres widens its end use for energy, drug delivery.
- Besides flexibility of material composition, the flexibility of designing different structures/morphologies widens the application of nanofibres [7].
- Human tissues are formed from different cells (functional cells, support cells) contained in an extracellular matrix (ECM). Electrospinning can form material of ECM dimensions. Nanofibres can be used for tissue engineering by developing functional tissue engineering products to mimic native ECM [8], which can actively integrate with biological systems such as cells, tissues.

- Cells are roughly 10-100 μm size. Cell sensing takes place at about 5-10 μm . Cells are sensitive to chemistry and topography on the macro, micro and nano scale. At this length scale material design can be done to help biology [9].

The above capabilities allow nanofibres to be used in different high end applications such as biomedical, defence and filtration. In the present work, different morphologies of Manukahoney(MH) –polyethylene oxide (MHPEO) nanofibres were produced by electrospinning. Depending on its end use different MHPEO nanofibre morphologies such as more merged or less merged mats can be made. Additionally, MHPEO fibres have shown bactericidal activity, and it has been proven that they can be used as functional fibres for biomedical enduses.

Fibres electrospun from Ethylcellulose (EC) with ethanol and toluene combination produced a series of different fibre morphologies from beaded to bead-less fibres. It is interesting to know that the shape and size of beads can be controlled by changing the ethanol: toluene ratio. The MHPEO and EC nanofibres were produced using single needle electrospinning. Single needle electrospinning is a low output method and has limitations such as needle blocking. In order to overcome limitations of needle electrospinning, researchers developed various needleless electrospinning methods. Bubble electrospinning is one of the recently invented electrospinning method. Bubble electrospinning can produce multiple jets at a time, so it is a high production method. Interestingly EC fibres had different morphologies by bubble electrospinning compared to single electrospinning with similar parametric variables.

8.2 MHPEO (Needle) Electrospinning

Manuka honey (MH) is widely used by ingestion or topically. MH honey is different due to its unique bactericidal activity called unique Manuka factor (UMF) indicated by numbers. Higher the UMF better is the antibacterial property. Use of MH in its present liquid/semisolid form limits its field of end use. MH in fibrous morphology can increase the enduses. MH alone cannot be spun on its own due to its viscoelastic properties. Polyethylene oxide can be used to spin the MH into nanofibres by electrospinning. There was a noticeable effect of the parameters such as MHPEO ratio, NTCD, applied voltage, feed rate on the fibre size and morphology. The average fibre diameters were produced from 0.198 μm to 0.924 μm by changing the parameters. Different morphologies such as flat, thick, merged fibres to round shaped, thin, unmerged fibres were obtained by changing all above parameters. The MHPEO nanofibre showed bactericidal activity at 50% (by wt. %) of MH proportion.

8.2.1 End Use

- MHPEO mat can be used as antibacterial and fast healing in wound healing.
- MHPEO fibres can be used in packaging as biomaterial.
- MHPEO fibre can be cross-linked to a different degree and can be used for slow release or controlled release of MH for medical applications.
- Cross linked MHPEO can be used for filtration.
- Apart from antibacterial activities the MHPEO mats maintains moisture and stickiness due to hygroscopic nature of the MH. These properties can be used to maintain moisture or stickiness.
- MHPEO fibres can be used as food using food grade PEO as matrix.
- MHPEO mats can be used in cosmetics to maintain moisture.

8.2.2 Further Work

- MHPEO electrospinning can be done with higher molecular weight PEO to reduce PEO proportion and to get more MH in the fibre.
- To control the water percentage of MH or to try dry powder of MH to have better control of parameters, as the water content in the MH has a significant effect on MHPEO fibre morphologies.
- To spin MHPEO fibres using wet spinning for conventional textile products.

8.3 Ethylcellulose (needle) electrospinning

EC is widely used in the pharmaceutical industry. It is a biocompatible polymer. The EC was successfully electrospun into nanofibres using different parameters. In present study we used an ethanol: toluene mixture to electrospin nano fibres. It is interesting to note that the effect of different solvent ratios of ethanol: toluene created different morphologies, from round shaped beads to smooth fibres.

8.3.1 End Use

- The beaded fibres can be used for drug loading and drug delivery, while bead-less fibres can be used for filtration.
- Not all medicines or additives are compatible with all solvents. The ethanol: toluene solvent system can be used to produce EC nanofibres with the any additives (for e.g. medicines) compatible with ethanol: toluene system.
- The ethanol: toluene solvent ratios can be used to design or engineer EC films/fibres at nanoscale with given mechanical and thermal properties, by

controlling the ethanol: toluene ratio without altering any processing or atmospheric parameters.

8.3.2 Further Work

- To load the EC fibres with drug/additive and study the effect of different bead morphology on loading and release of those drugs/additives
- To establish a numerical/mathematical relation between the solvent proportion/properties to control EC fibre/fabric properties.

8.4 Ethylcellulose (Bubble) Electrospinning

In the present study, EC fibres were electrospun into nanofibres by single needle electrospinning and bubble electrospinning. It was interesting to note that changing electrospinning method affected fibre morphology even for the same parameter values. Bubble electrospinning fibres followed different trend compared to needle electrospinning using the same parameters. Ethyl cellulose fibre diameters ranging from 0.188 μm to 0.396 μm can be obtained by changing different bubble electrospinning parameters such as solution surface to collector distance (SSCD) and applied voltage.

8.4.1 End Use

EC nanofibres can be used for drug delivery (same previous topic 1.4.1)

8.4.2 Further Work

- To study more parameters in bubble electrospinning to better understand the effect of parameters on fibre morphology.

8.5 Thermochromic Polypropylene

Thermochromic materials change their properties reversibly or irreversibly (usually optical) in the presence of heat. Traditionally, thermochromic textiles are produced by coating, spraying or printing thermochromic pigments on different forms of textiles such as fibres, yarns or fabrics. These methods add extra cost and need extra processing. Coating and printing should be fast enough to withstand washing and atmospheric parameters. In order to spray, coat or print there is a need of appropriate solvents. Thermochromic pigments are very sensitive to most solvents and can be easily destroyed. All above reasons limits the use of thermochromic pigments in textiles. Melt spinning of thermochromic pigments into filament can overcome all above disadvantages. Melt spinning of pigments into filament can be a challenge. As pigments may be destroyed due to heating and shear stresses by melt spinning. Uniform pigment

distribution is needed to achieve thermochromic filament. In order to do this, appropriate temperature profile and speeds/ draw ratio should be carefully established. We chose polypropylene as matrix to process thermochromic pigments.

Polypropylene is a polyolefin fibre. It is widely used in conventional and industrial textiles. Polypropylene is easily melt spinnable in textile forms.

8.5.1 End Use

- Thermochromic textiles can be used as visual sensor for temperature sensitive products and processes. Thermochromic pigments are available and can be developed for various temperature ranges using different materials.
- Thermochromic textiles can be used in textile design by incorporating heating element. Thermochromic pigments are available in various colours. Designs with different colours at different temperature can be produced or different designs can be obtained at different temperatures.
- Thermochromic textiles can be an added product in the textile fashion industry.
- Polypropylene can be dope dyed with such smart pigments as added value.

8.5.2 Further Work:

Present work can be extended as below:

- To optimize meltspinning parameters as the thermochromic fibre has more uneven surface compared to a neat polypropylene.
- To texturize thermochromic filament and act as staple fibre, and to study the processability in staple spinning.
- To study the weaving and knitting performance of a thermochromic filament.
- If the processability is poor in the above process, try to optimise its melt spinning parameters by more trial and error and improve its strength and evenness for better processability.
- To try different polymers such as nylon, polyester in place of polypropylene and to study compatibility or phase separation.
- It is very important to heat the filament to get the thermochromic effect. To incorporate a heating element by incorporating conductive additives at the dope dyeing stage in the filament stage or twisting with metallic wires at the yarn preparation stage. The resistivity of the conductive element can generate heat.
- To study the effect of different percentage of pigments on the melt processability and study the filament properties.

- To model the above processes to predict the effect of processing parameters on the thermochromic filament characteristics.
- To produce nanothermochromic fibres using melt electrospinning.

8.6 Bibliography

- [8.1] G. Cho, S. Lee, and J. Cho, "Review and Reappraisal of Smart Clothing," *International Journal of Human-Computer Interaction*, vol. 25, pp. 582-617, 2009.
- [8.2] L. V. Langenhove and C. Hertleer, "Smart clothing: a new life," *International Journal of Clothing Science and Technology*, vol. 16, pp. 63-72, 2004.
- [8.3] S. L. P. Tang and G. K. Stylios, "An overview of smart technologies for clothing design and engineering," *International Journal of Clothing Science and Technology*, vol. 18, pp. 108-128, 2006.
- [8.4] R. Shishoo, "Recent developments in materials for use in protective clothing," *International Journal of Clothing Science and Technology*, vol. 14, pp. 201-215, 2002.
- [8.5] D. Gupta, "Functional clothing— Definition and classification," *Indian Journal of Fibre & Textile Research*, vol. 36, pp. 321-326, December 2011 2011.
- [8.6] K. M. Sawicka and P. Gouma, "Electrospun composite nanofibres for functional applications," *Journal of Nanoparticle Research*, vol. 8, pp. 769-781, 2006.
- [8.7] D. Liang, B. S. Hsiao, and B. Chu, "Functional electrospun nanofibrous scaffolds for biomedical applications," *Adv Drug Deliv Rev*, vol. 59, pp. 1392-412, 2007.
- [8.8] C. P. Barnes, S. A. Sell, E. D. Boland, D. G. Simpson, and G. L. Bowlin, "Nanofibre technology: designing the next generation of tissue engineering scaffolds," *Adv Drug Deliv Rev*, vol. 59, pp. 1413-33, Dec 10 2007.
- [8.9] R. Gentsch and H. G. Börner, "Designing Three-Dimensional Materials at the Interface to Biology," vol. 240, pp. 163-192, 2010.

Chapter 9 : Conclusions

Smart, functional and structural ultrafine nano fibres were produced and characterized using different spinning methods in the present work. Antibacterial Manuka honey nanofibres with different morphologies (merged, unmerged) were produced successfully by needle electrospinning. Ethylcellulose nano fibres with different morphologies such as beaded fibres (round shaped, elongated shaped) and smooth bead-less fibres were produced by needle electrospinning and bubble electrospinning. In order to develop melt electrospinning, processing parameters of thermochromic polypropylene using a bench top melt extruder were studied.

Different smart materials were incorporated into different polymer matrix to spin smart and functional fibres. It is very important to investigate the optimum concentration, distribution and resultant effectiveness of the incorporated materials in the final matrix. It is also very important to balance the required properties of these fibres such as strength, functionalities/smartness and their processability. To produce the above mentioned smart, functional fibrous structures, effect of different electrospinning parameters on the morphologies and sizes of the ethylcellulose and Manuka honey nano fibres were studied. The fibre dimension and morphology (structure and shape) also adds functionality. For example, beaded fibres can be used for drug loading and smooth bead-less fibres can be used for high-end filtration.

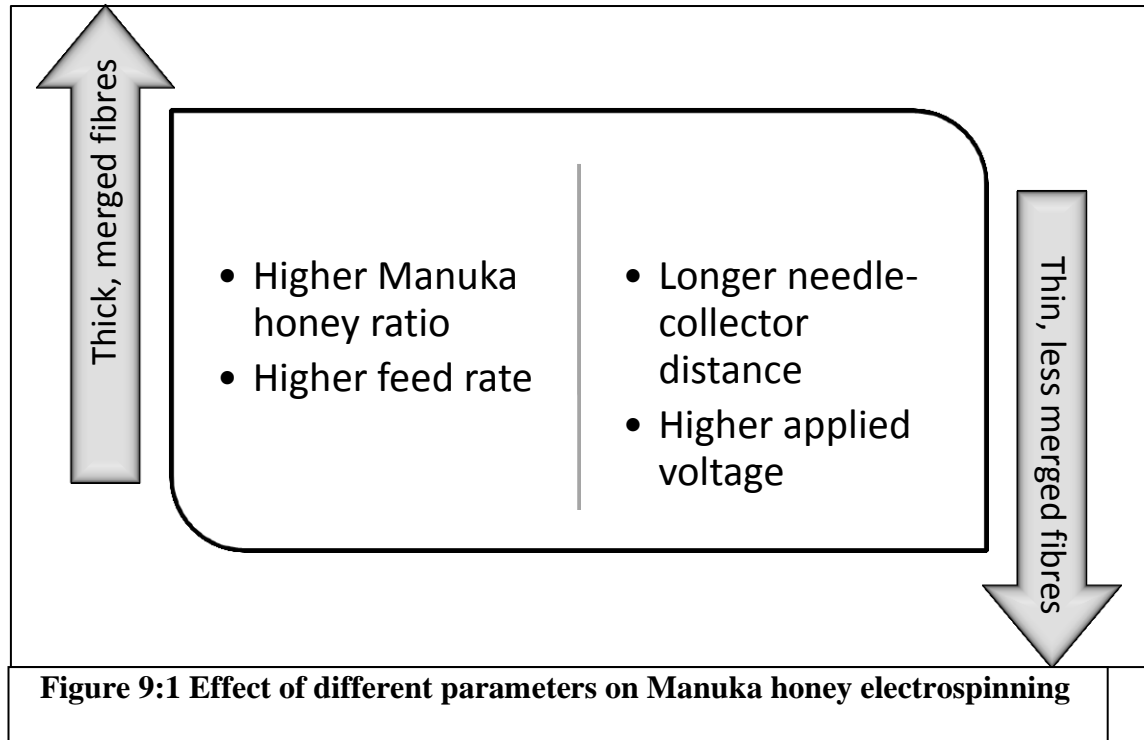
The following is the detailed discussion of the effect of various parameters on the properties and morphologies of fibres.

9.1 Antibacterial Manuka Honey Nano Fibres

The Manuka honey cannot be electrospun on its own, due to unfavourable Manuka honey properties such as viscosity, rheology and surface tension of Manuka honey. In the present work, Manuka honey (UMF 25%) nano fibres were successfully spun using poly ethylene oxide as a matrix polymer. It was also important to maintain antibacterial property of Manuka honey even after addition of polyethylene oxide. Results showed that Manuka honey nanofibres maintained its antibacterial property at 50% and higher concentration with polyethylene oxide.

In order to spin nano fibres, different proportions of Manuka honey: polyethylene oxide blends were electrospun. The Manuka honey fibres were studied for the thermal properties by DSC, blend by FTIR and fibre morphologies by SEM. Manuka honey:

Solution properties such as viscosity, surface tension, electrical conductivity and UV-visible spectra were also measured and compared for all the spinning solutions. The viscosity of all the Manuka honey: polyethylene oxide blends were lower compared to 15% polyethylene oxide aqueous solution. Viscosity of the Manuka honey: polyethylene oxide blend reduced as the Manuka honey proportion increased due to the increase in water content. The Manuka honey itself has water, apart from that Manuka honey is humectant and hygroscopic. Manuka honey attracts more water from the surroundings.



No clear trend was found between Manuka honey fibre morphologies and conductivity/surface tension. The fibre diameter increased with higher Manuka honey proportion, i.e. reduction in viscosity. Usually fibre diameter reduces as viscosity reduces. This reverse trend in Manuka honey is due to the hygroscopic and humectant nature of Manuka honey. The Manuka honey fibres become flatter, on reaching the collector at high speed due to more water content. At the same time, fibres on the collector absorbed water as well as spread more, which produced overall flatter and merged fibres due to more water content.

The Manuka honey fibre became thinner, round shaped and less merged as applied voltage and needle to collector distance increased (Figure 9:1). Higher applied voltage (in present study \rightarrow 25kV) further stretched Manuka honey fibres. Fibres dried faster as they became thinner which caused exposure of more surface area. Dried fibres did not merge or merged less at the contact point with each other. Similarly at longer needle to

collector distance fibres were stretched more and hence fibres dried faster as described earlier. Fibres reached thinner, dried and less merged at longer needle to collector distance (in present study \rightarrow 40cm). Fibres became flatter and merged with the faster feed rate. As the feed rate increased, more solution came out of the needle. Therefore, Manuka honey fibres became thicker, more merged and flatter with a faster feed rate.






In the present study, the thinnest fibres ($0.198\mu\text{m}$) were obtained at 30 cm needle to collector distance, 13kV applied voltage and 1.5 ml/hr feed rate using 16 gauge needle for 5% Manuka honey: polyethylene oxide solution. The thickest Manuka honey fibres ($0.924\mu\text{m}$) were obtained using 30 cm needle to collector distance, 10 ml/hr feed rate, 13kV applied voltage and 16 gauge needle for 15% Manuka honey : polyethylene oxide solution. The DSC results showed the influence of Manuka honey proportion on the melting point of Manuka honey electrospun mat. The melting point decreased compared to polyethylene oxide electrospun mat as the Manuka honey proportion increased. The melting point of polyethylene oxide mat was 67.4°C and 15% Manuka honey: polyethylene oxide was 61.1°C . The area under the DSC curve decreased as Manuka honey proportion increased, which indicates reduction in crystallization.

FTIR curves of Manuka honey: polyethylene oxide mat show respective peaks related to polyethylene oxide and Manuka honey. The 15% (wt/wt) polyethylene oxide and 15% (wt/wt) Manuka honey: polyethylene oxide did not show any anti-bacterial property. 50% (wt/wt) and 65% (wt/wt) Manuka honey: polyethylene oxide blend and 100% Manuka honey showed antibacterial activity. It can be concluded that Manuka honey fibres with higher proportion (in the present study \rightarrow 50% and more) of Manuka honey shows antibacterial activity.

9.2 Beaded and Smooth Ethylcellulose Nano Fibres by Needle Electrospinning

Size and shape (morphology / structure) of the fibres also adds functionality to the fibrous structures. Different morphologies can be electrospun from the same polymer such as beads, beaded fibres, smooth fibres, porous fibres, coiled fibres, flat fibres. by changing different parameters. It is very important to produce such different morphologies for different enduses. In present study, different morphologies were electrospun successfully from ethylcellulose by changing solvent combination. Ethylcellulose fibres were electrospun successfully and characterised by DSC, FTIR and SEM. The 15% (wt/wt) ethylcellulose was dissolved into different toluene: ethanol mixtures in the ratios of 0:100, 40:60, 50:50, 60:40, and 100:0. The fibres produced by different solvent mixtures gave different morphologies from round shaped beaded fibres

for 100% ethanol as solvent to elongated beaded fibres for 40:60 as well as for 50:50 toluene: ethanol and smooth (bead-less) thin fibres for 60:40 toluene: ethanol and smooth (bead-less), thick fibres for 100% toluene as solvents (Table 9:1).

Table 9:1 Effect of solvent on ethyl cellulose electrospinning		
Solvents (Ethanol: Toluene) ratio	Shape	Comment
100:0		Irregular / collapsed round bead on string
60:40		Irregular / collapsed elongated bead on string
50:50		Regular / solid elongated bead on string
40:60		Fibres
0:100		Thick fibres

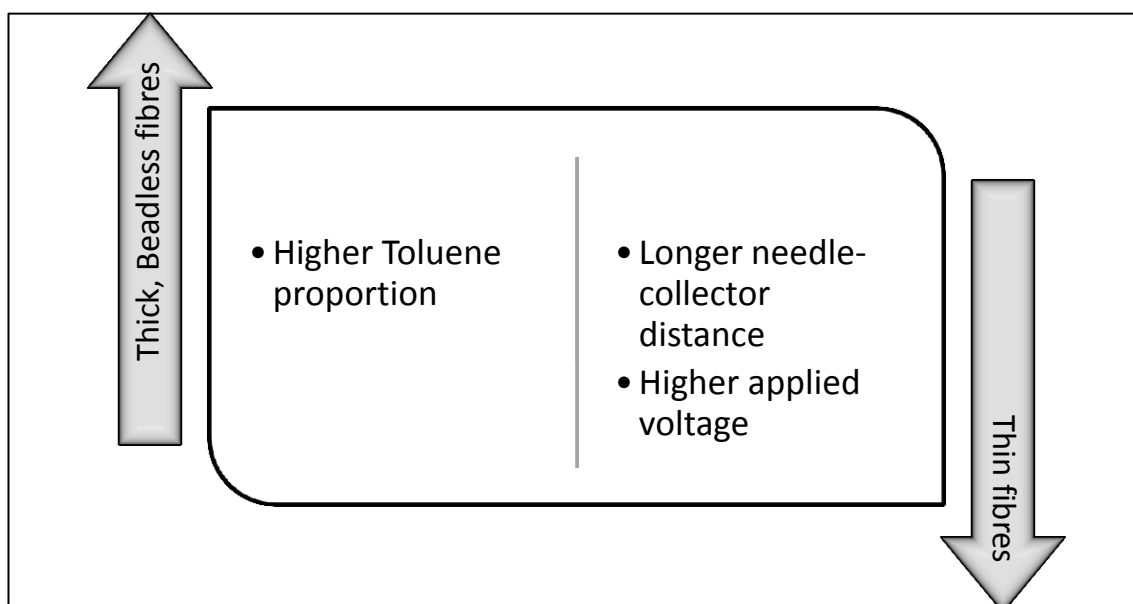


Figure 9:2 Effects of different parameters on Ethylcellulose needle electrospinning

All the parameters were kept same for the above experiment at 21kV applied voltage, 20cm needle to collector distance, 1.5ml/hr feed rate and 16 gauge needle.

Ethanol is a poor solvent for ethylcellulose compared to toluene. Ethylcellulose solution in ethanol has lower viscosity compared to the toluene as a solvent.

Less solubility of ethylcellulose in ethanol is also visible in the photograph (Chapter 5, Fig 1:5) showing higher turbidity. Higher solubility of ethylcellulose in toluene is visible by clear ethylcellulose solution in toluene. More beaded fibres at a higher ethanol proportion is due to low viscosity of the ethylcellulose solution in ethanol. As the toluene proportion is increased up to 100%, the ethylcellulose solution viscosity increases. Higher viscosity favours bead-less smooth fibres, so a higher proportion of toluene in solvent produces bead-less fibres. It indicates that selection of solvent has a measurable effect on electrospun fibre morphology. The 60:40 toluene: ethanol as solvent gave thin and bead-less fibres, hence we considered this solvent ratio for further experiment. In the present study (Figure 9:2), the thinnest average 15% (wt/wt) ethylcellulose fibre diameter ($0.483\mu\text{m}$) and at 30 cm needle to collector distance, 21kV voltage, 1.5ml/hr feed rate, 16 gauge needle and 60:40 toluene: ethanol solvent. The coarsest 15 % (wt/wt) ethylcellulose diameter ($0.631\mu\text{m}$) was obtained at 10 cm needle to collector distance in case of 60:40 toluene: ethanol as solvent.

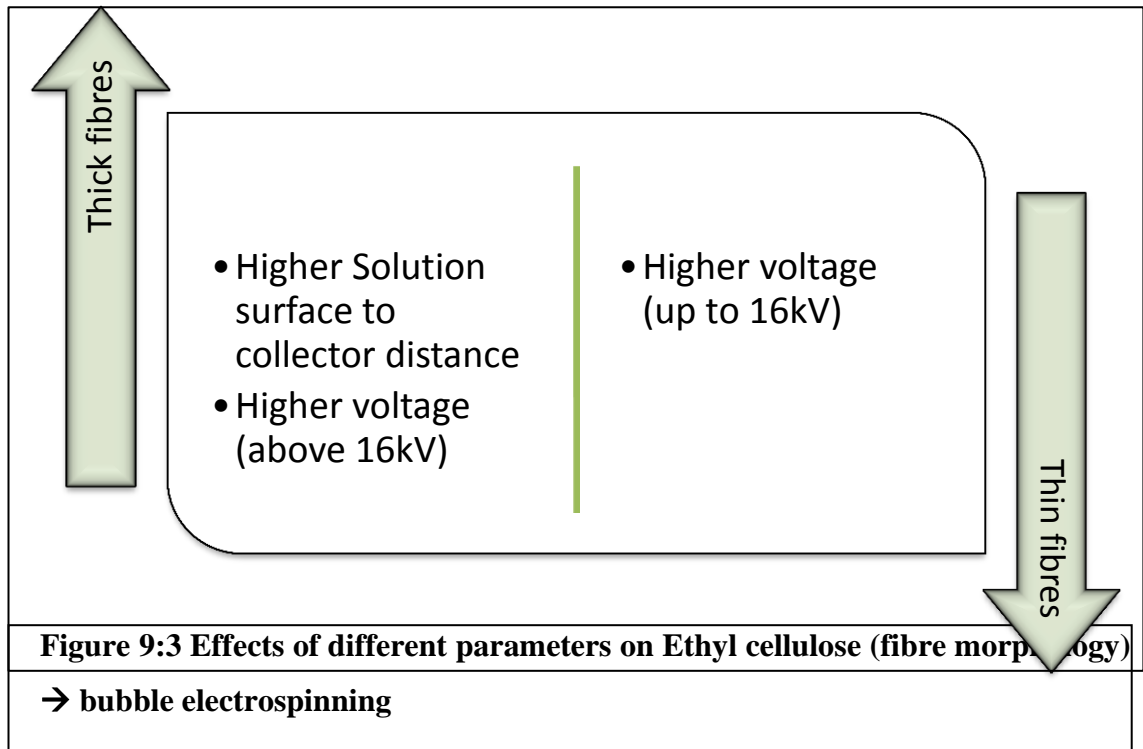
The DSC curve showed increased melting point with increase in toluene proportion as a solvent. The melting behaviour, glass transition temperature and crystallinity are correlated as the function of solvent chemistry.

The EC film mechanical properties and appearance were also affected with the change in ethanol: toluene ratio (Table 9:2).

Table 9:2 Ethyl cellulose solution and film visual property			
No.	Film detail	Film appearance	Film Flexibility
1	15EC100Et	Film with more white dots	Fragile & rigid
2	15EC50Et	Film with less white dots	semi fragile & rigid
3	15EC100To	Clear film	Pliable & flexible

9.3 Bubble Electrospinning of Ethylcellulose Eibres

Ethylcellulose fibres were also electrospun by bubble electrospinning and its results were compared with needle electrospinning results. In the bubble electrospinning of ethylcellulose (Figure 9:3), the coarsest average ethyl cellulose fibre ($0.49\mu\text{m}$) produced at 12kV applied voltage and 20cm solution surface to collector distance. The thinnest average ethylcellulose fibres produced ($0.188\mu\text{m}$) at 16kV applied voltage and 10 cm solution surface to collector distance.



9.4 Comparison between Ethylcellulose Needle Electrospeinning and Bubble Electrospeinning

Comparison was done between the conventional single needle electrospeinning with bubble electrospeinning fibre morphologies at the same parameters to understand the effect of single needle and bubble electrospeinning on fibre characteristics. Fibres were electrospeun at 0.7bar pressure by bubble electrospeinning and their size and appearance was compared with different single needle electrospeinning feed rates at 1.5 ml/hr, 5ml/hr and 10ml/hr. In the case of single needle electrospeinning, the feed rate can be controlled but in bubble electrospeinning feed rate depends entirely on the number and size of the bubbles produced, which is unpredictable. The bubble size and numbers depend on various process parameters such as the compressed force of the air, hose pipe diameter, and hose pipe depth in the bath of the reservoir. Therefore in this study, the average fibre diameter produced by both systems was considered as a milestone. Different feed rates in single needle electrospeinning revealed that fibre diameter at 1.5ml/hr feed rate is comparable to bubble electrospeinning fibre diameter produced by compressed air of 0.7bar capacity pump. Hence, 1.5 ml/hr federate was kept constant for all single needle electrospeinning experiments and the results were compared with the bubble electrospeinning results.

After standardization of the feed rate, the effects of needle to collector distance in single needle electrospeinning and solution surface to collector distance in bubble

electrospinning on fibre size and appearance were studied. The 10 , 20 and 30 cms needle to collector distance / solution surface to collector distance showed different results for single needle electrospinning and bubble electrospinning fibre morphology. A reduction of fibre diameter in single needle electrospinning with increasing the collector distance was found due to fibre stretching resulting by increased distance and time for fibre flight to collector. In bubble electrospinning, the opposite trend was found, i.e.; the fibre diameter increased with an increase in distance due to stress relaxation, drying and solution thickening by the compressed air flow.

As the applied voltage initially increased bubble electrospinning fibre diameter decreased and then increased with higher applied voltage. This is due to the interplay between bubble surface tension and the electrostatic force. In single needle electrospinning, fibre diameter decreased with increasing voltage due to the interplay between surface tension of the solution and the electrostatic force.

These changes in fibre morphology of single needle electrospinning and bubble electrospinning are due to different process parameters in fibre spinning, specifically the viscoelastic property of the solution in the case of single needle electrospinning and the viscoelastic force of the bubble in the case of the bubble electrospinning.

9.5 Thermochromic Polypropylene

Chromic materials are smart materials. Thermochromic materials change their properties (usually colour) as the temperature changes. Incorporating them into fibrous structure gives added value and dimension. In order to produce thermochromic filaments by melt electrospinning, it was necessary to study the processing of thermochromic pigments with polypropylene in melt spinning. For the proper blending of polymer matrix and pigments, it was necessary to spin thermochromic filaments by screw extruder. Similar feeding mechanism can be used to meltelectrospin the thermochromic filaments. The thermochromic pigments can be destroyed and affected by the temperature, the shear forces and the duration of exposure to the higher temperature. It was also necessary to decide spinnable concentration of thermochromic pigment. At the same time, it was also necessary to decide the minimum concentration required to maintain its thermochromism. In the present study we incorporated thermochromic pigments into polypropylene to produce thermochromic polypropylene by melt spinning.

In the present study, 35% UMB Blue thermochromic pigment and 65% polypropylene beads were fully mixed before feeding into bench top single screw extruder.

Thermochromic polypropylene filaments were coarser (90 tex) compared to neat polypropylene filaments (86 tex) using same processing parameters. The SEM image showed rough surface of thermochromic polypropylene compared to neat polypropylene due to the distribution of thermochromic pigments.

The differential scanning calorimetry results showed a distinct melting peak for thermochromic material at its activation temperature 37.5°C. The colour change from blue to colourless can be obtained by heating at body temperature (37°C), which is similar to activation temperature. The same phenomenon was observed, when sample was kept in oven and heated at 38°C. The colour change was reversible, so as the sample cooled down below activation temperature it again became coloured.

The solvent (methyl stearate) in thermochromic pigments is in solid phase at low temperature. When the colour forming components (organic acid and colorant) are in contact with each other, the colour can be seen. At low temperature, colour forming components are in contact, so they form colour. As temperature is raised to 37° C, the methyl stearate becomes liquid. The colour forming components lose their contact in liquid methyl stearate and colour cannot be seen.

Again when cooled down, the methyl stearate becomes solid. The colour forming components come in contact and form colour. Due to distribution, size and morphology of thermochromic pigments, the thermochromic polypropylene filament strength is reduced. It is still high enough for processability into textiles.

The optimum processing parameters were as noted below. The screw was heated by 3 temperature zones T1=201°C, T2=210°C and T3=220°C. Melting pump temperature T4=230°C. The two die zone temperatures T5=246°C and T6=240°C respectively. Melting pump rpm=4 and the extruder rpm=13.2. An initial trial and error were conducted to have continuous flow of material by changing temperature profiles and screw speeds, for eg higher pump speed (6.5 rpm), the neat polypropylene was processable. Polypropylene with thermochromic pigment showed phase separation and lumps of thermochromic pigments were coming along with the jet. It has very high breakage rate. This may be due to higher screw speed; it did not allow the pigment and matrix to mix well. At lower speed of 5 rpm, the breakage reduced with more continuity of polymer jet. At end 4.0 rpm was found as optimum speed for thermochromic polypropylene melt processability with nearly no breakage rate.

There were nearly no breakages observed in processing thermochromic polypropylene using above parameters. At the same time the thermochromic filament maintained its thermochromism and minimum required strength using above parameters.

The above temperature profile and parameters can be used as guideline for producing nano thermochromic polypropylene fibres by melt electrospinning.